Faculty of Pharmaceutical, Biomedical and Veterinary Sciences
Department of Veterinary Sciences

Integrated Approaches in Pediatric Pharmacotherapy: The Neonatal Göttingen Minipig Model for Drug Disposition in Perinatal Asphyxia and Therapeutic Hypothermia

PhD thesis submitted for the degree of Doctor in Veterinary Sciences at the University of Antwerp to be defended by

Marina-Stefania Stroe

Supervisor(s):
Prof. Dr. Steven Van Cruchten
Prof. Dr. Pieter Annaert
Prof. Dr. Karel Allegaert
Prof. Dr. Anne Smits
Antwerp, 2024

Composition of the PhD Examination Committee

Supervisors

Prof. Dr. Steven Van Cruchten
Comparative Perinatal Development, Faculty of Pharmaceutical, Biomedical and Veterinary Sciences, University of Antwerp, Antwerp, Belgium

Prof. Dr. Pieter Annaert
Drug Delivery and Disposition, Department of Pharmaceutical and Pharmacological Sciences KU Leuven, Leuven, Belgium
BioNotus GCV, Niel, Belgium

Prof. Dr. Karel Allegaert
Department of Development and Regeneration, KU Leuven, Leuven, Belgium
Department of Pharmaceutical and Pharmacological Sciences, KU Leuven, Leuven, Belgium
Department of Hospital Pharmacy, Erasmus MC, GA Rotterdam, the Netherlands
Child and Youth Institute, KU Leuven, Leuven, Belgium

Prof. Dr. Anne Smits
Department of Development and Regeneration, KU Leuven, Leuven, Belgium
Child and Youth Institute, KU Leuven, Leuven, Belgium
Neonatal Intensive Care Unit, University Hospitals Leuven, Leuven, Belgium

Internal committee members

Prof. Dr. Peter Bols
Laboratory of Veterinary Physiology and Biochemistry, Faculty of Pharmaceutical, Biomedical and Veterinary Sciences, University of Antwerp, Antwerp, Belgium

Prof. Dr. Antonius Mulder
Neonatal Intensive Care Unit, Antwerp University Hospital, Antwerp, Belgium

External committee members

Prof. Thomas Thymann, DVM, PhD
Comparative Pediatrics and Nutrition, Department of Veterinary and Animal Sciences, Faculty of Health and Medical Sciences, University of Copenhagen, Copenhagen, Denmark

Tim Bosmans, DVM, PhD, ECVAA residency trained
Clinic Manager & Teaching Supervisor, Anesthesia & Analgesia of Small Animals, Department of Small Animals, Faculty of Veterinary Medicine, University of Ghent, Ghent, Belgium

Table of Contents

TABLE OF CONTENTS

<p style="text-align: center;">TABLE OF CONTENTS</p>

TABLE OF CONTENTS

TABLE OF CONTENTS

List of Abbreviations

ADME	Absorption, distribution, metabolism, and excretion
ANOVA	Analysis of variance
AUC	Area under the curve
BE	Base excess
CL	Clearance
CYP	Cytochrome P450
CRI	Constant rate infusion
CV	Coefficient of variation
DMEs	Drug-metabolizing enzyme(s)
ECG	Electrocardiography
EEG	Electroencephalography
$EtCO_2$	End-tidal carbon dioxide
ETT	Endotracheal tube
ER	Extraction ratio
E_R	Expression ratio
EROD	Ethoxy resorufin-O-deethylase
FiO_2	Inspiratory oxygen fraction
FNT	Fentanyl
f_u	Fraction unbound
GFR	Glomerular filtration rate
GLMs	Göttingen Minipig liver microsomes
group C	Control
group H	Hypoxia
group H+TH	Hypoxia + therapeutic hypothermia
group TH	Therapeutic hypothermia
HCO_3	Bicarbonate
HIE	Hypoxic-ischemic encephalopathy
HR	Heart rate
IM	Intramuscular
IV	Intravenous
k	Elimination rate constant
Km	Michaelis-Menten constant
K_p	Partition coefficient
KPO_4	Potassium phosphate buffer
LC-MS/MS	Liquid chromatography-tandem mass spectrometry

LOD	Limit of detection
LLOQ	Lower limit of quantification
MDZ	Midazolam
MRI	Magnetic Resonance Imaging
MV	Mechanical ventilation
NADPH	Nicotinamide adenine dinucleotide phosphate regeneration system
N-FNT	Norfentanyl
NHPs	non-human primates
NICU	Neonatal intensive care unit
PA	Perinatal asphyxia
PCO_2	Partial pressure of carbon dioxide
PBPK	Physiologically-based pharmacokinetic(s)
PD	Pharmacodynamics
PHB	Phenobarbital
PK	Pharmacokinetics
PND1	Postnatal day 1 naive Göttingen Minipigs
PO_2	Partial pressure of oxygen
QC	Quality control
qPCR	quantitative Polymerase Chain Reaction
R_{ac}	Accumulation ratio
REST	Relative expression software tool
RFU	Relative fluorescence units
ROS	Reactive oxygen species
sO_2	Oxygen saturation
SpO_2	Fraction of oxygen-saturated hemoglobin
STSM	Short-Term Scientific Mission
TBI	Traumatic brain injury
TCO_2	Total carbon dioxide
TH	Therapeutic hypothermia
TPM	Topiramate
TPN	Total parenteral nutrition
$t_{1/2}$	Half-life
UVC	Umbilical venous catheter
V_d	Volume of distribution
Vmax	Maximal velocity of the reaction
1-OH-MDZ	1-Hydroxymidazolam

CHAPTER 1:
Introduction

Introduction

Pediatric drug therapy, especially in neonates, presents significant challenges. This subgroup is recognized to be the most vulnerable since growth and development are most pronounced during the early stages of life, affecting the body's response to drug administration. Among neonates, perinatal asphyxia (PA) is a notable condition often requiring therapeutic hypothermia (TH) alongside intensive care and drug treatment to reduce morbidity and mortality. In the context of supporting drug development and pharmacotherapy for this population, this study was undertaken to enhance our understanding of the effects of PA and TH. Given the physiological impacts of TH and PA, the primary hypothesis was that TH significantly reduces the metabolic clearance in asphyxiated neonates, necessitating adjustments in drug dosing. To investigate these effects, a neonatal Göttingen Minipig model was developed. Ultimately, integrating these findings, the optimized physiologically-based pharmacokinetic (PBPK) model is expected to be a reliable tool for accurately predicting drug exposure in asphyxiated neonates undergoing TH.

This chapter is structured in three sections. **Section 1** aims to familiarize the reader with current insights into neonatal drug disposition. **Section 2** further outlines the pathophysiological characteristics of system-specific functions in asphyxiated neonates. Recognizing the role of animal models in elucidating mechanisms in human diseases and exploring (patho)physiological factors influencing drug pharmacokinetics (PK), safety, and efficacy, **Section 3** delves into an analysis of animal models for pediatric drug development. The section particularly focuses on species selection for juvenile toxicity studies and introduces the chosen animal model for this research, the Göttingen Minipig.

1. Insights into neonatal drug disposition

Drug disposition and exposure holds a pivotal role in pharmaceutical research and development, guiding the identification of potential drugs and their safety, efficacy, and toxicity. It encompasses the fundamental PK processes: absorption, distribution, metabolism, and excretion (ADME). Conducting ADME studies is essential to gain insights into the behavior of drugs, facilitating the transition from preclinical animal studies to human clinical trials [1]. A specific challenge in drug research lies in the limited development and assessment of drugs, specifically for pediatric use. Most drugs are developed based on insights regarding the adult pathophysiology and adult indications, while knowledge of neonatal pathophysiological processes is relatively limited [2,3]. The expression "Children are not small adults" holds particular relevance in neonatal pharmacology, emphasizing that dose predictions for neonates cannot simply be extrapolated from the adult context, where methods such as rescaling body weight and body surface area are commonly employed [4,5]. The age- or weight- related changes in drug disposition can be attributed to physiological changes occurring in multiple organs and organ systems during development [6], as outlined in Figure 1. The application of PK in the pediatric field starts with understanding the maturational processes related to ADME from (preterm) neonates through adolescence [4], that will be further presented.

Figure 1. Developmental changes and physiological factors that influence drug disposition in neonates through adolescence. Adapted from Kearns et al. [6]. Created with BioRender.com. * Cytochrome P450 (CYP); glomerular filtration rate (GFR); uridine 5'-diphospho-glucuronosyltransferase (UGT); volume of distribution (V_d).
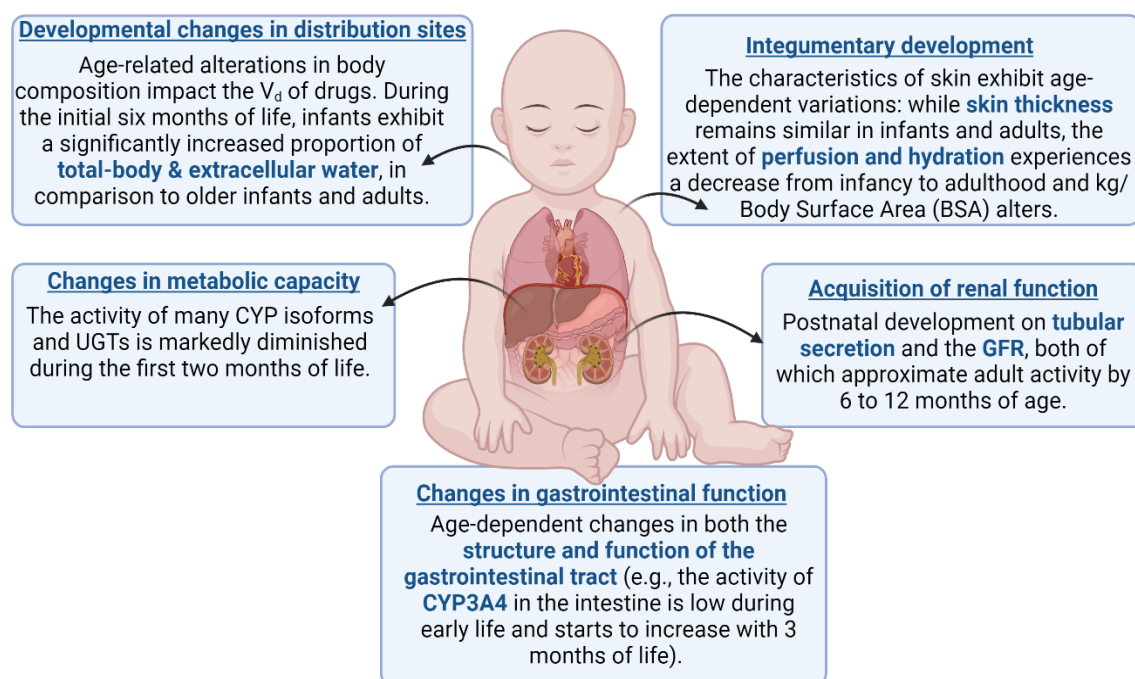
Gastrointestinal absorption of drugs is influenced by (1) its physicochemical properties, (2) physiological factors like gastric pH, the presence of drug-metabolizing enzymes (DMEs), and drug transporters (DT), and (3) environmental conditions, including food. These factors undergo changes during growth and development, leading to maturation-related alterations in the gastrointestinal system's absorptive capacity and first pass processes [7,8]. At birth, gastric pH is elevated, likely due to immature gastric secretory function and the ingestion of amniotic fluid [8]. The intestine contains various DMEs and DTs [7,9]. Notably, cytochrome P450 (CYP) 3A4 is the most prevalent DME in the intestine. While some DMEs, like glutathione peroxidase and alcohol dehydrogenase, remain relatively stable during growth, others, such as the uridine 5'-diphospho-glucuronosyltransferase (UGT) isoforms, exhibit abundance variations with age [7,10].

Upon absorption into the systemic circulation, compounds undergo distribution, transferring the drug to various organs and tissues [2,7,11]. The quantification of distribution is often expressed through the volume of distribution (V_d). Human neonates exhibit a higher proportion of body water per kilogram of body weight (70%) compared to adults (60%), leading to higher V_d for water soluble drugs. Additionally, human neonates have reduced plasma binding protein concentrations, including plasma globulins, albumin, and α-1 glycoprotein, compared to adults. This results in an increased free fraction of compounds, enhancing their ability to diffuse into different body compartments and penetrate deeper, consequently yielding to a higher V_d [7]. Chapter 4, "Drug disposition in neonatal Göttingen

Minipigs: exploring the effects of perinatal asphyxia and therapeutic hypothermia", will provide in-depth information on PK parameters, including V_d, as well as some potential factors responsible for PK alterations in neonatal Göttingen Minipigs.

Changes in metabolizing capacity during development can significantly impact the bioavailability (e.g., by first pass) and elimination of drugs. While developmental alterations in metabolism are recognized, there is limited information available regarding the impact of disease and conditions on specific drug metabolism in neonates. It is important to note that each metabolic pathway (e.g., CYP enzymes), has a distinct ontogeny that should be considered [12]. Further insights on this topic will be provided in Chapter 5, "Effects of hypothermia and hypoxia on cytochrome P450-mediated drug metabolism in neonatal Göttingen Minipigs". In addition to phase I metabolism, phase II metabolic pathways like glucuronidation and sulfation also display maturational changes. Developmental patterns also vary between the different UGT-isoenzymes. For instance, in humans, the expression of UGTs starts at 20 weeks of gestation and is enhanced by birth, independent from the gestational age, with a subsequent increase in the first weeks of life [13]. In a previous preclinical study, UGT activity was assessed in Göttingen Minipig liver microsomes [14]. Even if UGT activity assessed with human substrates is higher in (mini)pigs compared to humans, for the youngest age groups (fetal, postnatal day 1 and 3), low levels were detected [14].

Lastly, renal drug elimination depends on the glomerular filtration, the tubular excretion, and the tubular reabsorption. The glomerular filtration rate (GFR) is often used to quantify renal capacity. In human neonates, the GFR is 10-20 mL/minute, but its increases rapidly towards adult values of 70 mL/minute by 3-5 months of age. The renal tubule transporter system promotes the passage of drugs from the plasma into the tubule, but it has a reduced capacity of 20-30% in neonates compared to adults. In the end, in the distal part of the renal tubule, lipophilic drugs are reabsorbed by passive diffusion from the tubule back into the blood. Since reabsorption does not reach adult levels until 2 years of age, this developmental delay can cause alterations in the clearance of some drugs [7].

2. Pathophysiology of perinatal asphyxia , modulated by therapeutic hypothermia

In this thesis, Section 2 of Chapter 1 was adapted from the review article "Pharmacokinetics during therapeutic hypothermia in neonates: from pathophysiology to translational knowledge and physiologically-based pharmacokinetic (PBPK) modelling" authored by Leys K and Stroe M-S, et al., 2023, published in Expert Opinion on Drug Metabolism and Toxicology. The content has been modified and expanded to provide a more comprehensive understanding within the context of this thesis. This section is structured on two key aspects: (1) the pathophysiology of PA and (2) the pathophysiological implications of hypoxic-ischemic encephalopathy (HIE) on the brain.

2.1. Pathophysiology of the asphyxiated neonate receiving therapeutic hypothermia: definitions and general aspects

Perinatal asphyxia is a medical condition at delivery caused by oxygen deprivation, potentially resulting in HIE [15]. Approximately 0.5% of all live-born neonates are affected by PA, and

about 0.18% are diagnosed with HIE (mild, moderate, or severe). Perinatal asphyxia is still one of the most common causes of death in (near)term human neonates [16]. The complexity of PA pathophysiology is represented by its association with various risk factors during gestation [17]. These include chronic diseases in the mother (e.g., preeclampsia, hypertension, or diabetes), as well as placental issues (e.g., placental detachment, fetal-maternal hemorrhage, or inflammation). Fetal factors also can contribute, with the potential for anomaly or malformation, retarded intrauterine growth, and the development of neurological disorders or spinal cord injuries, among other conditions. These conditions can have profound implications for the neonate, particularly concerning the central nervous system [17]. Figure 2 provides a summary of PA pathophysiology, depicting organ injuries and the physiological imbalances, bridging both central and non-central nervous system, triggered in response to the hypoxic-ischemic injury. Oxygen deprivation is reflected in the diagnostic clues for HIE, consisting of clinical findings (Apgar score and Thomson score), and findings based on either laboratory values (arterial blood base excess, lactate, and pH for acidosis) or monitoring (electroencephalographic (EEG) activity) [15,18]. Therapeutic hypothermia (TH; target core temperature of 33.5 °C for 72 hours with subsequent slow rewarming at 0.5 °C/hour) is effective in reducing mortality or impaired neurodevelopmental outcome in moderate to severe HIE (number needed to treat 7, outcome variable decreases from about 55% to 45%) [19,20].

Figure 2. Prenatal risk factors for cerebral ischemic injury, with associated organ injuries and physiological imbalances in response to hypoxic-ischemic injury. Adapted from Mota-Rojas and Villanueva-Garcia et al. [17]. Created with BioRender.com. * Hypoxic-ischemic encephalopathy (HIE).
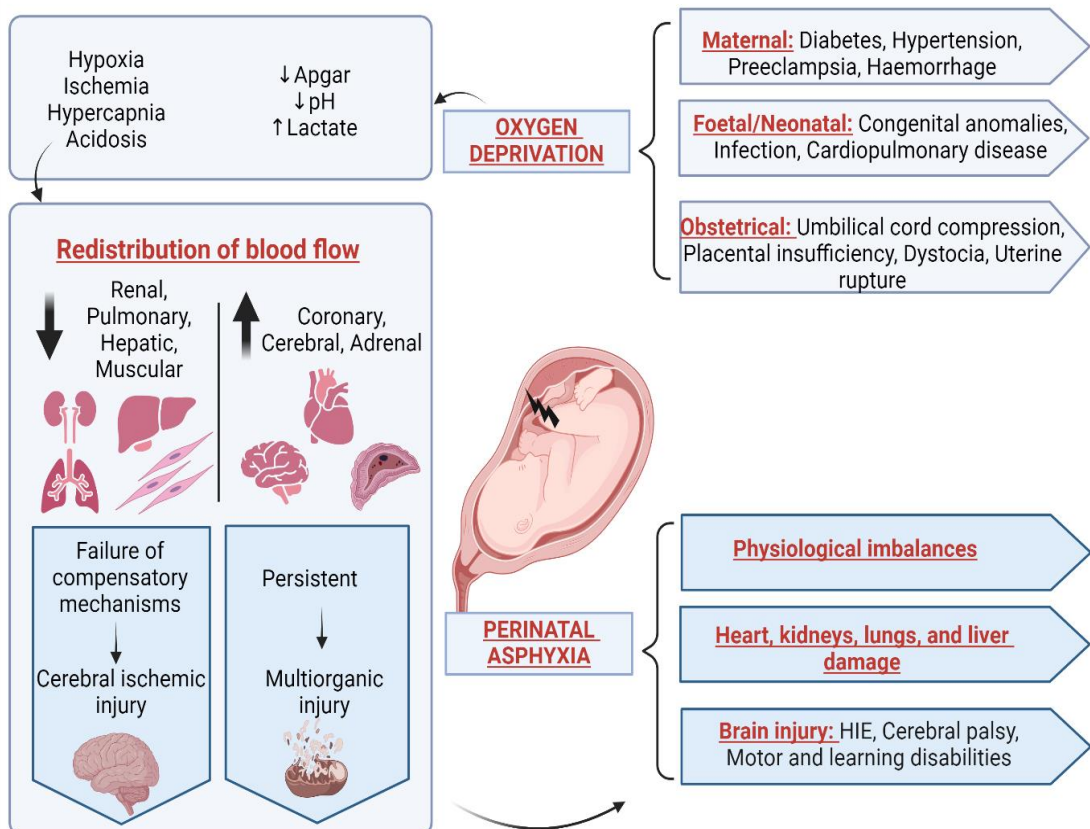
Perinatal asphyxia is affecting multiple organs, including but not limited to the central nervous system. The initial cardiovascular response to oxygen depletion results in organ-specific vasoconstriction. This subsequently results in perfusion and oxygen supply redistribution from non-vital organs to the heart and brain. Other organs, such as the kidneys, liver, lungs, muscles, and intestines, are in a low perfusion setting [21,22] (Figure 2). Therefore, it is essential to be aware that TH further modulates the "natural" progression of the pathophysiology of PA. As TH is only indicated in (near)term human neonates with moderate or severe HIE, this mainly refers to (patho)physiological parameters on cardiac output (CO; stroke volume, myocardial strain, and heart rate), regional blood flow (pulmonary hypertension, cerebral, renal, and hepatic blood flow), renal function (GFR), plasma composition (albumin, hematocrit, and α-1 glycoprotein), immunomodulation, and intestinal functions (gastric emptying, intestinal motility, and permeability). Using an exploratory search in PubMed on PA and TH in human neonates until November 2022, some of the pathophysiological characteristics of system-specific functions in asphyxiated neonates undergoing TH were listed in Table 1. This approach has the intention to provide the reader with a snapshot of system-specific observations, but is not complete, nor does it claim to be systematic.

Table 1. System-specific observations on the impact of perinatal asphyxia on neonatal physiology, with or without therapeutic hypothermia (TH). Reproduced from Leys K and Stroe M-S, et al. [23]. * Acute kidney injury (AKI); cardiac output (CO); C-reactive protein levels (CRP); electrocardiography (ECG); electroencephalography (EEG); hypoxic-ischemic encephalopathy (HIE); partial pressure of carbon dioxide (PCO_2); postnatal age (PNA); corrected QT Interval (QTc); serum creatinine (sCr).

System	Observations
Cardiovascular system	Asphyxia was the primary determinant of impaired myocardial function (strain rate about 50% slower), improving from day 4 (after TH) [24]. In a meta-analysis, short-term outcome studies suggest cardioprotective effects (via cardiac biomarkers, blunted myocardial dysfunction on ECG, and cardiac ultrasound) of TH [25]. The QTc interval is prolonged during TH and normalizes afterwards [26].
Renal system	Median sCr values over PNA days 1, 2, 3, 5, and 7 were 0.96, 0.80, 0.64, 0.75, and 0.47 mg/dL in PA/TH cases. This significantly differs from healthy controls: 0.71, 0.77, 0.67, 0.46, and 0.42 mg/dL, reflecting poorer kidney function in PA/TH cases [27,28]. In addition, a meta-analysis showed a significantly lower incidence of AKI in neonates treated with TH than in cases without TH (relative risk = 0.81, TH is protective) [25].
Coagulation system and acid-base balance	Compared to term controls, hematocrit is lower in asphyxiated term neonates (0.41 to 0.45 on day 1 of PNA versus 0.5 to 0.53 on day 5 of PNA) [29]. Albuminemia is decreased (24 g/L) in the setting of asphyxia and relates to the asphyxia severity grade (29 g/L in mild cases; 24 g/L

	in moderate cases; and 20 g/L in severe cases) [30]. Acidosis is a critical finding in these patients (umbilical cord pH<7 as one of the criteria). However, TH also affects blood gas parameters such as pH and PCO_2. At lower temperatures, the pH increases and PCO_2 decreases [31]. Umbilical cord blood lactate levels are significantly higher among neonates with HIE (mean 8.72±1.75 mmol/L, range 5.12-11.96 mmol/L) compared to those without HIE (mean 6.86±1.33 mmol/L, range 4.74–10.30 mmol/L; P=0.001) [32].
Digestive and hepatic system	The intestinal and hepatic blood flows are decreased in asphyxiated term neonates, reflected in increased (20-25%) regional flow velocity and reduced CO [29]. There is higher passive intestinal permeability (lactulose and renal lactulose/L-rhamnose test) up to at least day 9 of PNA in asphyxiated term neonates [33]. Hepatic injury, marked by raised liver enzyme levels, is common in PA; however, TH blunts the hepatic injury. The same holds for the inflammatory response (TH is associated with lower CRP) [30].
Central nervous system	Neurovascular coupling is impaired in neonates with asphyxia [34]. Seizures commonly occur and are associated with an adverse neurodevelopmental outcome [35].

2.2. The pathophysiological implications of hypoxic-ischemic encephalopathy on the brain

Three main consecutive phases associated with neuronal cell damage occur in neonates with HIE: (1) the primary phase, including a latent phase (from 6-12 hours), followed by (2) the secondary and (3) tertiary phases. A first peak of neuronal cell damage occurs during the primary phase and is caused by primary energy failure during the hypoxic event at birth. A second peak results from subsequent reoxygenation and reperfusion after birth ("reperfusion injury"; latent phase). In the primary phase, the acute hypoxia shortly before or during delivery results in primary oxygen and energy deficiency, resulting in depolarization, potassium efflux, sodium and calcium influx, adenosine triphosphate degradation, and finally resulting in cell necrosis if the event is sufficiently severe or prolonged. Subsequently, this results in the release of excitatory neurotransmitters, with glutamate as the most relevant compound (with subsequent N-methyl-D-aspartate receptor activation). However, the neonatal brain releases proportionally more inhibitory neurotransmitters, which is likely to contribute to the remarkable tolerance of the neonatal brain to hypoxia and ischemia [15,36]. The secondary phase further causes cell damage and induces an inflammatory response. The subsequent apoptotic activity and the down-regulation of trophic factors further contribute to neuronal cell injury. The secondary phase, represented by mitochondrial dysfunction and inflammatory response can last for days, while the tertiary phase can last up to weeks/years [15,36]. The primary phase is the time window relevant to initiate TH to blunt the secondary phase, while the secondary phase is the "main target time interval" for most ongoing drug development programs, like allopurinol, 2-iminobiotin, or erythropoietin [37-39]. Figure 3 resumes the phases of the hypoxic injury and the fundamental mechanisms.

Figure 3. Overview of the pathophysiological processes occurring during hypoxic-ischemic encephalopathy (HIE). Hypoxic-ischemic encephalopathy is a result of apoptosis or a reoxygenation-reperfusion injury after resuscitation. It is characterized by three phases: (1) the primary phase, including a latent phase, (2) the secondary energy failure and (3) a tertiary phase. This pathway leads to neuronal cell death, blood-brain barrier disruption and inflammation response. This physiopathology is outlined by 4 main events that are linked to each other all following their own pathway: oxidative stress, mitochondrial dysfunction with intracellular Ca^{2+} accumulation, excitotoxicity, and inflammation. Adapted from Greco et al. [40]. Created with BioRender.com. * Adenosine triphosphate (ATP), Deoxyribonucleic acid (DNA), reactive oxygen species (ROS).
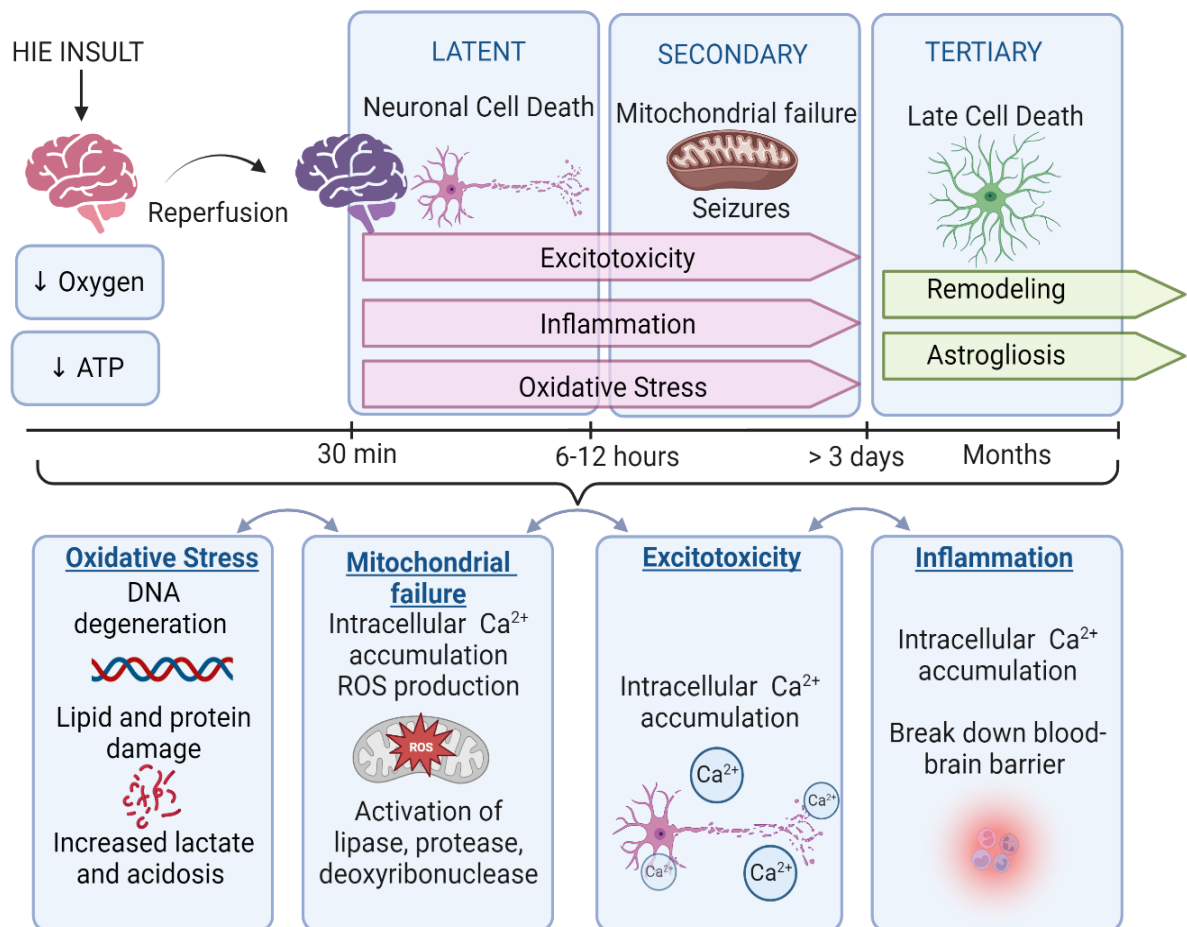
Several reviews have addressed the mechanisms governing neuroprotection during hypothermia in acute neurological diseases characterized by hypoxia (such as HIE) [41-43]. Across acute and subacute ischemic phases, TH has been described to specifically modulate cellular pathways leading to (1) excitotoxicity; (2) apoptosis; (3) inflammation; (4) free radical production. Moreover, TH modulates blood flow, slows overall cellular metabolism, and supports blood-brain barrier integrity. The latter is vital in determining the central nervous system access of administered drugs. In the acute phase, TH will cause a decrease in brain oxygen consumption and glucose metabolism of about 5%/°C. Hypothermia thus preserves adenosine triphosphate levels and pH, eventually preventing (excessive) lactate formation and acidosis. Furthermore, the effects of TH on the blood flow in damaged brain tissue during

reperfusion are characterized by a blunted overshoot as TH prevents the release of excitatory amino acids (e.g., glutamate). This is typically explained in terms of better maintenance of ion homeostasis, thus preventing necrosis.

3. Neonatal and juvenile animal models in pediatric drug discovery and development

Recognizing the valuable role of animal models in providing insights into mechanisms in human diseases, as well as exploring (patho)physiological factors influencing PK, safety, and efficacy of drugs, Section 3 of the introductory chapter analyzes animal models for pediatric drug discovery and development. The focus is on (1) species selection for juvenile toxicity studies, and it introduces the selected animal model for this research, the Göttingen Minipig (2).

3.1. Species selection for juvenile toxicity studies

To guide the design and safety monitoring of pediatric clinical trials, nonclinical and clinical data are valuable resources. When existing data are insufficient to ensure safety, a juvenile animal toxicity study is typically necessary. Usually a single relevant species, most commonly a rodent, is chosen as species of choice, while a non-rodent species can be appropriate when scientifically justified. Juvenile toxicity studies are complex, both conceptually and logistically [44]. Considering the continuous development of various organs at different rates, factors such as the comparative organ system development, discrepancy in drug PK/ADME between young animals and children, and the logistical requirements must be carefully addressed in the study design [23,44,45]. The majority of juvenile toxicity studies use rodents (>70%), with the rat being the most prevalent model, followed by dogs (9-12%), non-human primates (NHPs) (2-4%), and minipigs (1-2%), with other species (rabbit and sheep) being the least used [44]. The preference for rodent species is based on extensive experience, historical data, and the capacity to assess the entire postnatal development period. However, there are also some limitations concerning this species. Both strengths and limitations associated with using rodents in juvenile toxicity studies are summarized in Table 2 [17,44,45].

Table 2. Strengths and limitations of using rodents in juvenile toxicity studies [17,44,45].

	Strengths	Limitations
Rodent model for Juvenile toxicity studies	- extensive experience and historical background data. - can test full span of postnatal development. - easy to house, transport and manage. - short gestation time (21-23 days). - litters are easily produced and handled (5-10 liters per year). - ability to procure appropriate numbers of animals even for early age assessment. - easy cross-fostering and multiparity.	- may not be pharmacologically relevant. - rat pups' small size: limited routes of drug administration (the earliest day of dosing initiation is often based on the dosing route); limited blood sampling (usually sampling is terminal, thus requiring large numbers of offspring); not instrumented to monitor the hemodynamic indices; multiple biologic specimens are not feasible. - the potential immunogenic response.

As previously mentioned, the top three non-rodent species used for juvenile toxicity studies are the dogs, NHPs and minipigs. To provide a comparative overview, various characteristics of these animal species are presented in Table 3.

Table 3. Comparative features of the Göttingen Minipig, Beagle Dog, common marmoset, Cynomolgus monkey (Long-tailed macaque), and Rhesus macaque, used for juvenile toxicity studies. Adapted from Ellegaard et al. [46]. *[1] Data from the same breed is used to permit readily comparison.*

	Göttingen Minipig	Beagle Dog	Marmoset	Macaque
[1] Species/ Breed	Pig, *Sus scrofa*	Domestic dog, *Canis familiaris*	*Callithrix jacchus*	Cynomolgus monkey: *Macaca fascicularis;* Rhesus macaque: *Macaca mulatta*
Birth weight (kg)	0.45 (0.3-0.55)	0.25	0.25-0.35	Cynomolgus: 0.33-0.35 Rhesus: 0.40-0.55
Handling at birth	Easy; for juvenile studies they can be used from day 2 after birth	Easy	Not easy; neonates carried by family members	Not easy; neonates carried by mother

Sexual maturity (months)	Quick to mature. 3-4 (males), 4-5 (females); age to breed 5-9	7-8 (males), 8-14 (females); age to breed 12-24	16 months (males), 14 (females); age to breed 18-24	Cynomolgus: 36-48 months; age to breed 48-60. Rhesus: 36-48 (males), 24-36. (females); age to breed 48-60 (males), 36-48 (females)
Litters per year	2.1-2.3	1-2	1-2	1
Average offspring per breeding female per year	6.5 offspring × 2.2 litters per year= 14 offspring	6 offspring × 1.5 litters per year= 9 offspring	2 offspring × 1.5 litters per year= 3 offspring	1 offspring × 1 litter per year= 1 offspring
	Greater fecundity means fewer breeding animals are required than for NHPs . Also, more information can be obtained more quickly in reproductive toxicology studies			-
Male : female ratio	1:10	1:4-12	1:1	1:4 to 1:12
Health status	"Microbiologically defined status"	Conventional		Conventional. Not all colonies are Herpes B virus free; Herpes B virus is a serious health threat to animal handling staff
Transport	EU travel achieved within 24 hours for most countries			Import from third world countries means long and complex journeys, with loading/unloading. International journeys commonly last 30-70 hours therefore, minimizing journey duration is very important
Relocation	7-10 days is allowed for acclimatization following transport		7-28 days is allowed for acclimatization following transport	

Housing and husbandry (space)	Terrestrial, inquisitive	Terrestrial, inquisitive, and active	Arboreal (3 dimensional), inquisitive and highly active	
Handling and restraint	Fair; selected for docility	Good; docile and amenable socialized to humans	Poor; highly agile and active	Poor; highly agile, active, and strong. Risk of injury to handler from aggressive adult animals.
Human contact	Domesticated species		Non-domesticated species	
Human health and safety	Low risk of zoonoses	Low risk of zoonoses (technicians should be vaccinated against rabies); bite wounds can be severe	Low risk of zoonoses	Low risk of zoonoses but bite and scratch wounds can be severe. Exclude the use of Herpes B positive monkeys. Staff should be vaccinated against Hepatitis B
Animal care staff	May be difficult to find experienced staff; training is needed	Staff commonly more familiar with dog behaviors, due to their status as companion animals	May be difficult to find experienced staff; training is needed	

The biomedical community is increasingly recognizing the significance of pigs in research. In the past decade, researchers and clinicians have come to appreciate the utility of pigs in various research areas, such as providing organs for human transplants [47], advancing our knowledge of diseases like cancer [48,49], and serving in applications like surgical training (i.e., Orsi Academy, Belgium). Furthermore, Göttingen Minipigs have been selectively bred for its small size, pale skin, and docility in order to make them ideal animal models for laboratory biomedical research [46], and then for preclinical research on PK. The Göttingen Minipig breed exhibits continuous breeding, producing 2.1-2.3 litters annually. While its gestation period (114±4 days) surpasses the Beagle dogs (59-67 days) and falls short of NHPs (153-179 days in the Cynomolgus monkey; 146-180 days in the Rhesus macaque), both dogs and minipigs yield sizable litters of approximately 5-7 offspring, whereas the NHPs gives birth to a single offspring. Manipulating and cross-fostering offsprings are comparatively straightforward in minipigs and dogs but challenging in NHPs. The Göttingen Minipig reaches sexual maturity earlier (3-5 months) compared to dogs (7-14 months) and NHPs (Cynomolgus monkey 36-48 months). Some disadvantages include the more limited historical control data available for (mini)pigs than dogs and NHPs at present, the different placentation and a relatively more mature respiratory and musculoskeletal systems compared to human neonates [45]. Also,

when using the adult (mini)pigs the higher body weight, especially concerning the administration of compounds, which can be costly represent a drawback [46]. Obtaining neonatal non-rodent animals is always challenging. While Göttingen Minipigs are available across Europe, Asia, and the USA via 4 breeding facilities that can provide pregnant saws, the NHPs under 9-12 months is challenging, and purchasing pregnant animals is typically not an option from breeders of this species. Consequently, including neonatal NHPs in juvenile studies requires breeding at the research facility, posing logistical challenges [50].

Lastly, blood sampling and IV administration of drugs may be more challenging in pigs and NHPs than in dogs [45,46]. Minipigs have small ear veins, making them unsuitable for easy blood sampling (usually requiring sedation, and withdrawing large amounts of blood is challenging). Alternatively, blood sampling from the cranial vena cava is feasible, without sedation, allowing for larger blood samples. Although deeper location of the blood vessels makes blood sampling more challenging, samples can be taken with minimal distress when staff members are well trained. Due to the limited number of accessible superficial veins, in the Göttingen Minipig vascular access ports or chronic catheterization, are commonly used this involving surgery, anesthesia, and a recovery period. These are the preferred methods for frequent sampling since they are likely to improve the welfare of the animals. Available training courses with a focus on stress free handling and dosing, as well as surgical placement of temporary and chronic vascular catheters exists (e.g., Göttingen Minipigs Academy). On the other hand, blood is readily obtained from jugular or cephalic veins in dogs, while marmosets and macaques have specific methods and considerations for blood collection. Sampling in marmosets needs training and manual dexterity for blood sampling, with the femoral vein being the preferred method; the coccygeal vein is also an option. Their small size limits sequential samples from the same individual, potentially impacting study animal numbers. One solution is the micro sampling, using the capillary tube method, enabling the collection of small samples from the heel without the need for anesthesia. Macaques' larger size facilitates blood collection, but nevertheless accessing their blood vessels is more challenging than in dogs [46].

In conclusion, the minipig plays a part in the preclinical stages of drug development, although pharmaceutical companies may exhibit some hesitation, primarily stemming from lesser familiarity compared to the dog and NHPs. Nevertheless, selecting an animal model should hinge on its ability to replicate similar PK, pharmacodynamics, metabolic, safety, and toxicity profiles as observed in humans [51].

3.2. The Göttingen Minipig as a relevant animal model for biomedical research

The benefits of using small pigs, such as ease of handling, reduced food and space requirements, and lower quantities of pharmacological products and anesthetics in studies, prompted initial efforts to breed miniature pigs, and use them instead of the conventional (large) pig breeds. Subsequently, a diverse range of breeds and strains of miniature pigs have been developed and used in biomedical research, from which the Göttingen Minipig [52]. Except for some miniature pig (e.g., Westran, Yucatan, or the Micro-Yucatan), the breeds that are used in biomedical research are usually a product of crossbreeding (Table 4) [52]. Developed in the 1960s by Professor Fritz Haring at the Institute of Animal Breeding and Genetics at the University of Göttingen, Germany, the Göttingen Minipig (Figure 4 (A)) stands as the first European minipig breed. Comprising 59% Vietnamese Potbelly Pig (Figure 4 (B)),

33% Minnesota Miniature (Figure 4 (C)), and 8% German Landrace (Figure 4 (D)), this breed combines the high fertility of the Vietnamese with the docile behavior of the Minnesota Miniature. Currently, there are 4 breeding facilities worldwide (i.e., University of Göttingen, Germany; Ellegaard Göttingen Minipigs A/S, Dalmose, Denmark; North Rose, New York, US; and Tokyo, Japan), making the Göttingen Minipigs available for biomedical research across Europe, Asia, and the USA.

Table 4. Overview of minipig breeds used in biomedical research and their main biological characteristics. Reproduced from Köhn F. [52].

Breed	Origin	Birth weight (kg)	Adult weight (kg)	Piglets per litter	Colour
Clawn	crossbred	0.5	40	5	white
Göttingen	crossbred	0.45	45	6.5	white
Hanford	crossbred	0.73	80 - 95	6.7	white
Munich	crossbred	0.6 - 0.9	60 - 100	8.5	white, black, red, brown
Panepinto	crossbred	0.5 - 0.8	25 - 30	7	grey, black
Sinclair	crossbred	0.59	55 - 70	7.2	black, red, white, roan
Westran	native	0.93	80 -93	4.6	white
Yucatan	native	0.5 - 0.9	70 - 83	6	black, slate grey
Micro-Yucatan	native	0.6 - 0.7	55 - 70	6	black, slate grey

Figure 4. The origin of Göttingen Minipigs **(A)** depicted through images of the three breeds comprising its genetic foundation: **(B)** Vietnamese Potbelly Pig known for fertility and low body weight, **(C)** Minnesota Miniature recognized for small size and gentle temperament, and **(D)** German Landrace distinguished by light skin. Adapted from https://minipigs.dk/about-gottingen-minipigs/genetic-foundation .
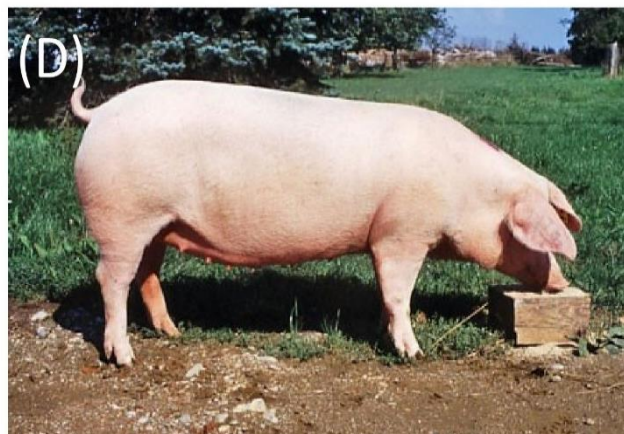
As mentioned in Section 3.1, the Göttingen Minipig stands out among non-rodent animal models, particularly for juvenile studies. Some examples of the many strengths that this species offers with some field of applications will be further presented.

First of all, it is important to highlight that both conventional pigs and minipigs represents excellent animal models for biomedical research. However, in view of nonclinical drug development, and then for PK preclinical research, the conventional pig is not used. The Göttingen Minipig is the most commonly used pig strain in Europe, as is the Beagle when using the dog and the Sprague Dawley or Wistar when using the rat [2]. The smaller size of Göttingen Minipigs, compared to that of larger conventional pigs, makes them more manageable in a laboratory environment. They exhibit characteristics suitable for research, including genetics and temperament. Göttingen Minipigs can be selectively bred under controlled conditions (genetically coherent, conventional, or specific pathogen-free, pigmented, or non-pigmented skin) and can be housed in laboratory conditions similar to those for dogs [53,54]. As such, they are well-characterized, and by using the same strain, pharmaceutical companies can rely on historical control data when interpreting findings in the safety studies [2].

In general, (mini)pigs and humans share many developmental milestones. The developmental patterns of the gastrointestinal tract, cardiovascular, central nervous system, and eye are largely comparable in both species, with renal, immune, and reproductive development occurring slightly earlier and more rapidly in humans than in pigs.

These data are illustrated in Figure 5. Additionally, high homology to the human Phase I drug metabolizing CYP family has already been described in Göttingen Minipigs (63-84% amino acid identity) [55,56] and the ontogeny of CYP enzyme activity in the juvenile Göttingen Minipig showed to be comparable to the corresponding age groups in human [14,57]. Our group has already reported on the age-related maturation of organ weights in the developing Göttingen Minipig [58] in an effort to further develop a PBPK model (Section 3.3., Chapter 6). This strengthens the expectation that establishing a disease animal model (i.e., PA model with TH in Göttingen Minipigs) could provide useful information for the human conditions.

Figure 5. Schematic representation of the postnatal development of different systems in human (top) and Göttingen Minipig (bottom). In lateral bars, the intensity of the maturation process is represented by dark (more intense) and light (less intense) tones. The time bar represents weeks (w), months (m) or year (y) of life. Reproduced from Ayuso et al. [45].
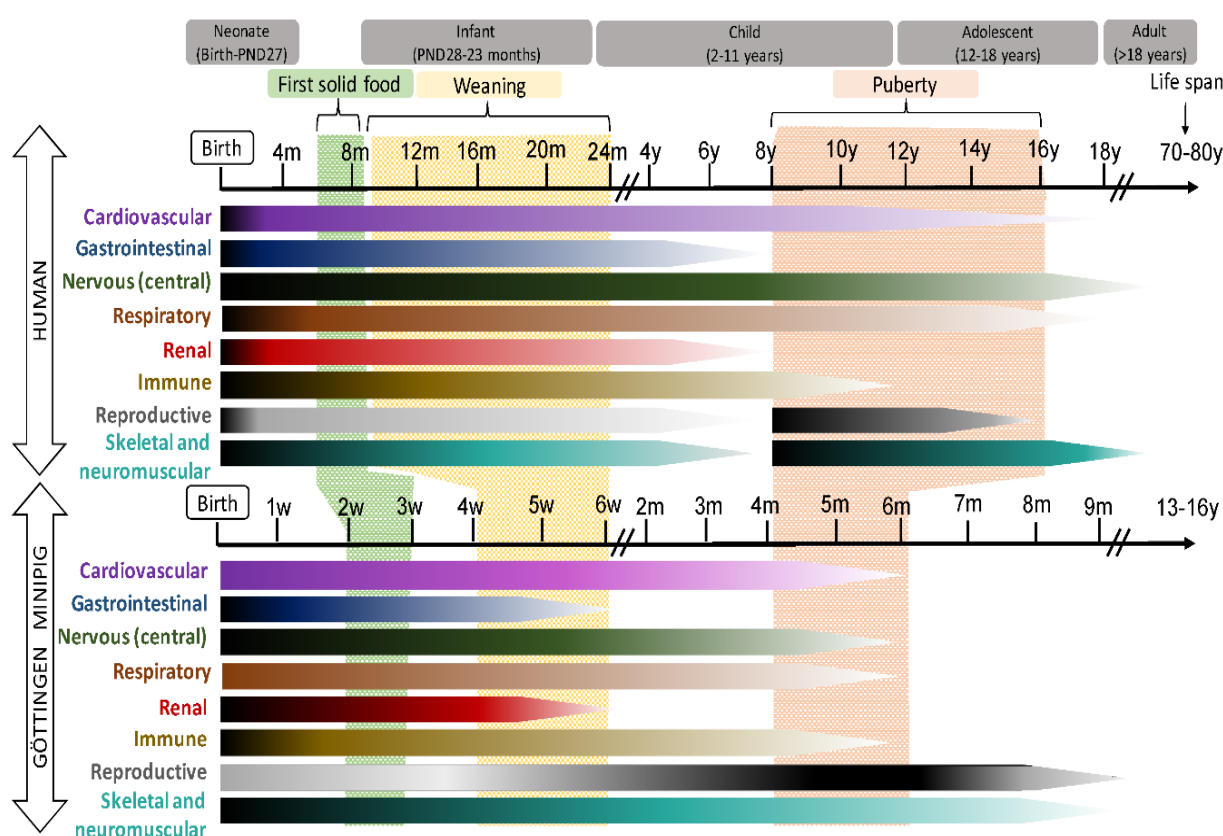
Göttingen Minipigs are applicable to all routes of drug administration: oral [59] (in food and water; capsule and tablets; oral gavage), parenteral [60-62] (intradermal, subcutaneous, IM, IV, intraperitoneal, intranasal), topical dermal applications [63], inhalations [64], osmotic pumps [46]. Due to the anatomical and physiological similarities with humans, the Göttingen Minipig is also a surgical model. Interventional catheter techniques, complex trauma procedures, (non)survival training classes, transplantations, endoscopic procedures, cardiac valve replacement and stent implantations are just some examples [65]. These make the Göttingen Minipigs valuable animal models for several clinical indications: cardiovascular [66-70], neurology [71], pain [72], dental [73], metabolism [74,75], skin [76,77], and acute and chronic intestinal inflammation [78,79]. This selection of papers using an unstructured

exploratory search in PubMed on Göttingen Minipig until December 2023 has the intention to provide the reader with a snapshot of the areas in which Göttingen Minipigs have excelled. It is important to note that the list of topics and papers is far from complete.

3.3. PBPK models in the Göttingen Minipig

When clinical data are limited or unavailable, the construction of a mechanistic framework for predicting drug exposure becomes crucial. Employing a "bottom-up" modelling strategy, such as PBPK models tailored to a corresponding animal model, offers a pathway to indirectly inform and enhance the desired PBPK models for the human target population. This approach is especially promising in the context of using animal models, with a special focus on juvenile animals [2,23]. An interesting example is the development of a PBPK model specifically designed to elucidate the PK of methylphenidate in both juvenile and adult populations, encompassing humans and NHPs [80]. Considering the aforementioned benefits provided by the Göttingen Minipig model, an increasing application of PBPK models is anticipated in (neonatal and juvenile) minipigs. This is expected to enhance the development of PBPK models in corresponding human populations. A guideline to enhance the construction of PBPK models for "novel" species, including minipigs, was already proposed [81]. This is quite interesting since only 5% of the parameters in the species models are "sensitive", therefore building minimal PBPK models to address the research questions (i.e., semi-mechanistic approach) should be considered [81].

In order to compare the juvenile Göttingen Minipig with the human pediatric population, efforts are ongoing to further characterize this animal model [14,57,58,82]. In this regard, a preliminary PBPK model for the adult Göttingen Minipig population has already been made [83,84] and the first steps have been taken to create a model for the juvenile population [57,58]. Regarding the adult Göttingen Minipig PBPK model, Suenderhauf and Parrott [83] were the first to publish a compilation of gastrointestinal pH values and transit times, along with organ sizes and blood perfusion rates. The PBPK model implementation of these physiological data was verified with moxifloxacin and griseofulvin, both after IV and oral administration [83]. Regarding the neonatal Göttingen Minipig PBPK model, Chapter 6 of this thesis explores the available information to establish a database for this age category and highlights current knowledge gaps. Initial midazolam and topiramate PBPK models using the neonatal Göttingen Minipig data were developed using PK-Sim® software (Open Systems Pharmacology Suite), incorporating literature findings and data resulted from the I-PREDICT project: Innovative physiology-based pharmacokinetic model to predict drug exposure in neonates undergoing cooling therapy. Ultimately, the insights gained during the development of PBPK models in the corresponding neonatal animal model are anticipated to contribute to the development of PBPK models for human neonates with specific conditions (i.e., PA/TH). Establishing both, a Göttingen Minipig and human neonatal PBPK model, is expected to be particularly valuable in predicting the impact of TH on the PK of essential drugs used in asphyxiated neonates [2,23].

4. References

1.   Caldwell J, Gardner I, Swales N. An introduction to drug disposition: the basic principles of absorption, distribution, metabolism, and excretion. Toxicol Pathol. 1995 Mar-Apr;23(2):102-14.
2.   Smits A, Annaert P, Van Cruchten S, et al. A Physiology-Based Pharmacokinetic Framework to Support Drug Development and Dose Precision During Therapeutic Hypothermia in Neonates. Front Pharmacol. 2020;11:587-587.
3.   Allegaert K, Smits A, Simons S, et al. Perspectives in Neonatal Pharmacology: Drug Discovery, Knowledge Integration and Structured Prioritization. Curr Pharm Des. 2018;24(41):4839-4841.
4.   Fernandez E, Perez R, Hernandez A, et al. Factors and Mechanisms for Pharmacokinetic Differences between Pediatric Population and Adults. Pharmaceutics. 2011 Feb 7;3(1):53-72.
5.   de Zwart LL, Haenen HE, Versantvoort CH, et al. Role of biokinetics in risk assessment of drugs and chemicals in children. Regul Toxicol Pharmacol. 2004 Jun;39(3):282-309.
6.   Kearns GL, Abdel-Rahman SM, Alander SW, et al. Developmental Pharmacology — Drug Disposition, Action, and Therapy in Infants and Children. New England Journal of Medicine. 2003;349(12):1157-1167.
7.   van den Anker J, Reed MD, Allegaert K, et al. Developmental Changes in Pharmacokinetics and Pharmacodynamics. J Clin Pharmacol. 2018 Oct;58 Suppl 10:S10-s25.
8.   Johnson TN, Bonner JJ, Tucker GT, et al. Development and applications of a physiologically-based model of paediatric oral drug absorption. Eur J Pharm Sci. 2018 Mar 30;115:57-67.
9.   Van Peer E, Verbueken E, Saad M, et al. Ontogeny of CYP3A and P-glycoprotein in the liver and the small intestine of the Göttingen minipig: an immunohistochemical evaluation. Basic Clin Pharmacol Toxicol. 2014 May;114(5):387-94.
10.   Kiss M, Mbasu R, Nicolaï J, et al. Ontogeny of Small Intestinal Drug Transporters and Metabolizing Enzymes Based on Targeted Quantitative Proteomics. Drug Metab Dispos. 2021 Dec;49(12):1038-1046.
11.   Allegaert K, van de Velde M, van den Anker J. Neonatal clinical pharmacology. Paediatr Anaesth. 2014 Jan;24(1):30-8.
12.   Ward RM, Benjamin D, Barrett JS, et al. Safety, dosing, and pharmaceutical quality for studies that evaluate medicinal products (including biological products) in neonates. Pediatr Res. 2017 May;81(5):692-711.
13.   Allegaert K, Simons SHP, Tibboel D, et al. Non-maturational covariates for dynamic systems pharmacology models in neonates, infants, and children: Filling the gaps beyond developmental pharmacology. Eur J Pharm Sci. 2017 2017/11//;109S:S27-S31.
14.   Van Peer E, Jacobs F, Snoeys J, et al. In vitro Phase I-and Phase II-drug metabolism in the liver of juvenile and adult Göttingen minipigs. Pharmaceutical research. 2017;34(4):750-764.
15.   Davidson JO, Gonzalez F, Gressens P, et al. Update on mechanisms of the pathophysiology of neonatal encephalopathy. Semin Fetal Neonatal Med. 2021 Oct;26(5):101267.

16. WHO. Levels and trends in child mortality report WHO, News Room, Fact-sheets2021 [04.10.2023]. Available from: https://www.who.int/news-room/fact-sheets/detail/levels-and-trends-in-child-mortality-report-2021

17. Mota-Rojas D, Villanueva-García D, Solimano A, et al. Pathophysiology of Perinatal Asphyxia in Humans and Animal Models. Biomedicines. 2022 Feb 1;10(2).

18. Michniewicz B, Szpecht D, Sowińska A, et al. Biomarkers in newborns with hypoxic-ischemic encephalopathy treated with therapeutic hypothermia. Childs Nerv Syst. 2020 Dec;36(12):2981-2988.

19. Abate BB, Bimerew M, Gebremichael B, et al. Effects of therapeutic hypothermia on death among asphyxiated neonates with hypoxic-ischemic encephalopathy: A systematic review and meta-analysis of randomized control trials. PLoS One. 2021;16(2):e0247229.

20. Sun YJ, Zhang ZY, Fan B, et al. Neuroprotection by Therapeutic Hypothermia. Front Neurosci. 2019;13:586.

21. O'Dea M, Sweetman D, Bonifacio SL, et al. Management of Multi Organ Dysfunction in Neonatal Encephalopathy. Front Pediatr. 2020;8:239.

22. Nestaas E, Walsh BH. Hypothermia and Cardiovascular Instability. Clin Perinatol. 2020 Sep;47(3):575-592.

23. [#a]Leys K, and[#b]Stroe M-S, Annaert P, et al. Pharmacokinetics during therapeutic hypothermia in neonates: from pathophysiology to translational knowledge and physiologically-based pharmacokinetic (PBPK) modeling. Expert Opinion on Drug Metabolism & Toxicology. 2023:1-17.

24. Nestaas E, Skranes JH, Støylen A, et al. The myocardial function during and after whole-body therapeutic hypothermia for hypoxic-ischemic encephalopathy, a cohort study. Early Hum Dev. 2014 May;90(5):247-52.

25. van Wincoop M, de Bijl-Marcus K, Lilien M, et al. Effect of therapeutic hypothermia on renal and myocardial function in asphyxiated (near) term neonates: A systematic review and meta-analysis. PLoS One. 2021;16(2):e0247403.

26. Allegaert K, Salaets T, Ward RM, et al. QTc Intervals Are Prolonged in Late Preterm and Term Neonates during Therapeutic Hypothermia but Normalize Afterwards. Children (Basel). 2021 Dec 8;8(12).

27. Keles E, Wintermark P, Groenendaal F, et al. Serum Creatinine Patterns in Neonates Treated with Therapeutic Hypothermia for Neonatal Encephalopathy. Neonatology. 2022;119(6):686-694.

28. Krzyzanski W, Smits A, Van Den Anker J, et al. Population Model of Serum Creatinine as Time-Dependent Covariate in Neonates. Aaps j. 2021 Jun 17;23(4):86.

29. Brucknerová I, Ujházy E, Dubovický M, et al. Early assessment of the severity of asphyxia in term newborns using parameters of blood count. Interdiscip Toxicol. 2008 Dec;1(3-4):211-3.

30. Muniraman H, Gardner D, Skinner J, et al. Biomarkers of hepatic injury and function in neonatal hypoxic ischemic encephalopathy and with therapeutic hypothermia. Eur J Pediatr. 2017 Oct;176(10):1295-1303.

31. Groenendaal F, De Vooght KM, van Bel F. Blood gas values during hypothermia in asphyxiated term neonates. Pediatrics. 2009 Jan;123(1):170-2.

32. Van Anh TN, Hao TK, Chi NTD, et al. Predictions of Hypoxic-Ischemic Encephalopathy by Umbilical Cord Blood Lactate in Newborns with Birth Asphyxia. Open Access Maced J Med Sci. 2019;7(21):3564-3567.

33. Beach RC, Menzies IS, Clayden GS, et al. Gastrointestinal permeability changes in the preterm neonate. Arch Dis Child. 1982 Feb;57(2):141-5.

34. Hermans T, Carkeek K, Dereymaeker A, et al. Assessing Neurovascular Coupling Using Wavelet Coherence in Neonates with Asphyxia. Adv Exp Med Biol. 2022;1395:183-187.

35. Zhou KQ, McDouall A, Drury PP, et al. Treating Seizures after Hypoxic-Ischemic Encephalopathy-Current Controversies and Future Directions. Int J Mol Sci. 2021 Jul 1;22(13).

36. Annink KV, Franz AR, Derks JB, et al. Allopurinol: Old Drug, New Indication in Neonates? Curr Pharm Des. 2017;23(38):5935-5942.

37. Maiwald CA, Annink KV, Rüdiger M, et al. Effect of allopurinol in addition to hypothermia treatment in neonates for hypoxic-ischemic brain injury on neurocognitive outcome (ALBINO): study protocol of a blinded randomized placebo-controlled parallel group multicenter trial for superiority (phase III). BMC Pediatr. 2019 Jun 27;19(1):210.

38. Favié LMA, Peeters-Scholte C, Bakker A, et al. Pharmacokinetics and short-term safety of the selective NOS inhibitor 2-iminobiotin in asphyxiated neonates treated with therapeutic hypothermia. Pediatr Res. 2020 Mar;87(4):689-696.

39. Wu YW, Comstock BA, Gonzalez FF, et al. Trial of Erythropoietin for Hypoxic-Ischemic Encephalopathy in Newborns. N Engl J Med. 2022 Jul 14;387(2):148-159.

40. Greco P, Nencini G, Piva I, et al. Pathophysiology of hypoxic-ischemic encephalopathy: a review of the past and a view on the future. Acta Neurol Belg. 2020 Apr;120(2):277-288.

41. Allen KA, Brandon DH. Hypoxic Ischemic Encephalopathy: Pathophysiology and Experimental Treatments. Newborn Infant Nurs Rev. 2011 Sep 1;11(3):125-133.

42. Yenari MA, Han HS. Neuroprotective mechanisms of hypothermia in brain ischaemia. Nat Rev Neurosci. 2012 Feb 22;13(4):267-78.

43. Kurisu K, Kim JY, You J, et al. Therapeutic Hypothermia and Neuroprotection in Acute Neurological Disease. Curr Med Chem. 2019;26(29):5430-5455.

44. Kim NN, Parker RM, Weinbauer GF, et al. Points to Consider in Designing and Conducting Juvenile Toxicology Studies. International Journal of Toxicology. 2017 2017/07/01;36(4):325-339.

45. Ayuso M, Buyssens L, Stroe M, et al. The Neonatal and Juvenile Pig in Pediatric Drug Discovery and Development. Pharmaceutics. 2021;13(1):44.

46. Ellegaard L, Cunningham A, Edwards S, et al. Welfare of the minipig with special reference to use in regulatory toxicology studies. Journal of Pharmacological and Toxicological Methods. 2010 2010/11/01/;62(3):167-183.

47. Sykes M. Developing pig-to-human organ transplants. Science. 2022 Oct 14;378(6616):135-136.

48. Kalla D, Kind A, Schnieke A. Genetically Engineered Pigs to Study Cancer. Int J Mol Sci. 2020 Jan 13;21(2).

49. Flisikowska T, Kind A, Schnieke A. Pigs as models of human cancers. Theriogenology. 2016 2016/07/01/;86(1):433-437.

50. Morford LL, Bowman CJ, Blanset DL, et al. Preclinical safety evaluations supporting pediatric drug development with biopharmaceuticals: strategy, challenges, current practices. Birth Defects Res B Dev Reprod Toxicol. 2011 Aug;92(4):359-80.

51. Bode G, Clausing P, Gervais F, et al. The utility of the minipig as an animal model in regulatory toxicology. J Pharmacol Toxicol Methods. 2010 Nov-Dec;62(3):196-220.

52. Köhn F. History and development of miniature, micro-and minipigs. The minipig in biomedical research. 2011:3-16.

53. Swindle MM, Makin A, Herron AJ, et al. Swine as models in biomedical research and toxicology testing. Vet Pathol. 2012 Mar;49(2):344-56.

54. Helke KL, Swindle MM. Animal models of toxicology testing: the role of pigs. Expert Opin Drug Metab Toxicol. 2013 Feb;9(2):127-39.

55. Puccinelli E, Gervasi P, Longo V. Xenobiotic Metabolizing Cytochrome P450 in Pig, a Promising Animal Model. Current drug metabolism. 2011 04/08;12:507-25.

56. Heckel T, Schmucki R, Berrera M, et al. Functional analysis and transcriptional output of the Göttingen minipig genome. BMC Genomics. 2015;16:932-932.

57. Buyssens L, De Clerck L, Schelstraete W, et al. Hepatic Cytochrome P450 Abundance and Activity in the Developing and Adult Göttingen Minipig: Pivotal Data for PBPK Modeling. Front Pharmacol. 2021;12:665644.

58. Van Peer E, Downes N, Casteleyn C, et al. Organ data from the developing Göttingen minipig: first steps towards a juvenile PBPK model. Journal of pharmacokinetics and pharmacodynamics. 2016;43:179-190.

59. Le Bars G, Dion S, Gauthier B, et al. Oral toxicity of Miglyol 812(®) in the Göttingen(®) minipig. Regul Toxicol Pharmacol. 2015 Dec;73(3):930-7.

60. Stroe M-S, Van Bockstal L, Valenzuela AP, et al. Development of a neonatal Göttingen Minipig model for dose precision in perinatal asphyxia: technical opportunities, challenges, and potential further steps [Methods]. Front Pediatr. 2023;11:662.

61. Langthaler K, Jones CR, Christensen RB, et al. Characterisation of intravenous pharmacokinetics in Göttingen minipig and clearance prediction using established in vitro to in vivo extrapolation methodologies. Xenobiotica. 2022 Jun;52(6):591-607.

62. Ding N, Yamamoto S, Chisaki I, et al. Utility of Göttingen minipigs for the prediction of human pharmacokinetic profiles after intravenous drug administration. Drug Metab Pharmacokinet. 2021 Dec;41:100408.

63. Dame MK, Paruchuri T, DaSilva M, et al. The Göttingen minipig for assessment of retinoid efficacy in the skin: comparison of results from topically treated animals with results from organ-cultured skin. In Vitro Cell Dev Biol Anim. 2009 Oct;45(9):551-7.

64. Koch W, Windt H, Walles M, et al. Inhalation studies with the Göttingen minipig. Inhal Toxicol. 2001 Mar;13(3):249-59.

65. Swindle MM. Swine in the laboratory: surgery, anesthesia, imaging, and experimental techniques. CRC press; 2007.

66. Pearson N, Boiczyk GM, Kote VB, et al. A Strain Rate-Dependent Constitutive Model for Göttingen Minipig Cerebral Arteries. J Biomech Eng. 2022 Aug 1;144(8).

67. Stubhan M, Markert M, Mayer K, et al. Evaluation of cardiovascular and ECG parameters in the normal, freely moving Göttingen Minipig. J Pharmacol Toxicol Methods. 2008 May-Jun;57(3):202-11.

68. Schuleri KH, Boyle AJ, Centola M, et al. The adult Göttingen minipig as a model for chronic heart failure after myocardial infarction: focus on cardiovascular imaging and regenerative therapies. Comp Med. 2008 Dec;58(6):568-79.

69. Basu D, Bornfeldt KE. Hypertriglyceridemia and Atherosclerosis: Using Human Research to Guide Mechanistic Studies in Animal Models. Front Endocrinol (Lausanne). 2020;11:504.

70. Sharp TE, 3rd, Scarborough AL, Li Z, et al. Novel Göttingen Miniswine Model of Heart Failure With Preserved Ejection Fraction Integrating Multiple Comorbidities. JACC Basic Transl Sci. 2021 Feb;6(2):154-170.

71. van der Staay FJ, Pouzet B, Mahieu M, et al. The d-amphetamine-treated Göttingen miniature pig: an animal model for assessing behavioral effects of antipsychotics. Psychopharmacology. 2009 2009/11/01;206(4):715-729.

72. Meijs S, Schmelz M, Meilin S, et al. A systematic review of porcine models in translational pain research. Lab Anim (NY). 2021 Nov;50(11):313-326.

73. Musskopf ML, Finger Stadler A, Wikesjö UME, et al. The minipig intraoral dental implant model: A systematic review and meta-analysis. PLOS ONE. 2022;17(2):e0264475.

74. Larsen MO, Rolin B. Use of the Göttingen minipig as a model of diabetes, with special focus on type 1 diabetes research. Ilar j. 2004;45(3):303-13.

75. Renner S, Blutke A, Dobenecker B, et al. Metabolic syndrome and extensive adipose tissue inflammation in morbidly obese Göttingen minipigs. Mol Metab. 2018 Oct;16:180-190.

76. Eirefelt S, Stahlhut M, Svitacheva N, et al. Characterization of a novel non-steroidal glucocorticoid receptor agonist optimized for topical treatment. Scientific Reports. 2022 2022/01/27;12(1):1501.

77. Eisler W, Baur J-O, Held M, et al. Assessment of Two Commonly used Dermal Regeneration Templates in a Swine Model without Skin Grafting. Applied Sciences. 2022;12(6):3205.

78. Singh VK, Thrall KD, Hauer-Jensen M. Minipigs as models in drug discovery. Expert Opin Drug Discov. 2016 Dec;11(12):1131-1134.

79. Stricker-Krongrad A, Shoemake CR, Pereira ME, et al. Miniature Swine Breeds in Toxicology and Drug Safety Assessments: What to Expect during Clinical and Pathology Evaluations. Toxicologic Pathology. 2015 2016/04/01;44(3):421-427.

80. Yang X, Morris SM, Gearhart JM, et al. Development of a physiologically based model to describe the pharmacokinetics of methylphenidate in juvenile and adult humans and nonhuman primates. PLoS One. 2014;9(9):e106101.

81. Schneckener S, Preuss TG, Kuepfer L, et al. A workflow to build PBTK models for novel species. Archives of Toxicology. 2020 2020/11/01;94(11):3847-3860.

82. Van Peer E, De Bock L, Boussery K, et al. Age-related Differences in CYP3A Abundance and Activity in the Liver of the Göttingen Minipig. Basic Clin Pharmacol Toxicol. 2015 Nov;117(5):350-7.

83. Suenderhauf C, Parrott N. A physiologically based pharmacokinetic model of the minipig: data compilation and model implementation. Pharmaceutical research. 2013;30(1):1-15.

84. Suenderhauf C, Tuffin G, Lorentsen H, et al. Pharmacokinetics of paracetamol in Göttingen minipigs: in vivo studies and modeling to elucidate physiological determinants of absorption. Pharmaceutical research. 2014;31:2696-2707.

CHAPTER 2:
Study aims and outline

Study aims and outline

Therapeutic hypothermia (TH) represents the standard of care for neonates with perinatal asphyxia (PA) and moderate to severe hypoxic-ischemic encephalopathy (HIE). To support drug development for this population, knowledge from clinical observations (pharmacokinetic (PK) and real-world data on physiology), preclinical (in vitro and in vivo animal model) data, and molecular and cellular biology insights can be incorporated into a physiologically-based pharmacokinetic (PBPK) model to serve as an integrative predictive modeling approach. This study hypothesized that systemic hypoxia, as well as TH, affect drug disposition. Given the effects of TH and PA on physiology, our primary hypothesis was that TH significantly decreases the metabolic clearance in asphyxiated neonates, requiring adjustments in drug dosing. We further hypothesized that PA and TH affect enzyme functionality, including gene and protein expression as well as enzymatic activities. A neonatal Göttingen Minipig model was developed to study these effects. Lastly, integrating these data, the optimized PBPK model will be a reliable tool to accurately predict drug exposure in asphyxiated neonates undergoing TH.

Chapter 1 introduces notions about neonatal drug disposition. The pathophysiological characteristics of system-specific functions in asphyxiated neonates and TH are further summarized. Since, animal models (e.g., Göttingen Minipig model) can provide useful information on pediatric drug discovery and development, these are covered in this chapter. After stating the aims of this thesis in **Chapter 2**, the methods and results are structured in **Chapters 3, 4, 5, and 6** reflecting the objectives: (1) the development of a neonatal Göttingen Minipig model for dose precision in PA together with the exploration of a conventional piglet hypoxia model, highlighting the importance of pilot studies (**Chapter 3**), (2) to unravel the impacts of hypoxia and TH on PK of 4 model drugs (**Chapter 4**), along with (3) assessing the effects of these two covariates on gene expression, protein abundance, and activity of major hepatic drug-metabolizing enzymes (DMEs) (**Chapter 5**), and finally, (4) to develop an pilot neonatal Göttingen Minipig PBPK model, as presented in **Chapter 6**, incorporating literature findings and data resulting from the I-PREDICT project (Figure 1).

Figure 1. The I-PREDICT project aims to improve dosage recommendation for drugs in neonates with perinatal asphyxia (PA) treated with therapeutic hypothermia (TH), by developing a physiologically-based pharmacokinetic (PBPK) model, combining preclinical (in vitro and animal data) and clinical data. Pharmacokinetic predictions of 4 model drugs (i.e., midazolam, fentanyl, phenobarbital, and topiramate) are investigated. The figure was reproduced from Leys K and Stroe M-S, et al. Created with BioRender.com.

* 1-Hydroxymidazolam (1-HMDZ); cytochrome P450 (CYP); midazolam (MDZ); physiologically-based pharmacokinetics (PBPK); pharmacokinetic (PK); temperature (T°).

TH: cooling core body T° to 33.5°C for 72 h

Perinatal asphyxia

Decreased body T° slows metabolic rate, preventing further brain damage

Better dosage recommendations

PBPK cooling model as an integrative predictive model in neonates

Venous blood

Arterial blood

Investigation of effect cooling and asphyxia on PK in the neonatal Göttingen Minipig

Phase I CYP enzymes

In vitro profiling of the effect of T° on
- gene expression
- protein abundance
- enzyme activity

Add-on pharmacotherapy: midazolam, phenobarbital, topiramate and fentanyl

- MDZ (ng mL^{-1})
- 1 H-MDZ (ng mL^{-1})

Time (h)

Change in PK during TH following PA?

Chapter 7 provides the general discussion of this thesis containing three key aspects: (1) a comparative analysis of conventional pigs versus the neonatal Göttingen Minipig model developed for PA, (2) an examination of various pharmacological strategies applicable to asphyxiated neonates undergoing TH and (3) future prospects on (neonatal) Göttingen Minipig PBPK modelling. **Chapter 8**, the final section of this thesis, reiterates the challenges and limitations encountered during this study and provides insights into future perspectives. Additionally, this chapter incorporates the outcomes of a Short-Term Scientific Mission (STSM) conducted as part of the European Cooperation in Science & Technology (COST) action titled "Maximizing Impact of Multidisciplinary Research in Early Diagnosis of Neonatal Brain Injury (AI-4-NICU)".

CHAPTER 3:
Development of a neonatal Göttingen Minipig model for dose precision in perinatal asphyxia

Development of a neonatal Göttingen Minipig model for dose precision in perinatal asphyxia

Abstract

Animal models are instrumental in understanding the mechanisms of human diseases, but also on exploring (patho)physiological factors affecting pharmacokinetics (PK) of drugs. For perinatal asphyxia (PA), a condition defined by oxygen deprivation in the perinatal period and possibly resulting in hypoxic-ischemic encephalopathy (HIE), therapeutic hypothermia (TH) together with symptomatic drug therapy, is the standard approach to reduce death and permanent brain damage. However, the impact of the systemic hypoxia during PA and/or TH on drug disposition is largely unknown. An animal model can provide useful information on these factors that cannot be assessed separately in patients. While the conventional pig is recognized for its relevance to PA, it is not used by pharmaceutical companies to develop new drug therapies. Instead, the Göttingen Minipig is the commonly used pig strain in nonclinical drug development. Therefore, the aim of this research was to develop the neonatal Göttingen Minipig model for dose precision in PA. The study involved 24 healthy male Göttingen Minipigs, within 24 hours of partus, weighing approximately 0.45-0.6 kg. These animals were instrumented for mechanical ventilation and multiple vascular catheters were inserted for maintenance infusion, drug administration and blood sampling. After premedication and induction of anesthesia, hypoxia was performed by ventilating them with a low-oxygen gas mixture. Blood gas analysis was used to determine the duration of the systemic hypoxic insult, to approximately 1 hour. Additionally, 4 drugs, with different physicochemical properties, PK characteristics and clinical relevance, were administered: midazolam (intermediate extraction ratio (ER)), fentanyl (high ER), phenobarbital (low ER) and topiramate (primarily renally excreted unchanged; explored as a potential neuroprotective drug when administered orally). This research aimed to establish the neonatal Göttingen Minipig model for dose precision in PA, allowing to separately study the effect of systemic hypoxia versus TH on drug disposition. The study demonstrated that the anatomy and physiology of neonatal Göttingen Minipigs are compatible with mechanical ventilation and multiple vascular access, in a 24-hour non-survival experimental setup, mimicking the clinical situation. Central venous catheterization proved to be the best method for vascular access. Peripheral catheterization was easiest in the epigastric vein. Finally, in this study we showed that systemic hypoxia could be induced in neonatal Göttingen Minipigs by ventilating with low-oxygen gas mixture. This is relevant information for laboratories using the neonatal Göttingen Minipig for other disease conditions or drug safety testing.

1. Introduction

Pigs are large animal models used in translational research, due to their anatomical, physiological, and biochemical similarities to humans [1,2]. Especially, for drug and food safety testing in the (very young) pediatric population the neonatal pig is considered a good model by regulatory bodies [3-5]. Also, for understanding the mechanisms of disease models in neonates, the neonatal pig can provide useful information. An example is the investigation of the pathophysiology of perinatal asphyxia (PA) in neonatal conventional piglets [6-8]. The neonatal conventional piglet has been very valuable in better understanding the impact and outcome of this condition in patients. However, less is known on the impact of PA versus therapeutic hypothermia (TH), which is the standard approach together with drug therapy, on drug disposition in these patients. The conventional pig is not used by pharmaceutical companies for drug discovery or development. Conversely, the Göttingen Minipig is the pig strain preferred by the pharmaceutical industry, as they are genetically coherent and well-characterized, and by using the same strain, pharmaceutical companies can rely on historical control data when interpreting findings in drug safety studies [9]. Minipigs have already been used as animal models for several clinical indications such as cardiovascular [10], dental conditions [11], diabetes [12], heart disease [13], skin conditions [14,15], and acute and chronic intestinal inflammation [2,16]. Furthermore, the neonatal Göttingen Minipig shares a striking number of developmental similarities with human neonates [17-21].

As the conventional pig is a well-established model for PA and the Göttingen Minipig is the preferred strain by the pharmaceutical industry, this latter strain provides opportunities for dose precision and potential new drug therapies in PA patients. This project aimed to develop a neonatal Göttingen Minipig model in a neonatal intensive care unit (NICU) -like setup, to separately study the effect of the systemic hypoxia versus TH on drug disposition. In this chapter, the complete setup of the neonatal Göttingen Minipig model for PA/TH, with a primary focus on addressing the challenges related to anesthesia, ventilation, and instrumentation, is presented aiming to optimize the procedures for reliable experimental outcomes.

2. Materials and equipment

2.1. Medication

The neonatal Göttingen Minipig groups and their therapeutic interventions are depicted in Figure 1. Fentanyl, midazolam, phenobarbital and topiramate were selected as model drugs based on their different physicochemical and/or pharmacokinetic (PK) characteristics and clinical relevance: fentanyl (cytochrome P450 (CYP) 3A4; high extraction ratio (ER)); midazolam (CYP3A4; intermediate ER), phenobarbital (CYP2C19; low ER), and topiramate (largely renally excreted unchanged). Fentanyl is a full μ opioid agonist, with more profound analgesic effects than morphine (100-fold more potent). The most common indications are pain management and anesthesia. Fentanyl can produce unconsciousness but is accompanied by significant adverse effects such as profound respiratory depression, bradycardia and/or hypotension [22]. Midazolam is one of the most used benzodiazepines for premedication and a co-induction agent with ketamine, propofol, or alfaxalone. It acts mainly as a sedative, through a depression of the limbic system, without analgesic properties. Additionally, it is used

to manage convulsions [23]. Phenobarbital is a barbiturate used primarily to manage convulsions, without having intrinsic analgesic activity. The anticonvulsive properties of phenobarbital are particularly useful because they tend to provide sufficient motor activity depression, without causing excessive sedation [24]. Lastly, topiramate is neuroprotective for hypoxia, ischemia, and convulsions in preclinical models [25].

Figure 1. Neonatal Göttingen Minipig groups and the therapeutic interventions. 4 conditions i.e., hypoxia, therapeutic hypothermia, hypoxia and therapeutic hypothermia and controls, with 6 piglets per condition (n=6), were investigated. * Degree Celsius (°C); hour (h); intramuscular (IM); minute (min); constant rate infusion (CRI); intravenous (IV); total parenteral nutrition (TPN).

Control (n=6): Normothermia (38 - 39.5 °C) + Normoxia (21% Oxygen)

Therapeutic hypothermia (n=6): Cooling treatment (33.5°C) + Normoxia (21% Oxygen)

Hypoxia (n=6): Hypoxia (15% Oxygen for ~1h) + Normothermia (38 - 39.5 °C)

Hypoxia + Hypothermia (n=6): (15% Oxygen for ~1h) + Cooling treatment (33.5°C)

Add-on drug treatment:

Premedication
➤ Tiletamine/zolazepam 4 mg/kg IM

Induction
➤ Isoflurane 3% in Oxygen, via face mask, 10 min

CRI
➤ Fentanyl 10 µg/kg/h IV
➤ Midazolam 0.4 mg/kg/h IV
➤ TPN 2-3 ml/kg/h IV

Loading dose
➤ Fentanyl 3 µg/kg IV
➤ Midazolam 0.3 mg/kg IV

Bolus
➤ Phenobarbital 20 mg/kg IV
➤ Topiramate 20 mg/kg IV

Bradycardia/Hypotension
➤ Atropine 0.05-0.1 mg/kg IV

2.2. Monitoring equipment

The heart rate via electrocardiogram (ECG), the fraction of oxygen-saturated hemoglobin (SpO_2) via pulse oximetry, end-tidal carbon dioxide ($EtCO_2$) and respiratory rate via capnograph, non-invasive blood pressure via blood pressure cuffs (size 1, 3-6 cm, orange fish, 98-0400-80-VET, Suntech Blood Pressure Cuffs), most reliable on radial and medial saphenous arteries, and rectal body temperature were assessed continuously using a multiparameter monitor (MONITOR uMEC12 Vet, Mindray Animal Medical). Mechanical ventilation (ADS 2000 Ventilator Machine), using a pediatric rebreathing circuit, was started immediately after intubation, using a pressure-controlled ventilation mode with a pre-set initial peak inspiratory pressure of 11-15 cm H_2O, leading to a tidal volume of 10 mL/kg, a respiratory rate varying from 15 to 30 breaths per minute, and inspiratory-to-expiratory ratio of 1-to-2 in order to

maintain an EtCO$_2$ between 35 to 45 mmHg. The most important materials and devices that were used are listed in Table 1.

Table 1. List of the most important materials and equipment necessary for the neonatal Göttingen Minipig model development.

Name	Company	Catalog Number	Comments
Doppler Vet BP with 1 probe	-	8289081	-
Blood Pressure Cuffs	Suntech	98-0400-80-VET	Size 1, 3-6 cm, orange fish
MONITOR uMEC12 Vet	Mindray Animal Medical	10004054	-
ADS 2000 Ventilator Machine	Engler Engineering Corporation	-	-
Uncuffed ETT, Mallinckrodt	Covidien	86233	2.5 mm I.D., 3.6 mm O.D.
Hydro-Therm™ Heat and Moisture Exchange (HME) Filter	Intersurgical	1442000	-
BD Microtainer® tube BD Microgard™ closure collections	BD	365974	K2EDTA, Closure Color Lavender
Vamin® 18gN/l Electrolyte-free	Fresenius Kabi	065201	-
Glucose 20%	Baxter B.V.	-	-
Intralipid® Caloric Agent Fat Emulsion 20% IV Solution Flexible Bag 500 mL	Fresenius Kabi, Baxter B.V.	12352211	Lipid Injectable Emulsion, Mfr. Std. Soybean Oil 20%
Vasofix® Safety IV Catheter	Braun	4269075	24 G (Yellow)
Venflon™ IV Catheter	BD	391451	22 G (Blue)
Discofix® three-way tap	Braun	48919458	-
Original Perfusor Line	Braun	8722870N	75 cm, 0.8 ml/m
(Arterial) Leader Catheter	Vygon	115090	3Fr, 8 cm, 24 ml/min
Single-lumen Umbilical (arterial) Catheter	Vygon	1270.02	PUR, 2.5 Fr, 30 cm, >3 ml/min
Animal Polster	Snögg	12116	Foam Dressing with Adhesive, 9cm x2m x5mm
Vicryl 4-0	Ethicon	329-8946	-
i-STAT® Alinity V	Abbott Point of Care	-	Point of Care Blood Gas analysis device

i-STAT® Alinity V CG4+ cartridge	Abbott Point of Care	10023271	-
Accutrend® Plus System	Roche	4015630056170 /5050499171	Lactate Meter
Accutrend® Lactate Strips	Roche	4015630004690	-
Gas Mix (15% oxygen, 85% nitrogen)	Nippon Gases, Denmark	-	On special order
WH underbed blanket	OK	OUB 60321	Heating blanket
Contour® XT	Ascensia Diabetes Care NV/SA	-	Blood Glucose Monitoring System

Figure 2. Overview of the surgery room at Ellegaard Göttingen Minipigs A/S, Dalmose, Denmark, featuring key materials and anesthesia equipment essential for developing the neonatal Göttingen Minipig model. * Intravenous (IV).

3. Methods

3.1. Experimental design and preanesthetic considerations

This study was conducted at Ellegaard Göttingen Minipigs A/S, Dalmose, Denmark (Figure 2), under Danish Ethical approval. All subjects were anesthetized throughout the entire procedure. Reproduction of this protocol had to be carried out in accordance with the national ethics and animal welfare guidelines and approved by local ethical committees. 4 conditions i.e., hypoxia (group H), therapeutic hypothermia (group TH), hypoxia + therapeutic hypothermia (group H+TH) and controls (group C), with 6 piglets per condition, were investigated. A power analysis was performed to determine the correct sample size. This was based on the standard deviation (SD) of dexmedetomidine clearance, from Ezzati et al. [8]. Using the clearance as the outcome variable for the 4 conditions, 6 piglets per condition are required to detect a 50% reduced clearance, as reported for dexmedetomidine [8], for the H+TH compared to controls (power of 80%; test-wise significance level of 0.05). Further, the procedures within 24 hours are detailed. These were repeated until the achievement of the total number of subjects (24 Göttingen Minipigs) required for the study. While accomplishing prolonged anesthesia, physiological parameters were recorded in individual anesthetic charts, every 10 minutes. Preanesthetic considerations, general risk factors, and optimization tracks, are presented in the study design algorithm depicted in Figure 3.

Neonatal male Göttingen Minipigs, weighing approximately 0.45-0.6 kg, coming from different litters were selected in the animal facility at Ellegaard Göttingen Minipigs A/S and immediately transferred to the adjacent operating room. They were clinically healthy, had suckled sufficient colostrum, received no iron injection and were not older than 24 hours. At arrival, they were accurately weighed and clinically checked. Animals were excluded in case of cardiac or respiratory decompensation at the thoracic auscultation and inspection, signs of hypoxia such as cyanosis, dyspnea with hyperventilation at visual inspection, rectal temperature below the neonatal pig thermal homeostasis threshold (38-39 °C) [26], congenital anomalies, or in case of a weight < 0.4 kg, considered too small for instrumentation.

Figure 3. Neonatal Göttingen Minipig study design algorithm. Preanesthetic considerations, with inclusion and exclusion criteria, general risk factors, and optimization (orange box) are depicted. This algorithm emphasizes the importance of planning and preparation in the development of the neonatal Göttingen Minipig asphyxia model. * hour (h); degree Celsius (°C); oxygen (O_2); inspiratory oxygen fraction (FiO_2); minute (min).
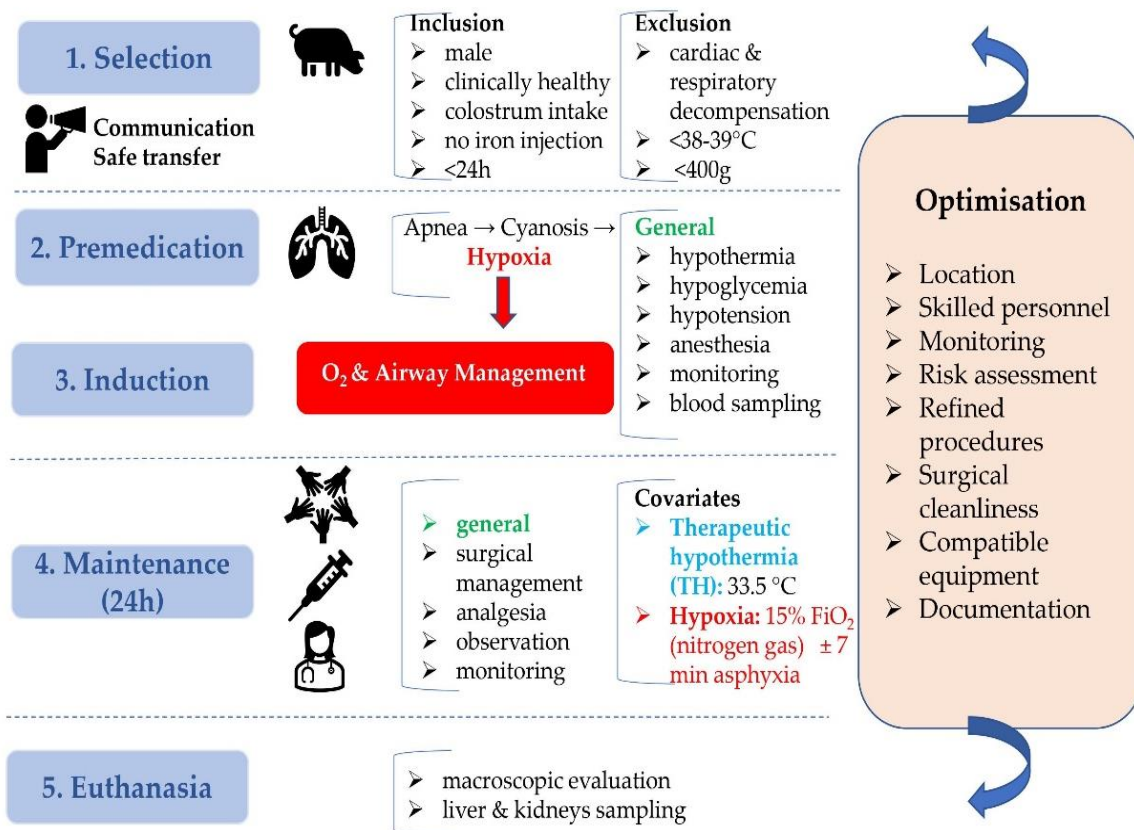
3.2. Anesthesia

The neonatal Göttingen Minipigs were premedicated intramuscularly (IM), with tiletamine/zolazepam (Zoletil® 50, Virbac), at 4 mg/kg. Zolazepam is a short-acting benzodiazepine derivative, with tranquilizing properties, available only in combination with tiletamine, a dissociative anesthetic and somatic analgesic [23]. This combination is routinely used IM in various animal species, including pigs, as part of research studies, to induce short-term anesthesia for surgical purposes and for immobilization [27]. This preparation was decided for premedication over alfaxalone (Alfaxan Multidose, Jurox), 5 mg/kg. Alfaxalone, a neuroactive steroid molecule [22], has already been documented to produce satisfactory induction and maintenance of anesthesia with minimal cardiovascular side effects in pigs [28]. Induction of anesthesia (Figure 4) was performed with isoflurane (IsoFlo®, Zoetis) 3% in oxygen, via face mask, for 10 minutes. If the jaws were relaxed and the palpebral reflex absent, intubation was achieved while placing the piglets in prone position, using uncuffed endotracheal tubes (ETT, Mallinckrodt, Covidien, 2.5 mm I.D. (internal diameter), 3.6 mm O.D. (outer diameter), 86233) and two laces on the upper and inferior jaws. Desensitization with Xylocaine® 10% spray, (AstraZeneca) was performed 30 seconds prior to intubation. Premeasuring and shortening the ETT for an acceptable length, as well as the use of a laryngoscope to visualize and displace the epiglottis from the soft palate, were crucial steps for optimal intubation. The ocular surface was kept moistened by applying Opticorn A (Ecupharm). An overview of the required materials during anesthesia induction is depicted in Figure 5.

Fentanyl (Fentadon®, Dechra), at 10 µg/kg/h, and midazolam (Midazolam, Accord®), at 0.4 mg/kg/h, were mixed in one syringe and administered intravenously (IV), at a constant rate infusion (CRI) of 2 mL/h. Additionally, a loading dose of fentanyl, at 3 µg/kg, and midazolam, at 0.3 mg/kg, were administered at the start of the CRI. After 2 hours from the start of the infusion and subsequently after 12 hours, the other two drugs from the study, phenobarbital (Luminal®, Desitin) and topiramate (10 mg/mL, Cas no 97240-79-4, Polpharma, solubilized in cyclodextrin matrix, Captisol®, Ligand Pharmaceuticals [25,29-31]), both at 20 mg/kg, were slowly and separately administered IV, with a 15 minutes delay in between administrations. Total parenteral nutrition (TPN) IV, CRI, followed by close monitoring of glucose status, at the start of the anesthesia and 12 hours later, was performed. The animals received 217 kj/kg/day, representing 50% of the total energetic requirement in neonatal conventional piglets (550 kj/kg/day), from which 8 g/kg/day amino acids (Vamin Fresenius Kabi, Nederland B.V.), glucose 20% (Baxter B.V.) and lipids (INTRALIPID® Fresenius Kabi, Lipid Injectable Emulsion, Mfr. Std. Soybean Oil 20%). The total infusion intake within a day, considering the dilution of drugs and TPN, was 6 mL/kg/h.

Figure 4. The induction of anesthesia was initiated with isoflurane using an anesthetic face mask **(A)**, followed by endotracheal intubation carried out using a laryngoscope **(B)**.

Figure 5. Overview of the required materials during anesthesia induction. * Central venous catheter (CVC).
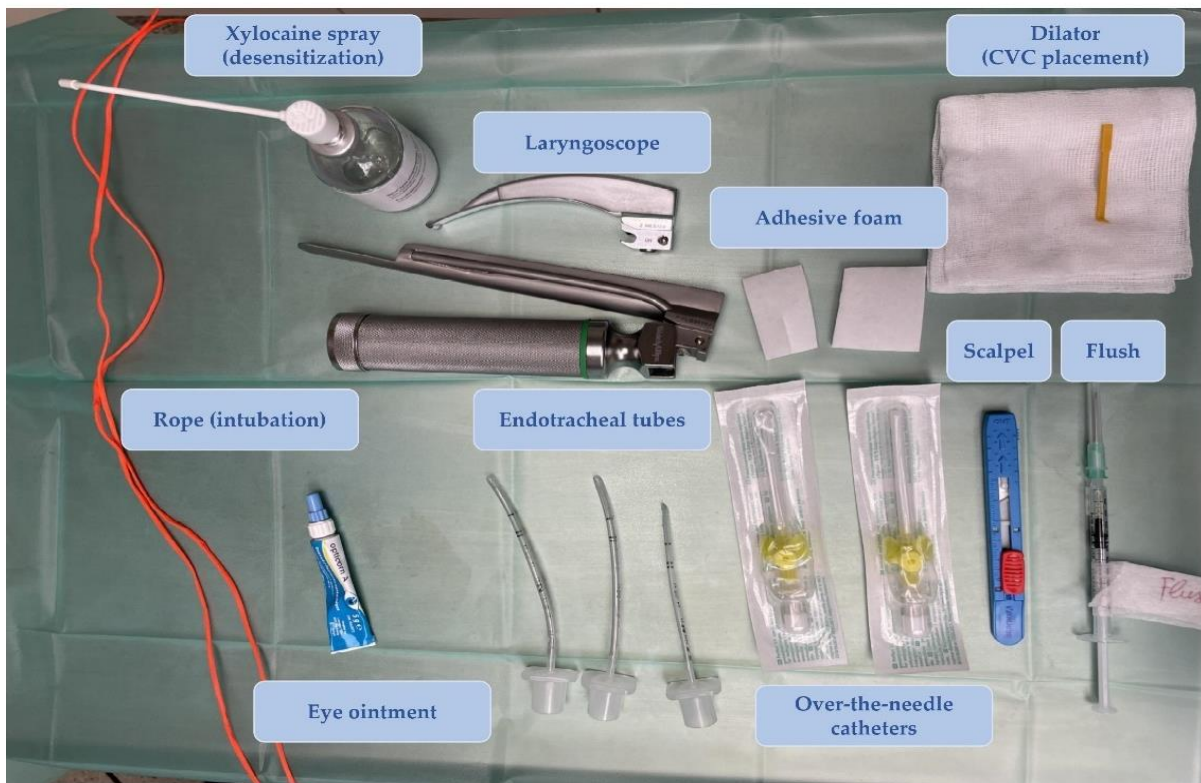
3.3. Vascular access and body fluids sampling

Central venous catheterization, more specifically of the external jugular vein or the junction of external and internal jugular veins [32], was ensured following aseptic procedures, using the modified Seldinger technique [33,34], while the piglets were positioned in dorsal recumbency. Since the vessels lay deep and are not visible, making the percutaneous technique [35] very challenging, we adapted the approach to a surgical one (Figure 6). To avoid the contamination of the blood sample with the drugs, this catheter was used exclusively for blood sampling.

Figure 6. Jugular vein catheterization via modified Seldinger technique in the neonatal Göttingen Minipig **(A)** incision of the skin in the neck region followed by dissection of the jugular vein, **(B)** passing one suture thread under the vein for better manipulation of the vessel and control of the bleeding, **(C)** puncture of the jugular vein with an over-the-needle catheter (BD Venflon™, 22 G, 391451), **(D)** pre-measure the final catheter (Arterial Leader Catheter, Vygon, 3Fr, 8 cm, 24 mL/min, 115090), **(E)** advance the round-tipped guide wire through the lumen of the over-the-needle catheter into the vessel and subsequently withdraw the over-the-needle catheter, **(F)** the final catheter can now be passed over the guide wire and inserted into the vessel to the required length; after that, the guide wire is withdrawn, the catheter is flushed and the skin is closed (Vicryl 4-0, Ethicon). For more stability, one extra suture can be used to restrain the catheter to the surrounding conjunctive tissue before closing the skin.
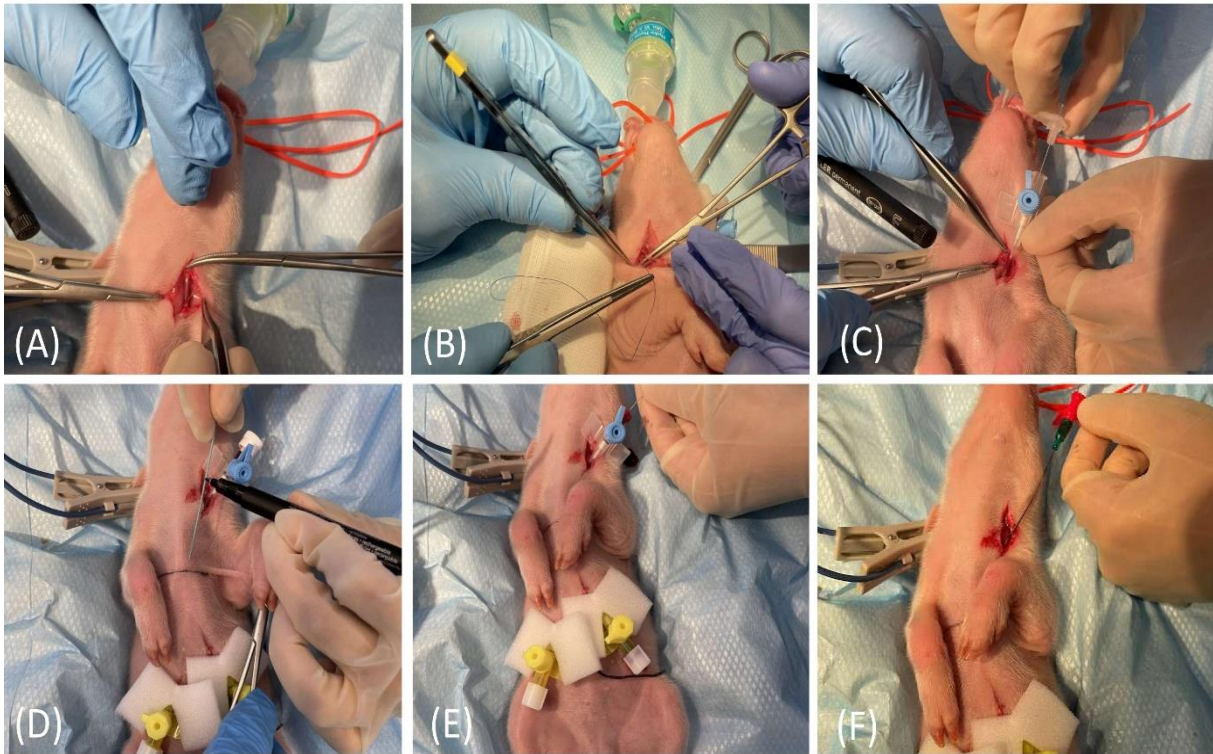
Additionally, for drug administration, two other catheters were placed: either two peripheral catheters or one peripheral and one central. The cranial superficial epigastric vein, also called the milk vein or subcutaneous abdominal vein, was documented for blood collection and fluid administration in adult conventional pigs [36] and Potbellied pigs [37]. The vein lies on the ventral portion of the abdomen, dorsolateral to the mammary chain [37]. The epigastric vein was visible in the neonatal Göttingen Minipig when placed in dorsal recumbency. An over-the-needle catheter (Figure 7, Vasofix® Safety IV Catheter, 24 G, 4269075) was inserted where the vein is most detectable, in a cranial direction, just lateral to the first and second teat. However, due to the lack of tonicity and thick skin, that makes difficult to penetrate, a small skin incision was performed before catheterization. The catheter placement was confirmed when a (low) blood flow was visible and was easily flushed. Alternatively, the lateral saphenous vein is a readily accessible vein in pigs [38-40]. Blood flows into the caudal femoral vein and then into the external iliac and caudal vena cava [38]. This was accessed with an over-the-needle catheter (Figure 8, Vasofix® Safety IV Catheter, 24 G, 4269075) in neonatal Göttingen Minipigs, placed in lateral recumbency.

Figure 7. Epigastric vein catheterization in the neonatal Göttingen Minipig: after visualization along the ventral portion of the abdomen and dorsolateral to the mammary chain, and aseptic preparation of the skin, **(A)** a small skin incision was performed before **(B)** catheterization with an over-the-needle catheter, followed by confirmation when a (low) blood flow is visible.

Figure 8. Lateral saphenous vein catheterization in the neonatal Göttingen Minipig with an over-the-needle catheter.

When the peripheral catheterization was considered challenging, mostly due to poor visualization, an umbilical venous catheter was placed. Since this catheter has a smaller diameter, a single-lumen umbilical catheter (Vygon, Umbilical arterial catheter PUR, 2.5 Fr, 30 cm, >3 mL/min, 1270.02) proved to be compatible (Figure 9).

The blood used for PK was limited to 500 μL per sampling and was withdrawn once pre-drug administration and subsequently 10 times after the drug administration, resulting in a total of 11 samples over the study period in each animal. The drug disposition results, based on the plasma concentrations measured at the different time points, as well as the effects of hypoxia and TH, will be presented in Chapter 4 of this thesis. In addition, a heparinized 1 mL syringe was prepared to draw 100 μL blood, followed by quick transfer into CG4+ i-STAT® Alinity V cartridge. Blood gas analysis was performed using the i-STAT® Alinity V. Urine samples were collected via cystocentesis, at the start of anesthesia, at 12 hours and 24 hours. Before cystocentesis, a quick ultrasound check of the urinary bladder was performed. The entire quantity of urine collected over 24 hours was recorded. Chapter 6 of this thesis will present the urinary output, along with creatinine levels and estimated glomerular filtration rates, in the neonatal Göttingen Minipig groups.

Figure 9. Umbilical venous catheter: after cutting the end of the umbilical cord with a scalpel to get a clean surface, leaving an approximate 0.5 cm overhang above the level of the nipple, **(A)** identify the vessels: the vein is large and thin walled, usually at the 12 o'clock position, while arteries are the two thick-walled, below the vein. Grasp the catheter (Vygon, Single-lumen umbilical arterial catheter, PUR, 2.5 Fr, 30 cm, >3 mL/min, 1270.02) between the thumb and forefinger, or with a forceps, and insert into the lumen of the dilated vein. Place in the inferior vena cava above the level of the diaphragm (between T8 and T9), above the liver. If resistance is met, withdraw slightly, rotate, and reinsert. **(B)** Confirm successful catheterization visually by observing blood return in the catheter or by attaching a syringe and aspirate to see if blood returns and flows easily in the syringe. Tie with suture (Vicryl 4-0, Ethicon) and restrain using the foam dressing with adhesive (Snögg Animal Polster, 9 cm x 2 m x 5 mm) and test the catheter again after fixation by withdrawing blood. Flush the catheter and attach the infusion.
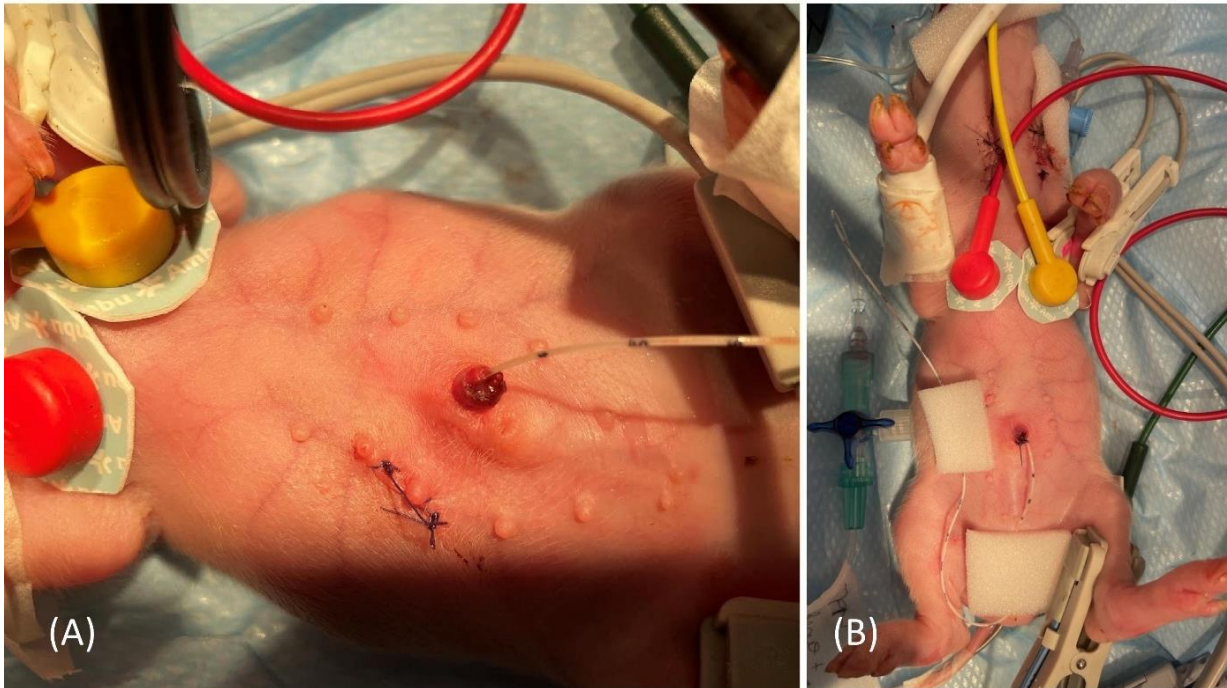
3.4. Hypoxia and therapeutic hypothermia

Using these instrumented Göttingen Minipigs (Figure 10), after stabilization for 30 minutes and determination of the individual blood gas baseline values, the experimental protocol of normocapnic alveolar hypoxia was started. The piglets were continuously monitored and anesthetized, with fentanyl and midazolam CRI, over the entire period of the insult. Hypoxia was induced by ventilation with a gas mixture containing 15% oxygen and 85% nitrogen. During the systemic hypoxic insult, blood gas analysis was performed at 30 minutes and approximately one hour after start. Once the blood lactate increased to the threshold of 8.7-10.7 mmol/L and pH decreased from the individual baseline determined before the insult, hypoxia was terminated targeting 1 hour insult. When the low-oxygen gas mixture ventilation was insufficient to achieve the targeted blood gas parameters, the occlusion of the ETT was performed for 7 minutes, thus adding hypercapnia to the hypoxia. The insult was followed by reoxygenation with 100% oxygen for 30 minutes and then 60% oxygen for the remaining time of the experiment. At the end of the hypoxia protocol, phenobarbital and topiramate were administered as mentioned above. The blood gas values were analyzed descriptively, with arithmetic means and standard deviations calculated to determine threshold values essential for developing the neonatal Göttingen Minipig model for PA, and statistically, to assess the impact of hypoxia on the measured parameters. The statistical analysis was performed in JMP® Pro 16 (SAS Institute Inc., Cary, NC, United States). Normality and homogeneity of variances were tested by the Shapiro-Wilk and Levene's test, respectively. The Student t-test was used to detect hypoxia-related differences between the control and the hypoxic groups and for each blood gas parameter. If assumptions could not be met, a non-parametric Wilcoxon/Kruskal-Wallis (rank sums) test was performed. A $P<0.05$ was considered statistically significant.

Whole body hypothermia was achieved in less than 90 minutes using cold packs and by stopping the heating devices, including infrared lamps, and heating mattresses (OUB 60321

WH underbed blanket, OK), and maintained for 24 hours, at a target rectal temperature of 33.5 °C, in line with the human neonatal target temperature in TH recommendations [41]. For the H+TH group, TH was started immediately after finishing the hypoxic insult.

Figure 10. Review of materials, anesthesia monitoring, and other equipment for the development of the neonatal Göttingen Minipig model for perinatal asphyxia and therapeutic hypothermia **(A)**, along with a detail on one neonatal Göttingen Minipig undergoing the experimental procedures **(B)**.
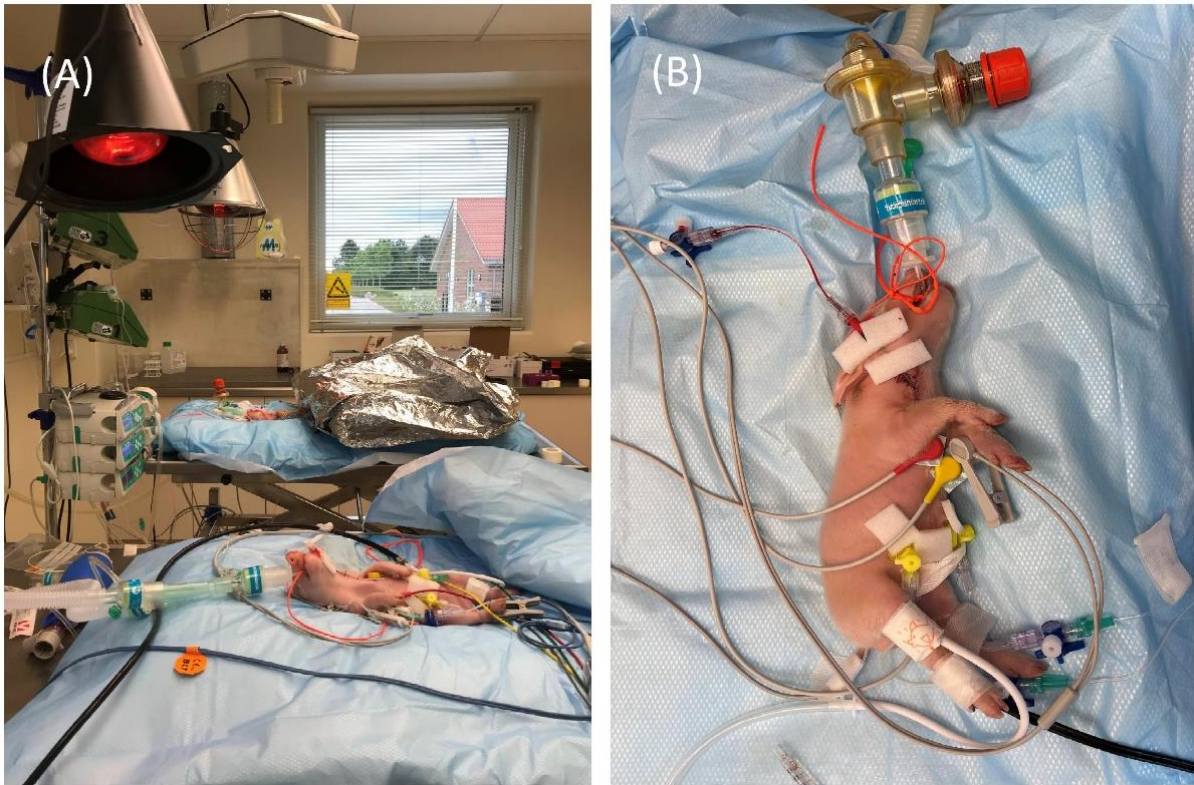
3.5. 24-hours survival

The experiment was ended after 24 hours. However, the intended experimental period was 96 hours, since TH in the NICU covers 72 hours, followed by gradual rewarming and maintenance of 36.5 °C for 24 hours [41]. The rationale for shortening the experimental period to 24 hours will be discussed later. The subjects were euthanized while under anesthesia by IV administration of pentobarbital-Natrium (30 mg/kg). After euthanasia, macroscopic evaluation of the abdominal and thoracic cavities was performed, with particular attention to the presence of effusions, organ macroscopic changes, and the catheters placement. The liver and kidneys were sampled, divided, snap-frozen, and stored at -80 °C for future in vitro investigations, which will be presented in detail in Chapter 5 of this thesis.

4. Results

4.1. Experimental length and subjects

Study procedures were well tolerated in 24 subjects with weight of 0.55 kg (±0.60, mean ±SD), minimum 0.43 and a maximum of 0.66 kg, 6 for each experimental group and for 24 hours.

Only one piglet achieved 48 hours of anesthesia (0.6 kg, group C), this length being the longest accomplished in the neonatal Göttingen Minipigs reported here. Therapeutic hypothermia was uneventful and easy to control by stopping the heating devices and maintaining it for 24 hours, at 33.5 °C. For the H+TH group, the duration was prolonged by approximately 2 hours since the TH started immediately after finishing the approximately 1-hour hypoxic insult and approximately 1-hour of instrumentation and stabilization.

Beside the 24 subjects, 2 other Göttingen Minipigs (group C) accomplished 24 hours of anesthesia. They were excluded because they developed sepsis. The hypotension (mean arterial blood pressure <30 mmHg), tachycardia (>200 beats per minute), hypoglycemia (blood glucose level <40 mg/dL), installed gradually, starting at approximately 12 hours. The experiment was terminated at 24 hours when extrasystoles and tachycardia were noticed on the ECG, as well as no response for the low blood glucose interventions and no urine production. Additionally, low pH (6.87), high partial pressure of carbon dioxide (PCO_2; 17.33 kPa) and a lactate of 1.04 mmol/L, were diagnostic clues for acidosis detected in one of the piglets. The necropsy of both Göttingen Minipigs revealed abdominal effusion and macroscopic changes in the lungs, liver, and intestines. The cause of sepsis is not clear, however we suspect a link between pneumonia, respiratory failure, and sepsis, since at that stage of the experimental design, the airway management did not include changeset of recumbency and mouth cleaning on a routine basis. Additionally, 2 other Göttingen Minipigs achieved 12 hours of anesthesia. The first piglet (group C) was intubated with an ETT with a 2.0 mm I.D. (Mallinckrodt, Covidien), which was too small, causing leakage. Due to the inefficient ventilation, this piglet was finally excluded from the study. The second piglet (group H) developed signs of sepsis similar with the ones described above. Slightly white plasma was observed after blood samples centrifugation in this piglet. The cause of the sepsis was confirmed at the necropsy by discovering gastric rupture. Lastly, one Göttingen Minipig (H+TH3, group H+TH) was excluded from the PK analysis due to epigastric catheter misplacement in the peritoneal cavity, and administration of drugs intraperitoneally. This animal was still used in the assessment of the hypoxic insult, as this technical error did not interfere with the physiology of the animal.

4.2. Anesthesia and airway management

Alfaxalone, at 5 mg/kg, and tiletamine/zolazepam, at 4 mg/kg, were the drugs tested in the neonatal Göttingen Minipig for premedication. Alfaxalone was well tolerated but provided light sedation and was insufficient for intubation in combination with isoflurane. Subsequently, the combination of tiletamine/zolazepam and isoflurane proved to be more effective and was used for all 24 subjects.

The 2.5 mm I.D. uncuffed ETT was the most adapted in ventilating the neonatal Göttingen Minipigs. This was preferred over a 2.0 mm I.D., which was too small, causing leakage of air and isoflurane, and a 3.0 mm I.D. or cuffed ETTs, which proved to be too big for the trachea. The airway management also included changeset of recumbency and mouth cleaning from mucus and debris approximately every 2 hours, while ETT suctioning was cautiously used.

All Göttingen Minipigs received TPN with 217 kj/kg/day, from which 8 g/kg/day amino acids were combined with glucose and lipids, administered at 2-3 mL/kg/h. The blood glucose level was checked, using a Contour® XT blood glucose monitoring system, since hypoglycemia represents a risk associated with prolonged anesthesia in neonates. In order to assess the

blood glucose status in the neonatal Göttingen Minipigs investigated, thresholds previously described as mild hypoglycemia (60 mg/dL) and moderate hypoglycemia (35 mg/dL) in the neonatal conventional piglets, were considered. This TPN formulation was sufficient to maintain normoglycemia over the entire length of the experiment. Consequently, the overall mean blood glucose levels in all combined groups before drug administration was 91.95 (SD ±25.60, minimum 42 and a maximum of 134) mg/dL, after 12 hours of anesthesia 86.42 (SD ±18.54, minimum 57 and a maximum of 128) mg/dL and at the end of the experiment 87.31 (SD ±25.65, minimum 30 and a maximum of 133) mg/dL.

4.3. Vascular access

3 different venous catheters were placed in each neonatal Göttingen Minipig: 43 central catheters (i.e., 38 jugular and 5 umbilical) and 29 peripheral catheters (i.e., 26 epigastric and 3 lateral saphenous). Central venous catheterization, using the modified Seldinger technique, showed to be the primary method for vascular access, either for sampling or drug administration, in neonatal Göttingen Minipigs. This method possessed internal consistency and reproducibility, since it was performed multiple times by the assessor and the technician, throughout the study. The peripheral catheterization was most feasible in the epigastric and the lateral saphenous veins. The auricular vein was considered too small in neonatal Göttingen Minipigs. The catheterization of the umbilical vein depended on the sufficient moisturizing of the umbilical cord after birth. Blood sampling was performed for blood gas analysis and for PK (Chapter 4). This was uneventful and easy to perform via the jugular catheters.

4.4. Hypoxia

Hypoxia was established for 51 (SD ±34.82, minimum 20 and a maximum of 145) minutes in neonatal Göttingen Minipigs. The body weight, the hypoxia duration, and the need for the ETT occlusion to induce the insult are depicted in Table 2. The oxygen deprivation was reflected in cyanosis, a drop of SpO_2 at approximately 40-20%, or tachycardic response (>200 beats per minute) followed by severe bradycardia (<75 beats per minute), with severe acidosis, cardiogenic shock and hypoperfusion to vital organs. Atropine, at 0.05-0.1 mg/kg, was used to correct severe bradycardia and hypotension in 7 neonatal Göttingen Minipigs.

Table 2. The body weight, the hypoxia duration, and the need for the ETT occlusion to induce the insult in neonatal Göttingen Minipigs. * Group hypoxia (H); group hypoxia and therapeutic hypothermia (H+TH); grams (g); minutes (min).

Animal	Group	Weight (g)	Duration of hypoxia (min)	Endotracheal tube obstruction
H1	H	521	20	-
H2	H	502	38	-
H3	H	430	35	-
H4	H	531	30	-
H5	H	547	20	Yes
H6	H	592	45	-
H+TH1	H+TH	530	45	-

H+TH2	H+TH	610	145	Yes
H+TH3 [1]	H+TH	540	50	-
H+TH4	H+TH	507	50	-
H+TH5	H+TH	552	55	-
H+TH6	H+TH	650	30	-
H+TH7	H+TH	521	100	Yes

[1] *For H+TH3 was noticed the misplacement of the epigastric catheter at the end of the experiment. Consequently, this subject was excluded from the PK analysis. Since this animal was excluded due to a technical and not a physiological issue, its blood gas analysis was still included in this table.*

Table 3. Overview of the descriptive (arithmetic mean ± standard deviation) data for (central venous) blood gas analysis, glucose, and body temperature at the moment of the collection. The assessment was performed at the end of the experiment (24 hours) for control (C) and therapeutic hypothermia (TH) groups. For hypoxia (H), and hypoxia and therapeutic hypothermia (H+TH) groups, the parameters were determined at the end of the hypoxic insult and additionally at the end of the 24 hours TH. Overview of the individual data that were considered for this table are detailed in Supplementary Table 1.* Base excess (BE); bicarbonate (HCO_3); fraction of oxygen saturation (on effective hemoglobin, sO_2); partial pressure of carbon dioxide (PCO_2); partial pressure of oxygen (PO_2); total carbon dioxide (TCO_2).

Parameter	C	TH	H	H+TH	
Time of measurement	24 hours	24 hours	End insult	End insult	TH
pH	7.26±0.12	7.1±0.12	6.96±0.08	6.96±0.18	7.16±0.07
PCO_2 (kPa)	9.82±3.01	14.47±2.93	16.83±0.99	14.43±2.4	13.95±3.08
PO_2 (kPa)	5.46±1.1	7.01±1.58	2.92±2.31	1.77±0.17	5.5±0.47
HCO_3 (mmol/L)	32.56±4.1	34.5±18.18	-	27.96±3.28	36.36±2.58
BE (mmol/L)	5.5±4.72	6±5.17	-	-2.33±3.78	8.33±2.51
sO_2 (%)	64.66±18.57	67.25±35.95	-	7.66±0.57	59.33±7.57
TCO_2 (mmol/L)	34.83±4.26	37.5±19.75	-	31±3	39.33±2.88
Lactate (mmol/L)	0.97±0.53	0.85±0.8	8.81±2.24	10.13±2.46	0.38±0.06
Glucose (mg/dL)	97.33±23.32	73.16±32.09	80.66±31.94	81.66±19.71	95±16.1
Temperature (°C)	37.7±0.4	34.1±0.95	37.35±1.63	36.01±0.92	33.75±0.75

Comparative overview of the descriptive data for blood gas analysis parameters, glucose, and body temperatures of the neonatal Göttingen Minipigs presented in function of group: C, TH (end of the experiment), H (end of hypoxic insult), and H+TH (end of hypoxic insult and end of

the 24 hours TH) groups are depicted in Table 3 (arithmetic mean ±SD) and individual parameters (Supplementary Table 1). Additionally, the trend lines for the key pharmacodynamic parameters in the assessment of the systemic hypoxic insult are presented in Supplementary Figure 2. Graphs were made in Microsoft Excel® version 16.0.1, 2021 (Microsoft Corporation, Redmond, WA, United States). An increase in blood lactate (mean 9.56, SD ±2.27 mmol/L) and a decrease in blood pH (mean 7.00, SD ±0.16) were used as biomarkers for the systemic hypoxic insult. The statistical analysis conducted to evaluate the impact of hypoxia on the measured parameters revealed that values were statistically significantly higher for PCO_2 (P=0.0073) and lactate (P=0.0039) while for pH (P=0.0032), partial pressure of oxygen (PO_2; P=0.037), oxygen saturation (sO_2; P=0.0325) were statistically significantly lower (Figure 11).

Figure 11. Hypoxia-related differences between the control and the hypoxic groups for blood gas analysis. The bars represent arithmetic means, and the error bars indicate standard deviations, showing the variability of the data set relative to the mean. The red bars correspond to hypoxia at the end of the insult (n=13, including the hypoxic neonatal Göttingen Minipigs from the H and H+TH groups), while the empty bars represent the control group (n=6). Values were statistically significantly higher for hypoxic (group H and H+TH) compared to controls for partial pressure of carbon dioxide (PCO_2; P=0.0073) and lactate (P=0.0039), while for pH (P=0.0032), partial pressure of oxygen (PO_2; P=0.037), oxygen saturation (sO_2; P=0.0325) were statistically significantly lower. Designed in GraphPad Prism version 8.0.2 (GraphPad Software, Inc. San Diego, California USA); p-value: *, P<0.05; **, P<0.005; ***, P<0.0005; ****, P<0.0001.
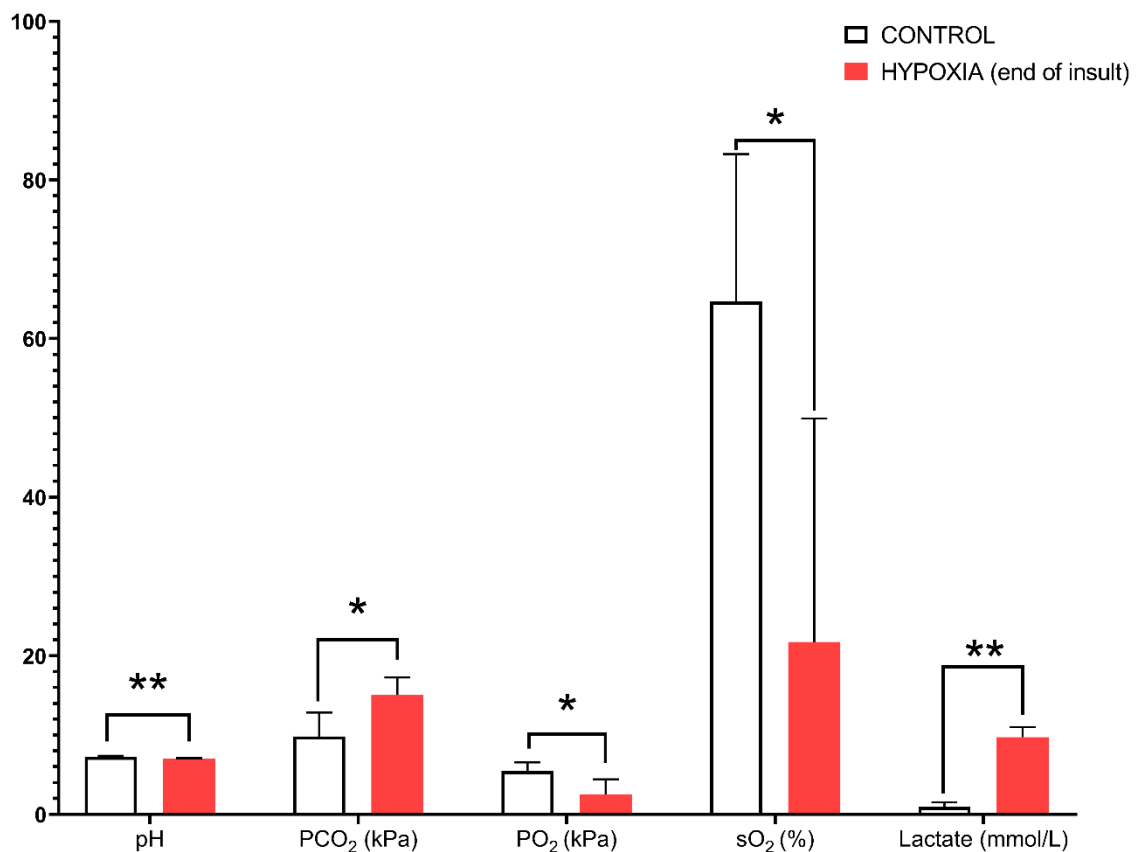
5. Discussion

5.1. Airway management

Due to the unique laryngeal anatomy and their predisposition for laryngospasm, endotracheal intubation is demanding in pigs [42,43]. Intubation is needed in PA studies since the ETT maintains a patent airway during general anesthesia, protects against aspiration, and allows positive pressure ventilation [44], as well as allows for the low-oxygen mixture ventilation. Both dorsal and ventral recumbency are alternatives for endotracheal intubation in pigs. In this study, ventral recumbency was used as it typically enables for smoother and faster intubation with reduced airway obstruction risks [43]. However, overextending the head in this position can increase the risk of laryngeal obstruction. Interestingly, dorsal recumbency allows the excessive pharyngeal tissue to "fall away" from the glottis, thus providing a good airway visualization [45].

In this study, the first piglet was intubated with an ETT that had an I.D. of 2.0 mm (Mallinckrodt, Covidien), which was too small, causing leakage. Due to the inefficient ventilation this first piglet was excluded from the study. Finally, the 2.5 mm I.D., 3.6 mm O.D. uncuffed ETT (Mallinckrodt, Covidien, 86233) was the most adapted in ventilating neonatal Göttingen Minipigs. This issue is also encountered when ventilating human neonates. Neonates are commonly ventilated using uncuffed endotracheal tubes. This may lead to a variable leakage around the ETT, depending on spontaneous breathing, the inspiratory pressure used, lung compliance, neck position and position of the ETT itself. Therefore, if the delivered tidal volume is measured only at inspiration, there can be a large discrepancy between pre-set and delivered volume, by overestimation [46]. The ETT patency is important for mechanical ventilation. Particularly in the NICU, for patients in whom small-sized ETTs are used, the risk of occlusion by secretions and subsequent need for reintubation may be high. Therefore, tube suction might be used in order to avoid obstruction from mucus and debris. On the other hand, ETT suctioning is associated with bradycardia, desaturation, atelectasis, increased intracranial pressure, bronchial perforation, and pneumothorax. Reducing the incidence of these side effects is inherent in the method in which ETT suctioning is performed. Limited frequency, shallow suctioning and preoxygenation are some beneficial practices [47]. For the airway management of the neonatal Göttingen Minipigs reported here, the mouth was cleaned every 2 hours together with changeset of recumbency while ETT suctioning was cautiously used. The ETT suction procedure was needed when secretions in the ETT where visible, the amplitude of the chest inflation at inspiration decreased, or abnormal breath sounds (i.e., wheezing) were observed. It was noted that the frequency of ETT suction and the reintubation need decreased when a predefined schedule of recumbency change was set-up. The piglets could experience arterial oxygen desaturation very rapidly during airway management and intubation [42]. Oxygen supplementation at 100%, 3 L/min was provided via face mask or ETT until the restoration of SpO_2. Proper oxygen management is crucial in neonatal resuscitation, as both insufficient and excessive oxygenation can be harmful [48]. In a previous study with neonatal piglets, hypoxia was followed by reoxygenation with 100% oxygen for 0.5 hours, then 21% oxygen for 3.5 hours [6]. Although our study did not focus on different oxygenation settings, we followed a similar protocol with successful resuscitation outcomes.

Pigs, like other mammals, are prone to respiratory depression under general anesthesia. Additionally, they are prone to suffer from partial airway obstruction, due to the species-specific reduced functional residual capacity of the lungs and the presence of excess tissue, in the oropharyngeal region. This increases the likelihood of peri-anesthetic hypoxia [44]. Furthermore, during spontaneous breathing, dependent lungs, understanding the lowest part of the lung in relation to gravity, tend to collapse if not periodically inflated. Atelectasis prevails in dependent lungs under general anesthesia. It is a position and pressure-dependent phenomenon and no matter the position, the gravity-dependent lung zones will always be susceptible to airway closure and atelectasis [49]. Areas of diffuse atelectasis will fail to oxygenate the blood. Therefore, venous admixture will lower blood oxygen levels [50].

Mechanical ventilation with intermittent positive inspiratory pressure and frequent recumbency changes maintained stable blood gas values in this study. Positive end-expiratory pressure (PEEP, baseline pressure maintained during expiration) is an important for preventing lungs from collapsing especially in human neonates [51,52]. This setting was more challenging to achieve in neonatal Göttingen Minipigs due to their smaller size and incompatibility with the ventilator used. Specific neonatal ventilators are recommended for further prolonged anesthesia studies using this model. Inadequate mode of ventilation can cause significant changes in their structure and function leading to ventilator induced lung injury [53]. This can be encountered in mechanically ventilated small animals and potentially result in excessive pressures (barotrauma), excessive distending volumes (volutrauma), alveolar damage resulting from transient and repeated closure and reopening of alveoli during the respiratory cycle (atelectotrauma), and biotrauma, in which the altered magnitude and pattern of lung stretch changes gene expression and cellular metabolism in a way that produces an overwhelming inflammatory response [50]. On the opposite side, small tidal volumes will produce an insufficient exchange of alveolar gases, no matter the respiratory rate or minute volume. This, in turn, would rapidly lead to carbon dioxide retention and the expected complications of hypercarbia and respiratory acidosis [46].

5.2. Vascular access

The main reason for using IV catheters is to facilitate multiple blood sampling and drug administration. It reduces animal stress, improves welfare, and reduces the number of personnel required [32]. Prompt placement of a peripheral IV catheter allows treatment of emergencies, if they arise, during induction. On the basis of this study, we recommend the use of the epigastric vein for IV administration of fluids and medications in neonatal Göttingen Minipigs. The piglets reported here were remarkably tolerant of this catheterization procedure and subsequent drugs and fluid administration. Catheter placement was successful when a preliminary incision of the skin was performed. As a limitation, the use of the epigastric vein for blood collection may prove to be inferior to other means of collection (i.e., central venous catheterization) because of the relatively low blood flow. Additionally, there is a risk of inadvertently entering the peritoneal cavity during attempted venipuncture by directing the stylet of the over-the-needle catheter too deeply. This last complication was detected in one neonatal Göttingen Minipig that was finally excluded from the study. Alternatively, the lateral saphenous vein was an appropriate peripheral catheterization in neonatal Göttingen Minipigs. However, compared with the epigastric vein, this was more difficult. This vein is embedded within subcutaneous fat and fascia and is not immediately apparent in pigs. It was

already reported that incision of the skin above the hock, below the fleshy portion of the leg, and more proximal to the Achilles tendon increase the ease of canulating this vessel [38]. Although peripheral veins were used successfully in several neonatal Göttingen Minipigs reported here, some piglets were more difficult to catheterize than others. When talking about very small subjects the target vessels are the central ones. Therefore, the central venous catheterization was the preferred method for vascular access in neonatal Göttingen Minipigs. The most common site is the neck, where the external jugular vein or the junction of external and internal jugular veins is catheterized [32]. In prolonged procedures, it is necessary to ensure a high level of surgical cleanliness when cannulating blood vessels. Infection becomes more likely the longer catheters are in place [50]. The umbilical venous catheterization is the most commonly used central lines in human neonates. It can be easily inserted soon after birth providing stable IV access for resuscitation medication, fluids, and parenteral nutrition [54]. As with other central catheters, thromboembolic events, bacteremia, and sepsis are common complications. Complications that are particular to umbilical venous catheters are the result of the catheter malposition in the heart, more specifically in the atria, resulting in cardiac arrhythmias, or in the portal system, resulting in serious hepatic injury. In these cases, the catheter must be withdrawn from the heart and returned to the inferior vena cava. On the other hand, hepatic necrosis can occur due to thrombosis of the hepatic veins or intravascular catheter complications, infusion of hypertonic or vasospastic solutions into the liver. Necrotizing enterocolitis and perforation of the colon and/or peritoneum have been reported following the positioning of the catheter in the portal system [55].

5.3. Blood sampling

Piglets are generally injected IM with iron after birth to prevent anemia and improve growth [56,57]. We observed that iron injection has an impact on the collected samples by coloring the plasma and other organs, thereby potentially influencing further in vitro investigations (e.g., proteomics, transcriptomics). This learning was aligned with the literature findings since it was documented that iron injections increase the hemoglobin concentration [56]. Additionally, hemoglobin in whole blood can lead to clogging of extraction matrices, which makes blood RNA isolation further difficult and gene expression analyses unreliable [58]. On the other hand, piglets are born with low iron stores and potentially become iron deficient. However, this might happen right before weaning (at approximately 20 days old) [57]. The neonatal Göttingen Minipigs recruited for our study did not receive iron supplementation since the follow-up of the pigs after birth was limited to 24 hours, as well as to prevent compromising future in vitro investigations. Blood sampling was uneventful and easy to perform via central venous access.

One limitation in the view of the blood sampling and the size of the model should be emphasized. As PK studies are demanding in terms of blood samples (preferably requiring rich data sets), the animal size and therefore volume of blood, that can be collected over 24 hours, represents a limitation. In our study design, this was accomplished, via micro sampling, the amount of blood collected was below 15% of the piglet's total blood volume, counting the samples for PK, blood gas analysis, and the possible blood loss during catheter placement. Since the sampling covered 24 hours while piglets received an IV infusion, no signs of cardiac decompensation were noticed. However, this degree of blood loss is sufficient to induce hypovolemia in certain individuals, especially when the collection is performed intensively at certain time periods. Therefore, for further perspectives in PK studies using the neonatal

Göttingen Minipig as model, the volume of blood collected should be cautiously determined, both from an ethical and study design validity points of view.

5.4. Hypoxic asphyxic insult

The most critical step in developing our model was generating a standardized hypoxic insult, as the primary goal was to induce a moderate to severe insult while ensuring animal survival. Literature reports variable durations of hypoxic insults, ranging from 12.5 minutes [8] to 2 hours [6], depending on the method used. The invasiveness of the procedures prior to the insult, which may result in pain, hypothermia, and potential blood loss, but also the age and weight of the piglets may impact this duration as well. Still, the variable duration of the insult in the different protocols is acceptable, as magnetic resonance spectroscopy analysis, EEG, brain histology, blood pressure and/or blood gas analysis [6-8,59] are used to assess the insult. Although variability in insult duration across different protocols is acceptable (Section 1.1., Methodological considerations from General Discussion), in our study, the mean duration of hypoxia was 51 minutes, with a range from 20 to 145 minutes. Table 2 shows that the duration of hypoxia was less than or equal to 45 minutes in 8 out of 13 neonatal Göttingen Minipigs. This deviation from the proposed hypoxia duration (approximately 1 hour) introduces variability between piglets, which could be considered a limitation of the study. However, this variability was necessary to harmonize the blood gas values, specifically lactate and pH levels, which were considered biomarkers in the determination of the severity of the hypoxic insult. Furthermore, monitoring laboratory indicators of acidosis via blood gas analysis, along with cardiac function through ECG, allowed us to adjust the hypoxic insult according to each piglet's tolerance resulting in an individualized approach to ensure a high survival rate.

On the other hand, when the ventilation with the low-oxygen gas mixture was insufficient to achieve the targeted blood gas threshold values, the ETT occlusion for 7 minutes was implemented (in 3 out of 13 neonatal Göttingen Minipigs), adding hypercapnia to the hypoxia. The duration of ETT was determined based on the recommended time for umbilical cord clamping in a conventional piglet model of asphyxia [60]. While the necessity of ETT occlusion in 3 out of 13 neonatal Göttingen Minipigs introduced additional variability into the study, we took all possible measures to prevent this outcome. In our pilot study (Section 9) - specifically designed for technical refinement - and in the first 4 experimental neonatal Göttingen Minipigs, this intervention was not required to achieve the targeted blood gas values. However, since this is the first neonatal Göttingen Minipig PA model, we could not have anticipated how neonatal Göttingen Minipigs would react under these specific experimental conditions. This unexpected variability highlights the challenges of establishing a new animal model. However, these adjustments were necessary to ensure that each neonatal Göttingen Minipig reaches the set physiological thresholds for the hypoxic insult, thus preserving the overall integrity and objectives of the research.

5.5. Blood gases and lactate

Blood gas analysis is useful for evaluating acid-base balance, ventilation, and oxygenation in critically ill patients. It measures three key parameters: the levels of free (unbound) oxygen (PO_2) and carbon dioxide (PCO_2) in the blood, and the blood pH, which reflects acidity or alkalinity. While PO_2 indicates oxygenation status, PCO_2 assesses ventilation, and the combination of pH, PCO_2, and bicarbonate (HCO_3) provides insight into acid-base balance [61].

While central venous blood can give useful information on pH, PCO_2, and HCO_3 levels, it is less reliable for determining PO_2 and sO_2. For accurate oxygenation assessment, arterial blood is preferred, although non-invasive pulse oximetry can often be sufficient. Central venous and arterial pH, PCO_2, and HCO_3 levels correlate well, with central venous pH typically being 0.03 units lower and PCO_2 0.6 kPa (5 mmHg) higher than arterial values [62]. Despite these differences, central venous blood gases can reliably reflect acid-base status when corrected values fall within the normal arterial range [63]. In our study, blood gas analysis, including lactate, was performed on all neonatal Göttingen Minipigs. In the control group, this analysis was conducted to establish baseline values for this model as well as to assess the ventilation and oxygenation. A slightly low pH was observed in some of the neonatal Göttingen Minipigs (Supplementary Table 1), likely due to ventilation challenges associated with this model (Section 5.1., Airway management). These challenges, along with the observed drop in pH, contributed to the decision to shorten the experimental duration to 24 hours (Section 5.6., Prolonged anesthesia). On the other hand, lactate and pH levels were measured as a biochemical marker of hypoxia. Lactate accumulates when aerobic metabolism is insufficient due to reduced oxygen delivery, necessitating anaerobic metabolism [64]. Elevated lactate levels can indicate HIE. A study of 41 infants with asphyxia found that umbilical cord blood lactate levels were significantly higher in those with HIE compared to asphyxic infants without HIE [65]. The optimal cutoff for detecting HIE was a lactate level of 8.12 mmol/L [65], which shows a similar threshold to that observed in our neonatal Göttingen Minipigs.

Finally, interpreting blood gases in hypothermia requires special consideration. Lower body temperatures increase the solubility of oxygen and carbon dioxide, potentially skewing blood gases results (i.e., pH increases and PCO_2 decreases) [66]. Blood gas analyzers warm samples to 37 °C, which can lead to inaccurately high PO_2 and PCO_2 readings and a lower pH when compared to the actual values in a hypothermic patient. To account for this, it is recommended to compare warmed blood gas results with normal values at 37 °C (alpha-stat approach) [67]. Although temperature adjustments might be necessary, they should be clearly indicated, and uncorrected blood gases values should be reported alongside corrected values. Currently, there is no data to guide temperature correction for oxygen delivery and demand outside 37 °C, so using uncorrected values is often sufficient [67,68].

5.6. Prolonged anesthesia

Monitoring of non-invasive vital signs should begin as soon as the animals are included in the study. The plan of anesthesia, mean arterial blood pressure, heart rate, SpO_2, body temperature and $EtCO_2$ can be readily obtained and monitored [50]. This is critical for the early detection of potential problems during the entire anesthetic period. In the perioperative mortality study by Brodbelt [69], many factors significantly contributed to mortality but through monitoring, the risk of death was significantly decreased [22,69]. One of the contributing factors in anesthesia-related death is hypothermia [69]. Neonatal and pediatric animals are highly susceptible to hypothermia because of their high body surface area-to-body mass ratio. As these animals can become quickly hypothermic under general anesthesia, the management should include numerous strategies [50]: creating warm conditions (bubble wrap insulations, with hot air blankets and/or heater pads), minimalization of the heat loss using intermittent positive pressure ventilation judiciously, favoring "low-flow" re-breathing systems and using heat moisture exchangers. However, these heat losses, promoted by surgery and anesthesia, proved to be useful in our study, for the hypothermia groups, by

inducing gradual cooling, over 90 minutes, in a less expensive setup than the clinical one (e.g., MiraCradle-Neonate Cooler).

Prolonged anesthesia may be required in studies using pigs as models for the human intensive care patient. In these type of studies, it is difficult to achieve a balance between prolonged anesthesia to maximize the data set and maintain a stable physiological state, and to minimize data variability and increase the study power [50]. Particularly, one limitation of our model refers to the duration of anesthesia. The initial target period was 96 hours, since TH in the human setting covers 72 hours, followed by gradual rewarming and subsequently maintenance of a body temperature at 36.5 °C during 24 hours [9]. However, after several attempts the length of the experiment was reduced to 24 hours and the dose regimen and sampling scheme were adapted accordingly. The rationale first of all relates to the complexity of the animal model with the logistical challenges (Section 1.1., Methodological considerations from General Discussion). Furthermore, there is also the need for skilled investigators in permanence for the entire length of the experiment, as well as a fully supplied operating suite, comparable to the human NICU, which is more sophisticated than the typical veterinary operating suite. The techniques in developing piglets for experimentation require experience to master, for the investigator and his assistant, and they must be comfortable with both the surgery and anesthesia. This was achieved by performing a preliminary pilot study in which we developed the PA model using conventional piglets to refine the techniques, and to optimize the experimental setup (Section 9). As a consequence of the 24 hours limitation, the rewarming was skipped in this study design, but it opened the possibility for further research directions.

Adjustments of anesthesia were performed to maintain homeostasis. Hypotension, hypoglycemia, shivering during TH, transitory insufficient anesthesia, and ventilation troubleshooting, such as carbon dioxide retention, high production of mucus, ETT leak, and lung atelectasis, are the main difficulties that were countered through comprehensive monitoring and customized procedures, as necessary. However, appropriate anesthetic management of neonatal and pediatric animals is often differently compared to adults. Clinically acceptable ranges can be different in neonates compared to adults; therefore the anesthesiologist should be familiar with the acceptable ranges for the species and age group of individuals that are being anesthetized [22]. Generally, neonatal, and juvenile animals have a higher heart rate but lower blood pressure than adults. For example, 45 mmHg represents the lower limit of autoregulation in neonatal swine for the mean arterial blood pressure [70,71], while 117.8 (in mean with SD ±4.7) mmHg was reported in freely moving adult Göttingen Minipigs [72]. Compared with the adult heart, the neonatal heart has limited myocardial contractile tissue, low ventricular compliance, limited cardiac reserve, cardiac output heart rate dependent and poor vasomotor control. The cardiovascular system must be supported with IV fluids and chronotropic support. Anticholinergic drugs are commonly used to treat and/or prevent anesthetic and preanesthetic bradycardia, decrease airway and salivary secretions, dilate the pupil, block vagally mediated reflexes (viscerovagal, oculocardiac, Branham), and block the effects of parasympathomimetic drugs [22]. In our study, atropine at 0.05-0.1 mg/kg was well tolerated by the neonatal Göttingen Minipigs. It represented a valuable drug used in stabilizing periods, after induction or hypoxic insult, when bradycardia and hypotension occurred. Since hypoglycemia is one of the most common neonatal anesthesia risks, TPN IV, CRI, followed by close monitoring of glucose status, every 12 hours, was performed. The TPN formulation for neonatal piglets consisted of 3200 to 3400

kj/L including: amino acids (45.5-54 g/L), glucose (72.5-116 g/L) and lipids (21-30.7 g/L) [73,74]. For the neonatal Göttingen Minipigs reported here, the TPN solution was administered continuously via the UVC or the peripheral catheters. The piglets received 217 kj/kg/day, from which 8 g/kg/day of amino acids were combined with glucose and lipids. This represents 50% of the total intake in neonatal piglets (550 kj/kg/day) and the energetic requirement necessary for the first 48 hours. Because of the high osmolarity of the TPN, supplemental crystalloids (e.g., 0.9% NaCl) were administered to maintain fluid homeostasis. Shivering, caused by light anesthesia and hypothermia, increases oxygen consumption (up to 200-300%). This increased oxygen demand may not be met by an increase in oxygen delivery, particularly if anesthetic-induced hypoventilation occurs [22]. The light anesthesia was addressed by starting the CRI of fentanyl and midazolam with loading doses, allowing the smooth change from gas anesthesia to total intravenous anesthesia (TIVA).

5.7. Comparative view on perinatal asphyxia animal models

Numerous models of hypoxia, hypoxia-ischemia, intraventricular hemorrhage, and focal stroke have been developed in rodents and in larger species to mimic the different types of injuries seen in the human neonates [75]. Although no animal model is perfectly ideal in terms of capturing the diversity and complexity of human pathology, the investigator must evaluate the strengths and limitations in the context of the research questions [76]. Firstly, the maturational pattern of the animal model should be as close as possible to the human neonate, for a better interpretation of the findings. Secondly, the body size at birth should allow the instrumentation (for hemodynamic and physiological measurements), in order to closely monitor the effects of hypoxia and reoxygenation, and the sampling (e.g., blood gas analysis to assess pulmonary gas exchange and acid-base status). This monitoring is crucial in reaching a degree of hypoxia likely to produce significant damage without excessive mortality, and it also helps ensure the reproducibility of the injury (e.g., a similar degree of acidosis with a similar descent over time). Lastly, the type, severity and duration of hypoxic insult are critical to the translational value of the model, which should approximate the clinical picture of PA [77].

The rat pup has been the most commonly used, and thus is probably the best characterized model in HIE research. The neonatal rat is altricial (born immature). At birth, its development corresponds to a 24- to 28-week human fetus [77]. The most commonly used non-rodent large mammal species to induce HIE in the immature brain are non-human primates (NHPs), sheep, rabbits, and pigs, species that have a white/gray matter ratio similar to the human brain [75]. An overview of the most important criteria in the differentiation of the rodent and non-rodent species for PA/HIE research are presented in Table 4. While impractical as a fetal model due to its large litter size (>10 piglets per litter), the neonatal piglet has been proven to be a valuable model to study HIE. After the rat, the neonatal pig model is the most frequently used. Its development corresponds to the 36- to 38-week human fetus [77]. A comparative overview of the different large animal models developed for PA/HIE, with their strengths and limitations, is provided in Table 5.

Table 4. Strengths and limitations of different animal models for * PA (perinatal asphyxia)/HIE (hypoxic-ischemic encephalopathy): rodent model versus large animal models.

Animal model for PA/HIE*	Strengths	Limitations
Rodent model	- postnatal cerebral development analogous to human development in the third trimester. - litters are easily produced and handled [76].	- lissencephalic cortex; the cerebral blood flow regulation and the white/gray matter ratios is different to the human brain. - limited behavioral repertoire [76]. - rodent brain regions are mature at a different pace, thus making it difficult to adhere to a single postnatal day, as a comprehensive representation of brain development [75]. - rat pups are generally not instrumented to monitor the hypoxia effects on hemodynamic indices, and this can make it difficult to control the degree of hypoxic-ischemic insult [77].
Large animal models	- gyrencephalic; the white/gray matter ratio is similar to the human brain. - when global hypoxia and hypotension are combined, the results in permanent brain injury, organ failure, post-hypoxic seizures, and abnormal neurology akin to human neonates are documented. - similar in survival rate. - among large neonatal animal models, other than nonhuman primates, the (neonatal) pigs are appropriate because their general brain and organ maturation at-term are similar to humans [76].	- high maintenance costs and long-term neurorehabilitation have dramatically limited the use of larger species over the past decade [75]. - ethical reasons [76].

Table 5. Comparative overview of the different large animal models used in the study of * PA (perinatal asphyxia)/HIE (hypoxic-ischemic encephalopathy), with their strengths and limitations. * Neonatal intensive care unit (NICU); therapeutic hypothermia (TH).

Animal model for PA/HIE*	Strengths	Limitations

Nonhuman primate	- anatomical and physiological similarities to humans [76,78] due to the phylogenetic proximity [77]. - similar pathological distribution of brain injury [78], allowing the investigation with sophisticated neurological tests [76].	- other (non-related brain) pathological processes secondary to asphyxia may be more appropriately assessed in other species [78]. - in terms of cerebral maturity, nonhuman primates are more precocious than humans and the model's equivalence to the human neonate is unknown [77]. - high economic handling costs, in addition to the ethical issues [76].
Sheep	- the instrumentation is feasible due to relatively large body size. - the litter size (1 or 2 offspring) is practical; it is a good model to reproduce the PA conditions prevailing in the womb [77]. - relatively low costs. - fetal physiology has already been extensively studied in sheep. - resistance to preterm labor following surgery [78].	- precocial species; studies are performed during pregnancy to correlate to relevant maturation stages in the human. - fetal models are complicated by maternal/placenta metabolism, which is not present in the HIE human situation [75]. - different placental flow patterns (cotyledonary placenta, in sheep versus mono-discoidal type, with a single disc, in humans) [78].
Rabbit	- useful animal model due to the possible application in both, basic research, and clinical applications. - their medium size greatly facilitates handling with reducing costs [76]. - model for cerebral blood flow [79].	- intrauterine ischemia is induced at approximately 22 days of gestation as equivalent to the preterm, and at the end of gestation, at 29 days, to mimic at-term injury [75].
Dog	- the neonatal beagle is known to have a germinal matrix layer similar to 30- to 32- week human gestational age and thus provides a good model for the developing nervous system research. - used for the study of regional cerebral blood flow, glucose, lactate and energy metabolism, autoregulation, maturation of	- inadequate ventilation, along with clinical risks comparable to the development of respiratory distress syndrome [23].

	germinal matrix, and drug effects [80].	
Pig	- development similar to (near)term human neonates, with comparable body systems and size at birth (1.5-2 kg). - the large body size at birth allows for sampling at early stages without hampering the physiology and also facilitates the adaptation of NICU equipment [77]. - as the piglet asphyxia model is well-characterized, this opens opportunities for pharmacological interventions and procedures applied in a clinical setting, such as TH [5].	- anesthesia and surgical trauma stress, limit this model in terms of survival length and number of invasive procedures performed. - skilled personnel experienced with surgery and anesthesia is the key for these types of experiments [6]. - logistical drawback of getting neonatal piglets in the research facility when no (pregnant) sows are housed on-site. - using older piglets (2 or more days of age) risks weakening the clinical relevance of the piglet model, as the model should be akin to the human neonatal metabolism [42].

6. Conclusion

In this study, a neonatal Göttingen Minipig model for dose precision in PA was developed. We showed that endotracheal intubation, vascular access, anesthesia, and mechanical ventilation are feasible in these very small animals. Therefore, this is useful information for scientists using the neonatal Göttingen Minipig for investigating disease conditions or for drug efficacy and safety testing, since it is the most commonly used pig strain in nonclinical drug development. This asphyxia model will be further used to assess the impact of systemic hypoxia and TH on drug disposition resulting in better drug dosing and drug exposure in human asphyxiated neonates. Besides the success of several challenging techniques achieved in this neonatal Göttingen Minipig asphyxia model, the current model also shows limitations such as the short survival duration (24 hours), which results in several consequences (e.g., no rewarming phase and limited PK profile of the drugs studied). Furthermore, additional diagnostic tools would be useful for the evaluation of HIE in this model.

7. References

1. Helke KL, Swindle MM. Animal models of toxicology testing: the role of pigs. Expert Opin Drug Metab Toxicol. 2013 Feb;9(2):127-39.
2. Singh VK, Thrall KD, Hauer-Jensen M. Minipigs as models in drug discovery. Expert Opin Drug Discov. 2016 Dec;11(12):1131-1134.
3. GUIDELINE IH. Nonclinical safety testing in support of development of paediatric pharmaceuticals S11. 2020.

4. Committee ES, Hardy A, Benford D, et al. Guidance on the risk assessment of substances present in food intended for infants below 16 weeks of age. EFSA Journal. 2017;15(5):e04849.

5. Ayuso M, Buyssens L, Stroe M, et al. The Neonatal and Juvenile Pig in Pediatric Drug Discovery and Development. Pharmaceutics. 2021;13(1):44.

6. Cheung P-Y, Gill RS, Bigam DL. A swine model of neonatal asphyxia. J Vis Exp. 2011 (56):3166.

7. Kyng KJ, Skajaa T, Kerrn-Jespersen S, et al. A Piglet Model of Neonatal Hypoxic-Ischemic Encephalopathy. J Vis Exp. 2015 (99):e52454-e52454.

8. Ezzati M, Broad K, Kawano G, et al. Pharmacokinetics of dexmedetomidine combined with therapeutic hypothermia in a piglet asphyxia model. Acta Anaesthesiol Scand. 2014 Jul;58(6):733-42.

9. Smits A, Annaert P, Van Cruchten S, et al. A Physiology-Based Pharmacokinetic Framework to Support Drug Development and Dose Precision During Therapeutic Hypothermia in Neonates. Front Pharmacol. 2020;11:587-587.

10. Pearson N, Boiczyk GM, Kote VB, et al. A Strain Rate-Dependent Constitutive Model for Göttingen Minipig Cerebral Arteries. J Biomech Eng. 2022 Aug 1;144(8).

11. Musskopf ML, Finger Stadler A, Wikesjö UME, et al. The minipig intraoral dental implant model: A systematic review and meta-analysis. PLOS ONE. 2022;17(2):e0264475.

12. Larsen MO, Rolin B. Use of the Göttingen minipig as a model of diabetes, with special focus on type 1 diabetes research. Ilar j. 2004;45(3):303-13.

13. Roh J, Hill JA, Singh A, et al. Heart Failure With Preserved Ejection Fraction: Heterogeneous Syndrome, Diverse Preclinical Models. Circulation Research. 2022;130(12):1906-1925.

14. Eirefelt S, Stahlhut M, Svitacheva N, et al. Characterization of a novel non-steroidal glucocorticoid receptor agonist optimized for topical treatment. Scientific Reports. 2022 2022/01/27;12(1):1501.

15. Eisler W, Baur J-O, Held M, et al. Assessment of Two Commonly used Dermal Regeneration Templates in a Swine Model without Skin Grafting. Applied Sciences. 2022;12(6):3205.

16. Stricker-Krongrad A, Shoemake CR, Pereira ME, et al. Miniature Swine Breeds in Toxicology and Drug Safety Assessments: What to Expect during Clinical and Pathology Evaluations. Toxicologic Pathology. 2015 2016/04/01;44(3):421-427.

17. Bode G, Clausing P, Gervais F, et al. The utility of the minipig as an animal model in regulatory toxicology. J Pharmacol Toxicol Methods. 2010 Nov-Dec;62(3):196-220.

18. Valenzuela A, Tardiveau C, Ayuso M, et al. Safety Testing of an Antisense Oligonucleotide Intended for Pediatric Indications in the Juvenile Göttingen Minipig, including an Evaluation of the Ontogeny of Key Nucleases. Pharmaceutics. 2021;13(9):1442.

19. Buyssens L, De Clerck L, Schelstraete W, et al. Hepatic Cytochrome P450 Abundance and Activity in the Developing and Adult Göttingen Minipig: Pivotal Data for PBPK Modeling. Front Pharmacol. 2021;12:665644.

20. Van Peer E, De Bock L, Boussery K, et al. Age-related Differences in CYP3A Abundance and Activity in the Liver of the Göttingen Minipig. Basic Clin Pharmacol Toxicol. 2015 Nov;117(5):350-7.

21. Van Peer E, Jacobs F, Snoeys J, et al. In vitro Phase I-and Phase II-drug metabolism in the liver of juvenile and adult Göttingen minipigs. Pharmaceutical research. 2017;34(4):750-764.

22. Grimm KA, Lamont LA, Tranquilli WJ, et al. Veterinary anesthesia and analgesia. John Wiley & Sons; 2015.

23. Duke-Novakovski T, Vries Md, Seymour C. BSAVA manual of canine and feline anaesthesia and analgesia. British Small Animal Veterinary Association; 2016. (Ed. 3).

24. Plumb D. Plumb's vet drug handbook: desk edition. Blackwell, Ames, IA; 2008.

25. Galinkin JL, Kurth CD, Shi H, et al. The plasma pharmacokinetics and cerebral spinal fluid penetration of intravenous topiramate in newborn pigs. Biopharmaceutics & drug disposition. 2004;25(6):265-271.

26. Villanueva-García D, Mota-Rojas D, Martinez-Burnes J, et al. Hypothermia in newly born piglets: Mechanisms of thermoregulation and pathophysiology of death. Journal of Animal Behaviour and Biometeorology. 2020 01/01;9:9:2101-9:2101.

27. Kumar A, Mann H, Remmel R. Pharmacokinetics of tiletamine and zolazepam (Telazol®) in anesthetized pigs. Journal of veterinary pharmacology and therapeutics. 2006;29(6):587-589.

28. Bigby SE, Carter JE, Bauquier S, et al. The use of alfaxalone for premedication, induction and maintenance of anaesthesia in pigs: a pilot study. Veterinary anaesthesia and analgesia. 2017;44(4):905-909.

29. Clark AM, Kriel RL, Leppik IE, et al. Intravenous topiramate: Comparison of pharmacokinetics and safety with the oral formulation in healthy volunteers. Epilepsia. 2013;54(6):1099-1105.

30. Clark AM, Kriel RL, Leppik IE, et al. Intravenous topiramate: Safety and pharmacokinetics following a single dose in patients with epilepsy or migraines taking oral topiramate. Epilepsia. 2013;54(6):1106-1111.

31. Vuu I, Coles LD, Maglalang P, et al. Intravenous Topiramate: Pharmacokinetics in Dogs with Naturally Occurring Epilepsy [Original Research]. Frontiers in Veterinary Science. 2016 2016-December-05;3(107).

32. Zeltner A. Catheters for Vascular Access and the Göttingen Minipig. Göttingen Minipigs Magazine. May 2013:3.

33. Seldinger SI. Catheter Replacement of the Needle in Percutaneous Arteriography: A new technique. Acta Radiologica. 1953 1953/05/01;39(5):368-376.

34. Song IK, Kim EH, Lee JH, et al. Seldinger vs modified Seldinger techniques for ultrasound-guided central venous catheterisation in neonates: a randomised controlled trial. British Journal of Anaesthesia. 2018 2018/12/01/;121(6):1332-1337.

35. Furbeyre H, Labussiere E. A minimally invasive catheterization of the external jugular vein in suckling piglets using ultrasound guidance. PLoS One. 2020;15(10):e0241444.

36. Framstad T, Sjaastad O, Aass R. Bleeding and intravenous techniques in pigs. 2004.

37. Snook CS. Use of the subcutaneous abdominal vein for blood sampling and intravenous catheterization in potbellied pigs. Journal of the American Veterinary Medical Association. 2001 15 Sep. 2001;219(6):809-810.

38. Benoit A, Dailey R. Catheterization of the caudal vena cava via the lateral saphenous vein in the ewe, cow, and gilt: an alternative to utero-ovarian and medial coccygeal vein catheters. Journal of animal science. 1991;69(7):2971-2979.

39.   Gasthuys F, Pollet L, Simoens P, et al. Anaesthesia for fluorescein angiography of the ocular fundus in the miniature pig. Veterinary Research Communications. 1990;14(5):393-402.

40.   Virolainen JV, Love RJ, Tast A, et al. Plasma progesterone concentration depends on sampling site in pigs. Animal reproduction science. 2005;86(3-4):305-316.

41.   NICE. National Institute for Health and Care Excellence. Interventional procedures guidance [IPG347]. Therapeutic hypothermia with intracorporeal temperature monitoring for hypoxic perinatal brain injury. Published on 26 May 2010, accessed on 25 April 2023. 2010.

42.   Whitaker EE, Zheng CZ, Bissonnette B, et al. Use of a Piglet Model for the Study of Anesthetic-induced Developmental Neurotoxicity (AIDN): A Translational Neuroscience Approach. J Vis Exp. 2017 Jun 11(124).

43.   Theisen M, Maas M, Hartlage M, et al. Ventral recumbency is crucial for fast and safe orotracheal intubation in laboratory swine. Laboratory animals. 2008 11/01;43:96-101.

44.   Steinbacher R, von Ritgen S, Moens YPS. Laryngeal perforation during a standard intubation procedure in a pig. Laboratory Animals. 2012 2012/07/01;46(3):261-263.

45.   Hodgkinson O. Practical sedation and anaesthesia in pigs. In Practice. 2007;29(1):34-39.

46.   Ahluwalia J, Morley C, Wahle HG. Volume Guarantee New Approaches in Volume Controlled Ventilation for Neonates. Lubeck: Drager Medizintechnik GmbH. 2014.

47.   Clifton-Koeppel R. Endotracheal Tube Suctioning in the Newborn: A Review of the Literature. Newborn and Infant Nursing Reviews. 2006 2006/06/01/;6(2):94-99.

48.   Kattwinkel J, Perlman JM, Aziz K, et al. Part 15: neonatal resuscitation: 2010 American Heart Association guidelines for cardiopulmonary resuscitation and emergency cardiovascular care. Circulation. 2010;122(18_suppl_3):S909-S919.

49.   Li C, Ren Q, Li X, et al. Effect of sigh in lateral position on postoperative atelectasis in adults assessed by lung ultrasound: a randomized, controlled trial. BMC Anesthesiology. 2022 2022/07/11;22(1):215.

50.   Clutton RE, Reed F, Eddleston M, et al. Prolonged anaesthesia in minipigs. Prolong Anaesth Minipigs. 2013:11-15.

51.   Holte K, Ersdal H, Eilevstjønn J, et al. Positive End-Expiratory Pressure in Newborn Resuscitation Around Term: A Randomized Controlled Trial. Pediatrics. 2020;146(4).

52.   Sam Wallis CF. Neonatal Ventilation – basics of mechanical ventilation. Bradford Teaching Hospitals NHS Fundation Trust. 17/09/2022 [cited. https://www.bradfordhospitals.nhs.uk/wp-content/uploads/2020/07/Neonatal-Ventilation.pdf

53.   Kuchnicka K, Maciejewski D. Ventilator-associated lung injury. Anaesthesiol Intensive Ther. 2013 Jul-Sep;45(3):164-70.

54.   D'Andrea V, Prontera G, Rubortone SA, et al. Umbilical Venous Catheter Update: A Narrative Review Including Ultrasound and Training. Front Pediatr. 2021 [cited 774705 p.]. DOI:10.3389/fped.2021.774705

55.   Hermansen MC, Hermansen MG. Intravascular catheter complications in the neonatal intensive care unit. Clin Perinatol. 2005 2005/03//;32(1):141-56, vii.

56.   Yu I, Lin J, Wu J, et al. Reevaluation of the necessity of iron injection to newborn piglets. Asian-australasian journal of animal sciences. 2002;15(1):79-83.

57. Chevalier TB, Monegue HJ, Lindemann MD. Effects of iron dosage administered to newborn piglets on hematological measures, preweaning and postweaning growth performance, and postweaning tissue mineral content. Journal of Swine Health and Production. 2021;29(4):189-199.

58. Meyer A, Paroni F, Günther K, et al. Evaluation of Existing Methods for Human Blood mRNA Isolation and Analysis for Large Studies. PLoS One. 2016;11(8):e0161778.

59. Robertson NJ, Faulkner S, Fleiss B, et al. Melatonin augments hypothermic neuroprotection in a perinatal asphyxia model. Brain. 2012;136(1):90-105.

60. van Dijk AJ, van Loon JPAM, Taverne MAM, et al. Umbilical cord clamping in term piglets: A useful model to study perinatal asphyxia? Theriogenology. 2008 2008/09/01/;70(4):662-674.

61. Gattinoni L, Pesenti A, Matthay M. Understanding blood gas analysis. Intensive Care Med. 2018 Jan;44(1):91-93.

62. Malatesha G, Singh NK, Bharija A, et al. Comparison of arterial and venous pH, bicarbonate, PCO2 and PO2 in initial emergency department assessment. Emerg Med J. 2007 Aug;24(8):569-71.

63. Sutton RN, Wilson RF, Walt AJ. Differences in acid-base levels and oxygen-saturation between central venous and arterial blood. Lancet. 1967 Oct 7;2(7519):748-51.

64. Jin ES, Sherry AD, Malloy CR. Metabolism of glycerol, glucose, and lactate in the citric acid cycle prior to incorporation into hepatic acylglycerols. J Biol Chem. 2013 May 17;288(20):14488-14496.

65. Van Anh TN, Hao TK, Chi NTD, et al. Predictions of Hypoxic-Ischemic Encephalopathy by Umbilical Cord Blood Lactate in Newborns with Birth Asphyxia. Open Access Maced J Med Sci. 2019 Nov 15;7(21):3564-3567.

66. Groenendaal F, De Vooght KM, van Bel F. Blood gas values during hypothermia in asphyxiated term neonates. Pediatrics. 2009 Jan;123(1):170-2.

67. Davis MD, Walsh BK, Sittig SE, et al. AARC Clinical Practice Guideline: Blood Gas Analysis and Hemoximetry: 2013. Respiratory Care. 2013;58(10):1694.

68. Shapiro BA. Temperature correction of blood gas values. Respir Care Clin N Am. 1995 Sep;1(1):69-76.

69. Brodbelt D. Perioperative mortality in small animal anaesthesia. The Veterinary Journal. 2009;182(2):152-161.

70. Larson AC, Jamrogowicz JL, Kulikowicz E, et al. Cerebrovascular autoregulation after rewarming from hypothermia in a neonatal swine model of asphyxic brain injury. J Appl Physiol (1985). 2013 Nov;115(10):1433-42.

71. O'Brien CE, Santos PT, Kulikowicz E, et al. Hypoxia-ischemia and hypothermia independently and interactively affect neuronal pathology in neonatal piglets with short-term recovery. Developmental neuroscience. 2019;41(1-2):17-33.

72. Carlsen MF, Christoffersen BØ, Lindgaard R, et al. Implantation of telemetric blood pressure transmitters in Göttingen Minipigs: Validation of 24-h systemic blood pressure and heart rate monitoring and influence of anaesthesia. Journal of Pharmacological and Toxicological Methods. 2022 2022/05/01/;115:107168.

73. Burrin D, Stoll B, Jiang R, et al. GLP-2 stimulates intestinal growth in premature TPN-fed pigs by suppressing proteolysis and apoptosis. American Journal of Physiology-Gastrointestinal and Liver Physiology. 2000;279(6):G1249-G1256.

74. Sangild PT, Thymann T, Schmidt M, et al. Invited review: the preterm pig as a model in pediatric gastroenterology. J Anim Sci. 2013 Oct;91(10):4713-29.

75. Mallard C, Vexler ZS. Modeling Ischemia in the Immature Brain. Stroke. 2015;46(10):3006-3011.

76. Mota-Rojas D, Villanueva-García D, Solimano A, et al. Pathophysiology of Perinatal Asphyxia in Humans and Animal Models. Biomedicines. 2022 Feb 1;10(2).

77. Chapados I, Cheung PY. Not all models are created equal: animal models to study hypoxic-ischemic encephalopathy of the newborn. Commentary on Gelfand SL et al.: A new model of oxidative stress in rat pups (Neonatology 2008;94:293-299). Neonatology. 2008;94(4):300-3.

78. Painter MJ. Animal models of perinatal asphyxia: Contributions, contradictions, clinical relevance. Seminars in Pediatric Neurology. 1995 1995/03/01/;2(1):37-56.

79. Raju TN. Some animal models for the study of perinatal asphyxia. Biol Neonate. 1992;62(4):202-14.

80. Ment LR, Stewart WB, Gore JC, et al. Beagle puppy model of perinatal asphyxia: Alterations in cerebral blood flow and metabolism. Pediatric Neurology. 1988 1988/03/01/;4(2):98-104.

8. Supplementary data

Supplementary Table 1. Supplementary blood gas analysis parameters, glucose, and body temperatures for the experimental study groups (control (C), therapeutic hypothermia (TH), hypoxia (H), hypoxia and therapeutic hypothermia (H+TH)), in neonatal Göttingen Minipigs. Blood gas analysis was performed with the i-STAT® Alinity V and the Accutrend® Plus System (Roche), using central venous blood. The assessment was performed at the end of the experiment (i.e., after 24 hours) for C and TH groups. For H, and H+TH groups, the parameters were determined during, at the end of the hypoxic insult and at the end of the 24 hours TH.
* Base excess (BE); bicarbonate (HCO_3); oxygen saturation (sO_2); partial pressure of carbon dioxide (PCO_2); partial pressure of oxygen (PO_2); total carbon dioxide (TCO_2); T °C (temperature at the moment of collection).

Control group (C) :

Subject	pH	PCO_2 (kPa)	PO_2 (kPa)	HCO_3 (mmol/L)	BE (mmol/L)	sO_2 (%)	TCO_2 (mmol/L)	Lactate (mmol/L)	Glucose (mg/dL)	T (°C)
C1	7.391	6.02	5.9	27.4	2	79	29	1.34	75	37.6
C2	7.145	12.19	5.8	31.5	3	62	34	1.73	133	37.7
C3	7.36	9.4	4.9	39.8	14	65	42	1.18	90	37.2
C4	7.079	14.46	3.8	32.1	2	31	35	0.3	96	37.8
C5	7.293	8.5	5.3	30.9	4	67	33	0.57	116	38.4
C6	7.336	8.4	7.1	33.7	8	84	36	0.72	74	37.5

Therapeutic hypothermia group (TH) :

Subject	pH	PCO_2 (kPa)	PO_2 (kPa)	HCO_3 (mmol/L)	BE (mmol/L)	sO_2 (%)	TCO_2 (mmol/L)	Lactate (mmol/L)	Glucose (mg/dL)	T (°C)
TH1	7.257	9.64	5.6	32.2	5	68	34	1	30	34.7
TH2	7.086	13.16	9	29.7	0	83	33	0.3	47	35.2
TH3	7.091	15.59	5.5	35.6	6	54	39	2.36	122	34.8
TH4	6.888	17.33	7.6	-	-	-	-	0.3	75	32.7
TH5	7.202	13.77	5.8	40.5	13	64	44	0.85	78	33.5
TH6	7.083	17.33	8.6	-	-	-	-	0.3	87	33.7

Hypoxia group (H):
During the hypoxic insult, blood gas analysis was performed at 30 minutes and approximately one hour after start. Once the blood lactate increased to the threshold of 8.7-10.7 mmol/L and pH decreased from the individual baseline determined before the insult, hypoxia was terminated, at approximately one hour. When the low-oxygen gas mixture ventilation was insufficient to achieve the targeted blood gas parameters, occlusion of the endotracheal tube (ETT) was performed for 7 minutes, thus adding hypercapnia to the hypoxia. * **Bold style**: Lactate measurements using the Accutrend® Plus System with the Accutrend® Lactate Strips (Roche). This monitoring system allows lactate determination more rapidly (90 seconds), using 1 drop of central venous blood.

Hypoxia group (H):

Time of experiment		pH	PCO$_2$ (kPa)	PO$_2$ (kPa)	HCO$_3$ (mmol/L)	BE (mmol/L)	sO$_2$ (%)	TCO$_2$ (mmol/L)	Lactate (mmol/L)	Glucose (mg/dL)	T (°C)	Length insult (minutes)	Comments
H1	Insult	7.08	15.4	6.4	34.1	4	64	38	5.87	120	37.9	20	
									5.7				
	End insult								**9.4**		38.3		
H2	Insult								**2.7**	72	37.1	38	
	End insult	6.91	17.3	1.7					10.38		37.4		
									10.3				
H3	Insult								**3.6**	117	33.9	35	
	Insult								**5.6**		34.1		
	End insult	6.9	17.3	1.7					7.96		34.1		
									8				
H4	Insult								**3.1**	42	38.6	30	
	End insult	6.97	17.3	1.9					11.81		38.4		
H5	Insult								**3.6**	78	37.5	20	Occlusion ETT for 7 min
	End insult								**7.7**		37.9		
H6	End insult								**6.2**	55	38	45	

Hypoxia and therapeutic hypothermia group (H+TH):

Time of experiment		pH	PCO$_2$ (kPa)	PO$_2$ (kPa)	HCO$_3$ (mmol/L)	BE (mmol/L)	sO$_2$ (%)	TCO$_2$ (mmol/L)	Lactate (mmol/L)	Glucose (mg/dL)	T (°C)	Length insult (minutes)	Comments
H+TH1	Preinsult	7.068	16.3	5	35.3	5	46	39	0.68		37.1	45	
	Insult	7.025	17.33	1.7					0.93		36.8		
	Insult								**2.3**		36.5		
	Insult	7.063	17.27	1.6	36.9	7	7	41	3.69		36.4		
	Insult								**6.2**	64	36		
	End insult								**10.7**		35.8		
	TH	7.244	11.72	5.8	38.1	11	68	41	0.38	90	34		
H+TH2	Preinsult								**1.9**	107	36.9	145	Occlusion ETT for 7 min
	Insult								**3.5**		37		
	Insult								**4.6**	79	37.2		
	Insult								**4.8**		37.4		
	Insult								**6.1**		37.5		
	End insult								**7.4**		36.5		
H+TH3	Preinsult								**1.5**	114	36.3	50	Note [1]
	Insult								**5.7**				
	End insult	7.115	13.05	1.6	31.5	2	8	34	8.19		38		
									7.6				
	TH	7.111	15.78	5.6	37.6	8	56	41	0.3	75	33.8		
H+TH4	Preinsult	7.275	10.08	3.9	35.1	8	45	37	2.96	89	37.3	50	
	Insult								**6.8**		37.3		

	End insult	7.054	11.95	1.8	25	-5	8	28	8.7		35.5		
									8.1				
H+TH5	Insult								**6**		36.4	55	
	Insult								**8.8**		36		
	End insult	6.983	15.39	1.7	27.4	-4	7	31	9.92	-	35.8		
H+TH6	Preinsult								**1.8**	85	37.9	30	
	Insult	6.84	17.33	3.5	-	-	-	-	4.22		37.9		
	End insult	6.688	17.33	2	-	-	-	-	11.2		36.3		
	TH	7.216	10.99	4.8	33.4	6	54	36	0.45	103	32.7		
H+TH7	Preinsult	7.244	12.3	5.4	39.9	13	63	43	1.96	59	36.4	100	Occlusion ETT for 7 min
	Insult								**4.5**		35.3		
	Insult	7.311	9.28	4.4	35.2	9	56	37	3.79		34.6		
									4.4				
	End insult								**14.8**				
	TH	7.085	17.33	5.8					0.39	112	34.5		

[1] *For H+TH3 the systemic hypoxic insult and 24 hours survival was achieved. However, at the end of the experiment, misplacement of the epigastric catheter was noticed. Consequently, this subject was excluded from the PK analysis. Since this animal was excluded due to a technical and not a physiological issue, its blood gas analysis parameters were still considered for the hypoxia statistical analysis.*

Supplementary Figure 1. Individual trend lines of the pharmacodynamic parameters and body temperatures at the moment of collection during the systemic hypoxic insult, in hypoxia (H) **(A)**, and hypoxia and therapeutic hypothermia (H+TH) **(B)** groups in neonatal Göttingen Minipigs.

* Beats per minute (bpm); end-tidal carbon dioxide ($EtCO_2$); heart rate (HR), fraction of oxygen-saturated hemoglobin (SpO_2).

(A)
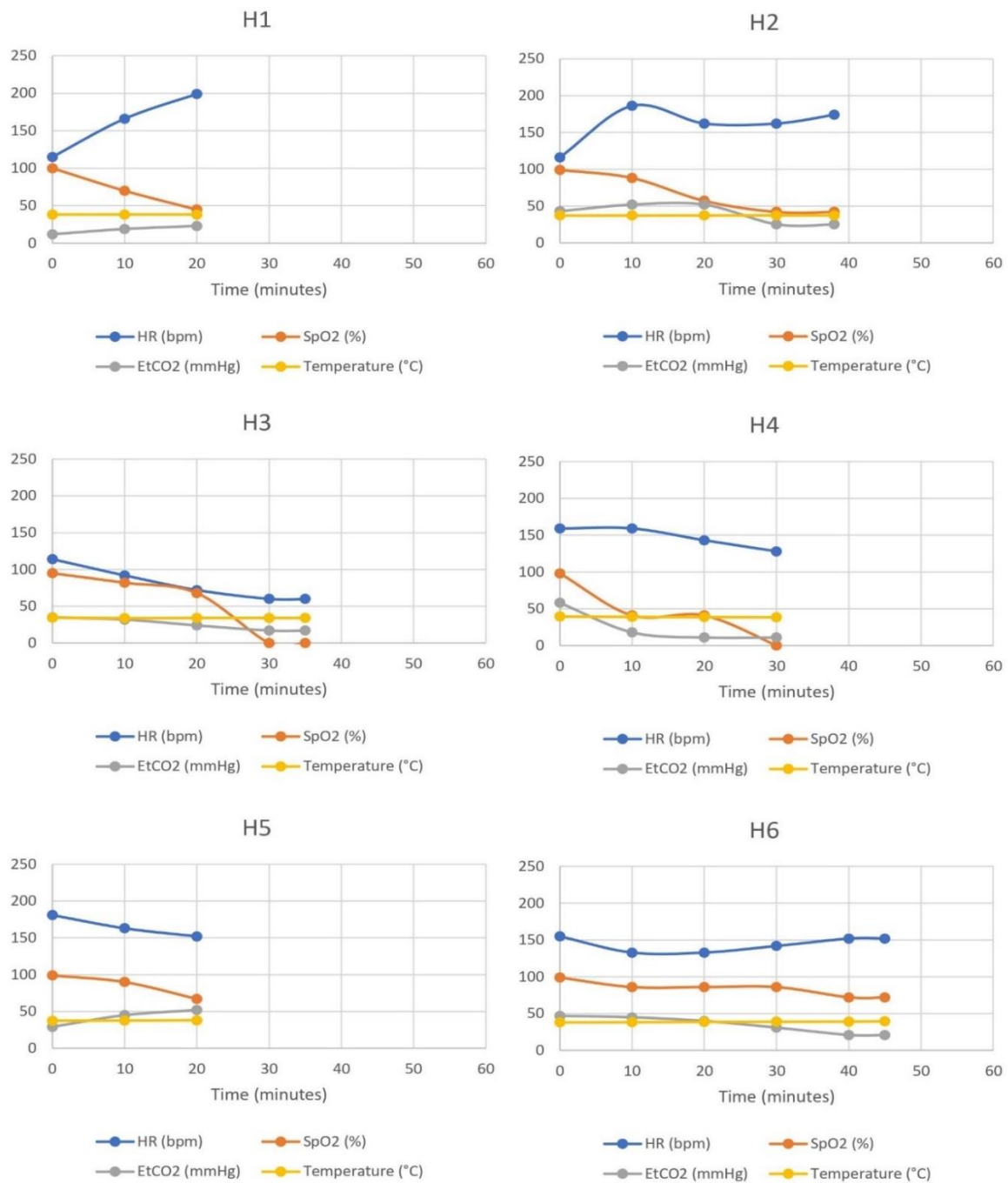
(B)

H+TH1
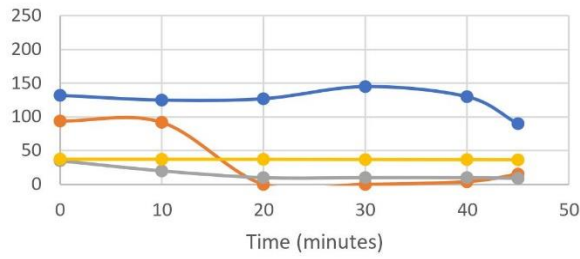
H+TH2
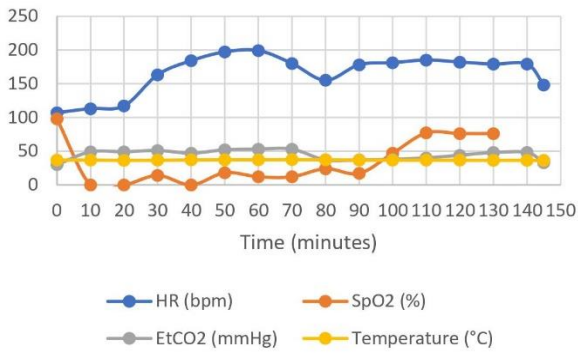
H+TH3 (Note 1)
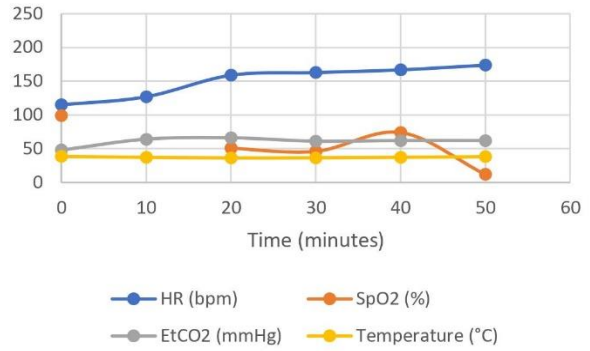
H+TH4
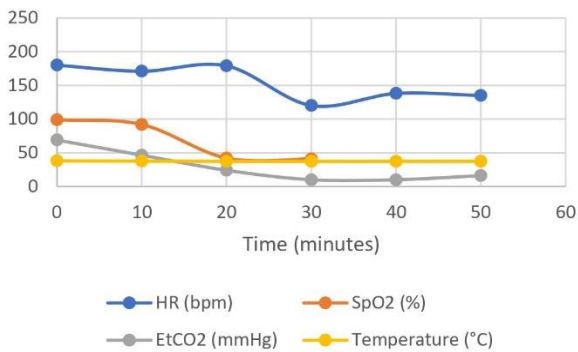
H+TH5
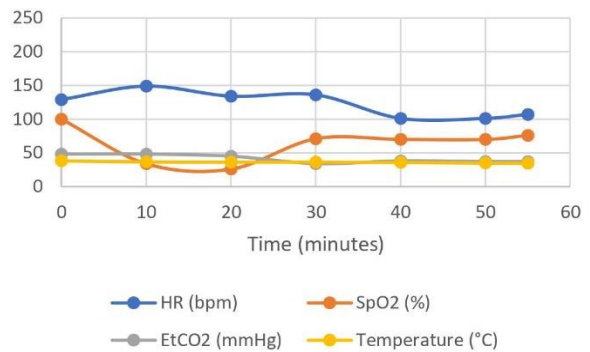
H+TH6
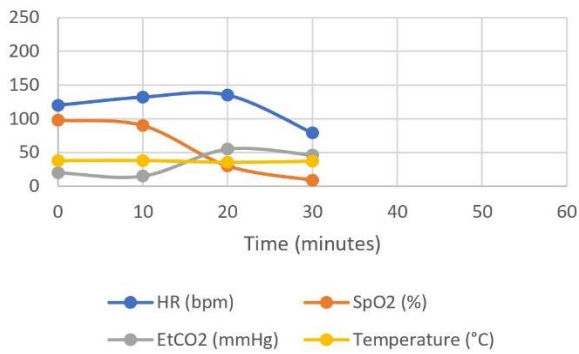
H+TH7
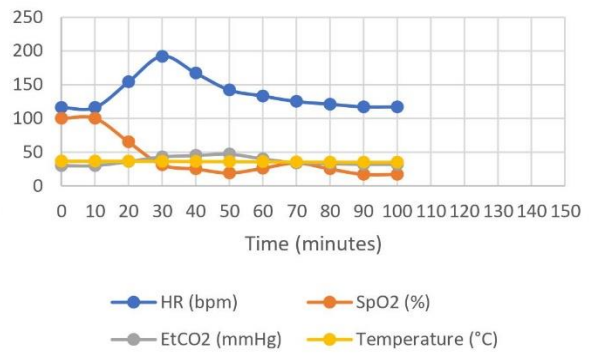
9. The value of pilot studies: conventional piglet hypoxia exploration

The techniques in developing piglets for experimentation require experience to master for the principal investigator and his assistant, that must be comfortable with both the surgery and anesthesia. This was achieved by performing a preliminary pilot study, involving conventional piglets, approved by the Ethical Committee of Animal Experimentation from the University of Antwerp (Belgium) (File 2020-62 entitled "I-PREDICT: Innovative physiology-based pharmacokinetic model to predict drug exposure in neonates undergoing cooling therapy using a pig model - pilot study"). This groundwork was essential before using Göttingen Minipigs in the main study (i.e., the development of a neonatal Göttingen Minipig model for dose precision in PA). Therefore, the aim of the pilot study was to develop the conventional piglet PA model to refine the techniques, and to optimize the experimental setup with a subsequent application in Göttingen Minipigs.

The sample size of the pilot study was determined by the experience and the personal judgment of the principal investigator and was limited to 8 animals. A research design of three experimental groups and one control group were conducted (Figure 12): the therapeutic hypothermia (TH) group included non-asphyxiated hypothermic piglets, the hypoxia (H) group included piglets undergoing systemic hypoxia (96% nitrogen; 4% oxygen) and the normothermia conditions, therapeutic hypothermia and hypoxia (H+TH) group contained hypoxic piglets undergoing TH and rewarming, and an additional control (C) group to which non-asphyxiated and non-hypothermic piglets were assigned. Due to the novelty of the procedures at the University of Antwerp, the experiments in the C group were performed during the first and second round in order to optimize the protocols and evaluate the consumables and devices. For every round of experiments, 2 conventional piglets out of the same litter were assigned to the intended group. These piglets were selected at the farm within 24 hours post-parturition and were approximately 5 hours of age. A general health check was performed at the farm in order make a suitable selection of the piglets used for this research (Table 6). The body weight was 1.12 (±0.13) kg (arithmetic mean ±SD), the piglets were evaluated clinically healthy and had suckled sufficient colostrum, in order to achieve normoglycemia and normotension, therefore, to enhance their survival. Piglets with lower/higher body weight or morbidities were excluded from the study. Thereafter, the selected piglets were transported to the central animal facility at University of Antwerp. Upon arrival, the piglets underwent a second physical examination and were accurately weighted. One piglet was examined and used in the experiment at the time for practical reasons. In the meantime, the second piglet remained in the transportation box until the first piglet was stabilized, being checked every 30 minutes.

Figure 12. The pilot study setup using conventional piglets (<24 hours of age); 2 rounds were conducted with the control group (hence 4 animals were used) while only 2 piglets were required for the hypoxia group, respectively one piglet for the therapeutic hypothermia and hypoxia and therapeutic hypothermia groups. Created with BioRender.com. * Sample size (n).

Control	Hypothermia	Hypoxia	Hypoxia + Hypothermia
n=4	n=1	n=2	n=1
Focus on monitoring and procedures, under normothermia and normoxia	Induction and maintenance of hypothermia (33.5°C) under normoxia	Induction of systemic hypoxia (96% nitrogen; 4% oxygen) under normothermia	Induction of systemic hypoxia followed by hypothermia
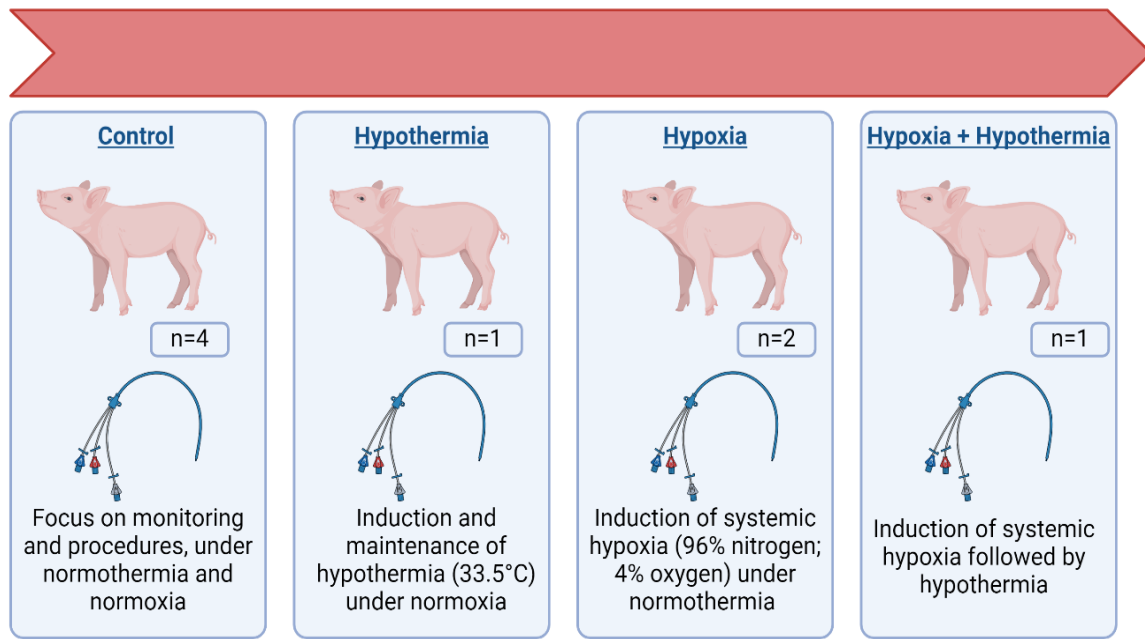
Table 6. Overview of the parameters considered in the examination of conventional piglets for the pilot study.

	Parameters
General	Normal attitude, active
Nervous system	Mentation, balance, absence of seizures Pupilar reflex, absence of miosis/mydriasis
Cardiovascular system	Thoracic auscultation: HR>160 beats per minute Pulse on the femoral artery: strong, synchrony with the heartbeat Oral cavity: color of mucosa (pink), capillary refill time (<2 seconds)
Respiratory system	Respiratory rate: 8-24 rpm SpO_2: >95%
Digestive and hepatic system	Absence of vomiting and internal parasites; existence of feces (yes/no) Glucose levels: 45-126 mg/dL
Renal system	Presence of urine (yes/no)

⚕	
Body temperature	38-39.5 °C

9.1. Anesthesia and venous access in the conventional piglet model

Figure 13. The anesthesia in the conventional piglets was initiated with sevoflurane using an anesthetic face mask **(A)** and maintained through an endotracheal tube **(B)**.
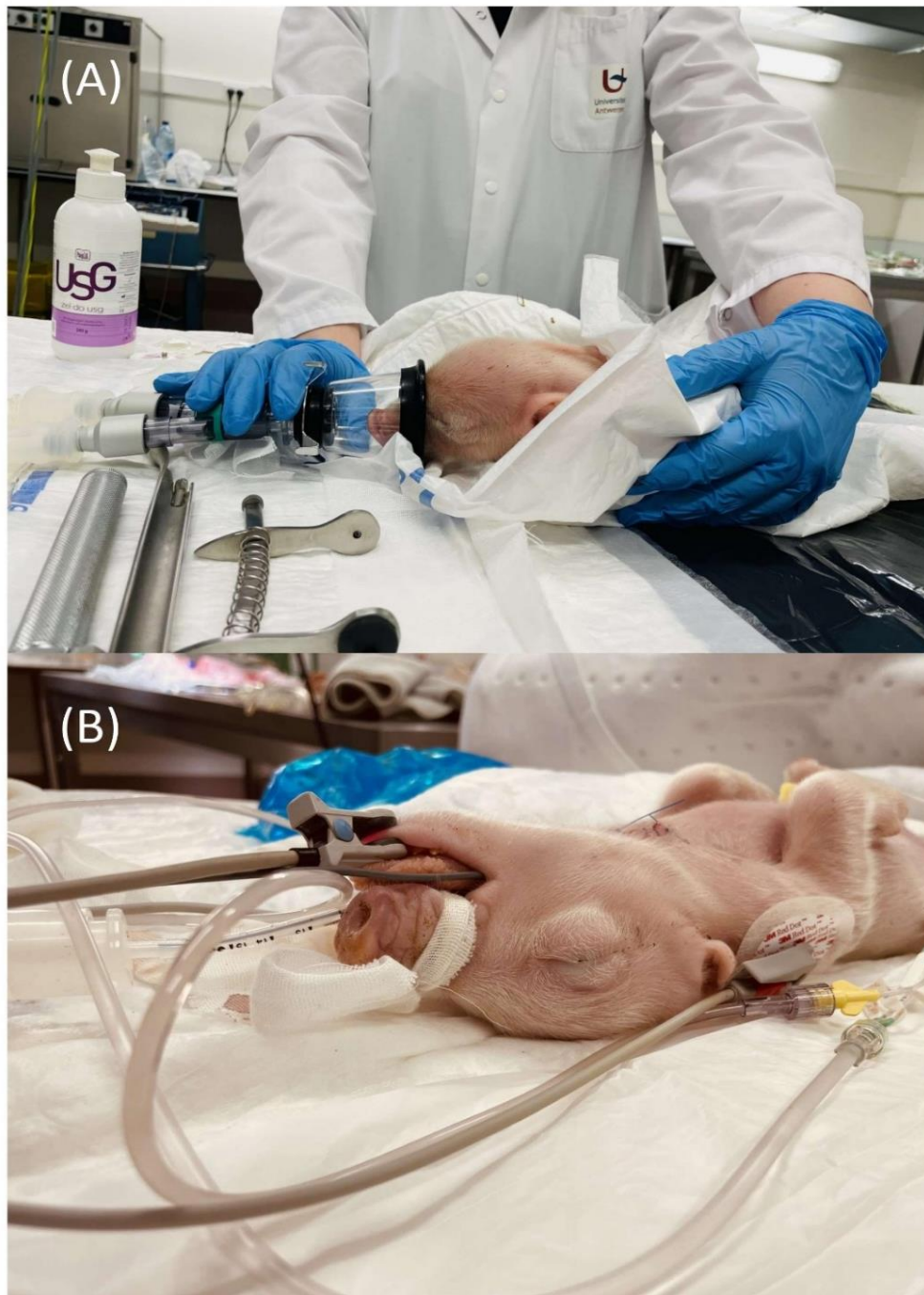
After positive physical evaluation, 0.3 mg/kg alfaxalone (Alfaxan, Zoetis), IM was administered as premedication. Subsequently, anesthesia was induced by sevoflurane (Dechra), 2-3% in 100% oxygen using an anesthetic face mask (Figure 13 (A)). The S/5 Aespire (Datex Ohmeda) machine was used for inhalant anesthesia, ventilation, and monitoring. The piglets were continuously monitored during the procedures. The cardiovascular system was checked using a pulse oximeter and ECG. Body temperature was monitored using an esophageal probe in a continuous manner and was controlled by heating blankets and hot packs, to maintain it at 38-39.5 °C. Glucose was measured at the start of the experiment and 2 hours later.

When venous access was established, a maximum of 0.2 mg/kg alfaxalone was administered IV to effect, together with the mask anesthesia for induction. For the maintenance of anesthesia, mechanical ventilation was provided using an ETT, the pediatric circle breathing system and the ventilator of the anesthetic machine. Between the pediatric breathing system and the anesthetics face mask, a heat and moisture exchanger (Tuoren) filter and a CO_2 flow sensor (from the capnograph), were present. When performing the intubation, a laryngoscope, and the desensitization of the larynx, provided by Xylocaine spray 10% (AstraZeneca), were carried out. Intubation was successfully established by using a 3.0 mm inner diameter endotracheal tube (Mallinckrodt™ Endotracheal tube, Covidien, Ireland; Figure 13 (B)). Regarding ventilation, pressure control ventilation with a pre-set initial peak inspiratory pressure of 11-13 cmH2O was used, leading towards a tidal volume of 8-10 mL/kg, a respiratory rate varying from 12-25 breaths/minute and an inspiratory-to-expiratory ratio of 1-to-2 in order to maintain an $EtCO_2$ between 35-45 mmHg.

Next, a pediatric double-lumen umbilical catheter (4 Fr, 20 cm length, 2x 0.19 mL, 11&12 mL/min; Vygon®) was inserted in the umbilical vein for maintenance fluids infusion: continuous IV infusion of fentanyl and midazolam in one lumen, and TPN infusion in the remaining lumen. For the insertion of the umbilical catheter, the upper part of the umbilical stump was cut (i.e., approximately 1 cm above the junction of the skin and the cord) to allow the identification of the umbilical vessels (Figure 14).

Figure 14. Umbilical venous catheterization in a conventional piglet. After cutting the end of the umbilical cord, the vessels were identified: the vein is large and thin walled, usually at the 12 o'clock position, while arteries are the two thick-walled, below the vein **(A)**. The catheter (double-lumen umbilical catheter; 4 Fr, 20 cm length, 2x 0.19 mL, 11&12 mL/min; Vygon®) was grasped between the thumb and forefinger and insert into the lumen of the dilated vein **(B).** Thereafter, the catheter was advances in the inferior vena cava, above the level of the diaphragm (between T8 and T9, above the liver) **(C)**. The confirmation of the successful catheterization was performed by observing blood return in the catheter or by attaching a syringe and aspirate to see if blood returns and flows easily in the syringe. The procedure was finalized with the fixation of the catheter suture (e.g., Vicryl 4-0, Ethicon), flushing, and attachment of the infusions.
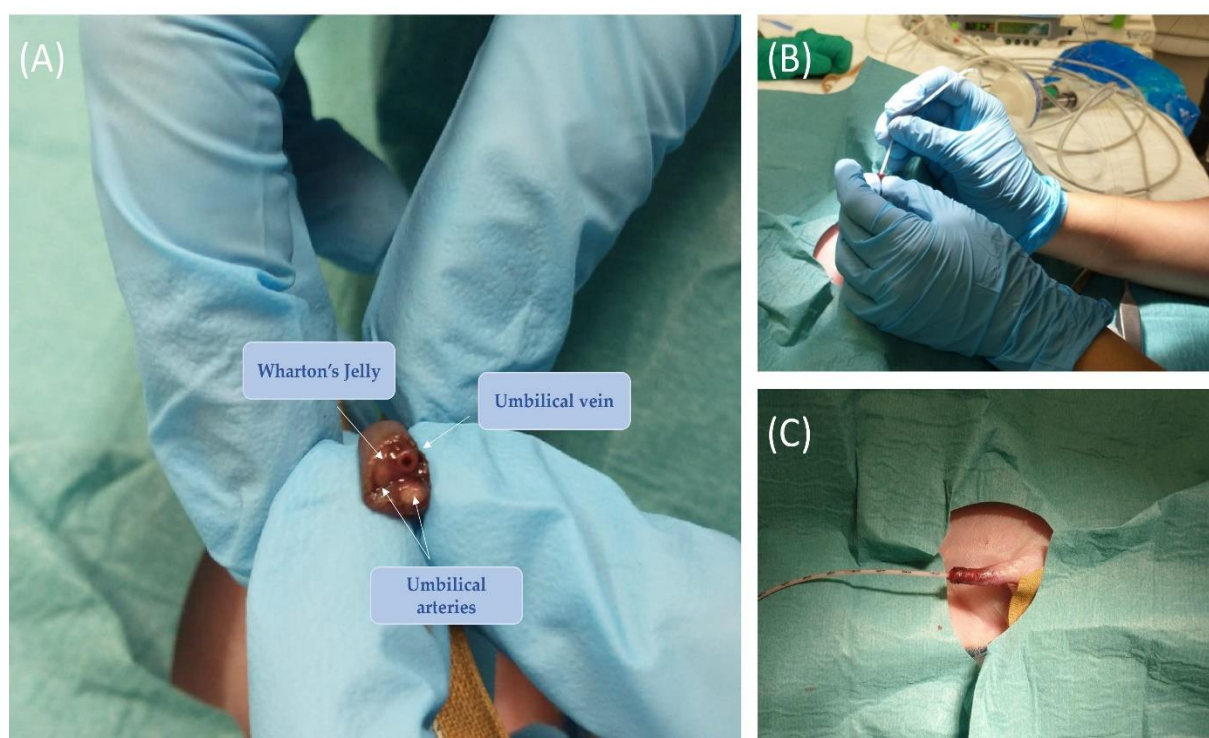
In order to facilitate multiple blood sampling, as well avoid the contamination of the blood sample with the studied drugs, a pediatric central venous catheter (Leader-Cath 2 E.L. Pediatric,3 Fr, 20G, 6 cm length; Vygon®) was placed percutaneously (Figure 15) or by making a small incision (Figure 16), in the external jugular vein. The catheterization was performed using the modified Seldinger technique, with an over-the-needle catheter (BD Venflon™, 22 G, 391451) used as a conduit for inserting the guide wire of the central venous catheter.

The TPN was infused via the umbilical catheter to maintain the normoglycemic status of the piglets. The TPN solution consisted of Baxter B.V.'s 20% glucose (34 mL/pig/day, hence 27 kcal), Vamin® 18 amino acids (8 g/kg/day, 70 mL/pig/day, hence 32.2 kcal), 20% Intralipid® emulsion (3 mL/day, hence 6 kcal), and Ringer's Lactate (Vetivex®), which consists of crystalloids and electrolytes (93 mL/pig) to obtain 200 mL of final TPN solution. This final solution was administered at the infusion rate of 4 mL/kg/h.

Midazolam (B. Braun; at 0.4 mg/kg/h) and fentanyl (Janssen; 10 µg/kg/h) were continuously and simultaneously infused (i.e., CRI) in the other lumen of the umbilical catheter to maintain general anesthesia. In case of hypotension and bradycardia, atropine (Sandoz) at 0.02-0.05 mg/kg IV was administered. After 2 hours from the initiation of general anesthesia, 20 mg/kg IV phenobarbital (Luminal®, Desitin) and topiramate (concentration of 10 mg/mL in 10% Captisol® diluted with sterile water, pH 7.5-8 and 20-22 °C temperature, starting from pure substance (CAS number 97240-79-4, supplied by Polpharma)) were slowly administered in the peripheral catheter. Blood sampling of 2 mL per sampling time point, using the BD Vacutainer® EDTA tubes, was performed using the central venous catheter, at the start of the experiment (i.e., time 0; T0), and at 1, 2, 4 and 6 hours from the experiment initiation. After sampling, the blood samples were centrifugated at 1500 g at room temperature for 15 minutes. The

resulting plasma was frozen at -80 °C. At the end of the experiment, urine was collected via cystocentesis and frozen at -80 °C.

Piglets were euthanized using pentobarbital sodium (Kela; 1.5 mL/5 kg IV). Death was confirmed by lack of heartbeat, pulse and breathing, a negative corneal and pedal withdrawal reflex, and greying of mucous membranes. During the subsequent necroscopy, the placement of the catheters and the presence of any other (macroscopical) lesions, that might be linked to the experimental procedure were investigated, in order to improve future rounds.

9.2. Therapeutic hypothermia, rewarming, and hypoxia in the conventional piglet model

Under general anesthesia, the stabilized and instrumented conventional piglets (i.e., maintained normothermic, normoglycemic, and normotensive) underwent the implementation of TH and systemic hypoxia protocols. Whole-body hypothermia was induced in less than 90 minutes and maintained for 12 hours, targeting a rectal temperature of 33.5 °C. This was achieved by discontinuing heating devices (i.e., including infrared lamp, warm packs, rescue blanket, heating mattress (OUB 60321 WH underbed blanket, OK)). For the H+TH group, TH started immediately after hypoxic insult completion. The piglets were then slowly rewarmed to normothermia (38.5 °C) at a rate of 0.5 °C/hour. Figure 17 depicts body temperature trends in the two hypothermic piglets (i.e., TH and H+TH groups).

Hypoxia was induced by a 4% oxygen and 96% nitrogen gas mixture, manually ventilated with the Veta3 anesthesia machine. Continuous monitoring included heart rate, systolic arterial pressure, $EtCO_2$ and SpO_2. Lactate and pH were assessed every 5-10 minutes. After an unsuccessful resuscitation attempt for the first piglet ventilated with the hypoxic gas mixture (approximately 30 minutes insult, Figure 18, (A)), subsequent hypoxic protocols were adjusted based on individualized lactate and pH thresholds (8.7-10.7 mmol/L and decreased pH from baseline). Hypoxia duration was then individualized, achieving acute insults of 10 minutes (Figure 18, (B)) and 15 minutes (Figure 18, (C)), followed by reoxygenation with 100% oxygen for 30 minutes and then 60% oxygen for the remaining experimental time.

Figure 15. Percutaneous external jugular vein catheterization in the conventional piglet model using a triangulation technique. **(A)** In dorsal recumbency, the neck was dissected to reveal landmarks and demonstrate the triangulation technique for identifying the external jugular vein. Dashed lines were drawn between palpable landmarks to create a large triangle, while solid lines extended from landmarks to midway points between primary lines, forming a smaller triangle. This smaller triangle, highlighted in yellow, aligns with the expected path of the external jugular vein and serves as an initial entry point for the introducer needle, following the approximate direction indicated by the blue line. Reproduced from Flournoy and Mani. **(B)** After premedication and mask induction a pediatric central venous catheter (Leader-Cath 2 E.L. Pediatric, 3 Fr, 20G, 6 cm length; Vygon®) was placed percutaneously using the technique, illustrated by from Flournoy and Mani. The monitoring was maintained using electrocardiogram (ECG).
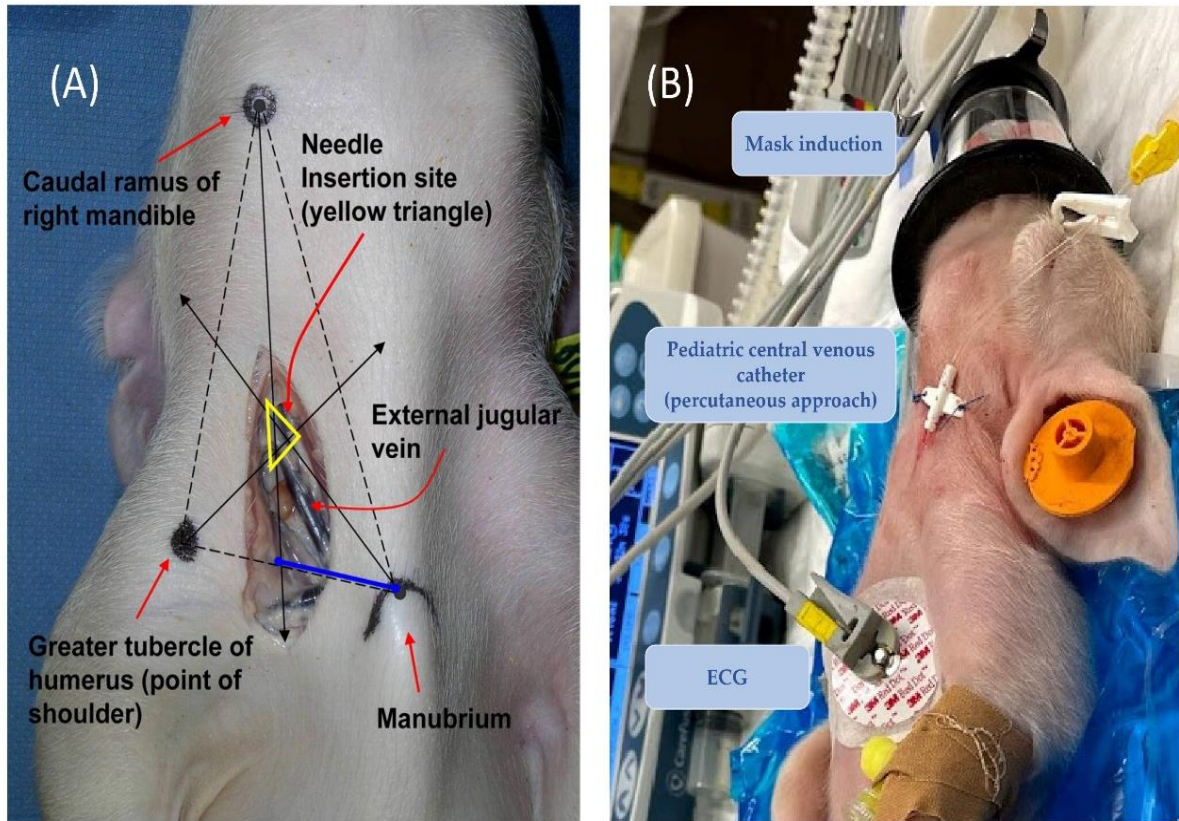
Figure 16. Anesthesia overview in the conventional piglet model. A peripheral catheter (Vasofix® Safety IV Catheter, 24 G, 4269075) on the epigastric vein, placed percutaneously, and a pediatric central venous catheter, placed surgically, ensured the drugs and maintenance infusions administration.
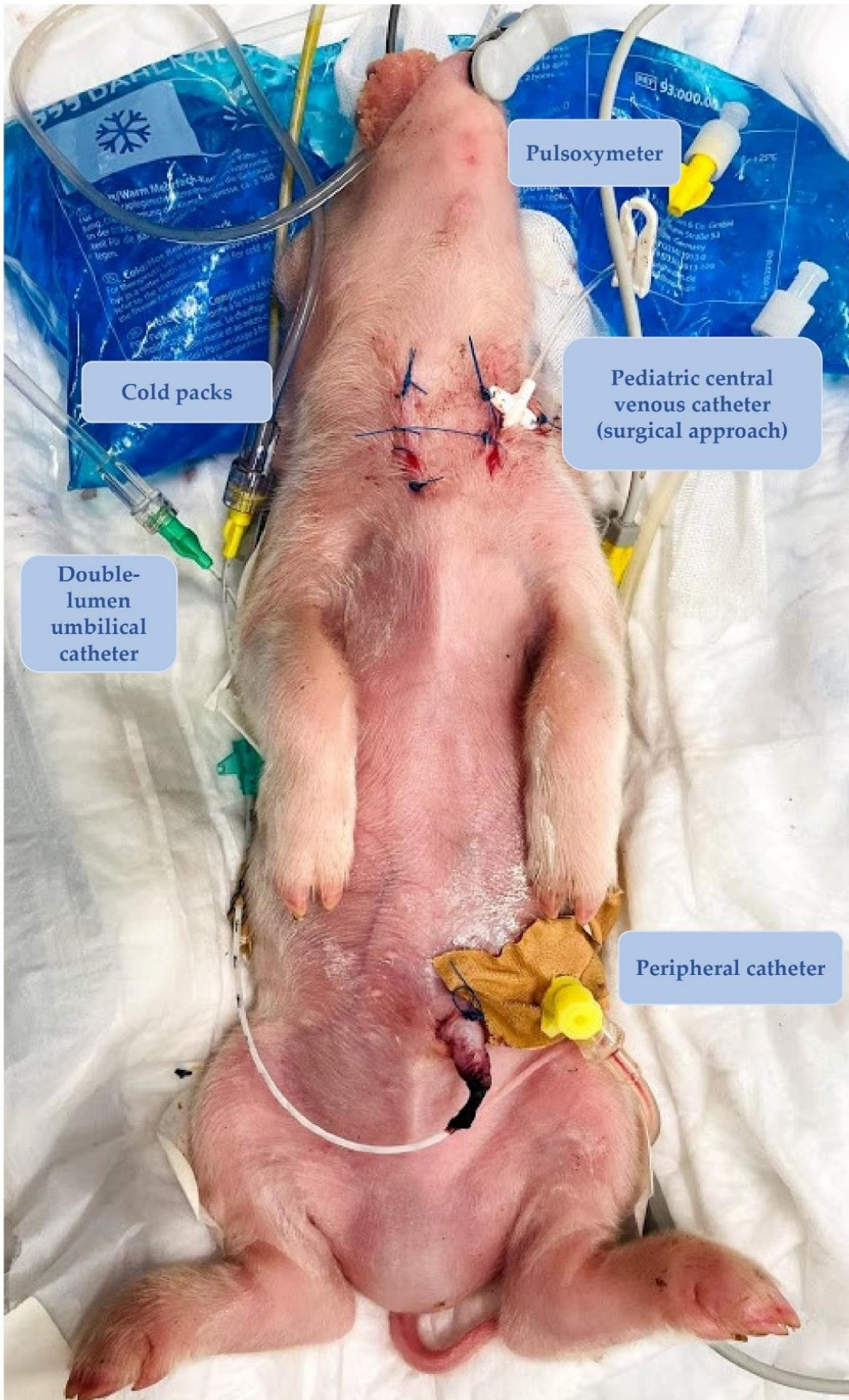
Figure 17. Body temperature trends in the two hypothermic conventional piglets (i.e., TH **(A)** and H+TH groups **(B)**).
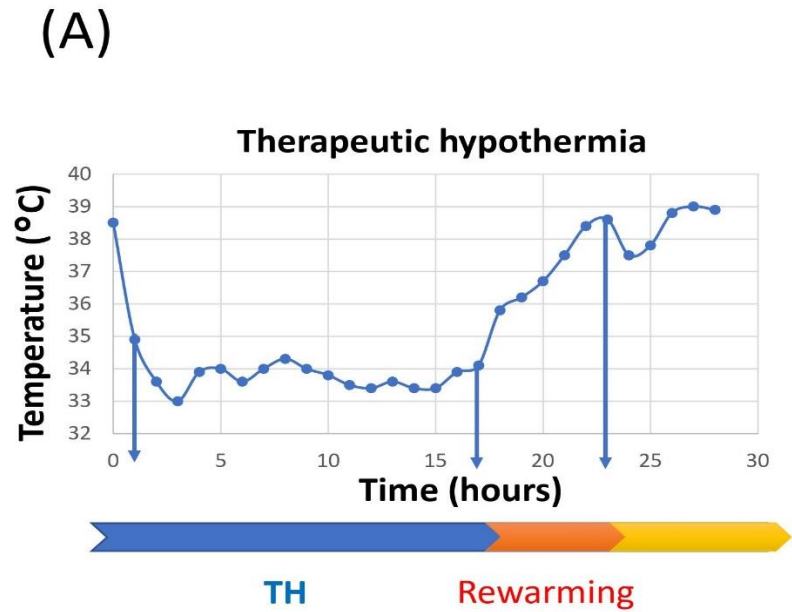
Therapeutic hypothermia Group	
Average TH	33.76 °C
Rewarming time	8 hours
Rewarming interval	33.9-38.6 °C
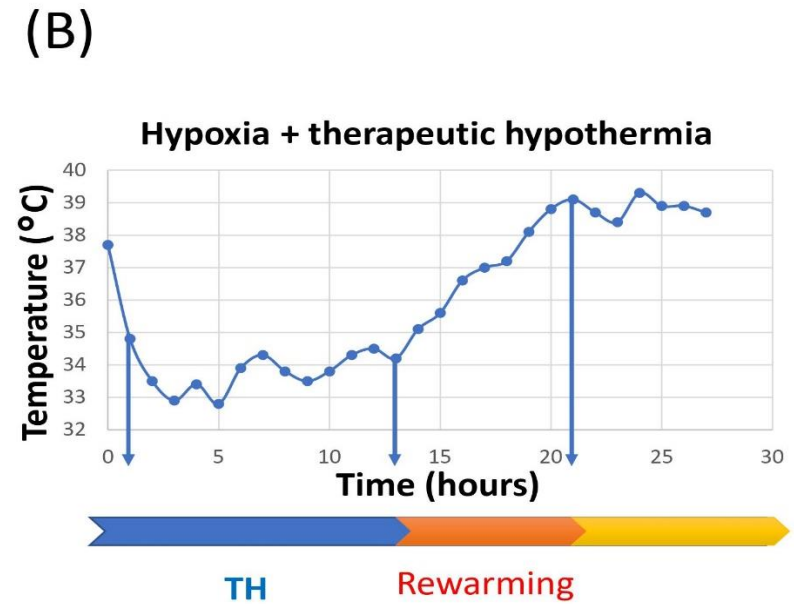
Hypoxia + Therapeutic hypothermia Group	
Average TH	33.82 °C
Rewarming time	7 hours
Rewarming interval	34.2 -38.8 °C

Figure 18. Lactate and pH trends in hypoxic conventional piglets. Hypoxia duration was individualized, achieving acute insults of 10 minutes **(B)** and 15 minutes **(C)**, followed by reoxygenation with 100% oxygen for 30 minutes and then 60% oxygen for the remaining experimental time.

CHAPTER 4:
Drug disposition in neonatal Göttingen Minipigs: exploring effects of perinatal asphyxia and therapeutic hypothermia

Drug disposition in neonatal Göttingen Minipigs: exploring effects of perinatal asphyxia and therapeutic hypothermia

Abstract

Asphyxiated neonates often undergo therapeutic hypothermia (TH) to reduce morbidity and mortality. Since both perinatal asphyxia (PA) and TH influence physiology, altered pharmacokinetics (PK) and pharmacodynamics (PD) are expected. Given that TH is the standard of care for PA with moderate to severe hypoxic-ischemic encephalopathy, disentangling the effect of PA versus TH on PK/PD is not possible in clinical settings. However, animal models can provide insights into this matter. The (neonatal) Göttingen Minipig, the recommended strain for nonclinical drug development, was selected as translational model. 4 drugs - midazolam (MDZ), fentanyl (FNT), phenobarbital (PHB), and topiramate (TPM), were intravenously administered under 4 conditions: control (C), therapeutic hypothermia (TH), hypoxia (H), hypoxia and TH (H+TH). Each group included 6 healthy male neonatal Göttingen Minipigs anesthetized for 24 hours. Blood samples were drawn at 0 (pre-dose), and 0.5, 2, 2.5, 3, 4, 4.5, 6, 8, 12, 24 hours post-drug administration. Drug plasma concentrations were determined using validated bioanalytical assays. The PK parameters were estimated through compartmental and non-compartmental PK analysis. The study showed a statistically significant decrease in FNT clearance (CL, 66% decrease) with approximately 3-fold longer half-life ($t_{1/2}$) in the TH group. The H+TH group showed a 17% reduction in FNT CL compared to the C group, however non-statistically significant. Although not statistically significant, trends towards lower CL and longer $t_{1/2}$ were observed in the TH and H+TH groups for MDZ and PHB. Additionally, TPM demonstrated a 28% decrease in CL in the H group compared to controls.

Significance statement

The overarching goal of this study using the neonatal Göttingen Minipig model was to disentangle the effects of systemic hypoxia and TH on PK, using 4 model drugs. Such insights can subsequently be used to inform and develop a physiologically-based pharmacokinetic model, which is useful for drug exposure prediction in human neonates.

1. Introduction

Hypoxic-ischemic encephalopathy (HIE), resulting from perinatal asphyxia (PA), is a severe medical condition associated with considerable neonatal morbidity and mortality. It affects 3 to 5 neonates out of every 1000 live births, with 0.5 to 1 per 1000 progressing to moderate or severe HIE [1]. Therapeutic hypothermia (TH) is the standard treatment for (near)term neonates with PA and moderate to severe HIE [1-4]. In these circumstances, most patients receive multiple drugs for sedation, analgesia, hemodynamic modulation, and treatment of suspected infections, convulsions, and other symptoms or diseases. Associated changes in pharmacokinetics (PK; concentration-time) and pharmacodynamics (PD; concentration-effect) may affect these treatment modalities and, consequently, the clinical outcome. More specifically, these alterations in absorption, distribution, metabolism, and excretion (ADME), may potentially lead to under- or overdosing of these patients [5].

In clinical studies, unraveling the effects of PA and TH on PK/PD is challenging, mainly because TH is the standard care for moderate to severe HIE [6]. Therefore, in this context, animal models offer insights into how systemic hypoxia and TH separately affect drug disposition. The pig represents a large animal model used in translational research, due to its anatomical, physiological, and biochemical resemblance to humans [7,8]. Pigs provide an advantage compared with other animal species, including rodents, dogs, and non-human primates, since their larger body size at birth enables sampling without substantially impacting physiology [9]. Additionally, the hypoxic insult and the resulting hemodynamic derangements can be managed in the pig model, in contrast to smaller animal models that often face limitations in terms of equipment for monitoring purposes [9,10]. Göttingen Minipigs are the preferred pig strain in nonclinical drug development because of their genetic consistency and well-documented characteristics, providing valuable historical control data for pharmaceutical companies in nonclinical safety studies [2,11-15]. Concerning drug development research, high homology to the human phase I drug metabolizing cytochrome P450 (CYP) family has already been described in minipigs (63-84% amino acid identity) [16,17] and the ontogeny of CYP enzymes activity in juvenile Göttingen Minipigs was shown to be comparable to the corresponding age groups in human [13,15].

The overarching goal of this study was to disentangle the effects of systemic hypoxia and TH on PK, using 4 model drugs selected based on their different physicochemical properties, PK characteristics and/or clinical relevance: midazolam (MDZ, intermediate extraction ratio (ER)), fentanyl (FNT, high ER), phenobarbital (PHB, low ER) and topiramate (TPM, primarily renally excreted unchanged; explored as a potential neuroprotective drug when administered orally, its current usage in clinical care is uncommon). Such insights can be used to inform and develop Göttingen Minipig and human physiologically-based pharmacokinetic (PBPK) models, which is the aim of the I-PREDICT project [2].

2. Materials and methods

2.1. Experimental study design

The animal study was conducted at Ellegaard Göttingen Minipigs A/S, Dalmose, Denmark, with approval from the Danish Ethics Committee (protocol code 2022-15-0201-01163 on the 5th of

April 2022). 4 conditions were investigated, i.e., control (C), therapeutic hypothermia (TH), hypoxia (H), hypoxia and TH (H+TH), with 6 neonatal (<24 hours of age) male Göttingen Minipigs per condition. A preliminary power analysis was performed to determine the correct sample size. This was based on the standard deviation (SD) of dexmedetomidine clearance (CL; [18]). Using CL as the outcome variable for the 4 conditions, 6 piglets per condition were required to detect a 50% reduction, as reported for dexmedetomidine [18], for the H+TH compared to controls (power of 80%; test-wise significance level of 0.05).

Figure 1. Neonatal Göttingen Minipig groups with their therapeutic interventions and sampling schedule. 4 conditions were investigated, i.e., control (C), therapeutic hypothermia (TH), hypoxia (H), hypoxia and TH (H+TH), with 6 piglets per condition (n=6). A blood sample was withdrawn pre-drug administration and subsequently, 10 times after the drug administration, resulting in a total of 11 samples over the study period for each Göttingen Minipig. Urine samples were collected at 12 hours and 24 hours via cystocentesis. Figure created with BioRender.com. * Degree Celsius (°C); hour (h); constant rate infusion (CRI); intravenous (IV).
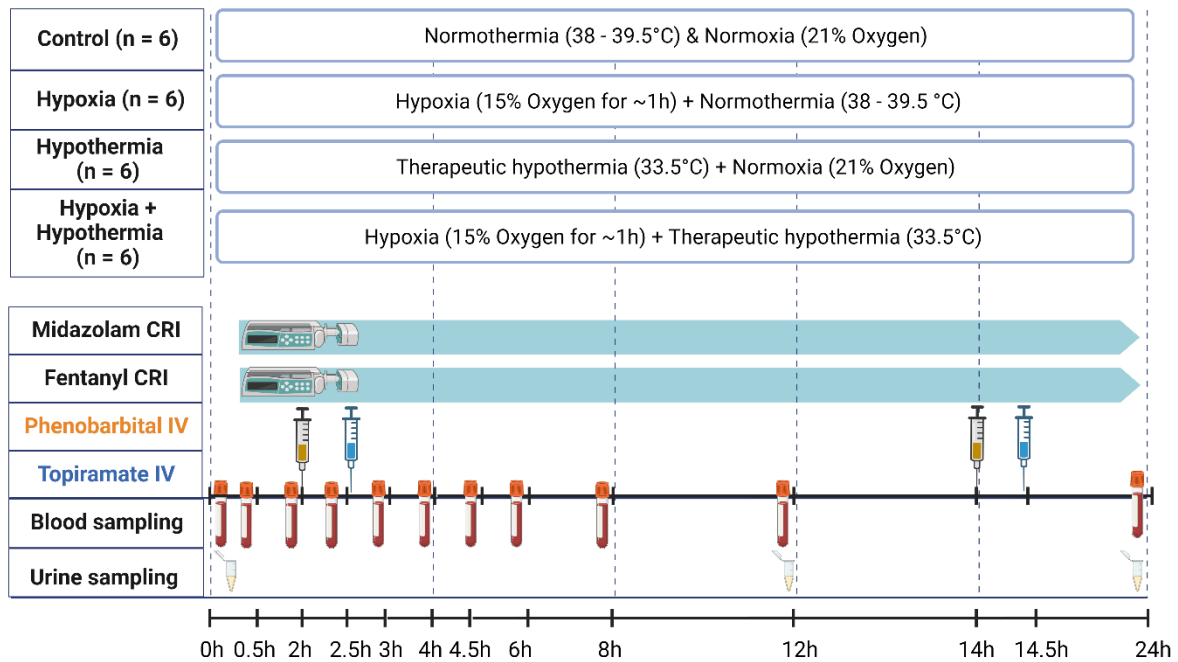
The Göttingen Minipigs' selection criteria and the study procedures to obtain the hypoxic and hypothermic conditions were previously described, together with their limitations and technical challenges (Chapter 3) [10]. The neonatal Göttingen Minipig groups, the drug administration and the sampling regimen are depicted in Figure 1. Briefly, within 24 hours of partus Göttingen Minipigs weighing approximately 0.6 kg were sedated with 4 mg/kg (Zoletil® 50, Virbac), containing tiletamine 50 mg/mL and zolazepam 50 mg/mL, intramuscularly, followed by induction of anesthesia with isoflurane (IsoFlo®, Zoetis). Given the demonstrated impact of inhalant anesthesia on drug disposition when used concomitantly with other drugs [19,20] and its non-inclusion in therapeutic approaches for neonates with PA/HIE, its administration was restricted to a 10-minute induction period and discontinued during maintenance. Mechanical ventilation was performed, and central venous and peripheral

catheters were inserted for continuous infusion, drug administration, and blood sampling. Heart rate (HR; measured via electrocardiogram monitoring), end-tidal carbon dioxide (EtCO$_2$) and respiratory rate (both measured via capnograph), rectal body temperature, as well as the fraction of oxygen-saturated hemoglobin (SpO$_2$; measured using a pulse oximeter) were assessed continuously. The urinary bladder was emptied before the start of the experiment. Urine samples were collected via cystocentesis at 12 and 24 hours, and the total volume of urine produced throughout the experiment was recorded. Chapter 6 of this thesis will present the urinary output, along with creatinine levels and estimated glomerular filtration rates, in the neonatal Göttingen Minipig groups.

2.2. Drug dosing and administration

Table 1 provides an overview of the study drugs, including details such as the drug class, clinical use, metabolic pathways in humans and pigs, metabolites, and some technical, physiological, and physicochemical information. The drug administration route was exclusively intravenous (IV). Midazolam at 0.4 mg/kg/h and FNT at 10 μg/kg/h were combined in a single syringe and administered IV using a constant rate infusion (CRI) of 2 mL/h till the end of the experiment. Before CRI initiation, a loading dose of MDZ (0.3 mg/kg) and FNT (3 μg/kg) was administered via IV bolus injection. 2 hours after the start of the infusion, and subsequently 12 hours later, PHB and TPM, both at a dose of 20 mg/kg, were slowly (short-time infusion of 10 minutes) and separately administered IV, with 15 minutes delay in between administrations. An IV formulation of TPM has been developed for research purposes of the long-term treatment of neonatal seizures, using a cyclodextrin matrix, Captisol® (Ligand Pharmaceuticals) [21-24]. A similar formulation was prepared in a laminar flow cabinet at a concentration of 10 mg/mL TPM in 10% Captisol® diluted with sterile water, pH 7.5-8 and 20-22 °C temperature, starting from TPM pure substance (CAS number 97240-79-4, supplied by Polpharma), at the University of Antwerp. To maintain homeostasis, an IV CRI of total parenteral nutrition (TPN) was administered until the end of the experiment. Glucose levels were closely monitored at the beginning of anesthesia and every 12 hours after. The Göttingen Minipigs received 217 kJ/kg/day, accounting for 50% of the energetic requirement in neonatal piglets (550 kJ/kg/day) [25,26]. This included 8 g/kg/day of amino acids (Vamin Fresenius Kabi, Nederland B.V.), 20% glucose (Baxter B.V.), and lipids (INTRALIPID® Fresenius Kabi, Lipid Injectable Emulsion, Mfr. Std. Soybean Oil 20%). The total volume of infusion, considering the dilution of drugs and TPN, was 6 mL/kg/h.

Table 1. Overview of the study drugs (i.e., midazolam (MDZ, [14,15,27,28]), fentanyl (FNT, [14,15,29-31]), phenobarbital (PHB, [4,15,27,32-34]) and topiramate (TPM, [21-24,35,36])) with the clinical use, metabolic pathways, and metabolites, as well as some technical, physiological, and physicochemical information. * Cytochrome P450 (CYP); extraction ratio (ER); fraction unbound (f$_u$).

Drug	Brand name, manufacturer, formulation	Primarily clinical use	Major adult human metabolites	Major adult human metabolic pathway	Major adult pig metabolic pathway	ER, Protein binding, f_u
MDZ	Midazolam, Accord®, solution for injection	Sedative, antiepileptic	1-Hydroxymidazolam	[1] CYP3A4; CYP3A5	CYP3A22; CYP3A29; CYP3A39 and CYP3A46	Intermediate ER, Albumin, 95%
FNT	Fentadon®, Dechra, solution for injection	Analgesia	Norfentanyl	[1] CYP3A4		High ER, Albumin and α-1 glycoprotein, 80-85%
PHB	Luminal®, Desitin, solution for injection	Antiepileptic	p-Hydroxy phenobarbital; conjugated p-Hydroxy phenobarbital	CYP2C9; CYP2C19; CYP2E1	CYP2C33, CYP2C42, and CYP2C49	Low ER, Albumin, 49%
TPM	10 mg/mL Topiramate (CAS number 97240-79-4, Polpharma) solubilized in 10% Captisol® Ligand Pharmaceuticals solution for injection	Neuroprotective antiepileptic	Primarily renally excreted unchanged			84%

[1] *In humans, CYP3A4 is hardly expressed in utero and evolves to adult levels after infancy. Instead, it is documented that CYP3A7 is most active in human fetal life and is almost absent after the first 2 weeks of postnatal life [37].*

2.3. Hypoxia and therapeutic hypothermia

Asphyxia and hypoxia are similar terms used to describe an inadequate oxygen supply to cells and tissues. Asphyxia happens when the air passage is blocked, while hypoxia occurs when there is an inadequate delivery, uptake, or utilization of oxygen by the body's tissues [38]. Nonetheless, the PA pathophysiology is complex, involving various risk factors such as gestational, fetal, and placental complications [39], one of the major cause being the interruption of placental blood flow [40]. The combination of reduced oxygen supply (hypoxia) and reduced blood supply (ischemia) may contribute to dysfunction in various neonatal organs [38]. In our study, the systemic hypoxic insult was induced by ventilating the neonatal Göttingen Minipigs with a gas mixture containing 15% oxygen and 85% nitrogen (i.e., 10 out of 13 subjects), or by combining the low oxygen gas mixture with asphyxia, performing endotracheal tube occlusion, for 7 minutes (i.e., 3 out of 13 subjects) [10]. The duration of endotracheal tube occlusion was determined based on the recommended time for umbilical cord clamping in a conventional piglet model of asphyxia [41]. An increase in blood lactate and a decrease in blood pH, previously observed in an asphyxia pig model [42] and in a pilot study conducted by our research group [10], were determined biomarkers to validate the systemic hypoxic insult. As result, the blood lactate values in Göttingen Minipigs were (arithmetic mean ±SD) 0.97±0.53 mmol/L under normoxic conditions, compared to 9.56±2.27 mmol/L under hypoxic conditions. For blood pH, the values were 7.26±0.12 under normoxic conditions and 7.00±0.16 under hypoxic conditions (complete descriptive data on blood gas analysis in Chapter 3).

2.4. Plasma sample preparation and storage

Blood samples were drawn from a central venous catheter placed in the jugular vein at 0 (pre-dose), and 0.5, 2, 2.5, 3, 4, 4.5, 6, 8, 12, 24 hours post-drugs administration. The start of the general anesthesia and co-administration of MDZ and FNT was designated as time 0 (T0). Separate sampling and administration lines were used to avoid contamination of the blood for PK analysis with the drugs. Therefore, two other IV catheters were placed for drug administration: either two peripheral IV catheters (on the epigastric and lateral saphenous veins), or one peripheral and one central (umbilical vein and other jugular vein). Micro sampling, with a volume of 500 µL per time point, was performed to ensure that all the collected volume remained below 15% of the total amount of the piglets' blood [43]. After each collection, all tubes (BD Microtainer, K2EDTA, Closure Color Lavender, 365974) were gently inverted to thoroughly mix the blood with the additive and centrifuged at 3000 g at room temperature, for 15 minutes. This resulted in 3 layers (from top to bottom): plasma, leucocytes (buffy coat), and erythrocytes. Immediately after this step, plasma was aspirated, and transferred to cryotubes which were stored at -80 °C until bioanalysis. The liquid chromatography tandem mass spectrometry (LC-MS/MS) quantification (Supplementary data) was achieved with two validated bioanalysis methods, presented in Supplementary Table 1 for MDZ, 1-hydroxymidazolam (1-OH-MDZ), FNT and norfentanyl (N-FNT) and Supplementary Table 2 for PHB and TPM.

2.5. Pharmacokinetic analysis

PKanalix®, MonolixSuiteTM (version 2021R2) [44] was used to estimate the PK parameters (volume of distribution (V_d), CL, and half-life ($t_{1/2}$)) of MDZ, FNT, PHB, and TPM, assuming a one-compartment model with first order elimination kinetics. The equations describing the concentrations following IV bolus administered drugs (i.e., PHB and TPM) and drugs administered via an IV bolus loading dose followed by an IV infusion maintenance dose (i.e., MDZ and FNT) are presented as supplementary data (Supplementary Figure 1). All plasma concentrations of MDZ and FNT within the first 24 hours were included in the analysis. Due to insufficient data between 12 and 24 hours, and the administration of a second bolus of PHB and TPM at the 12-hour mark, only data within the first 12-hour interval were included. Furthermore, the elimination rate constant (k) values were calculated through linear regression using R version 4.2.2 (2022-10-31 UCRT) and RStudio (2022.12.0 Build 353) for the drugs administered as bolus (i.e., PHB and TPM), while the one compartment model was used for the drugs administered as CRI (i.e., MDZ and FNT). The linear regression output of PHB and TPM are presented in Supplementary Table 3. As drug elimination rates in these neonatal Göttingen Minipigs were very limited, statistical significance ($P<0.05$) on the linear regression analysis for elimination slopes was used as selection criterion for subsequent calculation of k (13 subjects (54%) for PHB and 14 subjects (58%) for TPM, out of the initial 24 were included, as some subjects were excluded due to inaccurate k estimation (Supplementary Table 3)). PKanalix® was also used to calculate the area under the curve (AUC) values (0-12 hours) for the 4 model drugs as well as the MDZ and FNT metabolites, all based concentrations expressed in molar units. Regarding metabolites, when the concentrations of 1-OH-MDZ and N-FNT fell below the lower limit of quantification (LLOQ), these values were substituted with the respective LLOQ/2 for further analysis.
Microsoft Excel® version 16.0.1, 2021 (Microsoft Corporation, Redmond, WA, United States) was used to calculate the metabolite-to-parent drug ratio, based on molar AUC of the drugs administered continuously (i.e., MDZ and FNT) and their metabolites (i.e., 1-OH-MDZ and N-FNT). MS Excel® was also used to calculate the accumulation ratio (R_{ac}) by dividing the 24-hour plasma concentrations by plasma concentrations at 12 hours for each Göttingen Minipig, thereby assessing the capacity of drug removal from the body.

2.6. Statistical analyses of the pharmacokinetic and pharmacodynamic parameters

Firstly, given the non-normal distribution of the V_d, CL, $t_{1/2}$, and k datasets, the geometric mean was derived by applying a base 10 logarithm transformation, computing the mean of the logarithms, and subsequently converting the results back to the linear domain through antilog transformation. Secondly, 95% confidence intervals (CI) were calculated. Pharmacokinetic parameters values determined for each Göttingen Minipig categorized in function of the group (4 groups, with 6 values/group) were also used as input data for statistical analysis. Furthermore, the HR and the body temperature values recorded at 0, 0.5, 2, 2.5, 3, 4, 4.5, 6, 8, 10, 12, 14, 16, 18, 24 hours for each Göttingen Minipig were considered for statistical analysis. Since the PD data had normal distribution, the arithmetic means across all mentioned time points for each Göttingen Minipig were categorized in function of group, resulting in 4 groups, with 6 values/group. All the statistical analysis were performed in JMP® Pro 16 (SAS Institute Inc., Cary, NC, United States). The normality and homogeneity of variances were

tested by the Shapiro-Wilk and Levene's test, respectively. When necessary, a log transformation was applied to meet the assumptions for parametric testing. When the assumptions were fulfilled, One-Way Analysis of variance (ANOVA) was used for each estimated PK parameter to test the underlying null hypothesis of no difference between groups. Further, *P*<0.05 was considered statistically significant and a Tukey's-Kramer honestly significant difference method was conducted. When the normality and homogeneity of variances assumptions were not met, a non-parametric Wilcoxon/Kruskal-Wallis (rank sums) was performed, followed by nonparametric comparisons for each pair using the Wilcoxon method. Figures were designed in GraphPad Prism version 8.0.2 (GraphPad Software, Inc. San Diego, California USA).

3. Results

This study achieved the target sample size of 24 neonatal Göttingen Minipigs, with an equal distribution of 6 minipigs per group. A total of 311 plasma samples were analyzed. Metabolite concentrations were below the LLOQ in 83 samples, i.e., in 19 samples for 1-OH-MDZ and in 64 samples for N-FNT. The PK parameter values are detailed in Table 2 and illustrated in Figure 2 and Figure 3.

Table 2. A summary of the relevant pharmacokinetic (PK) parameters of the study drugs: **(A)** midazolam; **(B)** fentanyl; **(C)** phenobarbital; **(D)** topiramate, in neonatal Göttingen Minipigs stratified by the condition involved: control, therapeutic hypothermia and/or systemic hypoxia. Data are presented as geometric mean and 95% confidence intervals, with n representing the number of subjects per group considered for the calculations. * Area under the curve (AUC); clearance (CL); elimination rate constant (k); half-life ($t_{\frac{1}{2}}$); accumulation ratio (R_{ac}); volume of distribution (V_d).

Parameter / Group	Control	Hypoxia	Therapeutic hypothermia	Hypoxia and Therapeutic hypothermia
(A) Midazolam				
V_d (L/kg) (n=6)	1.64 (0.85; 3.17)	1.47 (0.50; 4.32)	1.55 (0.74; 3.25)	1.23 (0.56; 2.68)
CL (mL/kg/min) (n=6)	7.40 (3.90; 14.05)	5.89 (3.78; 9.19)	3.27 (2.31; 4.63)	6.04 (2.53; 14.44)
$t_{\frac{1}{2}}$ (hour) (n=6)	2.57 (1.78; 3.71)	2.89 (0.97; 8.56)	5.49 (2.58; 11.69)	2.34 (0.61; 9.09)
k (1/hour) (n=6)	0.27 (0.19; 0.39)	0.24 (0.08; 0.71)	0.12 (0.27; 0.06)	0.29 (0.07; 1.14)
24-hour plasma concentrations (ng/mL) (n=6)	1270.7 (703.96; 1837.44)	1201.16 (670.08; 1732.24)	2209.47 (1342.21; 3076.74)	1780.3 (598.89; 2961.71)
AUC 0-12 (hour*nmol/mL) (n=6)	26.23 (12.11; 40.34)	26.42 (9.08; 43.76)	35.93 (14.16; 57.69)	27.25 (14.64; 39.85)

ratios of metabolite-to-parent drug (n=6)	0.06 (0.01; 0.11)	0.07 (0.05; 0.09)	0.05 (0.02; 0.08)	0.05 (0.02; 0.09)
R_{ac} (n=6)	1.14 (0.78; 1.51)	0.97 (0.60; 1.35)	1.41 (1.03; 1.78)	1.47 (1.10; 1.85)

Parameter / Group	Control	Hypoxia	Therapeutic hypothermia	Hypoxia and Therapeutic hypothermia
(B) Fentanyl				
V_d (L/kg) (n=6)	3.43 (1.02; 11.45)	3.06 (1.07; 8.75)	3.34 (1.71; 6.52)	1.09 (0.56; 2.11)
CL (mL/kg/min) (n=6)	38.45 (26.43; 55.93)	27.79 (19.28; 40.05)	12.96 (5.11; 32.84)	31.98 (24.05; 42.52)
$t_{1/2}$ (hour) (n=6)	1.03 (0.29; 3.65)	1.27 (0.38; 4.16)	2.97 (0.76; 11.54)	0.39 (0.18; 0.87)
k (1/hour) (n=6)	0.67 (0.19; 2.38)	0.54 (0.16; 1.78)	0.23 (0.06; 0.90)	1.75 (0.79; 3.88)
24-hour plasma concentrations (ng/mL) (n=6)	5.32 (4.36; 6.28)	6.87 (2.88; 10.86)	14.56 (2.62; 26.51)	7.05 (3.80; 10.29)
AUC 0-12 (hour*nmol/mL) (n=6)	0.15 (0.10; 0.21)	0.20 (0.15; 0.25)	0.25 (0.14; 0.35)	0.19 (0.12; 0.26)
ratios of metabolite-to-parent drug (n=6)	0.11 (0.003; 0.27)	0.05 (0.03; 0.07)	0.06 (0.01; 0.11)	0.09 (0.04; 0.13)
R_{ac} (n=6)	1.18 (1.03; 1.33)	0.80 (0.44; 1.16)	1.49 (0.86; 2.11)	1.26 (1.11; 1.41)

Parameter / Group	Control	Hypoxia	Therapeutic hypothermia	Hypoxia and Therapeutic hypothermia
(C) Phenobarbital				
V_d (L/kg) (n=3)	0.61 (0.33; 1.14)	0.63 (0.56; 0.71)	0.66 (0.45; 0.96)	0.63 (0.21; 1.92)
CL (mL/kg/min) (n=3)	0.21 (0.07; 0.67)	0.13 (0.06; 0.28)	0.26 (0.05; 1.27)	0.15 (0.09; 0.24)
$t_{1/2}$ (hour) (n=3)	32.88 (11.37; 95.01)	55.41 (25.08; 122.38)	28.49 (5.00; 162.39)	44.47 (34.73; 56.93)
k (1/hour) (n=3)	0.00915 (0.00309; 0.02708)	0.00634 (0.00196; 0.02053)	0.01075 (0.00184; 0.06271)	0.00713 (0.00621; 0.00817)
24-hour plasma concentrations (µg/mL) (n=6)	49.50 (42.43; 56.57)	45.94 (38.05; 53.83)	44.77 (37.21; 52.33)	58.67 (43.75; 73.59)

AUC 2-12 (hour* nmol/mL) (n=6)	1156.60 (911.53; 1401.67)	1325.69 (934.76; 1716.62)	1164.04 (909.44; 1418.64)	961.34 (601.33; 1321.35)
R_{ac} (n=6)	1.88 (1.58; 2.20)	2.10 (1.56; 2.63)	1.85 (1.42; 2.27)	1.93 (1.75; 2.11)

Parameter / Group	Control	Hypoxia	Therapeutic hypothermia	Hypoxia and Therapeutic hypothermia
(D) Topiramate				
V_d (L/kg) (n=4)	0.77 (0.36; 1.63)	0.63 (0.53; 0.76)	0.85 (0.34; 2.12)	0.70 (0.58; 0.85)
CL (mL/kg/min) (n=4)	0.31 (0.29; 0.34)	0.22 (0.06; 0.77)	0.83 (0.09; 7.10)	0.33 (0.21; 0.54)
$t_{1/2}$ (hour) (n=4)	28.38 (12.29; 65.54)	32.67 (9.75; 109.41)	11.92 (3.45; 41.25)	24.22 (14.71; 39.87)
k (1/hour) (n=4)	0.01059 (0.00452; 0.02484)	0.00929 (0.00273; 0.03164)	0.02544 (0.00715; 0.09046)	0.01256 (0.00753; 0.02094)
24-hour plasma concentrations (µg/mL) (n=6)	30.01 (22.11; 37.92)	44.31 (34.02; 54.61)	37.26 (23.35; 51.16)	41.23 (35.01; 47.44)
AUC 2.5-12 (hour*nmol/mL) (n=6)	606.03 (475.74; 736.32)	707.62 (596.91; 818.34)	577.98 (380.03; 775.93)	764.83 (666.74; 862.92)
R_{ac} (n=6)	1.61 (1.34; 1.88)	1.77 (1.56; 1.98)	2.12 (1.72; 2.51)	1.71 (1.56; 1.85)

Figure 2. A summary of the relevant pharmacokinetic (PK) parameters of the study drugs in neonatal Göttingen Minipigs. The names of each group were abbreviated as the following - control (C), therapeutic hypothermia (TH), hypoxia (H), hypoxia and TH (H+TH). Data is presented as geometric mean and 95% confidence intervals: volume of distribution (V_d); clearance (CL); half-life ($t_{1/2}$); elimination rate constant (k); 24-hour plasma concentrations; area under the curve (AUC). The number of animals used in this analysis was 6 per group for each PK parameter and drug, with the exception of phenobarbital and topiramate, where 3 and 4 individuals, respectively, were used to calculate the geometric mean and 95% confidence intervals for V_d, CL, $t_{1/2}$, k.
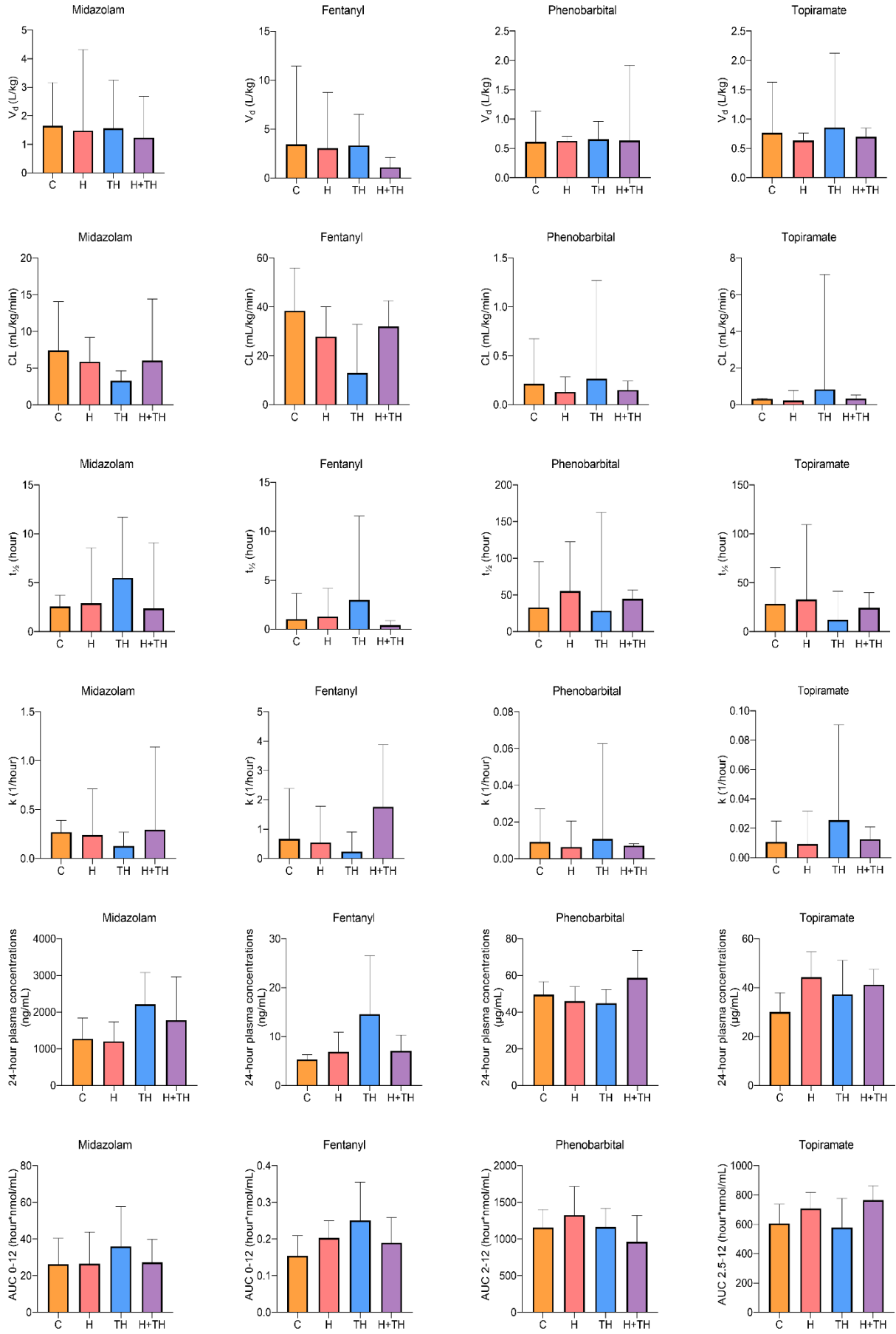
Figure 3. The accumulation ratio (R_{ac}) of **(A)** midazolam, **(B)** fentanyl, **(C)** phenobarbital, and **(D)** topiramate. The names of each group were abbreviated as the following - control (C), therapeutic hypothermia (TH), hypoxia (H), hypoxia and TH (H+TH). The bars represent medians with the whiskers presenting the interquartile range, which is the range between the first (25th percentile) and third quartiles (75th percentile). Datapoints that lie beyond the whiskers are outliers. The number of samples included was 6 per each group. A significantly higher R_{ac} was observed for TPM in the TH group ($P=0.0107$) compared to the C group and for FNT in the TH group ($P=0.0306$) and H+TH group ($P=0.0453$) compared with the H group. p-value: *, $P<0.05$; **, $P<0.005$; ***, $P<0.0005$; ****, $P<0.0001$.
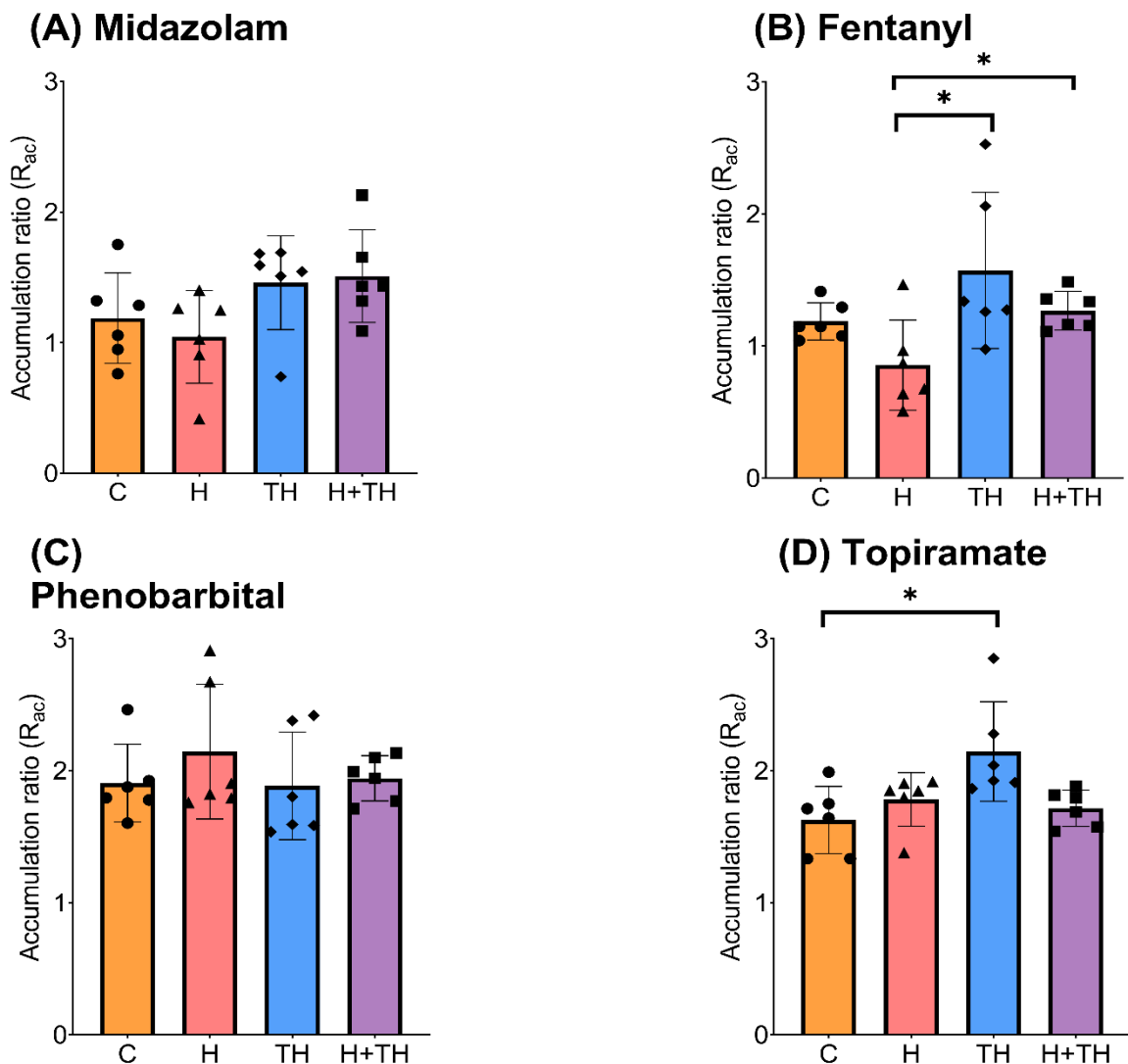
Figure 4. Pharmacokinetic parameter estimates of the study drugs in neonatal Göttingen Minipigs. The names of each group were abbreviated as the following - control (C), therapeutic hypothermia (TH), hypoxia (H), hypoxia and TH (H+TH). Data is presented as scatter plots, median with the whiskers presenting the interquartile range, which is the range between the first (25th percentile) and third quartiles (75th percentile), for: volume of distribution (V_d); clearance (CL); half-life ($t_{\frac{1}{2}}$); elimination rate constant (k); 24-hour plasma concentrations;

area under the curve (AUC). The number of animals used in this analysis was 6 per group for each PK parameter and drug, except for phenobarbital and topiramate, where 3 and 4 individuals, respectively, were used for V_d, CL, $t_{1/2}$, k. Datapoints that lie beyond the whiskers are outliers. Statistically significant differences were found only for fentanyl, with a significantly lower CL (*P*=0.0099) in the TH group compared to the control. Additionally, the 24-hour plasma concentrations were statistically significantly higher in the TH group compared to C (*P*=0.0026), H (*P*=0.0271) and H+TH (*P*=0.0337) groups. p-value: *, *P*<0.05; **, *P*<0.005; ***, *P*<0.0005; ****, *P*<0.0001.
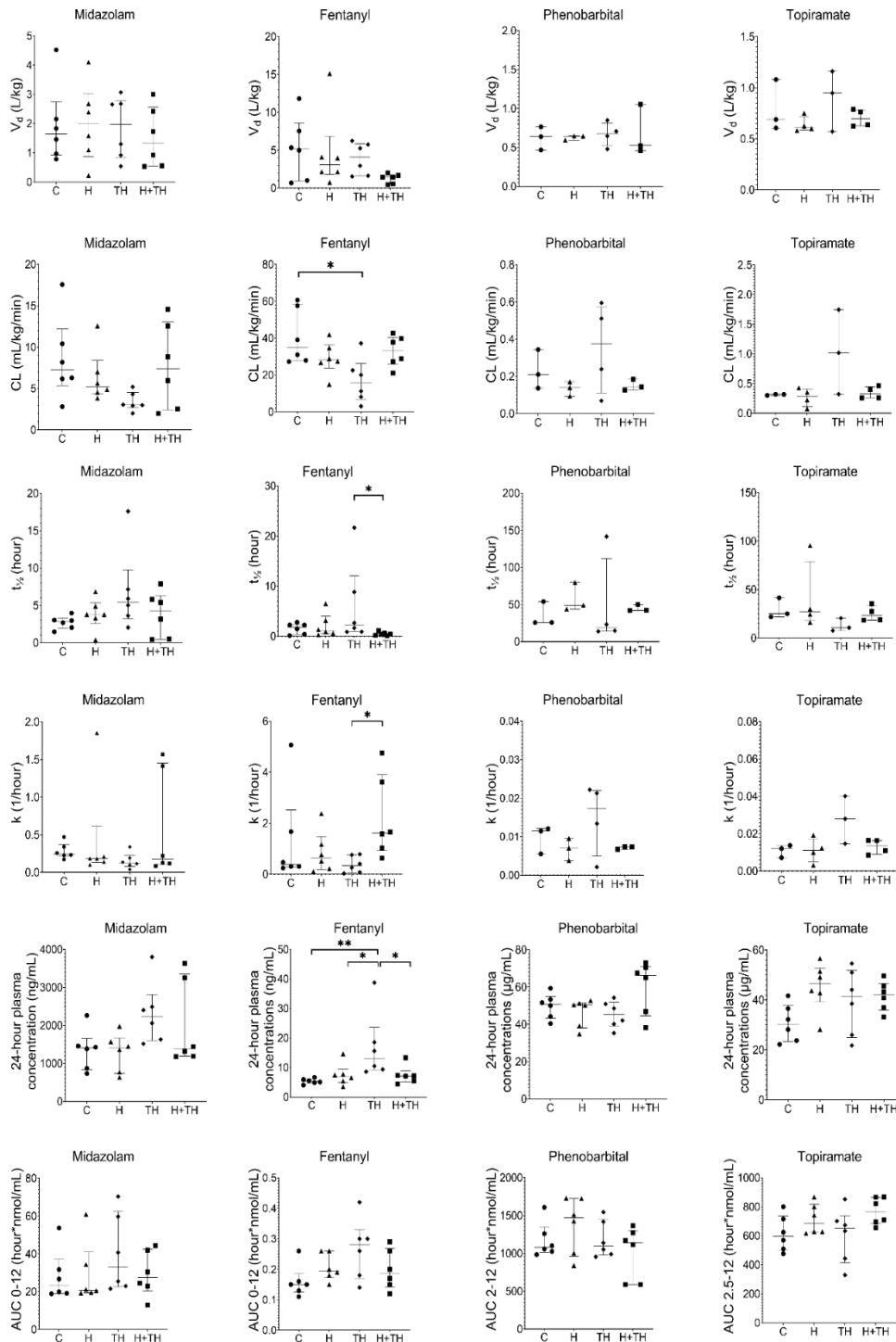
Statistical analysis was performed to detect any differences in PK between the investigated groups (Figure 4). Concerning FNT, a statistically significant decrease in FNT CL (P=0.0099; 66% decrease), with an approximately 3-fold longer $t_{1/2}$ was observed in the TH group compared to the C group. The 24-hour plasma concentrations were statistically significantly higher in the TH group compared to C (P=0.0026), H (P=0.0271) and H+TH (P=0.0337) groups. The H+TH group showed a 17% reduction in FNT CL with a 62% shorter $t_{1/2}$ compared to the C group, however non-statistically significant. Additionally, the $t_{1/2}$ of the H+TH group was significantly shorter (P=0.0244) than the TH group. A decrease in TPM CL of 28% for the H group was detected compared to the C group. No statistically significant differences were found for the investigated PK parameters between groups for MDZ and PHB, although modifications in the TH and H+TH groups were observed. Specifically, the TH group exhibited a 56% decrease in MDZ CL with approximately a 2-fold longer $t_{1/2}$ compared to the C group. Additionally, in the H+TH group, there was an 18% decrease in MDZ CL compared to the C group. For PHB, the H+TH group showed a 30% decrease in CL with a 35% longer $t_{1/2}$ compared to the C group.

Finally, to assess the extent of drug accumulation during repeated administrations, two graphical presentations were performed: a bar chart of the R_{ac} determined in each group (Figure 3) and a scatter plot of the plasma concentration at 12 and 24 hours (Figure 5), for each drug. Figure 5 revealed that plasma concentrations were higher at 24 hours compared to 12 hours, especially for PHB and TPM, due to the second bolus administered at the 12-hour mark, while for MDZ and FNT the 24-hour concentrations were comparable with the ones at 12 hours. This was confirmed with R_{ac} values, illustrated in Figure 3, where accumulation was close to 2 for PHB and TPM, while the R_{ac} of MDZ and FNT showed limited or no accumulation. A significantly higher R_{ac} was observed for TPM in the TH group (P=0.0107) compared to the C group and for FNT in the TH group (P=0.0306) and H+TH group (P=0.0453) compared with the H group.

Figure 5. Scatter plots of the 12 hours and 24 hours plasma concentrations of **(A)** midazolam, **(B)** fentanyl, **(C)** phenobarbital, and **(D)** topiramate in neonatal Göttingen Minipigs to assess the drugs accumulation pattern. Circle = control group (non-hypoxia, normothermia); triangle = hypoxia group; diamond = therapeutic hypothermia (TH) group; square = hypoxia + TH (H+TH) group; full red symbols = 24-hours concentrations, empty symbols = 12-hours concentrations.

(A) Midazolam

(B) Fentanyl

(C) Phenobarbital

(D) Topiramate
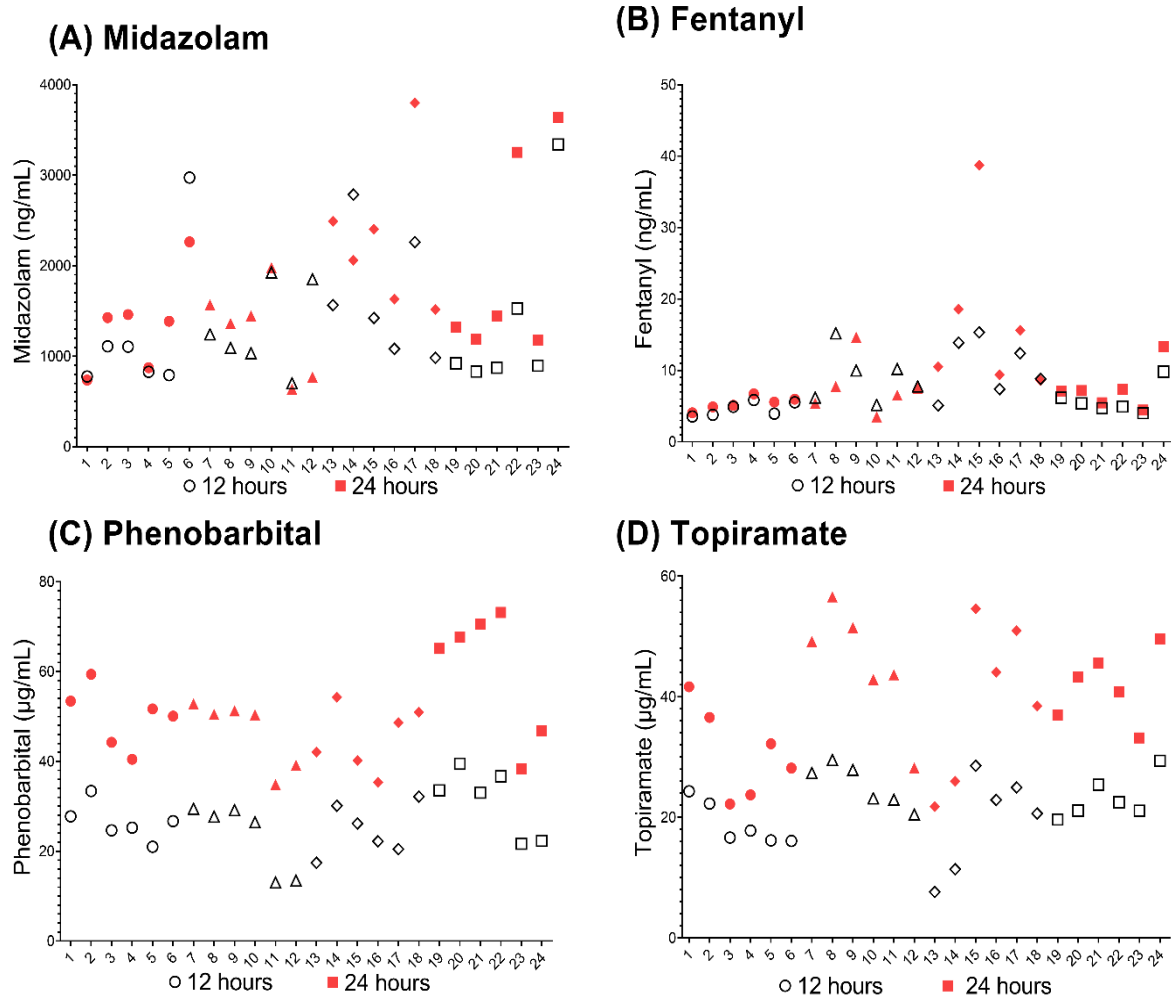
Bar charts of the HR and body temperature, based on the arithmetic means for each Göttingen Minipig across all mentioned time points, were designed with the purpose to detect any differences between the investigated groups (Figure 6, (A)). Statistically significant lower HR ($P<0.0001$) and body temperature ($P=0.0051$) were detected for both TH and H+TH groups compared to C and H groups. Moreover, the arithmetic mean (±SD) over time plots in each group are depicted, indicating successful control of these parameters in each neonatal Göttingen Minipig (Figure 6, (B)).

Figure 6. Hypoxia and/or therapeutic hypothermia-related differences in heart rate and body temperature during the 24-hour experiment. The statistical analysis **(A)** was performed using as input data the arithmetic mean across 0, 0.5, 2, 2.5, 3, 4, 4.5, 6, 8, 10, 12, 14, 16, 18, 24-hours' time points, for each neonatal Göttingen Minipig categorized in function of group: control (C), therapeutic hypothermia (TH), hypoxia (H), hypoxia and TH (H+TH). The trend lines for each group indicating successful control of hemodynamic parameters are depicted **(B)**. The bars represent arithmetic means, and the error bars indicate standard deviations. The number of samples included was 6 per each group. Statistically significant lower HR ($P<0.0001$) and body temperature ($P=0.0051$) were detected for both TH and H+TH groups compared to C and H groups. p-value: *, $P<0.05$; **, $P<0.005$; ***, $P<0.0005$; ****, $P<0.0001$. * °C, degree Celsius; bpm, beats per minute.

(A)

(B)
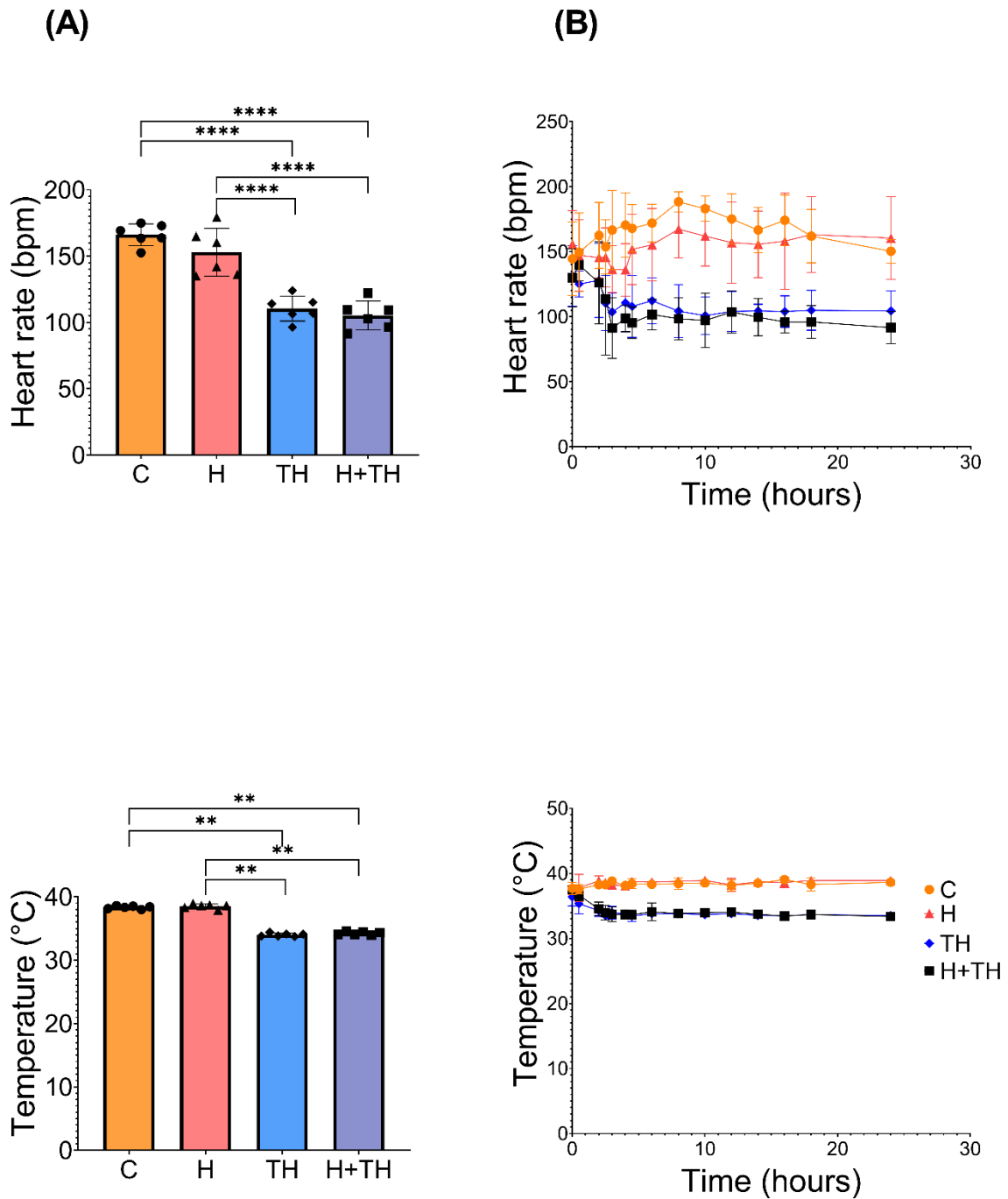
4. Discussion

The overarching goal of this study was to disentangle the effects of systemic hypoxia and TH on PK in neonatal Göttingen Minipigs, using 4 model drugs. The main study findings as well as the underlying mechanistic hypotheses, the alignment with the human clinical data, the challenges and limitations encountered, and potential further steps will be discussed.

4.1. Impact of therapeutic hypothermia on drug disposition in asphyxiated neonates

Given the influence of both TH and PA on physiology, our primary hypothesis in this study was that TH substantially decreases the metabolic CL in asphyxiated neonates, necessitating drug dosing adaptations. Data regarding the PK of various drugs in this specific population, as well as the gaps in understanding how PA and TH affect drug ADME have been previously reviewed [5,45,46]. For example, Lutz et al. reviewed 36 studies using 15 compounds [46]. It was shown that the impact of PA/TH on drug CL is dependent on the route of elimination and it was most pronounced for renal elimination during TH (i.e., no difference for PHB, -21% for 1-OH-MDZ, -24% for lidocaine, -21% to -47% for morphine, -25% to -35% gentamicin, -40% amikacin) [46]. By conducting an unstructured exploratory search in PubMed until December 2023, we compiled relevant PK parameter values for our study drugs in human neonates, undergoing TH or not (Table 3) to identify similarities and discrepancies with our Göttingen Minipig data.

Table 3. A summary of the relevant pharmacokinetic (PK) parameters of the study drugs: (A) midazolam; (B) fentanyl; (C) phenobarbital; (D) topiramate, in human neonates. Data are presented as mean and standard deviation (±SD). * Body weight (BW); degree Celsius (°C); clearance (CL); gestational age (GA); hypoxic-ischemic encephalopathy (HIE); sample size (n); postnatal day (PND); traumatic brain injury (TBI); therapeutic hypothermia (TH); half-life ($t_{½}$); volume of distribution (V_d).

Comments	Age	BW (kg)	n	$t_{½}$ (hour)	CL (mL/kg/min)	V_d (L/kg)	Ref
(A) Midazolam							
Neonates	GA 39.8±1.6	3.49±0.67	50	-	1.68	1.55	[4]
Mechanically ventilated neonates	PND 1-5	1.9±0.7	15	12±0.6	1.7±1.8	1.2±0.6	[47]
Mechanically ventilated neonates	PND 0-9	0.7-5.2	187	9.9	1.2±0.2	1±0.2	[48]
[1] Asphyxiated Neonates	GA, weeks +days 39+3 (36+0 to 41+4)	3.5 (2.15; 4.92)	53	5	0.94 (0.60; 1.27)	6.76 (5.85; 7.67)	[49]
(B) Fentanyl							
Neonates	PND 1	3.0±1.1	-	4.90±1.88	16.2±2.59	5.94±1.47	[50]
(C) Phenobarbital							

Neonates	GA ≥36 weeks	-	15	103	0.11	0.81	[51]
Asphyxiated Neonates	GA ≥36 weeks	-	10	148±55	0.08±0.03	0.97± 0.18	
HIE Neonates NonTH	PND 6.7± 8.4	3.26± 0.50	14	98.8± 26.4	0.04±0.021	0.41± 0.24	[52]
HIE Neonates TH	PND 3.04± 1.5	3.3± 0.7	26	120.3± 46.2	0.03±0.04	0.52± 0.14	
HIE Neonates TH (SHIVER)	GA 39.9 (36.0- 42.1)	3.62 (2.15- 4.92)	31	-	0.08±0.05	0.95	[53]
(D) Topiramate							
HIE Neonates TH (NeoNATI)	GA 38.8± 1.32	3.21± 0.53	21	35.6± 19.3	0.26±0.08	0.6-1	[35, 54]
HIE Neonates TH	GA 39± 1.6	3.25± 0.72	54	54.1± 23.6	0.33±0.21	-	[55]

[1] *Estimates for a neonate with a body weight of 3.5 kg. Data are presented as median and 95% confidence intervals.*

In this study, a statistically significant decrease in FNT CL by 66% was observed, leading to an approximately 3-fold longer $t_{1/2}$ in the TH group compared to the C group. Additionally, the 24-hour plasma concentrations were statistically significantly higher in the TH group compared to the three other groups investigated (i.e., C (P=0.0026), H (P=0.0271) and H+TH (P=0.0337)), as well as statistically significant higher FNT R_{ac} in the TH group (P=0.0306) and H+TH group (P=0.0453). This increase in drug concentrations and the inability to reach a steady state, in this timeframe, in the hypothermic groups provide further evidence for the limited FNT removal capacity, likely associated with reduced CL. According to thermopharmacological principles, CYP activity decreases at lower body temperatures [45]. As summarized by Tortorici et al (using non-clinical data), TH can decrease the systemic CL of drugs metabolized by CYPs, by 7-22% per degree Celsius below 37 °C [56]. Therefore, the TH impact on FNT metabolism could be attributed to the reduced CYP3A activity. However, it could also be associated with the diminished liver blood flow (Section 4.3., Impact of therapeutic hypothermia on cardiovascular processes driving drug disposition) [57,58]. Beside the TH group, the H+TH group also showed a reduction in FNT CL (i.e., 17%) compared to the C group, but at a lower extent than the TH group and non-statistically significant. This would typically increase $t_{1/2}$, as the drug is being eliminated more slowly. Contrary, in our study it was 62% shorter than control. Since $t_{1/2}$ is influenced by both CL and V_d, the lower V_d might overshadow the decrease in CL. Additionally, this discrepancy between the two hypothermic groups remains difficult to

explain based on our FNT study results, as the small sample size in relation with the interindividual variability and the limited experimental time (i.e., 24 hours) might play a role (Section 4.5., Challenges, limitations, and potential further steps). Furthermore, these findings rather have a scientific impact since the real-world setting is the combined occurrence of both hypoxia and TH.

Trends towards lower CL and longer $t_{\frac{1}{2}}$ of MDZ and PHB due to TH, and the inability to reach a steady state, provide evidence of the limited drug removal capacity in neonatal Göttingen Minipigs. Specifically, the TH group exhibited a 56% decrease in MDZ CL with approximately a 2-fold longer $t_{\frac{1}{2}}$, while for the H+TH group, there was an 18% decrease in MDZ CL compared to the C group. Regarding PHB, only the H+TH group demonstrated a potential trend, with a 30% decrease in CL with a 35% longer $t_{\frac{1}{2}}$ compared to the C group. A possible reason for the discrepancy between the TH and H+TH groups may lie in the small sample size, which limits the ability to draw robust conclusions. Future studies should include larger sample sizes and a longer duration of the experiment to better demonstrate these trends and clarify the effects of TH on drug disposition. On the other hand, our minipig data, indicating no statistically significant differences between groups, is consistent with previous findings that TH has no statistical significant effect on PHB [4,52,53] or MDZ [4,49] CL in human neonates with HIE. In the study by van den Broek, which assessed MDZ as an adjunct anticonvulsant under TH, it was observed that MDZ provided limited seizure control, achieving a 23% control rate after PHB administration [49]. Furthermore, 64% of participants experienced at least one hypotensive episode, and the concurrent use of inotropic medication led to a 33% decrease in MDZ CL, rendering it less suitable as a second-line anticonvulsant drug under TH [49]. On the other hand, the previously documented PK data for PHB indicated elevated plasma concentrations in neonates with PA/TH [59]. Because of its long $t_{\frac{1}{2}}$, small fluctuations in plasma concentrations (i.e., the difference between maximal and plasma trough concentration at steady state) occur for 24 hours. Specifically, the PHB $t_{\frac{1}{2}}$ decreases by 4.6 hours per day and is 67 hours in healthy infants 4 weeks of age [51]. Also in our study, the PHB concentration-time profiles exhibited shallow slopes following the first administration, indicating slow distribution and/or elimination.

Concerning drugs undergoing little or no hepatic metabolism (i.e., TPM), existing evidence suggests that TH following hypoxic-ischemic injury does not influence the PK [60,61]. This hypothesis was confirmed in our study since, despite a significantly higher R_{ac} for TPM in the TH group (P=0.0107), we could not detect a significant effect of TH on TPM PK in neonatal Göttingen Minipigs. Another example is a previous study by Filippi et al. involving 21 neonates with HIE undergoing 72 hours of whole-body TH (NeoNATI) and receiving oral TPM [35]. No statistically or clinically significant differences were observed for safety, primary or secondary outcomes. However, a reduction in the prevalence of epilepsy was observed in neonates co-treated with TPM. Furthermore, the group receiving TPM had a lower HR at 66-72 hours compared to controls (98-100 versus 100-112 beats per minute) and they exhibited a lower base excess after rewarming (-2.6 versus -0.2) [35]. In another study, 110 neonates were randomized, 57 to TPM and 53 to placebo at the initiation of TH [55]. The TPM group exhibited less seizure burden in the first 24 hours of TH (TPM, n=14 (25%) versus placebo, n=22 (42%)); needed less additional medication, and had lower mortality (TPM, n=5 (9%) versus placebo, n=10 (19%)). Although these results did not achieve statistical significance, a significant association was established between serum TPM levels and seizure activity [55]. In our study a decrease in TPM CL of 28% for the H group was detected compared to the C group. As sample

sizes were adapted during the analysis, the results are considered exploratory. These PK changes induced by hypoxia are expected since the hypoxic-ischemic injury itself can induce renal impairment (e.g., gentamicin in neonatal pigs [61] and human neonates [60]). Still, the influence of PA on renal tubular functions remains unclear, and additional research is needed to understand the underlying mechanisms.

4.2. Impact of therapeutic hypothermia on cardiovascular processes driving drug disposition

In addition to the potential direct impact on drug disposition, TH also has an impact on cardiovascular parameters [50,62]. Firstly, high ER drugs, such as FNT, are flow limited drugs meaning that upon IV administration, the systemic CL is highly dependent on the liver blood flow. For instance, in a study in juvenile conventional pigs exposed to mild hypothermia (31.6±0.2 °C for 6 hours) a reduction in cardiac index (41±15%) and organ blood flows was observed. In this context, this finding was correlated to a 25±11% increase in FNT plasma levels [62]. Data on organ blood flow, cardiac index, or cardiac output (CO) are typically needed to draw such conclusions. Although our study did not directly measure these parameters, we recorded the HR and detected statistically significant lower values in the hypothermic groups. It is crucial to emphasize that the pediatric cardiovascular system is characterized by a limited stroke volume, with CO substantially depending on HR, unlike the fully developed hearts [63]. This underlines the importance of HR as a key parameter in pediatric assessments. In a retrospective study, infants with PA/HIE exhibited a decrease in HR during the first day of life, dropping to 92 bpm at 12 hours after birth compared to normothermic infants (i.e., 118 bpm) [64]. Despite maintaining a consistently low rectal temperature, HR increased during the last day of TH to 97 bpm [64]. Additionally, in a study on healthy neonatal piglets, lower HR values were found during hypothermia compared to normothermia, with higher HR variability [65]. Temperature and HR variability were associated with hypothermia-induced bradycardia, reducing myocardial energy demands, and potentially impacting the sinus node and myocardium [65].

As HR impacts CO, the observed lower HR in our study could be linked to the lower capacity of drug removal from the body, as a possible mechanistic hypothesis. This trend was observed for FNT (high ER), while drugs with intermediate (MDZ) and low (PHB) ER were less impacted. Therefore, this might explain the more pronounced and statistically significant TH impact on FNT PK compared to MDZ, even though both drugs share the same metabolic pathway (i.e., hepatic CYP3A22, CYP3A29, CYP3A46 Göttingen Minipig metabolism [15]). Future experiments measuring organ blood flow, cardiac index, or CO would provide more comprehensive insights, especially in the context of PBPK modelling.

4.3. Challenges, limitations, and potential further steps

It is important to understand that by the nature of our study (i.e., co-administration of the study drugs), we could presume some possible drug-drug interactions. The use of CYP inhibitors and inducers can influence PK in a clinically relevant way [66]. In this regard, PHB is known to induce uridine 5'-diphosphate glucuronosyltransferases, CYP2C and CYP3A4 enzymes [67]. For example, in a previous study investigating human neonatal HIE cases, PHB, administered together with MDZ, increased the MDZ CL by a factor of 2.3, likely indicating drug-drug interactions [4]. Furthermore, since CYP3A4 inducers substantially decrease

systemic FNT exposure, they may lead to lower FNT plasma levels and risk inefficient pain relief [68]. On the other hand, the co-administration of IV TPM with PHB in dogs was linked to increased CL by approximately 5.6-fold and a corresponding 4-fold reduction in t½ [24]. Therefore, these subjects required a TPM dose adaptation to 25 mg/kg, compared to subjects on non-inducing drugs receiving 20 mg/kg to attain the target plasma concentration of 20-30 µg/mL, at 30 minutes post-dose [24].

Another consideration is the potential interaction of FNT co-administered with MDZ. It is well known that MDZ acts synergically with FNT due to a mutual potentiation between these two drug groups, leading in some cases to life-threatening complications such as respiratory and cardiac arrest [69]. Furthermore, MDZ can substantially inhibit the hepatic metabolism of N-FNT [70], which is particularly important for prolonged procedures. In these cases, elevated drug (and metabolite) levels relative to the desired ones can lead to potential side effects, emphasizing the critical importance of dose selection. To illustrate the rationale for the dosage regimens in our study, we have provided a comparative overview (Table 4) of some drug dosing recommendations and target concentrations in human neonates and (mini)pigs.

Table 4. Drug dosing and applied target concentrations in normothermia and hypothermia settings, human neonates, pigs and neonatal Göttingen Minipigs. * Intravenous (IV); therapeutic hypothermia (TH).

Drug	Species/Age	IV Bolus	IV Infusion	Target Plasma Concentration	Ref
Midazolam	Human Neonate	0.05-0.1 mg/kg	0.05-0.3 mg/kg/h	200 to 1000 ng/mL	[71]
	Human Neonate undergoing TH	0.05 mg/kg	0.05-0.1 mg/kg/h (max. 24 hours)		[71] [47]
	Pig	0.1-0.5 mg/kg	0.6-1.5 mg/kg/h	-	[72]
	Neonatal Göttingen Minipig	0.3 mg/kg	0.4 mg/kg/h	-	[10]
Fentanyl	Human Neonate	0.5-3 µg/kg	0.5-3 µg/kg/h	-	[71]
	Pig	50 µg/kg	100 µg/kg/h	-	[29]
	Neonatal Göttingen Minipig	3 µg/kg	10 µg/kg/h	-	[10]
Phenobarbital	Human Neonate	20 mg/kg (max. 40 mg/kg daily)	-	10-40 µg/mL; 3.2 to 75.2 mg/L	[51,71] [73]

	Neonatal Göttingen Minipig	20 mg/kg every 12 hours	-	-	[10]
Topiramate	Human Neonate	11-38.5 mg/kg/day	-	2-40 µg/mL	[74]
	Neonatal Pig	5 and 40 mg/kg	-	> 10 µM	[21]
	Neonatal Göttingen Minipig	20 mg/kg every 12 hours	-	-	[10]

Besides the success of developing the neonatal Göttingen Minipig model for dose precision in PA, the current study also shows some limitations. The limited survival duration of 24 hours has substantial implications, such as the absence of a rewarming phase and a restricted PK profile for the investigated drugs. Initially planned for 96 hours, the study duration was shortened due to logistical challenges and the need for extra experienced animal care staff. Consequently, the findings should be interpreted with caution compared to the human clinical setting, where TH covers 72 hours, followed by gradual rewarming and the subsequent maintenance at normothermia [2].

Substantial inter- and intra-patient PK variability has been reported in HIE patients. Notably, studies involving late preterm or term neonates with HIE treated with PHB consistently reported high coefficients of interindividual variability (CV) in CL and V_d. For instance, in a prospective study, CV values for CL ranged from 31% to 78%, and for V_d, ranged from 38% to 75% across different subgroups (normothermia, TH1 and TH2) [52]. Similarly, the SHIVER study reported a high CV for both PHB CL (43.1%) and V_d (8.4%) [53]. In the PharmaCool study, examining PHB and MDZ, high CV values were observed for PHB CL (54%) and V_d (36%), as well as for MDZ CL (79.2%) and V_d (96.6%) [4]. We also encountered high variability in PK, even if hemodynamic responses were harmonized in our animal model. Even though a power analysis was conducted prior to the study to determine the necessary sample size, challenges arose during the PK analysis. We had to exclude 11 subjects from the final statistical analysis of PHB and TPM due to inaccurate k estimation through linear regression. The omission of these observations represents a limitation since it might have induced a potential bias As a result, although our original intent was to have 6 animals per group, the effective sample size for some groups and parameters was reduced and then these results should be considered exploratory. Conducting experiments with larger sample size might overcome these limitations.

Our study showed statistically higher FNT plasma levels in the TH group by reducing CL and prolonging its $t_{½}$, but not in the H+TH group, which more closely reflects the clinical situation. This group was characterized by a lower CL, at a lower extent compared with TH group, but also by a lower V_d. Despite the expectation that a lower CL would typically result in a longer $t_{½}$, the shorter $t_½$ alongside reduced CL and a low V_d suggests a different interplay of PK factors. Possible reasons include increased plasma protein binding, alterations in tissue permeability, or physiological changes affecting drug distribution and elimination. In general, while pH and temperature changes can alter protein binding, these modifications usually do not impact the fraction unbound to a degree that affects the success of most therapies [75]. However, FNT is known to have clinically significant protein binding changes due to pH variations in humans

[76]. Drugs with a narrow therapeutic range, high ER, and IV administration - criteria that FNT meets in this study - are particularly sensitive to pH-dependent protein binding [76]. Therefore, based on current knowledge, pH changes are unlikely to pose major clinical consequences except for FNT, which was also used in our Göttingen minipig model. Collecting additional blood gas analysis data along with plasma protein levels could further elucidate the mechanisms behind PK changes induced by PA/HIE in this population. Future research should investigate the factors contributing to reduced V_d and CL, such as examining shifts in protein binding or potential drug interactions. Finally, besides clinical studies and nonclinical research, in silico modeling is paramount to gaining insights into dose precision in PA. As variability in maturational and non-maturational covariates can be substantial, PBPK models hold promise for the future. The PBPK approach accounts for neonatal distinctive physiology, and PK, and incorporates in vitro data from both human and juvenile animal models [9]. Furthermore, the effect of non-maturational covariates on drug disposition is needed to improve neonatal PBPK models since hypothermia in neonates is one of the conditions for which the development of a PBPK model is urgently needed. Smits et al. presented a stepwise multidisciplinary approach, and described the benefits and challenges in constructing a PBPK framework to predict drug disposition in asphyxiated neonates treated with TH (I-PREDICT project), as a future solution [2]. The minipig PBPK promises to generate unique insights on the relation between PA/TH and PK, to be translated into the human PBPK model, which can ultimately be used for more precise dosing in human neonates.

5. Conclusion

A neonatal Göttingen Minipig model was used to assess the impact of systemic hypoxia and TH separately on drug disposition, which provided insights that are difficult to obtain in a clinical setting. Our study showed statistically higher FNT plasma levels in the TH group by reducing CL and prolonging its $t_{1/2}$, but not in the H+TH group, which more closely reflects the clinical situation. Trends towards lower CL and longer $t_{1/2}$ of MDZ and PHB were also observed, however not statistically significant. The statistically significant influence of TH on HR in neonatal Göttingen Minipigs, in line with its well-documented influence in human neonates, could be mechanistically linked to its impact on high ER drugs such as FNT, whereas intermediate- (MDZ) and low- (PHB) ER drugs were less affected. Furthermore, a reduction in TPM CL in hypoxic Göttingen Minipigs was detected, suggesting that the hypoxic-ischemic injury itself can induce renal impairment. Discrepancies between the TH and H+TH groups were detected, likely due to the limited sample size and experimental duration. Since the number of Göttingen Minipigs available for the statistical analysis of V_d, CL, $t_{1/2}$, k, for PHB and TPM was adjusted during the analysis, the results should be considered exploratory at this point. Further research, including a larger sample size and a longer duration of the experiment, may help in better understanding these findings and their clinical implications. Finally, our study showed the potential of neonatal Göttingen Minipigs as a promising translational model for assessing the safety of therapies for pediatric conditions and it provides a valuable step towards developing a neonatal Göttingen Minipig PBPK model.

6. References

1. Jacobs SE, Berg M, Hunt R, et al. Cooling for newborns with hypoxic ischaemic encephalopathy. Cochrane Database Syst Rev. 2013 Jan 31;2013(1):Cd003311.
2. Smits A, Annaert P, Van Cruchten S, et al. A Physiology-Based Pharmacokinetic Framework to Support Drug Development and Dose Precision During Therapeutic Hypothermia in Neonates. Front Pharmacol. 2020;11:587-587.
3. NICE. National Institute for Health and Care Excellence. Interventional procedures guidance [IPG347]. Therapeutic hypothermia with intracorporeal temperature monitoring for hypoxic perinatal brain injury. Published on 26 May 2010, accessed on 25 April 2023. 2010.
4. Favié LMA, Groenendaal F, van den Broek MPH, et al. Phenobarbital, Midazolam Pharmacokinetics, Effectiveness, and Drug-Drug Interaction in Asphyxiated Neonates Undergoing Therapeutic Hypothermia. Neonatology. 2019;116(2):154-162.
5. Pokorna P, Wildschut ED, Vobruba V, et al. The Impact of Hypothermia on the Pharmacokinetics of Drugs Used in Neonates and Young Infants. Curr Pharm Des. 2015;21(39):5705-24.
6. Azzopardi D, Brocklehurst P, Edwards D, et al. The TOBY Study. Whole body hypothermia for the treatment of perinatal asphyxial encephalopathy: A randomised controlled trial. BMC Pediatrics. 2008 2008/04/30;8(1):17.
7. Helke KL, Swindle MM. Animal models of toxicology testing: the role of pigs. Expert Opin Drug Metab Toxicol. 2013 Feb;9(2):127-39.
8. Singh VK, Thrall KD, Hauer-Jensen M. Minipigs as models in drug discovery. Expert Opin Drug Discov. 2016 Dec;11(12):1131-1134.
9. Ayuso M, Buyssens L, Stroe M, et al. The Neonatal and Juvenile Pig in Pediatric Drug Discovery and Development. Pharmaceutics. 2021;13(1):44.
10. Stroe M-S, Van Bockstal L, Valenzuela AP, et al. Development of a neonatal Göttingen Minipig model for dose precision in perinatal asphyxia: technical opportunities, challenges, and potential further steps [Methods]. Front Pediatr. 2023;11:662.
11. Bode G, Clausing P, Gervais F, et al. The utility of the minipig as an animal model in regulatory toxicology. J Pharmacol Toxicol Methods. 2010 Nov-Dec;62(3):196-220.
12. Valenzuela A, Tardiveau C, Ayuso M, et al. Safety Testing of an Antisense Oligonucleotide Intended for Pediatric Indications in the Juvenile Göttingen Minipig, including an Evaluation of the Ontogeny of Key Nucleases. Pharmaceutics. 2021;13(9):1442.
13. Buyssens L, De Clerck L, Schelstraete W, et al. Hepatic Cytochrome P450 Abundance and Activity in the Developing and Adult Göttingen Minipig: Pivotal Data for PBPK Modeling. Front Pharmacol. 2021;12:665644.
14. Van Peer E, De Bock L, Boussery K, et al. Age-related Differences in CYP3A Abundance and Activity in the Liver of the Göttingen Minipig. Basic Clin Pharmacol Toxicol. 2015 Nov;117(5):350-7.
15. Van Peer E, Jacobs F, Snoeys J, et al. In vitro Phase I-and Phase II-drug metabolism in the liver of juvenile and adult Göttingen minipigs. Pharmaceutical research. 2017;34(4):750-764.
16. Puccinelli E, Gervasi P, Longo V. Xenobiotic Metabolizing Cytochrome P450 in Pig, a Promising Animal Model. Current drug metabolism. 2011 04/08;12:507-25.

17.   Heckel T, Schmucki R, Berrera M, et al. Functional analysis and transcriptional output of the Göttingen minipig genome. BMC Genomics. 2015;16:932-932.

18.   Ezzati M, Broad K, Kawano G, et al. Pharmacokinetics of dexmedetomidine combined with therapeutic hypothermia in a piglet asphyxia model. Acta Anaesthesiol Scand. 2014 Jul;58(6):733-42.

19.   Pypendop BH, Brosnan RJ, Siao KT, et al. Pharmacokinetics of remifentanil in conscious cats and cats anesthetized with isoflurane. Am J Vet Res. 2008 Apr;69(4):531-6.

20.   Avram Michael J, Krejcie Tom C, Niemann Claus U, et al. Isoflurane Alters the Recirculatory Pharmacokinetics of Physiologic Markers. Anesthesiology. 2000;92(6):1757-1768.

21.   Galinkin JL, Kurth CD, Shi H, et al. The plasma pharmacokinetics and cerebral spinal fluid penetration of intravenous topiramate in newborn pigs. Biopharmaceutics & drug disposition. 2004;25(6):265-271.

22.   Clark AM, Kriel RL, Leppik IE, et al. Intravenous topiramate: Comparison of pharmacokinetics and safety with the oral formulation in healthy volunteers. Epilepsia. 2013;54(6):1099-1105.

23.   Clark AM, Kriel RL, Leppik IE, et al. Intravenous topiramate: Safety and pharmacokinetics following a single dose in patients with epilepsy or migraines taking oral topiramate. Epilepsia. 2013;54(6):1106-1111.

24.   Vuu I, Coles LD, Maglalang P, et al. Intravenous Topiramate: Pharmacokinetics in Dogs with Naturally Occurring Epilepsy [Original Research]. Frontiers in Veterinary Science. 2016 2016-December-05;3(107).

25.   Sangild PT, Thymann T, Schmidt M, et al. Invited review: the preterm pig as a model in pediatric gastroenterology. J Anim Sci. 2013 Oct;91(10):4713-29.

26.   Burrin D, Stoll B, Jiang R, et al. GLP-2 stimulates intestinal growth in premature TPN-fed pigs by suppressing proteolysis and apoptosis. American Journal of Physiology-Gastrointestinal and Liver Physiology. 2000;279(6):G1249-G1256.

27.   Pacifici GM. Clinical pharmacology of midazolam in neonates and children: effect of disease-a review. Int J Pediatr. 2014;2014:309342.

28.   Zhou J, Poloyac SM. The effect of therapeutic hypothermia on drug metabolism and response: cellular mechanisms to organ function. Expert Opin Drug Metab Toxicol. 2011 Jul;7(7):803-16.

29.   Grimm KA, Lamont LA, Tranquilli WJ, et al. Veterinary anesthesia and analgesia. John Wiley & Sons; 2015.

30.   Ferreira A, Rodrigues M, Oliveira P, et al. Liquid chromatographic assay based on microextraction by packed sorbent for therapeutic drug monitoring of carbamazepine, lamotrigine, oxcarbazepine, phenobarbital, phenytoin and the active metabolites carbamazepine-10,11-epoxide and licarbazepine. Journal of Chromatography B. 2014 2014/11/15/;971:20-29.

31.   Bista SR, Haywood A, Hardy J, et al. Protein binding of fentanyl and its metabolite nor-fentanyl in human plasma, albumin and α-1 acid glycoprotein. Xenobiotica. 2015 Mar;45(3):207-12.

32.   Skaanild MT, Friis C. Analyses of CYP2C in porcine microsomes. Basic Clin Pharmacol Toxicol. 2008 Nov;103(5):487-92.

33.   Boréus LO, Jalling B, Kållberg N. Phenobarbital metabolism in adults and in newborn infants. Acta Paediatr Scand. 1978 Mar;67(2):193-200.

34. Zhao M, Ma J, Li M, et al. Cytochrome P450 Enzymes and Drug Metabolism in Humans. Int J Mol Sci. 2021 Nov 26;22(23).

35. Filippi L, Fiorini P, Catarzi S, et al. Safety and efficacy of topiramate in neonates with hypoxic ischemic encephalopathy treated with hypothermia (NeoNATI): a feasibility study. J Matern Fetal Neonatal Med. 2018 Apr;31(8):973-980.

36. Christensen J, Højskov CS, Dam M, et al. Plasma concentration of topiramate correlates with cerebrospinal fluid concentration. Ther Drug Monit. 2001 Oct;23(5):529-35.

37. van Groen BD, Nicolaï J, Kuik AC, et al. Ontogeny of Hepatic Transporters and Drug-Metabolizing Enzymes in Humans and in Nonclinical Species. Pharmacol Rev. 2021 Apr;73(2):597-678.

38. Matara D-I, Pouliakis A, Xanthos T, et al. Microbial Translocation and Perinatal Asphyxia/Hypoxia: A Systematic Review. Diagnostics. 2022;12(1):214.

39. Mota-Rojas D, Villanueva-García D, Solimano A, et al. Pathophysiology of Perinatal Asphyxia in Humans and Animal Models. Biomedicines. 2022 Feb 1;10(2).

40. Rainaldi MA, Perlman JM. Pathophysiology of Birth Asphyxia. Clin Perinatol. 2016 Sep;43(3):409-22.

41. van Dijk AJ, van Loon JPAM, Taverne MAM, et al. Umbilical cord clamping in term piglets: A useful model to study perinatal asphyxia? Theriogenology. 2008 2008/09/01/;70(4):662-674.

42. Orozco-Gregorio H, Mota-Rojas D, Alonso-Spilsbury M, et al. Importance of blood gas measurements in perinatal asphyxia and alternatives to restore the acid base balance status to improve the newborn performance. American Journal of Biochemistry and Biotechnology. 2007;3(3).

43. Frankel DAZ, Acosta JA, Anjaria DJ, et al. Physiologic Response to Hemorrhagic Shock Depends on Rate and Means of Hemorrhage. Journal of Surgical Research. 2007 2007/12/01/;143(2):276-280.

44. ©Lixoft. PKanalix® documentation 2023 MonolixSuite™ (version 2021R2, Lixoft application). Available from https://pkanalix.lixoft.com/. Accessed on 02/07/2023.

45. van den Broek MP, Groenendaal F, Egberts AC, et al. Effects of hypothermia on pharmacokinetics and pharmacodynamics: a systematic review of preclinical and clinical studies. Clin Pharmacokinet. 2010 May;49(5):277-94.

46. Lutz IC, Allegaert K, de Hoon JN, et al. Pharmacokinetics during therapeutic hypothermia for neonatal hypoxic ischaemic encephalopathy: a literature review. BMJ Paediatr Open. 2020;4(1):e000685.

47. Jacqz-Aigrain E, Daoud P, Burtin P, et al. Pharmacokinetics of midazolam during continuous infusion in critically ill neonates. European journal of clinical pharmacology. 1992;42:329-332.

48. Burtin P, Jacqz-Aigrain E, Girard P, et al. Population pharmacokinetics of midazolam in neonates. Clin Pharmacol Ther. 1994 Dec;56(6 Pt 1):615-25.

49. van den Broek MP, van Straaten HL, Huitema AD, et al. Anticonvulsant effectiveness and hemodynamic safety of midazolam in full-term infants treated with hypothermia. Neonatology. 2015;107(2):150-6.

50. Ziesenitz VC, Vaughns JD, Koch G, et al. Pharmacokinetics of Fentanyl and Its Derivatives in Children: A Comprehensive Review. Clin Pharmacokinet. 2018 Feb;57(2):125-149.

51. Pacifici GM. Clinical Pharmacology of Phenobarbital in Neonates: Effects, Metabolism and Pharmacokinetics. Curr Pediatr Rev. 2016;12(1):48-54.

52.   Pokorná P, Posch L, Šíma M, et al. Severity of asphyxia is a covariate of phenobarbital clearance in newborns undergoing hypothermia. The Journal of Maternal-Fetal & Neonatal Medicine. 2019 2019/07/18;32(14):2302-2309.

53.   van den Broek MPH, Groenendaal F, Toet MC, et al. Pharmacokinetics and Clinical Efficacy of Phenobarbital in Asphyxiated Newborns Treated with Hypothermia. Clinical Pharmacokinetics. 2012 2012/10/01;51(10):671-679.

54.   Filippi L, la Marca G, Fiorini P, et al. Topiramate concentrations in neonates treated with prolonged whole body hypothermia for hypoxic ischemic encephalopathy. Epilepsia. 2009 Nov;50(11):2355-61.

55.   Nuñez-Ramiro A, Benavente-Fernández I, Valverde E, et al. Topiramate plus Cooling for Hypoxic-Ischemic Encephalopathy: A Randomized, Controlled, Multicenter, Double-Blinded Trial. Neonatology. 2019;116(1):76-84.

56.   Tortorici MA, Kochanek PM, Poloyac SM. Effects of hypothermia on drug disposition, metabolism, and response: a focus of hypothermia-mediated alterations on the cytochrome P450 enzyme system. Critical care medicine. 2007;35(9):2196-2204.

57.   Hines RN. Ontogeny of human hepatic cytochromes P450. J Biochem Mol Toxicol. 2007;21(4):169-75.

58.   Gow PJ, Ghabrial H, Smallwood RA, et al. Neonatal hepatic drug elimination. Pharmacol Toxicol. 2001 Jan;88(1):3-15.

59.   Filippi L, la Marca G, Cavallaro G, et al. Phenobarbital for neonatal seizures in hypoxic ischemic encephalopathy: a pharmacokinetic study during whole body hypothermia. Epilepsia. 2011 Apr;52(4):794-801.

60.   Liu X, Borooah M, Stone J, et al. Serum gentamicin concentrations in encephalopathic infants are not affected by therapeutic hypothermia. Pediatrics. 2009 Jul;124(1):310-5.

61.   Satas S, Hoem NO, Melby K, et al. Influence of mild hypothermia after hypoxia-ischemia on the pharmacokinetics of gentamicin in newborn pigs. Biol Neonate. 2000;77(1):50-7.

62.   Fritz HG, Holzmayr M, Walter B, et al. The effect of mild hypothermia on plasma fentanyl concentration and biotransformation in juvenile pigs. Anesth Analg. 2005 Apr;100(4):996-1002.

63.   Duke-Novakovski T, de Vries M, Seymour C. BSAVA Manual of Canine and Feline Anaesthesia and Analgesia. British Small Animal Veterinary Association; 2016.

64.   Elstad M, Liu X, Thoresen M. Heart rate response to therapeutic hypothermia in infants with hypoxic–ischaemic encephalopathy. Resuscitation. 2016 2016/09/01/;106:53-57.

65.   Pedersen MV, Andelius TCK, Andersen HB, et al. Hypothermia and heart rate variability in a healthy newborn piglet model. Scientific Reports. 2022 2022/10/31;12(1):18282.

66.   Kokubun H, Ebinuma K, Matoba M, et al. Population pharmacokinetics of transdermal fentanyl in patients with cancer-related pain. J Pain Palliat Care Pharmacother. 2012 Jun;26(2):98-104.

67.   Dowd FJ, Johnson B, Mariotti A. Pharmacology and therapeutics for dentistry-E-book. Elsevier Health Sciences; 2016.

68.   Kuip EJ, Zandvliet ML, Koolen SL, et al. A review of factors explaining variability in fentanyl pharmacokinetics; focus on implications for cancer patients. Br J Clin Pharmacol. 2017 Feb;83(2):294-313.

69.   Ben-Shlomo I, Abd-El-Khalim H, Ezry J, et al. Midazolam acts synergistically with fentanyl for induction of anaesthesia. British Journal of Anaesthesia. 1990;64(1):45-47.

70. Labroo RB, Paine MF, Thummel KE, et al. Fentanyl metabolism by human hepatic and intestinal cytochrome P450 3A4: implications for interindividual variability in disposition, efficacy, and drug interactions. Drug Metab Dispos. 1997 Sep;25(9):1072-80.

71. Dutch-Children's-Formulary. Medicine Midazolam, Fentanyl, Phenobarbital Dutch Children's Formulary. 2023.

72. Swindle MM. Swine in the laboratory: surgery, anesthesia, imaging, and experimental techniques. CRC press; 2007.

73. Völler S, Flint RB, Stolk LM, et al. Model-based clinical dose optimization for phenobarbital in neonates: An illustration of the importance of data sharing and external validation. Eur J Pharm Sci. 2017 Nov 15;109s:S90-s97.

74. Glauser TA, Miles MV, Tang P, et al. Topiramate Pharmacokinetics in Infants. Epilepsia. 1999;40(6):788-791.

75. Roberts JA, Pea F, Lipman J. The Clinical Relevance of Plasma Protein Binding Changes. Clinical Pharmacokinetics. 2013 2013/01/01;52(1):1-8.

76. Hinderling PH, Hartmann D. The pH Dependency of the Binding of Drugs to Plasma Proteins in Man. Therapeutic Drug Monitoring. 2005;27(1):71-85.

7. Supplementary data

7.1. Quantitative determination of analytes by LC-MS/MS

The Göttingen Minipig plasma samples were analyzed in the bioanalytical laboratory of BioNotus, Belgium to determine concentrations of midazolam (MDZ), fentanyl (FNT), phenobarbital (PHB), and topiramate (TPM) and the metabolites 1-hydroxymidazolam (1-OH-MDZ) and norfentanyl (N-FNT), using a validated liquid chromatography-mass spectrometry (LC-MS/MS) method. The samples were extracted using protein precipitation and reversed-phase liquid chromatography. The study was performed on a Shimadzu Nexera X2 UHPLC, coupled with Sciex TQ 6500+ system. The data was acquired and processed via Analyst® version 1.7.3 software. The lower limit of quantification (LLOQ) concentrations were 0.1, 0.2, 5 and 10 ng/mL; 1 and 0.5 µg/mL for N-FNT, FNT, 1-OH-MDZ, MDZ; PHB and TPM, respectively. The upper limit of quantification concentrations were 20, 40, 1000 and 2000 ng/mL, 200 and 100 µg/mL for N-FNT, FNT, 1-OH-MDZ, MDZ, PHB and TPM, respectively. Quality control (QC) and calibration curve standard working solutions were prepared in advance and stored at -20°C (Greenland Mega Line freezer with logging). The QC samples were freshly prepared for each batch using an internal lot of pooled Göttingen Minipig plasma. Calibration curve samples were freshly prepared for each run. The calibration curve consists of a control blank, a zero standard (blank + internal standard (IS)) and 8 non-zero calibration curves standard covering the concentration ranges. Analyte to IS peak area ratio values were used to set up the calibration curves, to determine QC and unknown sample concentrations. A linear regression with a weighting factor of l/x2 was used to obtain the best fit for the calibration curve data. All concentration values were reported with three decimals. The following criteria were used for the validity of the analytical run: acceptable system suitability test, interference from the blank and blank + IS, if any, at the retention time of the analyte, must not exceed 20.0% of the response of the analyte in LLOQ sample; interference from the blank, if any, at the retention time of the IS, must not exceed 5.0% of the mean response of the IS from the acceptable

calibration curve standard and QC samples; at least 75% of calibration curve standards (8 standards) should be within ±15.0% of their nominal value (±20.0% for calibration curve standard 1); at least 67% of overall QC samples (low QC, medium QC and high QC) and at least 50% at each level should be within ±15.0% of their nominal values.

Summary of the two analytical methods used for the determination of the plasma concentration of the target drugs in the neonatal Göttingen Minipigs are presented in Supplementary Table 1 for MDZ, 1-OH-MDZ, N-FNT and FNT and Supplementary Table 2 for PHB and TPM. The LC-MS/MS quantification was based on two separate methods, with different calibration ranges: MDZ (10-2000 ng/mL), 1-OH-MDZ (5-1000 ng/mL), FNT (0.2-40 ng/mL), N-FNT (0.1-20 ng/mL), for the first method, and PHB (1-200 µg/mL), TPM (0.5-100 µg/mL), for the second method. All batches met the acceptance criteria for calibration curve standard and QC samples, demonstrating satisfactory performance of the method during the bioanalytical study phase.

Supplementary Table 1. Summary of the analytical method of midazolam (MDZ), 1-hydroxymidazolam (1-OH-MDZ), norfentanyl (N-FNT) and fentanyl (FNT).

Parameter		Parameter Value	Comments
Matrix		Minipig plasma	Ellegaard Göttingen Minipigs
Sample preparation: Extraction		Phospholipid extraction using Phree plate.	N/A
Calibration Range	N-FNT	0.1 ng/mL – 20 ng/mL	N/A
	FNT	0.2 ng/mL – 40 ng/mL	N/A
	1-OH-MDZ	5 ng/mL – 1000 ng/mL	N/A
	MDZ	10 ng/mL – 2000 ng/mL	N/A
Regression Type		Linear	$1/(\text{concentration})^2$
Data Calculation		Peak area ratio	N/A
Sample volume		100 µL	N/A
Analytical Instrument		LC: Shimadzu Nexera X2	N/A

		MS/MS detector: Sciex TQ6500+	
Column		Kinetex® F5 2.6 µm, 50 × 2.1 mm	Manufacturer: Phenomenex United States
Column Temperature		40 °C	N/A
Autosampler Temperature		15 °C	N/A
Flow rate		0.4 mL/min	N/A
Injection volume		10 µL	N/A
Mobile Phase	Line A	0.1% (v/v) formic acid in Water	Gradient mode, 5 to 40%B.
	Line B	0.1% (v/v) formic acid in acetonitrile	
Run time		7.2 min.	N/A
Retention Times	N-FNT	2.75 min	N/A
	FNT	4.55 min	N/A
	1-OH-MDZ	4.19 min	N/A
	MDZ	4.37 min	N/A
MRM transitions	N-FNT	233.05 / 84, 233.05 / 150	N/A
	FNT	337.28 / 188.1, 337.28 / 105.0	N/A
	1-OH-MDZ	342.0 / 140.2, 342.0 / 176.1	N/A
	MDZ	326.03 / 309.0, 326.03 / 249.1	N/A
Reference Standards:		MDZ and FNT supplied by the client,	N/A

	1-OH-MDZ and N-FNT supplied by Cayman	

Supplementary Table 2. Summary of the analytical method of phenobarbital (PHB) and topiramate (TPM).

Parameter		Parameter Value	Comments
Matrix		Minipig plasma	Ellegaard Göttingen Minipigs
Sample preparation: Extraction		Protein precipitation.	N/A
Calibration Range	TPM	0.5 µg/mL – 100 µg/mL	N/A
	PHB	1 µg/mL – 200 µg/mL	N/A
Regression Type		Linear	$1/(concentration)^2$
Data Calculation		Peak area ratio	N/A
Sample volume		10 µL	N/A
Analytical Instrument		LC: Shimadzu Nexera X2 MS/MS detector: Sciex TQ6500+	N/A
Column		Kinetex® F5 2.6 µm, 50 × 2.1 mm	Manufacturer: Phenomenex United States
Column Temperature		40 °C	N/A
Autosampler Temperature		15 °C	N/A
Flow rate		0.4 mL/min	N/A
Injection volume		1 µL	N/A

Mobile Phase	Line A	0.1% (v/v) acetic acid in Water	Isocratic mode, 20%B.
	Line B	0.1% (v/v) acetic acid in acetonitrile	
Run time		3.0 min	N/A
Retention Times	TPM	1.9 min	N/A
	PHB	1.3 min	N/A
MRM transitions	TPM	338.1 / 78, 338.1 / 96.0	N/A
	PHB	231.1 / 42, 231.1 / 188.1	N/A
Reference Standards:		TPM and PHB supplied by the client.	N/A

7.2. Pharmacokinetic analysis

A one-compartment model with administration via IV bolus and/or IV infusion, assuming linear elimination was used to analyze the PK of PHB, TPM, MDZ and FNT, resulting in estimates for V_d, volume of distribution; CL, clearance; $t_{1/2}$, half-life; k, elimination rate constant. PKanalix®, MonolixSuiteTM (version 2021R2) (©Lixoft) was used as software platform. The equations describing the concentrations following IV bolus administered drugs (i.e., PHB and TPM, 1st Equation) and drugs administered via an IV bolus loading dose followed by an IV infusion maintenance dose (i.e., MDZ and FNT, 2nd Equation) were:

$$C_p = \left(\frac{LD}{V_d}\right) e^{-kt} \qquad \textit{(1st Equation)}$$

$$C_p = \left(\frac{MD/T_{inf}}{V_d k}\right) + \left[\left(\frac{LD}{V_d}\right) e^{-kt} - \left(\frac{MD/T_{inf}}{V_d k}\right) e^{-kt}\right] \qquad \textit{(2nd Equation)}$$

Where C_p denotes the predicted plasma concentrations, MD is the total dose infused over the infusion duration T_{inf}, LD represents the loading dose (or the bolus dose), V_d is the volume of distribution, k is the elimination rate constant, τ represents the dosing interval, n is the nth dose given in that dosing interval, and t denotes the corresponding time for the concentration. The equation employed to estimate the clearance (CL) and half-life ($t_{1/2}$) were:

$$CL = kV_d \qquad \textit{(3rd Equation)}$$

$$t_{1/2} = \frac{0.693}{k} = \frac{0.693 * V_d}{CL}$$

(4th Equation)

A schematic representation of the compartmental models used is depicted as **Supplementary Figure 1.** Figure created with BioRender.com. * Predicted plasma concentrations (C_p); elimination rate constant (k); LD represents the loading dose (or the bolus dose); MD is the total dose infused over the infusion duration T_{inf}; corresponding time for the concentration (*t*); volume of distribution (V_d).
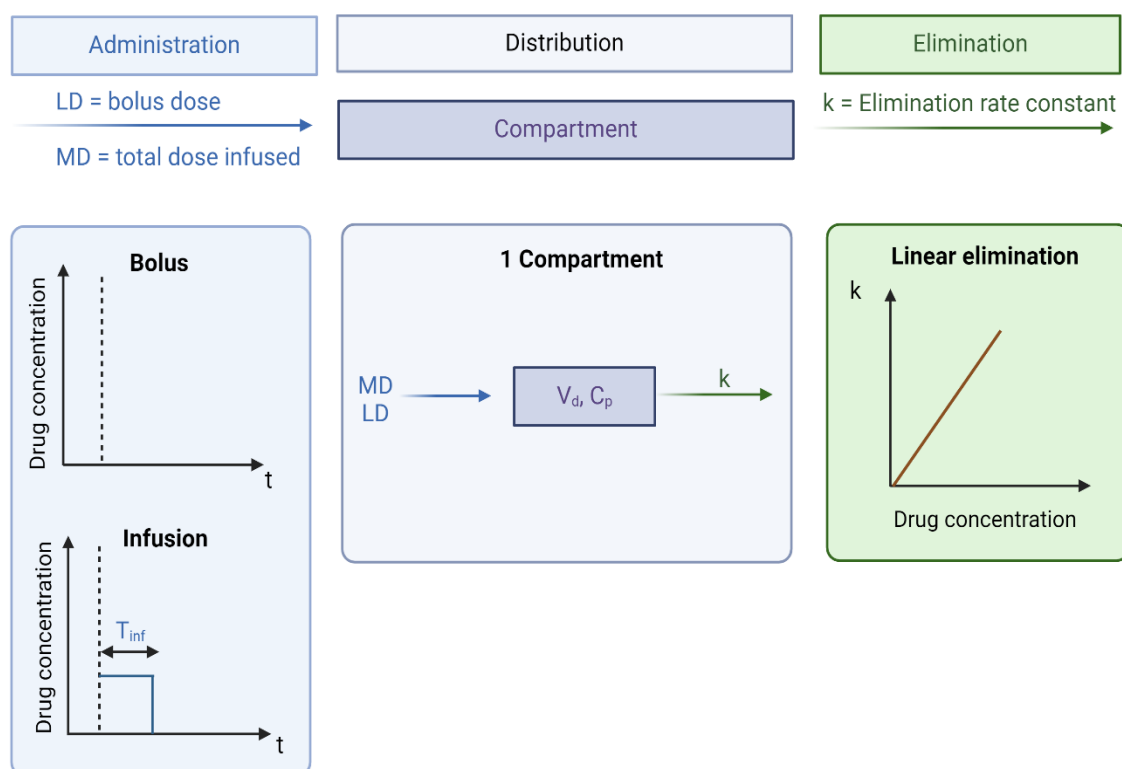
7.3. Elimination rate constants

Supplementary Table 3. Linear regression output required for the estimation of the elimination rate constants (k, 1/hour). The names of each group were abbreviated as the following - control (C), therapeutic hypothermia (TH), hypoxia (H), hypoxia and TH (H+TH).

ID	Intercept	k (1/hour)	R squared	p-value slope	Observations
Phenobarbital					
C1	2.00317	-0.0015	0.03373	0.69343	Excluded
C2	2.07334	0.01145	0.84785	0.00117	
C3	2.03483	-0.0013	0.1232	0.44014	Excluded
C4	2.14078	0.00553	0.95617	0.00073	
C5	2.29179	0.0121	0.81931	0.00505	
C6	2.07792	0.009	0.11587	0.45502	Excluded
H1	2.21021	0.0096	0.76826	0.05112	

H2	2.05102	-0.00303	0.22169	0.34593	Excluded
H3	2.13402	0.0038	0.66427	0.02551	
H4	2.14461	0.0071	0.94824	0.00102	
H5	1.786	0.0026	0.27028	0.29043	Excluded
H6	1.76833	-0.00001	0.00001	0.99595	Excluded
TH1	2.12878	0.0213	0.84804	0.00324	
TH2	2.28173	0.0134	0.91866	0.0101	
TH3	2.09709	0.0052	0.54639	0.05764	Excluded
TH4	2.00995	0.0021	0.66481	0.04799	
TH5	2.1789	0.0222	0.73596	0.01353	
TH6	2.18931	0.005	0.6035	0.06914	Excluded
H+TH1	2.12396	-0.0038	0.4334	0.15516	Excluded
H+TH2	2.30293	0.006	0.53246	0.06268	Excluded
H+TH4	2.23242	0.0074	0.75657	0.02432	
H+TH5	2.28723	0.0073	0.92361	0.00056	
H+TH6	1.84959	-0.00991	0.83359	0.00409	Excluded
H+TH7	2.05173	0.0067	0.7603	0.02354	
Topiramate					
C1	2.00935	0.0276	0.60118	0.12342	Excluded
C2	1.75503	0.0072	0.78959	0.01793	
C3	1.80493	0.0104	0.47663	0.12895	Excluded
C4	2.02226	0.0137	0.99328	0.00023	
C5	1.96306	0.0121	0.93083	0.00184	
C6	1.95058	0.024	0.64956	0.05283	Excluded
H1	1.99751	0.0087	0.66889	0.18214	Excluded
H2	1.98203	0.0032	0.78286	0.01914	
H3	2.03226	0.01	0.96986	0.00034	
H4	2.06422	0.0192	0.83308	0.03054	
H5	1.90233	0.0054	0.22619	0.3404	Excluded
H6	1.92623	0.0123	0.97506	0.00024	
TH1	1.81479	0.0401	0.90279	0.00104	
TH2	1.86357	0.028	0.99955	0	
TH3	1.85476	-0.00204	0.01372	0.8512	Excluded
TH4	1.8262	-0.00017	0.04675	0.72687	Excluded
TH5	2.05084	0.0147	0.95028	0.00478	
TH6	1.99102	0.0205	0.5274	0.10217	Excluded
H+TH1	1.93429	0.0163	0.72126	0.03237	
H+TH2	1.89979	0.0085	0.88278	0.01767	
[1] H+TH4	2.0035	0.011	0.95207	0.00088	
H+TH5	2.00897	0.0164	0.9417	0.0013	
H+TH6	1.8605	0.006	0.47282	0.13113	Excluded
H+TH7	1.9745	0.0028	0.51097	0.1104	Excluded

CHAPTER 5:
Effects of hypothermia and hypoxia on cytochrome P450-mediated drug metabolism in neonatal Göttingen Minipigs

Effects of hypothermia and hypoxia on cytochrome P450-mediated drug metabolism in neonatal Göttingen Minipigs

Abstract

Asphyxiated neonates often undergo therapeutic hypothermia (TH) to reduce morbidity and mortality. As perinatal asphyxia and TH impact neonatal physiology, this could also influence enzyme functionality. Therefore, this study aimed to unravel the impact of age, hypothermia, and hypoxia on porcine hepatic cytochrome P450 (CYP) gene expression, protein abundance, and activity. Hepatic CYP expression, protein abundance, and activity were assessed in naive adult and neonatal Göttingen Minipigs, alongside those from an (non-survival) in vivo study, where 4 conditions: control (C), therapeutic hypothermia (TH), hypoxia (H), hypoxia and TH (H+TH), were examined. Naive neonatal Göttingen Minipigs exhibited 75% lower general CYP activity and different gene expression patterns than adults. In vitro hypothermia (33 °C) decreased general CYP activity in adult liver microsomes by 36%. Gene expression was not different between TH and C, while hypoxia up-regulated several genes (i.e., CYP3A29 (expression ratio; E_R=5.1472) and CYP2C33 (E_R=3.2292) in the H group, and CYP2C33 (E_R=2.4914) and CYP2C42 (E_R=4.0197) in the H+TH group). The medical treatment and the interventions over 24 hours, along with hypoxia and TH, affected the protein abundance. These data on CYP expression, abundance, and activity in young animals can be valuable in building physiologically-based pharmacokinetic models for neonatal drug dose predictions.

1. Introduction

Despite advances in perinatal medicine, the incidence of perinatal asphyxia (PA), a medical condition at delivery caused by oxygen deprivation, which can result in hypoxic-ischemic encephalopathy (HIE), has not decreased in the last decade [1]. Asphyxiated (near)term neonates with moderate to severe HIE often undergo therapeutic hypothermia (TH) along with intensive care and drug therapy to reduce morbidity and mortality [2]. Since PA and TH affect neonatal physiology, we hypothesize that these two non-maturational covariates impact drug disposition, including enzyme functionality, in these patients.

Cytochrome P450 (CYP) enzymes are important drug metabolizing enzymes (DMEs), facilitating the excretion of drugs from the body [3,4]. Despite previous research on DMEs in humans [5], the influence of maturational (i.e., weight, age, ontogeny of absorption, distribution, metabolism, and excretion), but also non-maturational (i.e., disease (PA/HIE), and therapies (TH, drug interactions)) on CYP enzymes in neonatal populations remains largely unexplored [6,7]. In this regard, non-clinical data from an adequate animal model under experimental conditions can provide valuable insights into these covariates that cannot be studied separately in humans. While no animal model can perfectly capture the diversity and complexity of human pathology, the strengths and limitations must be evaluated in the context of the research purposes [8]. Although the rat pup is the most commonly used and probably the best-characterized model in HIE research, the piglet offers unique advantages in closely replicating human neonatal conditions [9]. Firstly, the body size of piglets at birth support instrumentation for hemodynamic and physiological measurements and facilitate sampling. This size limitation of the rat pups restricts the ability to perform extensive blood sampling (e.g., for drug pharmacokinetic (PK) and blood gas analysis) without compromising physiology [9]. Secondly, the maturational pattern of the animal model should closely match that of human neonates for better interpretation of findings, specifically to be pharmacologically relevant. In this regard, it is relevant to note that (i) there is a high homology between human and porcine CYPs [10,11] and (ii) the ontogeny of CYP activities was comparable between juvenile Göttingen Minipigs and humans [12,13]. For this purpose, the (neonatal) Göttingen Minipig was selected as translational model, as this is the preferred pig strain in non-clinical drug development [14]. Göttingen Minipigs offer several advantages over other pig strains due to their genetic consistency and well-documented characteristics, providing valuable historical control data for pharmaceutical companies in non-clinical safety studies [4,12-16].

It is crucial to acknowledge that CYPs can be evaluated at various levels, including mRNA, protein abundance, and enzyme activity. All these levels are important particularly in distinguishing between acute and prolonged temperature-induced modifications: while alterations in expression levels require a period for manifestation, changes in enzymatic activity can manifest promptly. Therefore, this study aimed to investigate the impact of age, hypothermia, and hypoxia on hepatic CYP expression, abundance, and activity in Göttingen Minipigs. In our study, sex differences in DMEs have been investigated at activity level using fluorogenic substrates. We did not examine sex differences at the gene and protein expression levels, but other studies have addressed these aspects [13,17,18]. Additionally, the effects of medical treatment and interventions, denoting general anesthesia with mechanical ventilation and the administration of 4 drugs - midazolam, fentanyl, phenobarbital, and topiramate - over 24 hours, were evaluated. The genes of interest for this research were the

orthologous porcine isoforms of the human CYP1A2, i.e. CYP1A2; human CYP3A4, i.e. CYP3A22, CYP3A29, and CYP3A46; human CYP2C8, CYP2C9, CYP2C19, CYP2C18, i.e. CYP2C33 and CYP2C42; human CYP2D6, i.e. CYP2D25; and human CYP2E1, i.e. CYP2E1. The choice of the target genes was driven by the substantial homology (i.e., 63-84 % identity in amino acids) between human and (mini)pig CYP isoforms [10]. Additional CYPs were identified and quantified using a proteomics approach. For CYP activity, two substrates were selected for this study: Vivid® 7-benzyloxy-methyl resorufin, a fluorogenic substrate with general affinity for most CYPs, and 7-ethoxy resorufin, employed in the ethoxyresorufin-O-deethylase (EROD) assay, commonly used to assess CYP1A activity in humans, but also other vertebrates [19,20]. Besides general CYP activity, CYP1A activity and, more specifically, 7-ethoxy resorufin was selected for evaluation due to (i) its well-conserved nature among species [21], (ii) high catalytic activity of 7-ethoxy resorufin by human and porcine CYP1A [22] and (iii) the presence of CYP1A activity in neonatal piglets, in contrast to several other CYPs [12].

2. Materials and methods

2.1. Experimental study design

An overview of the study design and the methods used to investigate the impact of age, hypothermia, and hypoxia on hepatic CYP expression, abundance, and activity in Göttingen Minipigs is provided in Figure 1. The protocols and the use of animals were approved by the Ethical Committee of Animal Experimentation from the University of Antwerp (Belgium) (ECD 2012-30) (i.e., adult Göttingen Minipigs and resulting liver tissues [12]) and by the Danish Ethical Committee, 2022-15-0201-01163, on the 5th of April 2022 (i.e., neonatal Göttingen Minipigs and resulting liver tissues were collected after an 24 hours non-survival in vivo study, conducted at Ellegaard Göttingen Minipigs A/S, Dalmose, Denmark). In this in vivo study, 4 conditions were investigated: controls (group C), hypoxia (group H), therapeutic hypothermia (group TH), and hypoxia and TH (group H+TH). The Göttingen Minipigs' selection criteria and the study procedures to obtain the hypoxic and hypothermic conditions were previously described, together with their limitations and technical challenges (Chapter 3) [23].

Figure 1. Overview of the methods and study design used to investigate the impact of age, sex, hypothermia, and hypoxia on hepatic CYP expression, abundance, and activity in Göttingen Minipigs. Created with BioRender.com. * 7-benzyloxy-methyl resorufin (BOMR); complementary DNA (cDNA); cytochrome P450 (CYP); 7-ethoxy resorufin (ER); Michaelis-Menten constant (Km); liquid chromatography tandem mass spectrometry (LC-MS/MS); postnatal day 1 denoted as naive Göttingen Minipigs (PND1); therapeutic hypothermia (TH); maximal velocity of the reaction (Vmax).
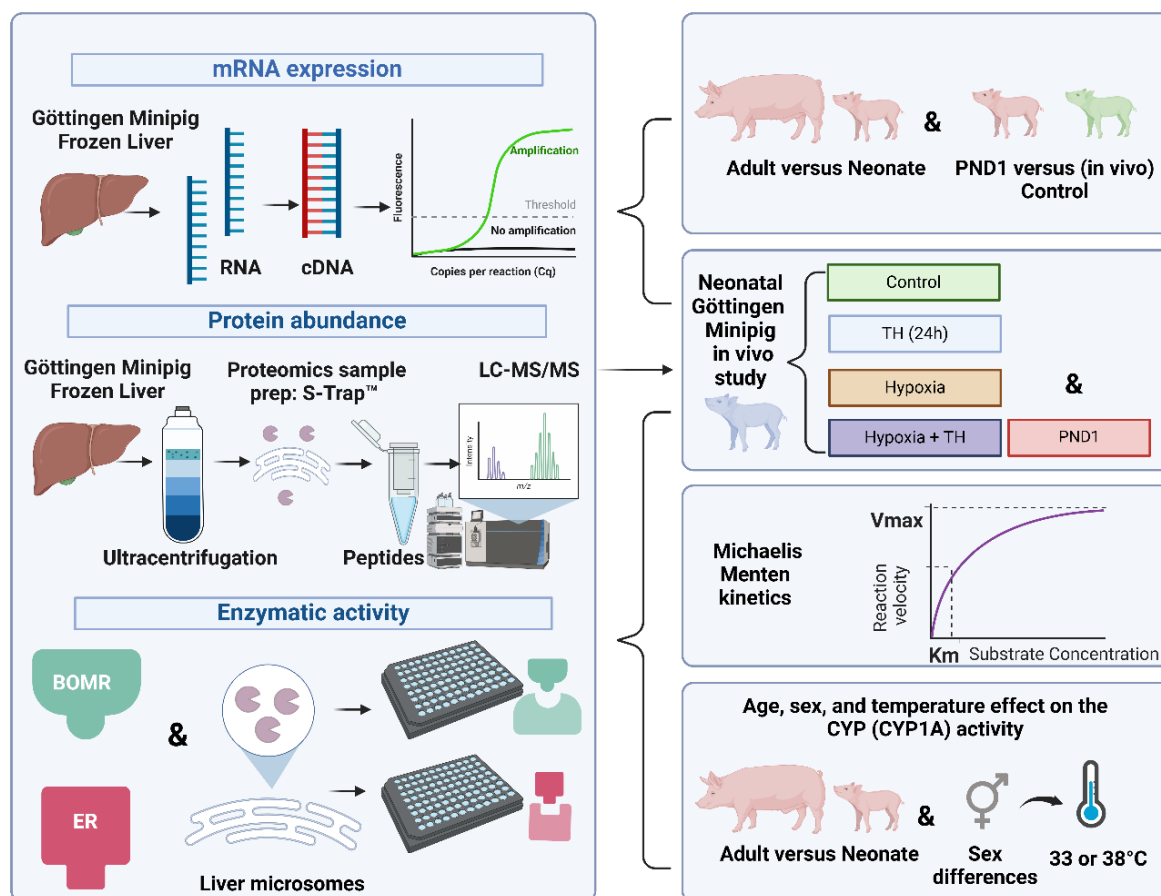
2.2. Hepatic CYP-mRNA expression in Göttingen Minipigs

2.2.1 Samples and target genes

Hepatic CYP expression levels were evaluated using quantitative PCR (qPCR). Firstly, to assess the impact of age, frozen liver samples from adult (n=6) versus neonatal (<24 hours of age denoted as postnatal day, PND1; n=6) naive male Göttingen Minipigs were used. Secondly, the impact of TH and hypoxia in Göttingen Minipigs undergoing 24 hours general anesthesia was assessed in 6 males, <24 hours of age, per condition (i.e., controls (C), hypoxia (H), TH, and hypoxia and TH (H+TH)). Moreover, to assess the potential impact of medical treatment and interventions on gene expression levels, we compared 6 postnatal day 1 (PND1) Göttingen Minipigs (naive) with those undergoing 24 hours of general anesthesia with mechanical ventilation, along with administration of the 4 candidate drugs, referred as the in vivo control group. The target genes in (mini)pigs with the specific primers and the template used for their design are listed in Supplementary Table 1.

2.2.2. Primer design

The primer design was performed with the Primer-BLAST tool (https://www.ncbi.nlm.nih.gov/tools/primer-blast/). Before this, all transcript variants for the porcine sequences were searched on the ENSEMBL platform [24]. This is recommended since it allows visualization of the future primers into the specific pig sequences. Therefore, this

check ensured the primers' specificity and their design in different exons or to span exon-exon junctions, a condition required to prevent genomic deoxyribonucleic acid (DNA) amplification. The ApE software v2.0.55 (M Wayne, CA, USA) and the Florence Corpet tool (http://multalin.toulouse.inra.fr/multalin/) were used for the multiple sequence alignment of all transcript variants found in ENSEMBL. Next, a search using the standard nucleotide BLAST tool with the conserved region was accomplished to identify the most complete sequence in The National Center for Biotechnology Information (NCBI) database. Finally, the primers were generated using the Primer-BLAST tool, ensuring the specificity and inclusion of all transcript variants available in ENSEMBL. The primer pair specificities were verified with the same Primer-BLAST tool by copying the newly designed primers and checking the products on intended targets to verify whether they correspond to the specific pig sequence. After this validation, the primers were ordered at Integrated DNA Technologies (IDT, https://eu.idtdna.com/pages/products/custom-dna-rna/dna-oligos) and used in the incoming PCR and qPCR experiments.

2.2.3. Choice of reference genes

According to The Minimum Information for Publication of qPCR Experiments guidelines, at least two reference genes are recommended for assay validation [25]. Consequently, the chosen reference genes in our study were Hypoxanthine phosphoribosyltransferase 1 (HPRT1) and Ubiquitin C (UBC). The reference genes were validated using the GeNorm software (M<1.5 represents high expression stability) [26], as well as statistical tests (i.e., One-Way Analysis of Variance (ANOVA)), used to show no significant difference in expression among groups (P>0.05). Reference gene primers were designed using the primer BLAST tool, following the same strategy already mentioned for the target genes, and are listed in Supplementary Table 1. The subsequent steps, including RNA extraction and quality check (Supplementary Table 2), complementary DNA synthesis, and conventional PCR (Supplementary Table 3), are provided as supplementary data.

2.2.4. qPCR

When the products of the conventional PCR were verified as specific and without contamination, a qPCR protocol was performed. The reaction efficiencies were tested for the reference and target genes and are listed in Supplementary Table 2. The main qPCR experiment, including 36 samples, was counting 32 plates. To correct for plate-to-plate variation, a calibrator consisting of 2 samples with primers of a reference gene (HPRT1 in our case) was included in each plate. Cytochrome P450 3A22 was amplified at a lower temperature (i.e., 58 °C) instead of the default (i.e., 60 °C). The reference genes were run at both temperatures to ensure proper normalization at different temperatures. The results following inefficient or unspecific amplifications detected on the melt curve were excluded. Due to low target amplification, 2 samples were excluded entirely from the analysis (i.e., 1 C and 1 PND1). The relative expression software tool (REST) [27] was used to test the differences in gene expression, with reference genes used to normalize the target gene expression. The REST uses a mathematical model for calculating gene expression ratios (E_R) by considering each gene's previously determined efficiency (i.e., target and reference gene), allowing for a

statistical evaluation of the calculated E_R. The E_R were determined using the following formula to calculate gene expression ratios between two groups (i.e., adult - neonate; naive male Göttingen Minipigs (PND1) - in vivo control (Figure 2); control - covariate-treated group (Figure 3)):

$$Relative\ gene\ expression\ ratio\ = \frac{(E_{gene\ of\ interest})^{\Delta Cq\ gene\ of\ interest^{(control-treatment)}}}{(E_{referance\ gene})^{\Delta Cq\ referance\ gene^{(control-treatment)}}}$$

Where, E = reaction efficiency, ΔCq = cycle threshold value. The relative expression software tool incorporates PCR efficiencies and ΔCq values for both target and reference genes, it converts the PCR reaction efficiencies into integer numbers, then use ΔCq for control and treatment to calculate the E_R. Unlike other statistical methods, REST does not assume a normal distribution, which cannot be expected every time when using ratios.

2.3. Hepatic CYP-protein abundance in Göttingen Minipigs

2.3.1. Samples

4 conditions, i.e., C, H, TH, and H+TH, with 6 male Göttingen Minipigs per condition, were needed to determine potential in vivo systemic hypoxia and/or TH-related differences at the level of protein abundance. Additionally, to differentiate whether there is an impact of the 24 hours general anesthesia, 6 naive male Göttingen Minipigs (PND1) were included in the analysis. Samples were analyzed at ProGenTomics, Ghent, Belgium, using a validated liquid chromatography-tandem mass spectrometry (LC-MS/MS) based quantitative proteomics method [13,28].

2.3.2. LC-MS/MS experimental set-up

Starting from the same frozen liver tissue samples used for mRNA quantification (Section 2.2.1.), 30 neonatal Göttingen Minipig liver microsomal (GLMs) samples were isolated following a protocol reported previously [4] and stored at -80 °C until use. Further, the total protein amount was determined by a bicinchoninic acid assay (Pierce™ BCA Protein Assay Kit, ThermoFisher), with bovine serum albumin as standard. Depending on the amount of each sample, the microsomal samples were further diluted to 200 µg protein, using MilliQ ultrapure water, for each sample. They underwent the S-Trap™ mini spin column digestion protocol (Protifi, steps and required reagents listed in Supplementary Table 4). The protein was trapped using the S-Trap™ mini spin columns over 1.5 mL Eppendorf tubes and biding/washing buffer. The protein digestion into peptides was performed using Tryp/Lys solution overnight at 37 °C. Peptides were eluted with one incubation (1 minute) and one centrifugation (1 minute, 4 000 g) step in between each reagent and vacuum dried (38 °C). Before running on a Zeno7600 QTOF instrument (Sciex), the samples were resuspended in 50 µL 0.1% formic acid ($\pm$4 µg/µL) and quantified with Lunatic (Unchained Labs, $\pm$1 µg/µL). All samples were randomized to avoid systematic variation and interspersed with quality control (QC) samples to monitor instrumental variation. Further, 1.6 µg of each sample was spiked with 200 fmol Hi3 E. coli standard before injection. LC-separation was done with a Nano Acquity system coupled to a

YMC-Triart C18 analytical column using a 20-minute gradient. For the mobile phases, 0.1% formic acid in water was used as solvent A, and 0.1% formic acid in acetonitrile was used as solvent B. All samples were acquired on the Zeno7600 in data-dependent acquisition mode. The total scan time was 0.76 seconds, and each scan cycle allowed for the fragmentation of a maximum of 40 precursor ions with an intensity threshold of 200 cps. The Zeno pulse in the time-of-flight (TOF) accelerator was active, allowing a duty cycle increase and, thus, an increase in intensity. The mass range was set to m/z 400-1200 for precursor scans and 140-1800 for fragment scans. The mass spectrometry proteomics data have been deposited to the ProteomeXchange Consortium via the PRIDE [29] partner repository with the dataset identifier PXD049275 and project DOI: 10.6019/PXD049275 (reviewer account details, Username: reviewer_pxd049275@ebi.ac.uk; Password: cTWObixM).

2.3.3. Data and statistical analysis

Data analysis was performed using Progenesis QI (Nonlinear Dynamics) version 2.3 (Waters). All samples were aligned to a QC sample to compensate for drifts in retention time between runs. Relative quantification was performed with all runs normalized to all proteins. Peptide identification was performed with Mascot 2.8 by searching in an updated database of reviewed *Sus scrofa* entries (Swiss-Prot), supplemented with unreviewed CYP proteins and fragments of interest (TrEMBL). 3 samples (2 C and 1 H) were considered outliers and were excluded from analysis.

The statistical analysis was performed in JMP® Pro 16 (SAS Institute Inc., Cary, NC, United States) using the relative quantification values for each Göttingen Minipig categorized in function of group, as input data. Normality and homogeneity of variances were tested using Shapiro-Wilk and Levene's test, respectively. If necessary, a logarithm transformation was performed to meet the assumptions for parametric testing. If the assumptions were fulfilled, One-way ANOVA was used to test the underlying null hypothesis that there was no difference between groups and for each target gene. Further, if the $P<0.05$, this was considered statistically significant, and a post hoc Tukey's-Kramer honestly significant difference (HSD) method was performed to detect the covariate-related differences. If the normality and homogeneity of variances assumptions could not be met, a non-parametric Wilcoxon/Kruskal-Wallis (rank sums) was performed, followed by nonparametric comparisons for each pair using the Wilcoxon method.

2.4. CYP-activity in Göttingen Minipig liver microsomes

2.4.1. Samples and substrates

This investigation aimed to assess the impact of age, sex, and temperature (in vitro) on general CYP activity and CYP1A, in particular. The experiments with both substrates (i.e., the Vivid® 7-Benzyloxy-methyl resorufin Screening Kit (Thermo Scientific™ Pierce™) and 7-ethoxy resorufin, CAS number 5725-91-7 (Sigma-Aldrich)) were performed at 38 °C and 33 °C. The resulting fluorescence signal intensity was proportional to the resorufin concentration formed by the CYP enzymes.

Firstly, to evaluate the influence of age and sex, GLMs were used, with 4 samples allocated to each combination of age and sex groups (i.e., adult, neonatal, females, and males). Secondly, to assess the potential immediate effect of hypothermia, two different temperature exposure

conditions were established (i.e., 38 °C, close to in vivo normothermia in pig [30] versus 33 °C, reflecting human neonatal target temperature for TH [2]). Thirdly, the same GLMs samples extracted from experimental and PND1 Göttingen Minipigs, described in previous sections, were used to evaluate the effects of in vivo TH and systemic hypoxia on the activity. The workflow, data, statistical analysis, and results of the in vivo TH and hypoxia effects on the activity are presented in supplementary data (Supplementary Figure 1).

Depending on the amount of each sample that was obtained by the bicinchoninic acid assay assay, GLMs were further diluted with 0.01 M potassium phosphate (KPO_4) buffer (451201; Corning Incorporated, Corning, NY, USA, pH 7.4) to the optimal protein amount determined for each assay. Human liver microsomes were used as a positive control and an inter-plate calibrator to better detect plate-to-plate variations. Insect Cell Control Supersomes™ (Corning Incorporated, Corning, NY, USA) were chosen as negative control due to their stability and lack of CYP activity [12,20].

2.4.2. General CYP-activity assay with Göttingen Minipig liver microsomes

The Vivid® 7-Benzyloxy-methyl resorufin stock solution was prepared by dissolving 0.1 mg of Vivid® substrate in 150 µL acetonitrile and stored at -20 °C until use. The working solution consisted of Vivid® stock solution, the Nicotinamide adenine dinucleotide phosphate (NADPH) regenerating system, and 0.1M KPO_4 buffer. Firstly, the concentration of 1.2 µM 7-Benzyloxy-methyl resorufin was chosen as the optimal (and final) substrate concentration. The substrate concentration was determined based on the Michaelis-Menten kinetics, Michaelis-Menten constant (Km) and maximal velocity (Vmax) of the reaction, using non-linear regression in GraphPad Prism version 8.0.2 (Inc. San Diego, California USA): Km of 0.6126 µM and Vmax of 169.5 pmol/min/mg microsomal protein for pooled neonatal GLMs; Km of 1.251 µM and Vmax of 104.7 pmol/min/mg microsomal protein for pooled adult GLMs. Furthermore, since CYP enzymes require NADPH because it serves as an electron donor in their catalytic cycle and GLMs lacks NADPH, a NADPH-regenerating system was used (Solution A, 451220 and Solution B, 451200; Corning). Therefore, 1.3 mM NADP+, 3.3 mM glucose-6-phosphate, 3.3 mM magnesium chloride, and 0.4 U/mL glucose-6-phosphate dehydrogenase were needed in each incubation well. The entire working solution (i.e., containing the substrate, the NADPH-regenerating system, and 0.1M KPO_4 buffer) was finally mixed and stored in the incubator at either 33 °C or 38 °C. Secondly, a 9-point resorufin red fluorescent standard curve (500, 250, 125, 62.50, 31.25, 15.65, 7.81, 3.91, and 0 nM) was prepared to estimate the resulting fluorescent signal. Lastly, GLMs extracted from adult and neonatal, female, and male Göttingen Minipigs were diluted in 0.1 M KPO_4 buffer (pH 7.4) at the optimal (and final) sample concentration of 75 µg/mL microsomal protein. Once everything was prepared, the samples were pipetted into a 96-well flat-bottom black polystyrene plate (Greiner). The final volume per well was 100 µL ((i) the diluted microsomes with the substrate; (ii) the standard curve). Therefore, 50 µL diluted GLMs, human liver microsomes and Insect Cell Control Supersomes™ were pipetted in duplicate and 50 µL of working solution (including the substrate prepared at 2x concentration) were pipetted into each well, that contained the above (sample or control), to activate the CYP-enzymes. The measurements were performed using the Tecan Infinite® 200 PRO microplate reader.

2.4.3. CYP1A-activity assay with Göttingen Minipig liver microsomes

The 7-ethoxy resorufin stock solution was prepared by dissolving 0.5 mg substrate in 2.073 mL dimethyl sulfoxide to obtain a concentration of 10 mM. As for the fluorescent resorufin standard (CAS number 635-78-9 (Sigma-Aldrich)) stock solution, 10 mM resorufin in dimethyl sulfoxide was used. Both stock solutions were stored at -20 °C until use. Depending on the linear formation of resorufin over time and the highest reaction velocity, the optimal microsomal protein amount was determined to be 100 µg/mL. To obtain the optimal substrate concentration, it was observed that enzyme kinetics are different with age (Table 1, Supplementary Figure 2), contrary to 7-Benzyloxy-methyl resorufin, where one substrate concentration could cover both adult and neonatal age groups. Therefore, substrate concentrations (96, 48, 24, 12, 6, 3, 1.5, 0.75 µM) were tested on 4 samples from each age group (i.e., adults and neonatal GLMs). The NADPH regenerating system was prepared at the same target concentrations as 7-Benzyloxy-methyl resorufin but together with the GLMs instead of the working solution to facilitate the serial dilution of the substrate. A 9-point resorufin standard curve was prepared (512, 256, 128, 64, 32, 16, 8, 4, and 0 nM). Further, the samples were pipetted into a 96-well flat-bottom black polystyrene plate. The final volume per well was 100 µL. Further, the impact of age, sex, temperature (33 °C and 38 °C) were determined using the EROD assay. Considering the inclusion of neonatal Göttingen Minipig samples, 12 µM ER was chosen as the optimal substrate concentration to which all GLMs were exposed (Table 1). The measurements were performed using the Tecan Infinite® 200 PRO microplate reader.

Table 1. The age and temperature effects on the CYP1A Michaelis-Menten kinetics observed in neonatal compared to adult Göttingen Minipigs. Data are presented as geometric mean and 95% confidence intervals, with 4 subjects per group considered for the calculations. Michaelis-Menten plot analysis of each individual are depicted as Supplementary Figure 2. * 7-ethoxy resorufin (ER); Michaelis-Menten constant (Km); maximal reaction velocity (Vmax).

Göttingen Minipig age category	Temperature (°C)	Vmax (pmol/min/mg protein)	Km (µM)
Adult	38	3773.69 (1146.26; 12423.61)	23.17 (5.84; 91.89)
Neonate	38	733.48 (69.14; 7780.65)	5.44 (1.21; 24.41)
Adult	33	2695.15 (571.99; 12699.12)	21.82 (5.53; 86.03)
Neonate	33	505.45 (42.79; 5970.67)	5.02 (1.45; 17.37)

2.4.4. Data and statistical analysis

Firstly, the mean relative fluorescence units (RFU) of the resorufin standard curve triplicate measurements were corrected with the blank arithmetic mean. Linear regression was performed in which the X-axis represented the resorufin concentration (nM), and the Y-axis was the corresponding RFU. The mean RFU of the duplicate GLM samples was also corrected, but this time with the arithmetic mean of the Insect Cell Control Supersomes™, as they served as the negative control. Next, the concentration of formed resorufin (nM) was calculated by dividing the RFUs by the standard curve linear regression slope. Finally, the reaction velocities

of the CYP-enzymes were obtained and were expressed in pmol/min/mg microsomal protein. Additionally, the limit of detection (LOD) and the lower limit of quantification (LLOQ) [31] were determined by using the arithmetic mean and SD of the Insect Cell Control Supersomes™. Calculations were made in Microsoft Excel® version 16.0.1, 2021 (Microsoft Corporation, Redmond, WA, United States). The Michaelis-Menten EROD kinetic parameters (i.e., Km, Vmax) for the two temperature treatments and ages were calculated using non-linear regression in GraphPad Prism Software.

Regarding the statistical analysis, data represented by the 7-Benzyloxy-methyl resorufin reaction velocities, as well as reaction velocities and enzyme kinetics (Km, Vmax) obtained with EROD, assessing the impact of age, sex, and temperature was fitted into a linear mixed model (JMP® Pro 16) having as fixed factors age, temperature, sex, and their interaction. Normality and homogeneity of variances were tested on the residuals using Shapiro-Wilk and Levene's tests. If necessary, a logarithm transformation was performed to meet the assumptions for parametric testing. The starting model was gradually simplified using stepwise backward modelling, where all non-significant effects were removed step by step. Furthermore, a Student's t-test was used to detect sex-related differences within each age group.

3. Results

Supplementary Table 5 provides an overview of the mRNA expression, protein abundance, and enzyme activity statistically significant results, grouped according to the covariate studied. Detailed results will be presented in the subsequent sections, each focusing on a specific technique.

3.1. CYP-mRNA expression in Göttingen Minipigs

The detailed results represented by gene E_R, standard errors, 95% confidence intervals, and P are depicted in Supplementary Table 6. Concerning the age-related differences (Supplementary Table 6 (A), Figure 2, (A)), significantly lower CYP3A22 (P=0.0005, E_R=0.026), CYP3A29 (P=0.001, E_R=0.004), CYP3A46 (P=0.002, E_R=0.004), CYP2C42 (P=0.0115, E_R= 0.248), and higher CYP2E1 (P=0.0335, E_R=8.8197) expressions were observed in neonates compared to adult Göttingen Minipigs and no differences were noted for CYP1A2, CYP2C33, and CYP2D25. We also examined whether the medical treatment and interventions influenced gene expression. This involved analyzing hepatic CYP expression in naive neonatal Göttingen Minipigs compared to controls from the in vivo study. These results showed that 6 out of 8 target genes were profoundly affected (Supplementary Table 6 (B), Figure 2, (B)): CYP1A2 (P=0.019, E_R=0.2742), CYP2C33 (P=0.0265, E_R=0.5257), and CYP2E1 (P=0.0335, E_R=0.2412) were down-regulated, while CYP3A22 (P=0.006; E_R=16.1198), CYP3A46 (P=0.006; E_R=3.637), and CYP2C42 (P=0.0285; E_R=3.6426) were up-regulated. To assess the effect of the covariates (TH and H), we compared the covariate-treated groups with the in vivo controls (Supplementary Table 6 (C)). Gene E_R, graphed as box and whisker plots, and null hypothesis observations are depicted in Figure 3. The results showed that 24 hours TH did not affect gene expression compared to in vivo controls. However, hypoxia enhanced the expression of CYP3A29 (P=0.026, E_R=5.1472) and CYP2C33 (P=0.0025, E_R=3.2292), while the combination of

hypoxia and TH enhanced the expression of CYP2C33 (*P*=0.003, E$_R$=2.4914) and CYP2C42 (*P*=0.04, E$_R$=4.0197) compared to in vivo controls.

Figure 2. The gene expression ratios and standard errors following the relative expression software tool for 8 target genes in Göttingen Minipigs: the age-related differences: adult (n=6) versus neonatal (<24 hours of age denoted as postnatal day, PND1; n=6) male Göttingen Minipigs without medical treatment and interventions **(A)**; medical treatment and interventions -related differences: naive neonatal male Göttingen Minipigs (<24 hours of age denoted as postnatal day, PND1; n=6) versus treated neonatal male Göttingen Minipigs (<24 hours of age undergoing medical treatment and interventions denoted as (in vivo) control Göttingen Minipigs ; n=6) **(B)**. Concerning the age-related differences, significantly lower CYP3A22, CYP3A29, CYP3A46, CYP2C42, and higher CYP2E1 expressions were observed in neonates compared to adult Göttingen Minipigs and no differences were noted for CYP1A2, CYP2C33, and CYP2D25. Concerning the medical treatment and interventions -related differences results showed that 6 out of 8 target genes were profoundly affected: CYP1A2, CYP2C33, and CYP2E1 were down-regulated, while CYP3A22, CYP3A46, and CYP2C42 were up-regulated. The detailed results represented by gene E$_R$, standard errors, 95% confidence intervals, and *P* are depicted in Supplementary Table 6. * Cytochrome P450 (CYP).

(A)   Adult versus Neonate   **(B) PND1 versus (in vivo) Control**
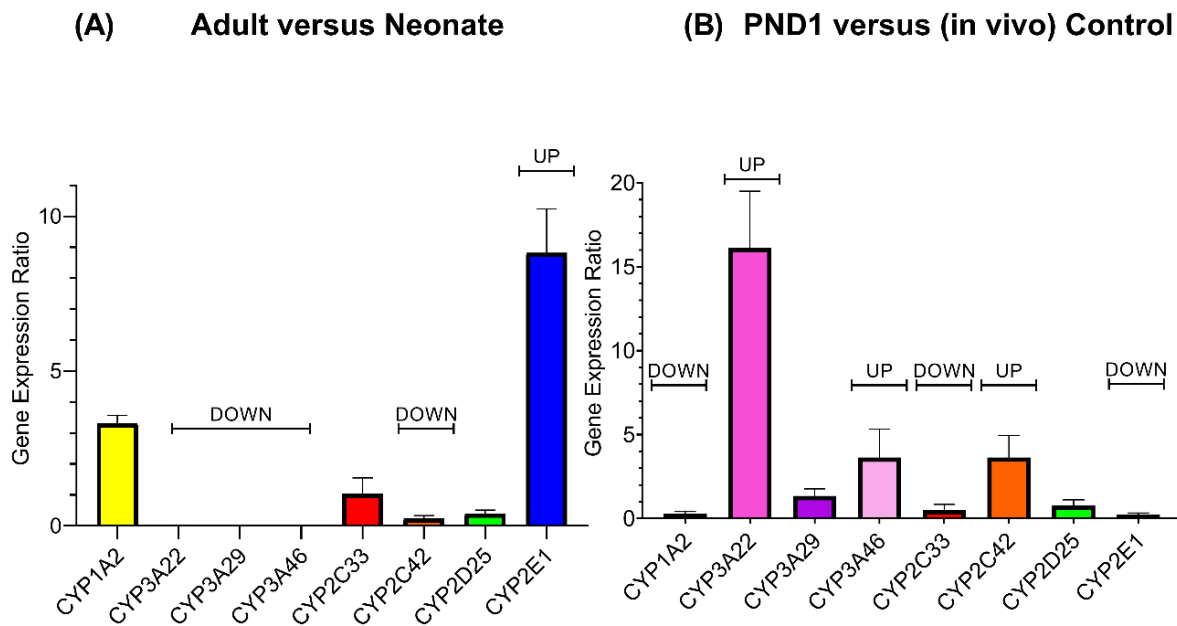
Figure 3. Hypoxia (H) and/or therapeutic hypothermia (TH) gene expression-related differences for 8 target genes: CYP1A2, CYP3A22, 29 and 46 **(A)**, and CYP2C33 and 42, CYP2D25, CYP2E1 **(B)**, investigated in neonatal Göttingen Minipigs. To assess the effect of the covariates (H and TH), the covariate-treated groups were compared with the in vivo controls. Gene expression ratios (E$_R$) following the relative expression software tool were graphed as box and whisker plots. The box represents the inter-quartile range for the observations, with a median line, and the whiskers are the upper and lower 25% observations from the randomized bootstrapping. Additionally, the null hypothesis (H0) observations graph displays the observations for the random permutations used in calculating the *P*. Each observation is

displayed as an open circle. The arithmetic mean is shown as a red dot. The mean must be toward the outer 5% of observations (up or down) to be statistically significant. If the mean E_R is within the middle of the observations, there is no statistically significant difference between the treated and control groups for the respective gene. Conversely, if the mean E_R is outside of 95% of the observations, there is a statistically significant difference between the treated and the control groups for the respective gene. Further, the position of the mean is such that it shows the gene expression is down- or up- regulated. Hypoxia enhanced the expression of CYP3A29 and CYP2C33, while H+TH enhanced the expression of CYP2C33 and CYP2C42 in the neonatal Göttingen Minipigs compared to in vivo controls; no significant differences were detected between the groups due to TH. * Cytochrome P450 (CYP).
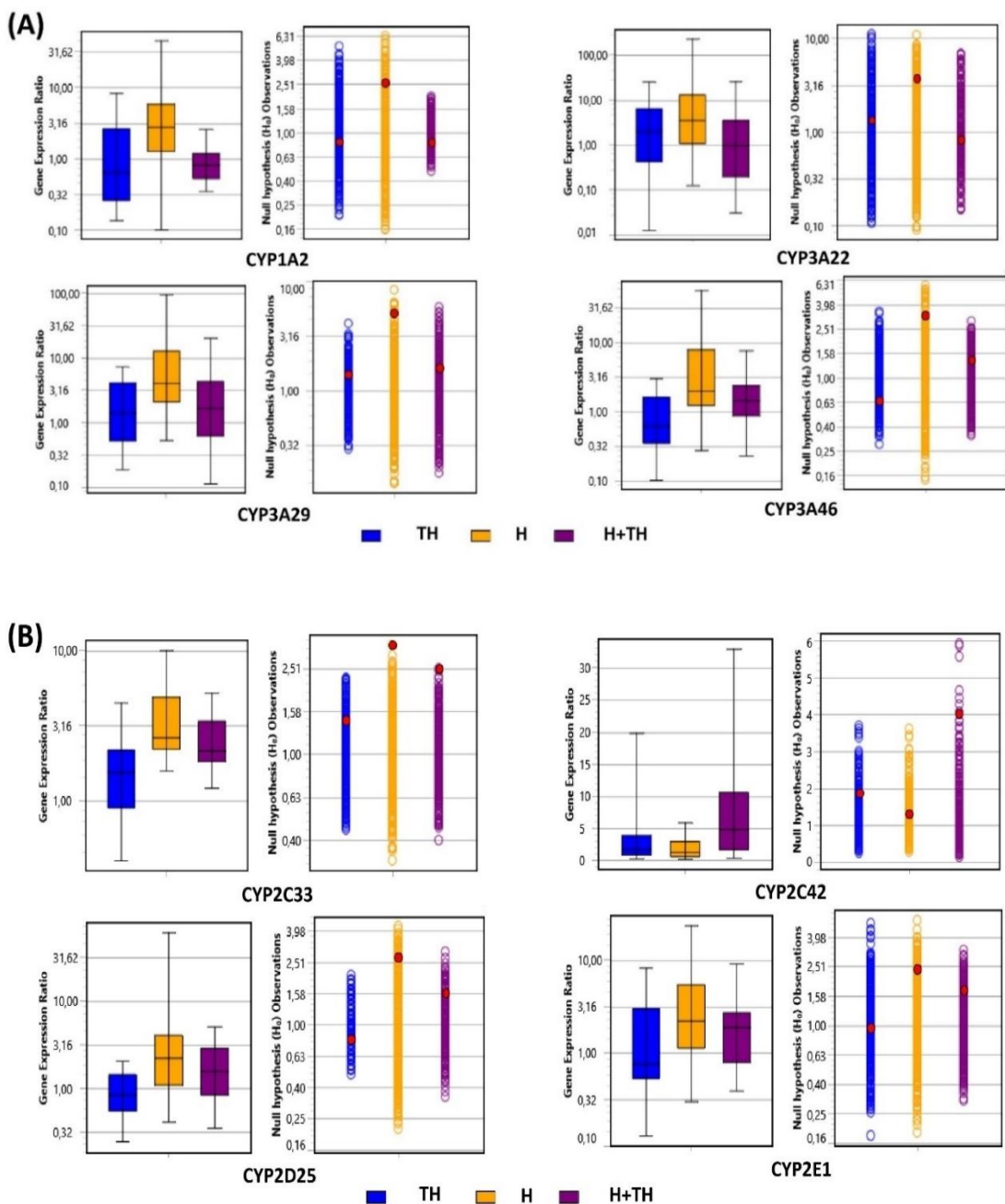
3.2. CYP-protein abundance in neonatal Göttingen Minipigs

16 CYP proteins were identified in the neonatal GLMs: CYP1A1, CYP1A2, CYP2A6, CYP3A22, CYP4A21, CYP20A1, CYP27A1, CYP51A1, CYP2B22, CYP8B1, CYP2C33, CYP2C34, CYP2C42, CYP2C49, CYP2D6, and CYP2E1. For these CYPs, the relative protein abundance was further statistically investigated (Figure 4). Significant differences were detected for CYP51A1, CYP2B22, CYP2C34, CYP2C42, CYP2D6, CYP2E1. Lower CYP51A1 protein abundance was detected in the hypothermic groups when compared to minipigs without medical treatment and interventions (TH versus PND1 (P=0.0291) and H+TH versus PND1 (P=0.0167)) and with hypoxic minipigs (H versus TH (P=0.0104) and H versus H+TH (P=0.0060)). In contrast, higher CYP2B22 protein abundance was detected in the hypothermic groups when compared to minipigs without medical treatment and interventions (PND1 versus TH (P=0.0202) and PND1 versus H+TH (P=0.0202)). Similarly, increased CYP2C34 protein abundance was detected in the TH group (P=0.0098), when compared to minipigs without medical treatment and interventions, and trends towards higher protein abundance in the other treated groups (i.e., C, H, H+TH). The medical treatment and interventions over the 24 hours period enhanced CYP2C42 protein abundance for which statistically significant higher values were detected for H (P=0.0008), TH (P=0.0392) and H+TH (P=0.0346) treatment groups, when compared to minipigs without medical treatment and interventions. For CYP2D6, the medical treatment and interventions enhanced the abundance of the in vivo treated groups (i.e., statistically significantly the TH group (P=0.0371) and trends towards higher protein abundance in the C and H+TH groups), but not of the hypoxic Göttingen Minipigs. The protein abundance for this later group was significantly lower than controls (P=0.0143), TH (P=0.0075) and H+TH (P=0.0105). In contrast, hypoxia enhanced CYP2E1 abundance (P=0.0362) compared to controls.

Figure 4. Hypoxia (H) and/or therapeutic hypothermia (TH) protein abundance-related differences for 16 genes: CYP1A1, CYP1A2, CYP2A6, CYP3A22, CYP4A21, CYP20A1, CYP27A1, and CYP51A1 **(A)** and CYP2B22, CYP8B1, CYP2C33, CYP2C34, CYP2C42, CYP2C49, CYP2D6, and CYP2E1 **(B)**. The statistical analysis was performed using the relative protein abundance data for each individual categorized in the function of the group: neonatal Göttingen Minipigs without medical treatment and interventions (<24 hours of age denoted as postnatal day, PND1), control (C), therapeutic hypothermia (TH), hypoxia (H), hypoxia and TH (H+TH). The bars represent arithmetic means, and the error bars indicate standard deviations. The sample size was 6 neonatal Göttingen Minipigs per group, except for the C and H groups, which included 4 and 5 subjects, respectively. Statistically significant differences were detected for CYP51A1, CYP2B22, CYP2C34, CYP2C42, CYP2D6, and CYP2E1. p-value: *, P <0.05; **, P<0.005; ***, P<0.0005; ****, P<0.0001. * CYP, Cytochrome P450.

(A)

(B)

CYP2B22

CYP8B1

CYP2C33

CYP2C34

CYP2C42

CYP2C49

CYP2D6

CYP2E1
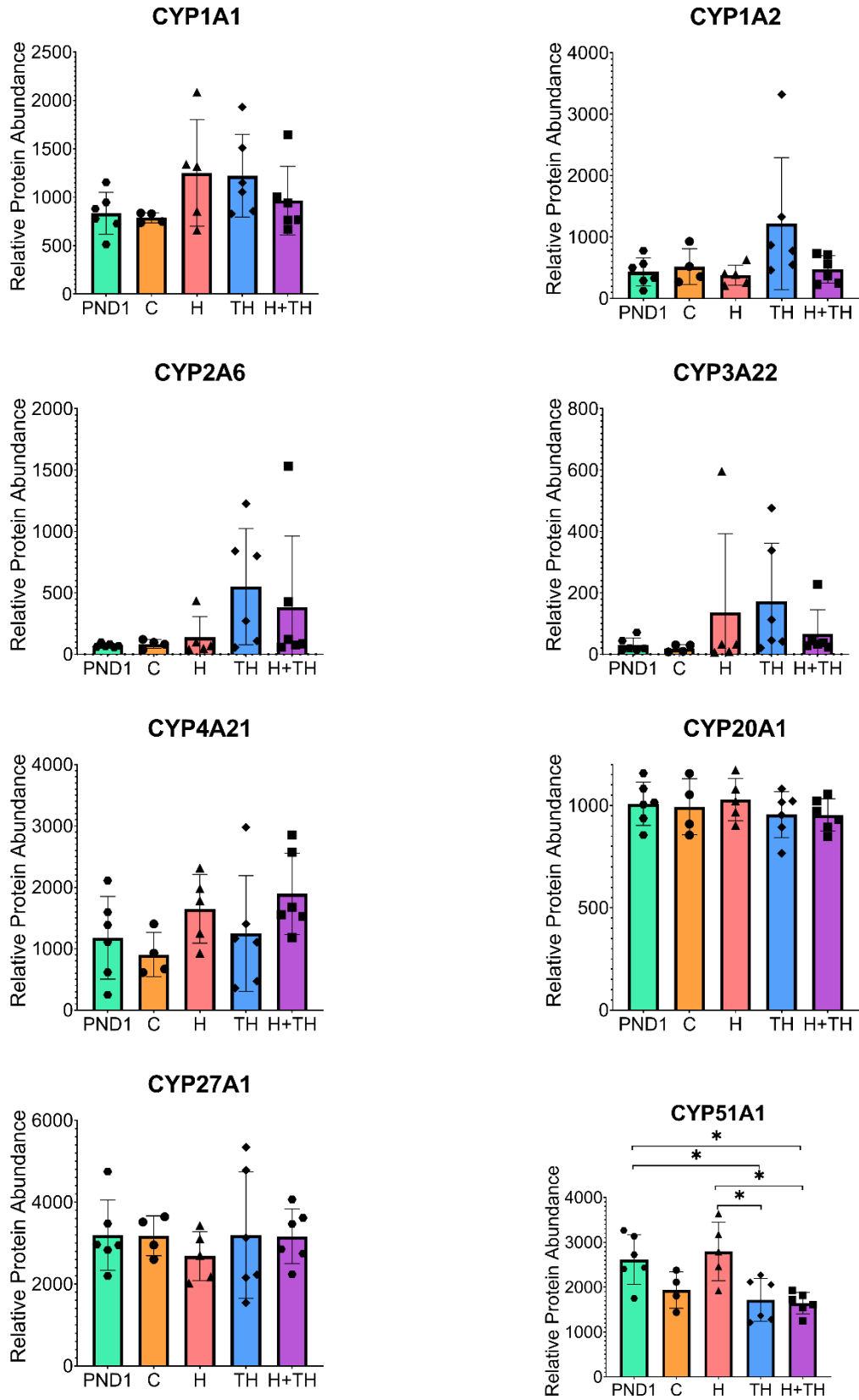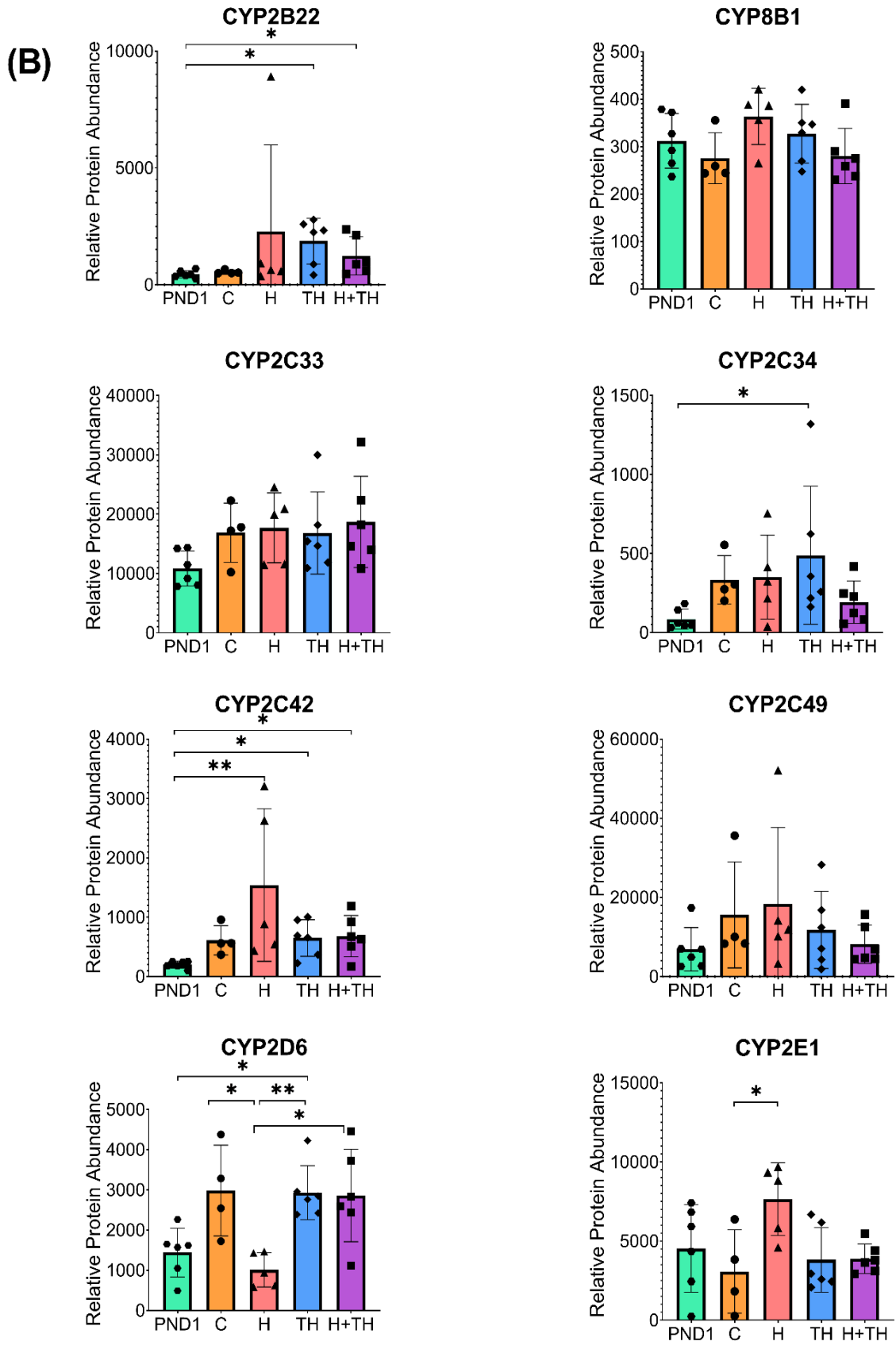
3.3. CYP-activity in Göttingen Minipigs

Figure 5. Hepatic cytochrome P450 (CYP) activity in Göttingen Minipig liver microsomes: The effect of age, sex, and temperature (immediate) on the general CYP and CYP1A activity. General CYP activity was significantly influenced by age at both 33 °C (P =0.0001) and 38 °C (P=0.0006), with a 75% difference in reaction velocities between adults and neonates. Temperature had a significant effect only in adults, with a 36% decrease in reaction velocity at 33 °C compared to 38 °C (P=0.0153), while no temperature effect was observed in neonates. For CYP1A activity, sex (P=0.0004) and age (P=0.0240) were significant factors, while temperature had no effect.* Lower limit of quantification (LLOQ); p-value: *, $P<0.05$; **, $P<0.005$; ***, $P<0.0005$; ****, $P<0.0001$; ns, non-significant.
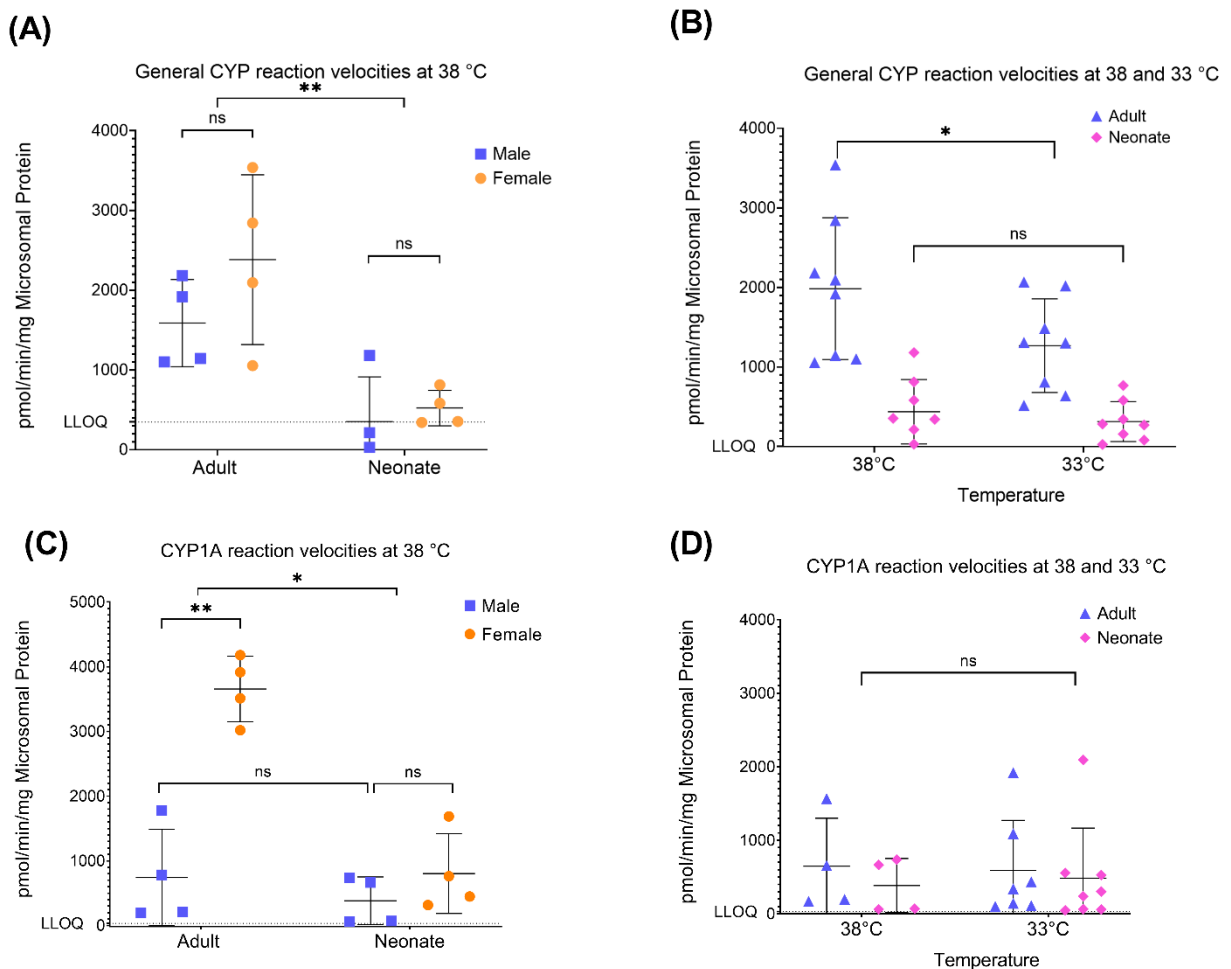
3.3.1. Age, sex, and temperature effects on the general CYP-activity

To determine the significance of the general CYP-activity findings related to sex and age (Figure 5, (A)), a linear mixed modelling analysis was conducted. The p-values of sex*age interaction and sex factor were >0.05 and, therefore, non-significant. However, age statistically significantly influenced general CYP activity in GLMs at 33 °C (P=0.0001) and 38 °C (P=0.0006; 75% difference between adult and neonatal general CYP reaction velocities). Using a similar methodology, the impact of age versus temperature and their interaction on the

general CYP-activity (Figure 5, (B)) was checked using linear mixed modelling. Temperature and age*temp showed a statistically significant influence. However, this must be interpreted cautiously since most neonatal reaction velocities were below LOD/LLOQ levels (i.e., LOD=223 and LLOQ=349 pmol/min/mg microsomal protein at 38 °C; LOD=141 and LLOQ=315 pmol/min/mg microsomal protein at 33 °C). The temperature only statistically significantly influenced adults (P=0.0153), represented by 36% decrease at 33 °C compared to 38 °C reaction velocities, and no influence was detected in neonates.

3.3.2. Age, sex, and temperature effects on the CYP1A-activity

3.3.2.1. The effects of age and temperature on CYP1A kinetics

A statistically significantly lower Km (P=0.0027; 77% decrease) and Vmax (P=0.0128; 81% decrease) were observed in neonates compared to adult Göttingen Minipigs at 38 °C, while temperature and the interaction age*temperature were non-significant factors (Figure 6). Given the non-normal distribution, the geometric mean and 95% confidence intervals were more suitable to overview these datasets and are provided (Table 1). The geometric mean was derived by applying a base 10 logarithm transformation, computing the mean of the logarithms, and subsequently converting the results back to the linear domain through antilog transformation. Based on these findings, the optimal substrate concentration was 54 μM for adult and 12 μM for neonatal GLMs.

Figure 6. Effect of age and temperature on the cytochrome P450 (CYP) 1A kinetics. The sample size consisted of 4 male Göttingen Minipigs for each age group (adults and neonates). Statistically significant lower Michaelis-Menten constants (Km) (P=0.0027) **(A)** and maximal velocity (Vmax) (P=0.0128) **(B)** of the reactions were observed in neonates compared to adults Göttingen Minipigs while temperature and the interaction age*temperature were non-significant factors. p-value: *, P<0.05; **, P<0.005; ***, P<0.0005; ****, P<0.0001.
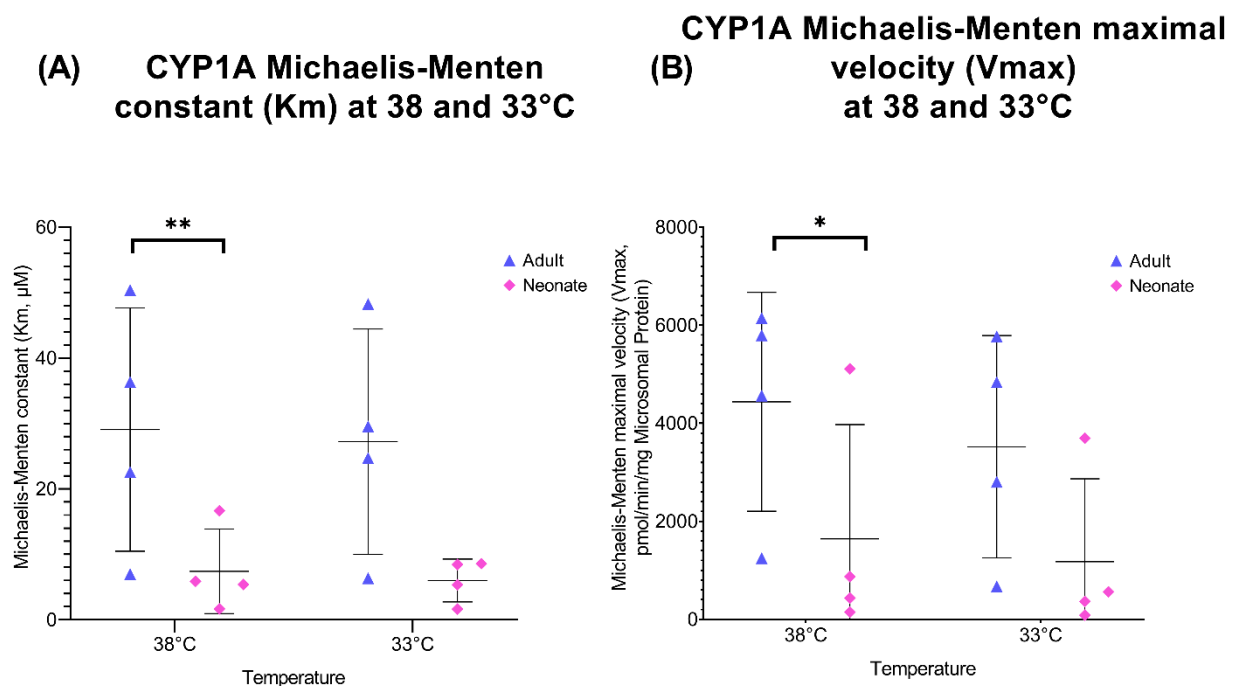
3.3.2.2. The effects of age, sex, and temperature on the CYP1A-reaction velocities

To determine the significance of the EROD findings related to sex, age, and temperature (Figure 5, (C) and (D)), a linear mixed model was conducted on the reaction velocities obtained from GLMs from both age and sex exposed to the two temperature treatments, incubated with 12 µM ER. We selected the Km concentration determined for neonates (12 µM) rather than the adult Km concentration. This decision was made to prevent substrate inhibition, especially considering the inclusion of neonatal samples, and to maintain a linear curve. All non-significant factors were removed step by step until sex (P=0.0004) and age (P=0.0240) remained significant. Therefore, CYP1A activity was not affected by temperature (Figure 5, (D)). Given the different optimal substrate concentrations for the two age groups (Section 3.3.2.1.), a Student's t-test was also employed to assess the significance of the EROD findings concerning sex (Figure 5, (C)). Only adult GLMs exposed to 54 µM 7-ethoxy resorufin showed statistically significant sex difference (5-fold higher reaction velocities in females compared to males, P=0.0011) and no difference between neonatal females and males, exposed to 12 µM ER. This confirms the findings revealed by the linear mixed modelling.

4. Discussion

4.1. Age

It is essential to recognize that each metabolic pathway, including those governed by CYP enzymes, follows a unique ontogeny pattern [32]. Cytochrome P450 3A4 is one of the most essential DMEs in humans and shows significant similarities with CYP3A in the Göttingen Minipig [4,12]. In humans, CYP3A4 is hardly expressed in utero and evolves to adult levels after infancy. Both abundance and activity of CYP3A increase gradually in juvenile Göttingen Minipigs but remain below the adult levels [4]. Instead, it is documented that CYP3A7 is most active in human foetal life and is almost absent after the first 2 weeks of postnatal life [6]. Other studies suggest that the "foetal" CYP3A7 isoform remains the dominant CYP3A enzyme until 1 year of age [3]. Contrastingly, a specific CYP3A "foetal" isoform homologue in the Göttingen Minipig is absent. 4 isoforms have been identified in the porcine CYP3A subfamily, from which CYP3A22 and CYP3A29 are considered CYP3A4 homologues in Göttingen Minipigs, while CYP3A39 and CYP3A46 cannot be excluded [12]. Our results are consistent with these previous findings, as we identified CYP3A22, CYP3A29, and CYP3A46 through qPCR and CYP3A22 through proteomics. Due to their high sequence similarity, the primers intended for CYP3A39 exhibited mismatches with unintended targets, predominantly CYP3A22 and CYP3A29. Considering that CYP3A39 is not deemed critical for metabolism in pigs and is considered a synonym for CYP3A22, we excluded it from further analysis. Concerning age-related differences, our study showed lower gene expression of CYP3A22, CYP3A29, and CYP3A46 in neonates compared to adult Göttingen Minipigs. These results are consistent with previously published ontogeny data from a proteomics study in the Göttingen Minipig, which revealed a gradual increase of CYP3A22, CYP3A29, and CYP3A46, reaching their highest levels in adulthood [13]. Additionally, in the same study, a correlation analysis between CYP protein abundance and activity indicated a clear association between CYP3A22 abundance and the metabolism of midazolam, a substrate highly specific to both porcine and human CYP3A [13].

Regarding other Göttingen Minipig CYPs, our investigations showed statistically significantly lower CYP2C42 and higher CYP2E1 gene expression in neonates compared to adult Göttingen Minipigs. A gradual increase in protein abundance was already demonstrated for CYP2C33, CYP2C34, CYP2C36, CYP4A21, CYP4V2_2a, and CYP27A1, with the highest levels observed at the adult age, while CYP1A2, CYP2A19, CYP2D6, CYP2D25, and CYP2E1 reached their maximum protein abundance already at PND28 [13]. Regarding CYP activity, our data agree with these findings as age statistically significantly influenced the general CYP activity in GLMs. The reaction velocities determined with neonatal GLMs were 75% lower than adults. For CYP1A activity, a significantly lower Km (77% decrease) and Vmax (81% decrease) were observed in neonates compared to adult GLMs. Furthermore, age was identified as a significant factor (*P*=0.0240) when analyzing CYP1A reaction velocities obtained from female GLMs. Interestingly, this was not observed when analyzing the male GLMs data at 33 °C and 38 °C.

4.2. Sex

Göttingen Minipigs show more sex-related expression and activity differences than other pig breeds [17,33]. For instance, CYP1A activity was 2-4 times higher in female than in male Göttingen Minipigs, which exhibited similar activity levels to conventional pigs [17]. Our data support these findings regarding CYP1A activity, with sex being identified as a significant factor (*P*=0.0004) with 5-fold higher reaction velocities in female than male adult GLMs. Similarly, CYP2A activity was 70-fold higher in female compared to male Göttingen Minipigs, but this time, a similar pattern was also observed in conventional pigs [17]. Notably, in vivo studies involving sexually mature male Göttingen Minipigs revealed that castration led to a 10-fold increase in CYP2A activity in GLMs, demonstrating sexual regulation of this gene [34,35]. Such sex differences are not observed in humans for CYP1A2 [36] and CYP2A6 [37].

4.3. Hypothermia

During hypothermia, most cellular processes are slowed down, including DMEs activity [38]. Our results showed that general CYP activity in adult GLMs decreased significantly (by 36%) when exposed to in vitro hypothermia (33 °C). Additionally, lower CYP51A1 protein abundance was detected in the TH groups. On the other hand, the CL of intermediate- (midazolam) and low- (phenobarbital) extraction ratio drugs can be reduced during cooling [38]. Our drug disposition data in neonatal Göttingen Minipigs (Chapter 4) [39] sustain this since we observed trends towards lower CL and longer half-life for midazolam and phenobarbital. We also noted statistically higher fentanyl plasma levels in the TH group due to reduced CL (66% decrease) with approximately 3-fold longer half-life. The significant influence of TH on heart rate in neonatal Göttingen Minipigs, consistent with its well-documented effect in human neonates, could be mechanistically linked to its impact on high extraction ratio drugs, like fentanyl. In contrast, intermediate- and low- extraction ratio drugs were less affected [39]. Another example is a study examining the impact of hypothermia on midazolam metabolism, primarily mediated by CYP3A2 in the liver, in rats [40]. This investigation was conducted at two levels: evaluating in vitro CYP3A2 activity and in vivo PK. Firstly, suspended rat hepatocytes were subjected to midazolam incubations at 37 °C, 32 °C, and 28 °C. The midazolam Km remained the same, while the Vmax decreased. Secondly, concerning the in vivo findings, midazolam

plasma concentrations were higher at 28 °C. Additionally, the fraction unbound (f_u) of midazolam in serum at 28 °C was half of the f_u at 37 °C [40].

Contrastingly, a small number of genes, which code for proteins participating in cold cell adaptation, are activated by hypothermia [41]. In a previous study, rats were exposed to 4 °C for 1, 5, or 10 days to study the effect of in vivo cold exposure on CYP1A1 and CYP1A2 activity and protein expression level in the liver and lungs [41]. In the liver, there was a decrease in both CYP1A1 and CYP1A2 activities on day 1 but an increase on days 5 and 10. In contrast, there was no change in CYP1A1 activity in the lungs, whereas CYP1A2 activity was below LOD at all time points during exposure to cold [41]. In our study, the temperature was a non-significant factor for CYP1A kinetics and reaction velocities in GLMs.

4.4. Hypoxia

It is well known that acute systemic hypoxia in humans down-regulate specific CYP isoforms and up-regulate CYP3A4 and P-glycoprotein, changing the drug CL and the kinetics [42]. In an in vivo study performed in rabbits subjected to an 8% fraction of inspired oxygen (FiO$_2$) for 48 hours, hypoxia down-regulated hepatic CYP1A1, CYP1A2, CYP2B4, CYP2C5, and CYP2C16 and up-regulated CYP3A6. Furthermore, in the same study, rats exposed to an 8% FiO$_2$ for 48 hours exhibited up-regulation of hepatic CYP3A11 and P-glycoprotein [43]. Our study results align with these findings regarding hypoxia-induced changes in CYP3A. We observed a statistically significant up-regulation of CYP3A29 mRNA, the only CYP3A Göttingen Minipig isoform that showed significant changes in gene expression in response to hypoxia.

Our study revealed increased mRNA expression of CYP3A29 and CYP2C33 in the H group, and the combination of hypoxia and TH elevated CYP2C33 and CYP2C42 mRNA expression compared to in vivo controls. These changes in gene expression were not reflected at the protein level for CYP2C enzymes (i.e., CYP2C33, CYP2C34 and CYP2C49 were not statistically significantly influenced by hypoxia), except for CYP2C42, where the H group exhibited a statistically significantly higher protein abundance compared to minipigs without medical treatment and interventions (i.e., PND1). These findings are consistent with another study conducted in rats where the influence of acute and chronic, middle- and high- altitude hypoxia was investigated on activity and protein abundance levels [44]. The protein abundance of CYP2C9, and CYP2C19 in the acute and chronic, middle- and high- altitude hypoxia groups was not significantly different from the controls (plain group). Still, the protein abundance of CYP2C19 increased significantly by 87.5% in the acute high-altitude hypoxia group compared to the chronic middle-altitude hypoxia group [44]. Therefore, it can be concluded that the effects of hypoxia are diverse and can vary depending on the CYP-isoform, and the specific level of investigation and, moreover, are influenced by the intensity and manner of hypoxia induction.

Cytochrome P450 2E1, known for its high oxidase activity, is involved in hypoxic injury [45]. A study using a CYP2E1-overexpressing HepG2 cell line demonstrated a substantial increase in CYP2E1 expression, catalytic activity, reactive oxygen species (ROS) production, and cell death during hypoxia [46]. Specifically, CYP2E1 showed a 720-fold increase in CYP2E1 expression and a prominent band in the Western blot analysis, associated with a 150-fold increase in CYP2E1 catalytic activity. The CYP2E1 produced 2.3-fold more ROS and 1.9-fold more cell death in this hypoxia model [46]. Our results, indicating a statistically significant increase in CYP2E1 protein abundance in the H group compared to in vivo controls, align with these previous findings. These results show that CYP2E1 in the liver may be involved in hypoxic injury.

An inflammatory reaction partially prevents both the down-regulation of CYP1A1/2 and the up-regulation of CYP3A6 produced by hypoxia [42]. This phenomenon has been demonstrated in rabbits exposed to moderate in vivo hypoxia, indicating that the up-regulation of CYP3A6 is dependent on the p42/44 Mitogen-activated Protein Kinase molecular mechanism, a pathway associated with the production of inflammatory mediators. This supports the hypothesis that proinflammatory cytokines (i.e., hypoxia-inducible factors and activator protein 1) may play a role in the signaling pathway leading to CYP3A6 induction by hypoxia [47]. The inflammatory reaction alone down-regulates CYP1A1/2 and CYP3A6, and hypoxia alone down-regulates CYP1A1/2 and up-regulates CYP3A6, although the combination of hypoxia and the inflammatory reaction down-regulates CYP1A1/2 marginally and partially prevents CYP3A6 up-regulation [42]. This was also the case in our study where CYP1A2 was one of the genes for which there was no significant response to hypoxia. Lastly, in addition to the in vitro and animal investigations, a population PK model was constructed to examine the effects of inflammation and organ failure on midazolam, in critically ill children [48]. The model revealed that inflammation and organ failure significantly decrease midazolam CL, a surrogate marker of CYP3A-mediated drug metabolism (i.e., the inflammatory markers C-reactive protein of 300 mg/L was associated with a 65% lower CL). Consequently, critically ill patients administered drugs metabolized by CYP3A may face heightened drug concentrations and the potential for associated toxicity [48]. These findings imply that various factors can influence the effects of hypoxia on enzyme functionality and drug metabolism. Consequently, it can be generalized that in cases of acute hypoxia, the PK of drugs metabolized by CYP enzymes may be changed, necessitating dose modifications. The following section lists the potential effect of administering drugs (e.g., phenobarbital) and other interventions (e.g., mechanical ventilation, MV) on enzyme functionality correlated with our findings.

4.5. Medical treatment and interventions

Hypoxia is usually not isolated but is associated with an underlying acute inflammatory process [49]. This connection between hypoxia and inflammation could potentially explain the differences observed between our naive neonatal Göttingen Minipig group (i.e., PND1) and the treated group (i.e., in vivo control, normothermic, normoxic, but undergoing 24 hours of general anesthesia). The impact of MV on human gene expression in tissues other than the lungs is poorly explored. A study performed to detect MV marker genes in 6 representative tissues (i.e., liver, fat, skin, (tibial) nerve, muscle, and lung) showed that MV is associated with reduced development, movement, and higher inflammation and injury not only in lungs but also in peripheral tissues [50]. Our data prove that medical treatment and interventions during 24 hours impact gene expression. The results showed that CYP1A2, CYP2C33, and CYP2E1 were down-regulated, while CYP3A22, CYP3A46, and CYP2C42 were up-regulated. Furthermore, literature findings showed that an inflammatory reaction down-regulates CYP1A, CYP2B, CYP2C and CYP3A subfamilies [49]. We observed this reduced gene expression for CYP1A2, CYP2C33, and CYP2E1 but not for CYP3A. One mechanistic explanation for why the mRNA expression of the CYP3A22 and CYP3A46 isoforms was increased in the treated (i.e., in vivo control group) compared to the naive (i.e., PND1 group) Göttingen Minipigs can rely upon a possible phenobarbital-mediated gene and enzyme induction since this drug was part of the medication. The ability of phenobarbital to modulate the metabolism of drugs and other xenobiotics in mammals has already been documented [51]. Phenobarbital induce 5'-diphosphate glucuronosyltransferases, CYP2C, and CYP3A enzymes in humans [52]. Since

phenobarbital is an inducer of CYP3A and midazolam is a CYP3A substrate, the co-treatment with phenobarbital might impact midazolam CL. For example, data collected in a prospective study, on days 2-5 after birth, from 113 neonates treated with phenobarbital, 118 treated with midazolam, and 68 treated with both drugs showed that phenobarbital significantly increased midazolam CL by a factor of 2.3, indicating potential drug-drug interaction [53]. Therefore, in regulating CYP genes, the medication must also be considered when interpreting findings.

Lastly, we did not find any significant differences between the treated and naive Göttingen Minipigs for CYP3A22 protein abundance, this up-regulation being observed just at the level of mRNA expression. This highlights again the difficulties in interpreting study endpoints, when looking at different levels. This is crucial because protein and mRNA expression often do not reflect activity, whereas enzyme activity governs the required dosage. Consequently, short-term, and long-term activity measurements are imperative to grasp the mechanism, whether directly at the protein level (catalytic activity) or at the expression level.

5. Conclusion

This study offers valuable insights into the impact of age, TH, and systemic hypoxia and the medical treatment and interventions (i.e., MV) on various CYPs. In vitro investigations showed differences in CYP gene expression and activity between neonatal and adult Göttingen Minipigs, highlighting again the role of maturation in drug metabolism. Regarding non-maturational factors, CYP activity in adult GLMs decreased by 36% after exposure to in vitro hypothermia. Although no differences were observed in gene expression in response to in vivo TH, the expression of CYP3A29, CYP2C33, and CYP2C42 genes was altered due to hypoxia in neonatal Göttingen Minipigs. The medical treatment and interventions over 24 hours, along with hypoxia and TH, affected the protein abundance of CYP51A1, CYP2B22, CYP2C34, CYP2C42, CYP2D6, and CYP2E1. These data on CYP expression, abundance, and activity in neonatal Göttingen Minipigs can subsequently support the construction of PBPK models and enhance dose precision in human neonates.

6. References

1.   Pokorna P, Wildschut ED, Vobruba V, et al. The Impact of Hypothermia on the Pharmacokinetics of Drugs Used in Neonates and Young Infants. Curr Pharm Des. 2015;21(39):5705-24.
2.   Azzopardi D, Brocklehurst P, Edwards D, et al. The TOBY Study. Whole body hypothermia for the treatment of perinatal asphyxial encephalopathy: A randomised controlled trial. BMC Pediatrics. 2008 2008/04/30;8(1):17.
3.   Hines RN. The ontogeny of drug metabolism enzymes and implications for adverse drug events. Pharmacol Ther. 2008 May;118(2):250-67.
4.   Van Peer E, De Bock L, Boussery K, et al. Age-related Differences in CYP3A Abundance and Activity in the Liver of the Göttingen Minipig. Basic Clin Pharmacol Toxicol. 2015 Nov;117(5):350-7.
5.   Hines RN. Developmental expression of drug metabolizing enzymes: impact on disposition in neonates and young children. Int J Pharm. 2013 Aug 16;452(1-2):3-7.

6.   Allegaert K, Simons SHP, Tibboel D, et al. Non-maturational covariates for dynamic systems pharmacology models in neonates, infants, and children: Filling the gaps beyond developmental pharmacology. Eur J Pharm Sci. 2017 2017/11//;109S:S27-S31.

7.   Allegaert K, Mian P, van den Anker JN. Developmental Pharmacokinetics in Neonates: Maturational Changes and Beyond. Curr Pharm Des. 2017;23(38):5769-5778.

8.   Mota-Rojas D, Villanueva-García D, Solimano A, et al. Pathophysiology of Perinatal Asphyxia in Humans and Animal Models. Biomedicines. 2022 Feb 1;10(2).

9.   Chapados I, Cheung PY. Not all models are created equal: animal models to study hypoxic-ischemic encephalopathy of the newborn. Commentary on Gelfand SL et al.: A new model of oxidative stress in rat pups (Neonatology 2008;94:293-299). Neonatology. 2008;94(4):300-3.

10. Puccinelli E, Gervasi P, Longo V. Xenobiotic Metabolizing Cytochrome P450 in Pig, a Promising Animal Model. Current drug metabolism. 2011 04/08;12:507-25.

11. Heckel T, Schmucki R, Berrera M, et al. Functional analysis and transcriptional output of the Göttingen minipig genome. BMC Genomics. 2015;16:932-932.

12. Van Peer E, Jacobs F, Snoeys J, et al. In vitro Phase I-and Phase II-drug metabolism in the liver of juvenile and adult Göttingen minipigs. Pharmaceutical research. 2017;34(4):750-764.

13. Buyssens L, De Clerck L, Schelstraete W, et al. Hepatic Cytochrome P450 Abundance and Activity in the Developing and Adult Göttingen Minipig: Pivotal Data for PBPK Modeling. Front Pharmacol. 2021;12:665644.

14. Smits A, Annaert P, Van Cruchten S, et al. A Physiology-Based Pharmacokinetic Framework to Support Drug Development and Dose Precision During Therapeutic Hypothermia in Neonates. Front Pharmacol. 2020;11:587-587.

15. Bode G, Clausing P, Gervais F, et al. The utility of the minipig as an animal model in regulatory toxicology. J Pharmacol Toxicol Methods. 2010 Nov-Dec;62(3):196-220.

16. Valenzuela A, Tardiveau C, Ayuso M, et al. Safety Testing of an Antisense Oligonucleotide Intended for Pediatric Indications in the Juvenile Göttingen Minipig, including an Evaluation of the Ontogeny of Key Nucleases. Pharmaceutics. 2021;13(9):1442.

17. Skaanild MT, Friis C. Cytochrome P450 sex differences in minipigs and conventional pigs. Pharmacol Toxicol. 1999 Oct;85(4):174-80.

18. Rasmussen MK, Scavenius C, Gerbal-Chaloin S, et al. Sex dictates the constitutive expression of hepatic cytochrome P450 isoforms in Göttingen minipigs. Toxicology Letters. 2019 2019/10/10/;314:181-186.

19. Verbueken E, Bars C, Ball JS, et al. From mRNA Expression of Drug Disposition Genes to In Vivo Assessment of CYP-Mediated Biotransformation during Zebrafish Embryonic and Larval Development. Int J Mol Sci. 2018 Dec 10;19(12).

20. Saad M, Matheeussen A, Bijttebier S, et al. In vitro CYP-mediated drug metabolism in the zebrafish (embryo) using human reference compounds. Toxicology in Vitro. 2017;42:329-336.

21. Achour B, Barber J, Rostami-Hodjegan A. Cytochrome P450 Pig liver pie: determination of individual cytochrome P450 isoform contents in microsomes from two pig livers using liquid chromatography in conjunction with mass spectrometry [corrected]. Drug Metab Dispos. 2011 Nov;39(11):2130-4.

22. Messina A, Chirulli V, Gervasi PG, et al. Purification, molecular cloning, heterologous expression and characterization of pig CYP1A2. Xenobiotica. 2008 Dec;38(12):1453-70.

23. Stroe M-S, Van Bockstal L, Valenzuela AP, et al. Development of a neonatal Göttingen Minipig model for dose precision in perinatal asphyxia: technical opportunities, challenges, and potential further steps [Methods]. Front Pediatr. 2023;11:662.

24. Corpet F. Multiple sequence alignment with hierarchical clustering. Nucleic Acids Res. 1988 Nov 25;16(22):10881-90.

25. Bustin SA, Benes V, Garson JA, et al. The MIQE guidelines: minimum information for publication of quantitative real-time PCR experiments. Clin Chem. 2009 Apr;55(4):611-22.

26. Nygard AB, Jørgensen CB, Cirera S, et al. Selection of reference genes for gene expression studies in pig tissues using SYBR green qPCR. BMC Mol Biol. 2007 Aug 15;8:67.

27. Pfaffl MW, Horgan GW, Dempfle L. Relative expression software tool (REST) for group-wise comparison and statistical analysis of relative expression results in real-time PCR. Nucleic Acids Res. 2002 May 1;30(9):e36.

28. Millecam J, De Clerck L, Govaert E, et al. The Ontogeny of Cytochrome P450 Enzyme Activity and Protein Abundance in Conventional Pigs in Support of Preclinical Pediatric Drug Research. Front Pharmacol. 2018;9:470.

29. Perez-Riverol Y, Bai J, Bandla C, et al. The PRIDE database resources in 2022: a hub for mass spectrometry-based proteomics evidences. Nucleic Acids Res. 2022 Jan 7;50(D1):D543-d552.

30. Swindle MM. Swine in the laboratory: surgery, anesthesia, imaging, and experimental techniques. CRC press; 2007.

31. Sengul U. Comparing determination methods of detection and quantification limits for aflatoxin analysis in hazelnut. J Food Drug Anal. 2016 Jan;24(1):56-62.

32. Ward RM, Benjamin D, Barrett JS, et al. Safety, dosing, and pharmaceutical quality for studies that evaluate medicinal products (including biological products) in neonates. Pediatr Res. 2017 May;81(5):692-711.

33. Rasmussen MK. Porcine cytochrome P450 3A: current status on expression and regulation. Arch Toxicol. 2020 Jun;94(6):1899-1914.

34. Gillberg M, Skaanild M, Friis C. Changes in hepatic cytochrome 2A, 2E, and 3A expression in the Göttingen minipig following castration. J Vet Pharm Ther. 2003;26.

35. Skaanild MT. Porcine cytochrome P450 and metabolism. Curr Pharm Des. 2006;12(11):1421-7.

36. Shimada T, Yamazaki H, Mimura M, et al. Interindividual variations in human liver cytochrome P-450 enzymes involved in the oxidation of drugs, carcinogens and toxic chemicals: studies with liver microsomes of 30 Japanese and 30 Caucasians. J Pharmacol Exp Ther. 1994 Jul;270(1):414-23.

37. Chauret N, Gauthier A, Martin J, et al. In vitro comparison of cytochrome P450-mediated metabolic activities in human, dog, cat, and horse. Drug Metab Dispos. 1997 Oct;25(10):1130-6.

38. Zhou J, Poloyac SM. The effect of therapeutic hypothermia on drug metabolism and response: cellular mechanisms to organ function. Expert Opin Drug Metab Toxicol. 2011 Jul;7(7):803-16.

39. Stroe M-S, Huang M-C, Annaert P, et al. Drug disposition in neonatal Göttingen Minipigs: Exploring Effects of Perinatal Asphyxia and Therapeutic Hypothermia. Drug Metabolism and Disposition. 2024.

40. Miyamoto H, Matsueda S, Moritsuka A, et al. Evaluation of hypothermia on the in vitro metabolism and binding and in vivo disposition of midazolam in rats. Biopharmaceutics & Drug Disposition. 2015;36(7):481-489.

41. Maria LP, Alevtina Yu G. Comparison of the Effects of Cold on Cytochromes P450 1A in the Rat Lungs Versus Liver. Advances in Biochemistry. 2013;1(2):7-12.

42. du Souich P, Fradette C. The effect and clinical consequences of hypoxia on cytochrome P450, membrane carrier proteins activity and expression. Expert Opin Drug Metab Toxicol. 2011 Sep;7(9):1083-100.

43. Fradette C, Batonga J, Teng S, et al. Animal models of acute moderate hypoxia are associated with a down-regulation of CYP1A1, 1A2, 2B4, 2C5, and 2C16 and up-regulation of CYP3A6 and P-glycoprotein in liver. Drug Metab Dispos. 2007 May;35(5):765-71.

44. Li X, Wang X, Li Y, et al. Effect of exposure to acute and chronic high-altitude hypoxia on the activity and expression of CYP1A2, CYP2D6, CYP2C9, CYP2C19 and NAT2 in rats. Pharmacology. 2014;93(1-2):76-83.

45. Caro AA, Cederbaum AI. Oxidative stress, toxicology, and pharmacology of CYP2E1. Annu Rev Pharmacol Toxicol. 2004;44:27-42.

46. Alwadei N, Rashid M, Chandrashekar DV, et al. Generation and Characterization of CYP2E1-Overexpressing HepG2 Cells to Study the Role of CYP2E1 in Hepatic Hypoxia-Reoxygenation Injury. International Journal of Molecular Sciences. 2023;24(9):8121.

47. Fradette C, du Souich P. Hypoxia-inducible factor-1 and activator protein-1 modulate the upregulation of CYP3A6 induced by hypoxia. Br J Pharmacol. 2003 Nov;140(6):1146-54.

48. Vet NJ, Brussee JM, de Hoog M, et al. Inflammation and Organ Failure Severely Affect Midazolam Clearance in Critically Ill Children. Am J Respir Crit Care Med. 2016 Jul 1;194(1):58-66.

49. Dumais G, Iovu M, du Souich P. Inflammatory reactions and drug response: importance of cytochrome P450 and membrane transporters. Expert Rev Clin Pharmacol. 2008 Sep;1(5):627-47.

50. Somekh J, Lotan N, Sussman E, et al. Predicting mechanical ventilation effects on six human tissue transcriptomes. PLoS One. 2022;17(3):e0264919.

51. Kemper B. Regulation of Cytochrome P450 Gene Transcription by Phenobarbital. In: Moldave K, editor. Progress in Nucleic Acid Research and Molecular Biology. Vol. 61: Academic Press; 1998. p. 25-64.

52. Dowd FJ, Johnson B, Mariotti A. Pharmacology and therapeutics for dentistry-E-book. Elsevier Health Sciences; 2016.

53. Favié LMA, Groenendaal F, van den Broek MPH, et al. Phenobarbital, Midazolam Pharmacokinetics, Effectiveness, and Drug-Drug Interaction in Asphyxiated Neonates Undergoing Therapeutic Hypothermia. Neonatology. 2019;116(2):154-162.

7. Supplementary materials

7.1. Supplementary tables

Supplementary Table 1. Target and reference genes in (mini)pigs with the specific primers. * Cytochrome P450 (CYP); The National Center for Biotechnology Information (NCBI).

Homo sapiens	Sus scrofa orthologues	Primer	Input PCR template in NCBI primer blast
CYP1A2	CYP1A2	Forward primer: AGGAGCGCTATCGGGACTTTG Reverse primer: TGGTAATTGTATCAAATCCGGCTCC	**NM_001159614.1.** Sus scrofa cytochrome P450 family 1 subfamily A member 2 (CYP1A2), mRNA
CYP3A4	CYP3A22	Forward primer: AGCCTGTGCTGGCTATGAGA Reverse primer: CCGCTGGACCAAAATTCCGC	**NM_001195509.1** Sus scrofa cytochrome P450 family 3 subfamily A member 22 (CYP3A22), mRNA
	CYP3A29	Forward primer: TACCTGCCCTTTGGGACTGG Reverse Primer: TGTGTAAGCCCTTGCGTGGT	**EU918131.1** Sus scrofa breed Bama miniature cytochrome P450 CYP3A, mRNA
	CYP3A46	Forward primer: TGATGGTGCCAATCTTTGCG Reverse primer: GAGGGCAAACCTCATGCCAA	**NM_001134824.1** Sus scrofa cytochrome P450 family 3 subfamily A member 46 (CYP3A46), mRNA
CYP2C8 CYP2C9	CYP2C33	Forward primer: CAGCCTGCCGTGGTCTTACA Reverse primer: GGGAGAAGCGCCGTATTTGC	**NM_214414.1** Sus scrofa cytochrome P450 family 2 subfamily C member 33 (CYP2C33), mRNA
CYP2C8 CYP2C18 CYP2C9 CYP2C19	CYP2C42	Forward primer: CATCCCCAAGGGCACAACAA Reverse primer: CCCTCTCCCACACAAATCCG	**NM_001167835.1** Sus scrofa cytochrome P450 C42 (CYP2C42), mRNA
CYP2D6	CYP2D25	Forward primer: CGAGTACAACGACCCTCGCA Reverse primer: GAAGAGCTTGGCACACAGCC	**NM_214394.1** Sus scrofa cytochrome P450 family 2 subfamily D member 6 (CYP2D6), mRNA
CYP2E1	CYP2E1	Forward primer: AATCCCCACGTTCCAAGTGC Reverse primer: TTCCCCATCCCGAAGTCACG	**NM_214421.1** Sus scrofa cytochrome P450 family 2 subfamily E member 1 (CYP2E1), mRNA
-	Hypoxanthine phosphoribosyl transferase 1 (HPRT1)	Forward primer: GGACTTGAATCATGTTTGTG Reverse primer: CAGATGTTTCCAAACTCAAC	**NM_001032376.2** Sus scrofa hypoxanthine phosphoribosyltransferase 1 (HPRT1), mRNA
	Ubiquitin C (UBC)	Forward primer: CTTGGTCCTGCGCTTGAGG Reverse primer: AAGTGCAATGAAATTTGTTGAAAGC	**XM_003483411.4** Sus scrofa ubiquitin C (UBC), transcript variant X1, mRNA

Supplementary Table 2. The concentration and the purity (ratio A260/A280 and A260/A230) of the isolated total RNA from 36 Göttingen Minipigs frozen liver samples: naive adult (n=6, males, M1, M2, M3, M4, M5, M6) and neonatal (n=6, < 24 hours of age, males, postnatal day, PND1 1, PND1 2, PND1 3, PND1 4, PND1 5, PND1 6) Göttingen Minipigs' to assess the age-related differences; 6 males, <24 hours of age Göttingen Minipigs per condition: hypoxia (H; H1, H2, H3, H4, H5, H6), therapeutic hypothermia (TH; TH1, TH2, TH3, TH4, TH5, TH6), hypoxia and TH (HTH; HTH1, HTH2, HTH3, HTH4, HTH5, HTH6), and in vivo controls (C; C1, C2, C3, C4, C5, C6) to assess the impact of hypothermia and hypoxia, were selected.

Sample	Group	Concentration (ng/µL)	A260/A280	A260/A230
C1	Control	3432.3	2.06	2.1
C2		7820.6	2.06	2.09
C3		3105.8	2.07	2.16
C4		2971.1	2.07	2.23
C5		3376.4	2.06	2.21
C6		5107.4	2.09	2.26
TH1	Therapeutic hypothermia	7797.3	2.04	2.05
TH2		2204.8	2.05	2.1
TH3		13567.2	2.05	1.97
TH4		3051.2	2.09	1.98
TH5		4236.3	2.08	2.06
TH6		4509.1	2.1	2.08
H1	Hypoxia	3002.8	2.08	1.94
H2		4579.3	2.09	1.88
H3		2235.7	2.08	2.19
H4		2466.6	2.04	1.99
H5		7081.1	2.06	1.85
H6		1929.1	2.1	2.07
HTH1	Hypoxia and Therapeutic hypothermia	8528.5	2.06	1.99
HTH2		3278	2.05	2.06
HTH3		1834.7	2.09	2.2
HTH4		2581.7	2.04	2.21
HTH5		4194.1	2.07	2.09
HTH6		6469.4	2.05	2.04
PND11	Postnatal day	3038.3	2.06	2.23
PND12		2771.3	2.05	2.27
PND13		4539.8	2.07	1.84
PND14		4908.7	2.05	2.07
PND15		1684.9	2.06	1.97
PND16		1676.7	2.06	2.01
M1	Adult	1160.4	2.04	1.87
M2		1189.8	2.04	2.09
M3		2570.9	2.05	2.07
M4		3235.2	2.07	2.01
M5		2560.2	2.05	2
M6		1192	2.01	2.02

Supplementary Table 3. Optimization steps (i.e., primer concentrations, efficiency, gradient temperature (58 °C, 60 °C, and 62 °C)) were conducted to identify the optimal conditions for amplification, using conventional PCR. * degree Celsius (°C); Cytochrome P450 (CYP); Hypoxanthine phosphoribosyl transferase 1 (HPRT1); Ubiquitin C (UBC).

Sus scrofa orthologues	Primer (µL)	Efficiency	Information	Temperature (°C)
HPRT1	0.5	0.9742	Reference and Inter-plate Calibrator	60
		0.9271	Reference and Inter-plate Calibrator	58
UBC	0.5	0.8104	Reference	60
		0.9482	Reference	58
CYP3A22	0.5	0.8982	Target	58
CYP3A29	0.5	0.913	Target	60
CYP3A46	0.5	0.9266	Target	60
CYP1A2	0.3	0.8915	Target	60
CYP2D25	0.3	0.8526	Target	60
CYP2C33	0.5	0.8468	Target	60
CYP2C42	0.3	0.8313	Target	60
CYP2E1	0.5	0.8692	Target	60

Supplementary Table 4. S-Trap™ mini spin column digestion protocol (Protifi) steps and required reagents and solutions.

	Reagents and solutions	Quantity
(2x) Lysis Buffer	10 % sodium dodecyl sulphate (SDS))	23 µL
Reducer	5 mM dithiothreitol (DTT) final concentration in 27.5 µL	2 µL
Alkylator	methyl methanethiosulphonate (MMTS), 500 mM MMTS in isopropanol	2 µL
Acidifier	phosphoric acid, pH ≤ 1	5 µL
Biding / Washing buffer	final concentration of 100 mM triethylammonium bicarbonate (TEAB) in 90% methanol	350 / 400 µL
Tryp/Lys Solution	Tryp/Lys solution in 50 mM TEAB	1 µg / 125 µL
Elution Solution	80 µL 50 mM TEAB, 80 µL 0.2 % formic acid (FA) and 80 µL 50 % acetonitrile	

Supplementary Table 5. Overview of the statistically significant results for mRNA expression, protein abundance, and enzyme activity, grouped according to the covariate studied: age, sex, hypothermia, hypoxia, medical treatment, and interventions. * Cytochrome P450 (CYP); Michaelis-Menten constant (Km); hypoxia (H); postnatal day 1 denoted as naive Göttingen Minipigs (PND1); therapeutic hypothermia (TH); maximal reaction velocity (Vmax).

Assay	Studied Effect	Target CYP	Treatment Group	Control Group	Expression Ratio / % Difference	P	Result
qPCR	Age	CYP3A22	Neonate	Adult	0.026	0.0005	Down-regulated
qPCR		CYP3A29	Neonate	Adult	0.004	0.0010	Down-regulated
qPCR		CYP3A46	Neonate	Adult	0.004	0.0020	Down-regulated
qPCR		CYP2C42	Neonate	Adult	0.250	0.0115	Down-regulated
qPCR		CYP2E1	Neonate	Adult	8.820	0.0335	Up-regulated
Fluorometry		General CYP	Neonate reaction velocities	Adult reaction velocities	75%	0.0006	Lower
Fluorometry		CYP1A	Neonate Km	Adult Km	77%	0.0027	Lower
Fluorometry		CYP1A	Neonate Vmax	Adult Vmax	81%	0.0128	Lower
Fluorometry		CYP1A	Neonate reaction velocities	Adult reaction velocities	62%	0.0240	Lower
Fluorometry	Sex	CYP1A	Female	Male	5-fold higher reaction velocities in females compared to males	0.0011	Higher
Fluorometry	Hypothermia	General CYP	Adult 33°C (in vitro)	Adult 38°C (in vitro)	36%	0.0153	Lower
Proteomics		CYP51A1	TH	PND1		0.0291	Lower
Proteomics		CYP51A1	H+TH	PND1	-	0.0167	Lower
Proteomics		CYP51A1	TH	H		0.0104	Lower

Proteomics		CYP51A1	H+TH	H		0.0060	Lower
Proteomics		CYP2B22	TH	PND1		0.0202	Higher
Proteomics		CYP2B22	H+TH	PND1		0.0202	Higher
Proteomics		CYP2C34	TH	PND1		0.0098	Higher
qPCR	Hypoxia	CYP3A29	H	C	5.147	0.0260	Up-regulated
qPCR		CYP2C33	H	C	3.229	0.0025	Up-regulated
qPCR		CYP2C33	H+TH	C	2.491	0.0030	Up-regulated
qPCR		CYP2C42	H+TH	C	4.019	0.0400	Up-regulated
Proteomics		CYP2D6	H	C		0.0143	Lower
Proteomics		CYP2D6	H	TH	-	0.0075	Lower
Proteomics		CYP2D6	H	H+TH		0.0105	Lower
Proteomics		CYP2E1	H	C		0.0362	Higher
qPCR	Medical treatment and interventions	CYP1A2	C	PND1	0.274	0.0190	Down-regulated
qPCR		CYP3A22	C	PND1	16.120	0.0060	Up-regulated
qPCR		CYP3A46	C	PND1	3.637	0.0060	Up-regulated
qPCR		CYP2C33	C	PND1	0.526	0.0265	Down-regulated
qPCR		CYP2C42	C	PND1	3.643	0.0285	Up-regulated
qPCR		CYP2E1	C	PND1	0.241	0.0335	Down-regulated
Proteomics		CYP2C42	H	PND1		0.0008	Higher
Proteomics		CYP2C42	TH	PND1	-	0.0392	Higher
Proteomics		CYP2C42	H+TH	PND1		0.0346	Higher
Proteomics		CYP2D6	TH	PND1		0.0371	Higher

Supplementary Table 6. The gene expression ratios, standard errors, 95% confidence intervals (CI), and p-values following the relative expression software tool: the age-related differences **(A)**; medical treatment and interventions during the 24-hour experiment- related differences **(B)**; hypoxia (H) and/or therapeutic hypothermia (TH)- related differences within the controls and the treated groups **(C)**.

(A) Age-related differences: Adult versus Neonate

Gene	Treatment Group	Expression Ratio	Standard Error	95% CI	*P*	Result
CYP1A2	Neonate	3.3142	0.259 - 39.936	(0.109; 67.186)	0.2815	No difference
CYP3A22	Neonate	0.0259	0.011 - 0.065	(0.003; 0.114)	0.0005	**Down**
CYP3A29	Neonate	0.0043	0.002 - 0.01	(0.001; 0.015)	0.001	**Down**
CYP3A46	Neonate	0.0039	0.002 - 0.008	(0.001; 0.011)	0.002	**Down**
CYP2C33	Neonate	1.0443	0.506 - 2.188	(0.339; 3.060)	0.8945	No difference
CYP2C42	Neonate	0.2484	0.085 - 0.602	(0.052; 1.301)	0.0115	**Down**
CYP2D25	Neonate	0.4005	0.112 - 1.257	(0.029; 1.973)	0.1795	No difference
CYP2E1	Neonate	8.8198	1.414 - 71.118	(0.293; 123.636)	0.0335	**Up**

(B) Medical treatment and interventions -related differences: PND versus (in vivo) Control

Gene	Treatment Group	Expression Ratio	Standard Error	95% CI	*P*	Result
CYP1A2	Control	0.2742	0.143 - 0.5	(0.086; 1.104)	0.019	**Down**
CYP3A22	Control	16.1198	3.388 - 68.883	(1.689; 200.174)	0.006	**Up**
CYP3A29	Control	1.3465	0.422 - 4.699	(0.235; 9.973)	0.601	No difference
CYP3A46	Control	3.637	1.695 - 9.495	(1.208; 19.049)	0.006	**Up**
CYP2C33	Control	0.5257	0.321 - 0.885	(0.223; 1.069)	0.0265	**Down**
CYP2C42	Control	3.6426	1.315 - 9.887	(0.615; 25.340)	0.0285	**Up**
CYP2D25	Control	0.7896	0.325 - 1.869	(0.214; 4.998)	0.598	No difference
CYP2E1	Control	0.2412	0.089 - 0.56	(0.066; 2.138)	0.0335	**Down**

(C) Hypoxia (H) and/or therapeutic hypothermia (TH) -related differences within the controls and the treated groups: (in vivo) Control versus Treated groups.

Gene	Treatment Group	Expression Ratio	Standard Error	95% CI	*P*	Result
CYP1A2	Hypothermia	0.8358	0.201 - 4.044	(0.136; 8.409)	0.773	No difference

| CYP1A2	Hypoxia	2.6047	0.741 - 14.349	(0.101; 45.468)	0.2705	No difference
CYP1A2	Hypothermia and Hypoxia	0.8332	0.453 - 1.461	(0.35; 2.619)	0.5	No difference
CYP3A22	Hypothermia	1.3434	0.195 - 10.430	(0.013; 25.917)	0.7875	No difference
CYP3A22	Hypoxia	3.7489	0.498 - 25.036	(0.126; 233.081)	0.2085	No difference
CYP3A22	Hypothermia and Hypoxia	0.8295	0.125 - 6.014	(0.031; 26.166)	0.8215	No difference
CYP3A29	Hypothermia	1.4067	0.449 - 5.610	(0.186; 7.391)	0.5285	No difference
CYP3A29	Hypoxia	5.1472	1.080 - 17.481	(0.529; 96.761)	0.026	**Up**
CYP3A29	Hypothermia and Hypoxia	1.6089	0.455 - 7.223	(0.113; 20.517)	0.4755	No difference
CYP3A46	Hypothermia	0.6474	0.231 - 1.931	(0.102; 3.026)	0.438	No difference
CYP3A46	Hypoxia	3.2560	1.004 - 11.663	(0.274; 56.88)	0.119	No difference
CYP3A46	Hypothermia and Hypoxia	1.3857	0.549 - 3.297	(0.229; 7.639)	0.4745	No difference
CYP2C33	Hypothermia	1.4352	0.758 - 2.726	(0.398; 4.519)	0.3085	No difference
CYP2C33	Hypoxia	3.2292	1.968 - 5.431	(1.584; 10.101)	0.0025	**Up**
CYP2C33	Hypothermia and Hypoxia	2.4914	1.723 - 4.336	(1.212; 5.262)	0.003	**Up**
CYP2C42	Hypothermia	1.881	0.701 - 5.903	(0.296; 19.858)	0.307	No difference
CYP2C42	Hypoxia	1.3035	0.446 - 3.784	(0.203; 5.922)	0.6045	No difference
CYP2C42	Hypothermia and Hypoxia	4.0197	1.099 - 13.749	(0.394; 32.953)	0.04	**Up**
CYP2D25	Hypothermia	0.8068	0.386 - 1.532	(0.245; 2.083)	0.593	No difference
CYP2D25	Hypoxia	2.7106	0.856 - 7.838	(0.414; 61.954)	0.1385	No difference
CYP2D25	Hypothermia and Hypoxia	1.6028	0.783 - 3.930	(0.352; 5.127)	0.2665	No difference
CYP2E1	Hypothermia	0.9596	0.184 - 3.907	(0.130; 8.324)	0.9485	No difference
CYP2E1	Hypoxia	2.4256	0.670 - 9.425	(0.305; 23.544)	0.166	No difference
CYP2E1	Hypothermia and Hypoxia	1.7281	0.566 - 4.526	(0.395; 9.175)	0.237	No difference

7.2. Supplementary figures

The effects of therapeutic hypothermia and hypoxia induced in vivo on the activity

To investigate the impact of TH and systemic hypoxia on general CYP and CYP1A activities, preliminary experiments were carried out using the 30 liver microsomes obtained from instrumented Göttingen Minipigs, including the naive neonatal minipigs (PND 1). These samples were incubated with BOMR, respectively, with ER substrate, at 38 °C, since the treatment conditions (i.e., in vivo control (C), therapeutic hypothermia (TH), hypoxia (H), hypoxia and TH (H+TH)) were performed in vivo. The experimental procedures followed the same steps outlined in the optimized BOMR protocol, referring to the standard curve, the optimal substrate (i.e., 1.2 µM BOMR; 12 µM ER) and microsomal protein concentrations (i.e., 75 µg/mL for BOMR respectively, 100 and 500 µg/mL for EROD assay).

The reaction velocities data were analyzed by One-Way ANOVA to test the underlying null hypothesis of no difference between the 5 groups investigated and for each assay. Normality and homogeneity of variances were tested by the Shapiro-Wilk and Levene's test and a logarithm transformation was required to meet the assumptions for parametric testing. No statistically significant differences observed between the groups investigated in both assays.

Supplementary Figure 1. In vivo therapeutic hypothermia (TH) and systemic hypoxia effects on enzyme activity assessed with Vivid® BOMR (7-benzyloxy-methyl resorufin) **(A)** and the ethoxyresorufin-O-deethylase (EROD) **(B)** assays in neonatal Göttingen Minipig liver microsomes. * Microsomal protein (MP). The statistical analysis was performed using the reaction velocities for each individual categorized in the function of group as input data: neonatal Göttingen Minipigs without medical treatment and interventions (<24 hours of age denoted as postnatal day, PND1), control (C), therapeutic hypothermia (TH), hypoxia (H), hypoxia and TH (H+TH).

(A) General CYP Reaction Velocities   (B) CYP1A Reaction Velocities
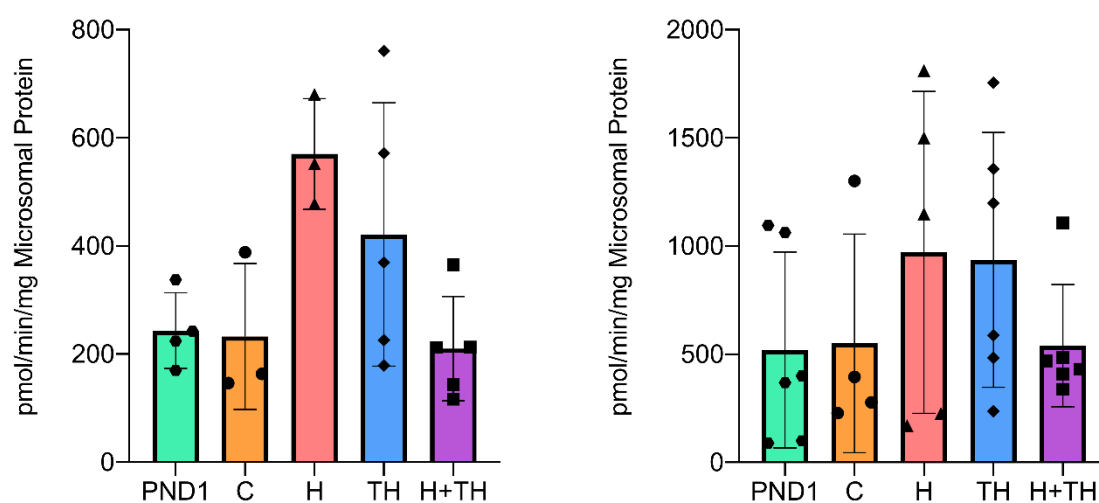
Supplementary Figure 2. Michaelis-Menten plot analysis. The age and temperature effects on the CYP1A Michaelis-Menten kinetics observed in adult (n=4) **(A)** compared with neonatal (n=4) **(B)** Göttingen Minipigs.
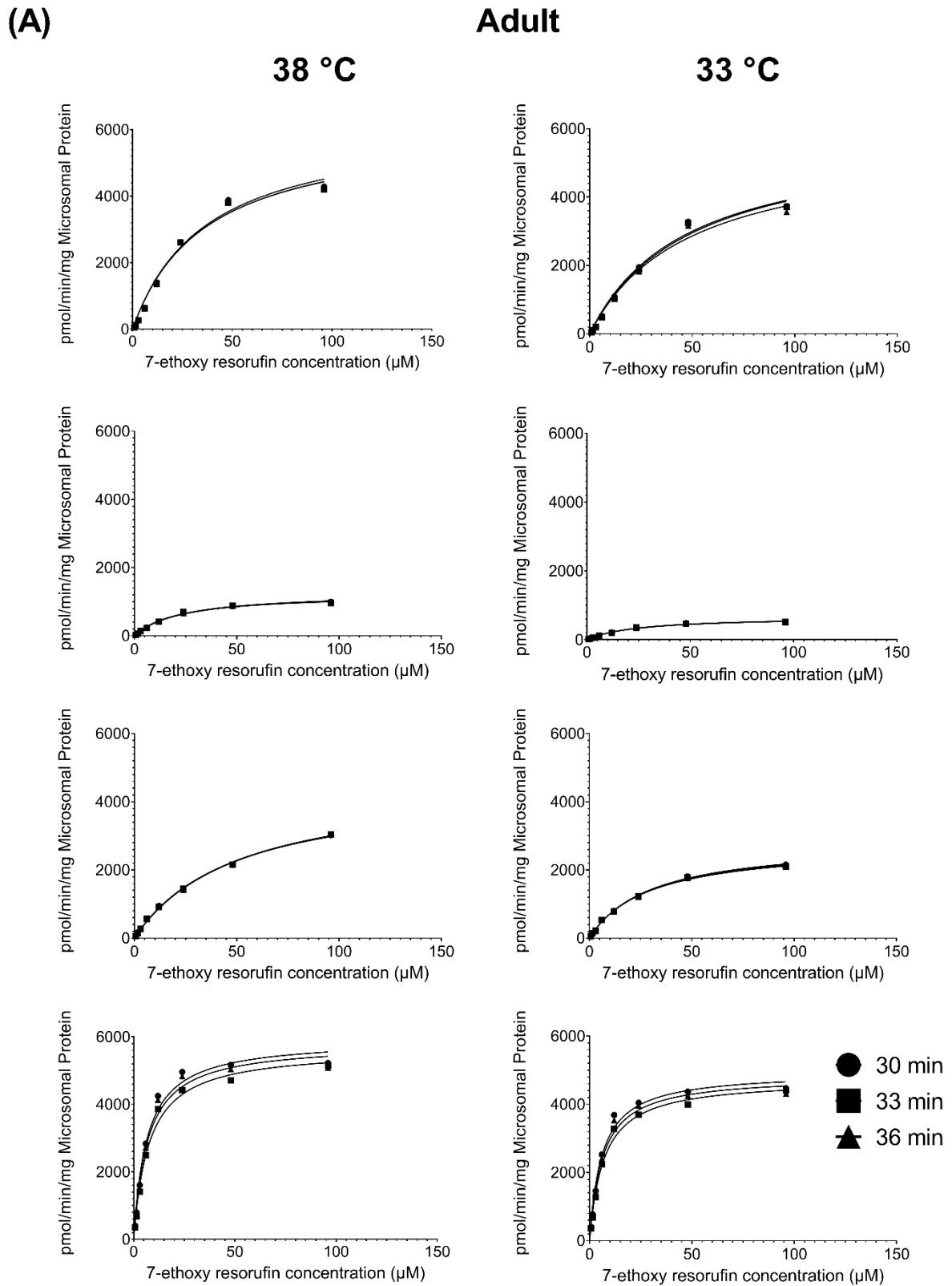
(B)   **Neonate**
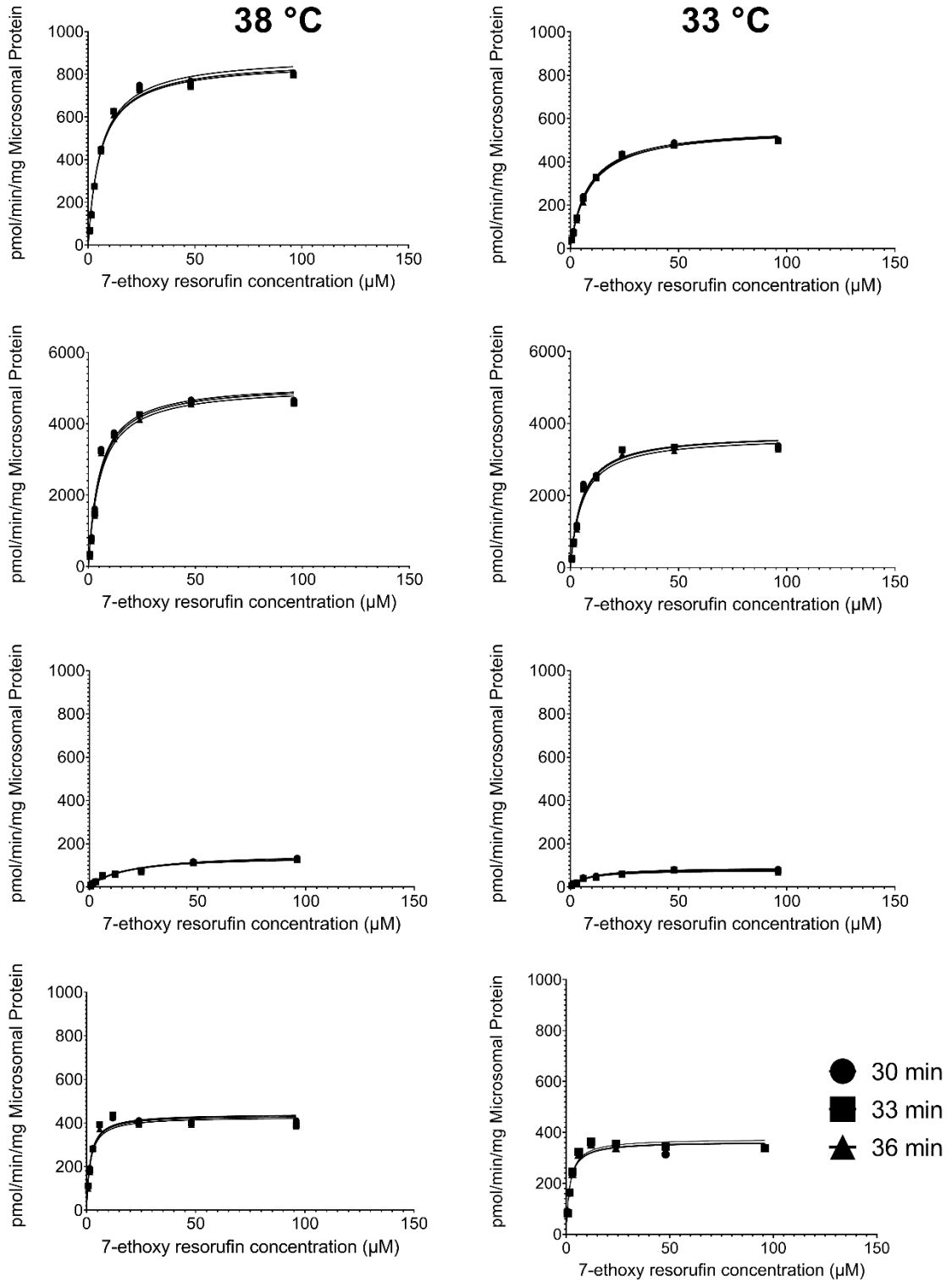
CHAPTER 6:
Enhancing pediatric pharmacotherapy knowledge: a neonatal Göttingen Minipig physiologically-based pharmacokinetic (PBPK) model with midazolam and topiramate as model drugs

In this thesis, Chapter 6 explores the available information to establish a pilot neonatal (juvenile) Göttingen Minipig PBPK model and highlights current knowledge gaps (unpublished work).

Enhancing pediatric pharmacotherapy knowledge: a neonatal Göttingen Minipig physiologically-based pharmacokinetic (PBPK) model with midazolam and topiramate as model drugs

Abstract

Physiologically-based pharmacokinetic (PBPK) modelling and simulation (M&S) is a bottom-up computational approach to predict pharmacokinetics (PK) based on population- and drug-specific data. For the pediatric population, animal models, such as juvenile animals, offer promise. Conversely, hypothermia in neonates is one of the conditions for which the development of PBPK models is urgently needed. This highlights the growing importance of special populations PK in PBPK modeling, where species models help the study of disease and treatment scenarios not feasible in clinical settings, enhancing the translational value of PBPK models. Following a translational and multidisciplinary approach, our study aimed to develop a human and minipig PBPK framework to describe and predict the impact of hypothermia on drug disposition in neonates. This chapter explores the available information to establish a database for the neonatal (juvenile) Göttingen Minipig physiological model and highlights current knowledge gaps. Initial PBPK models were developed for two model drugs using PK-Sim® software, incorporating (patho)physiological and PK data resulted from the I-PREDICT project. Simulations were conducted for two drugs, administered intravenously that display different physicochemical properties, PK characteristics and/or clinical relevance. Midazolam (MDZ) is a sedative and antiepileptic drug, with intermediate hepatic extraction ratio, while topiramate (TPM) is primarily renally excreted unchanged and explored as a potential neuroprotective drug when administered orally. Initial steps were hereby taken to construct hypothermia PBPK models, considering therapeutic hypothermia as non-maturational covariate. The validity of the MDZ and TPM PBPK models was assessed by comparing model-based predictions with observed plasma concentrations in Göttingen Minipigs exposed to hypothermia versus control conditions. A middle-out approach was employed, meaning that some parameters were estimated by fitting to observed in vivo data. This chapter provides insights into the state of the art of neonatal Göttingen Minipig PBPK M&S approaches and underscores the need for further research in this area.

1. Introduction

Asphyxiated neonates often undergo therapeutic hypothermia (TH) to reduce morbidity and mortality [1-4]. We hypothesized that both hypoxia and TH influence drug disposition in neonates. Using adequate preclinical data from an animal model, such as the neonatal Göttingen Minipig, offers valuable insights into these two covariates that cannot be studied separately in the clinical situation. Therefore, following a translational and multidisciplinary approach, the aim of the I-PREDICT project was to initiate the development of a physiologically-based pharmacokinetic (PBPK) modelling and simulation framework to describe and predict the impact of TH on drug disposition in asphyxiated neonates.

Physiologically-based pharmacokinetic models use drug-specific information and physiological data to create predictive models that mathematically describe the underlying physiological and biochemical processes explaining absorption, distribution, metabolism, and excretion (ADME) of xenobiotics, including medication [5]. Generally, PBPK models offer a mechanistic approach to predict drug exposure in specific populations through a comprehensive bottom-up approach. The input data comprises: (i) drug-specific information, encompassing physicochemical properties and in vitro disposition data (such as metabolic rates, plasma protein binding, and transepithelial permeability); and (ii) quantitative representation of the physiology of the biological system under investigation (e.g., neonatal humans or (mini)pigs) [6]. Additionally, for neonatal PBPK models, knowledge on ontogeny and maturation of different systems has to be integrated [1]. In situations where there is insufficient or no clinical data for model validation, constructing a PBPK model for a relevant animal model holds the potential to indirectly enhance the intended PBPK model in the human target population [1,6]. Juvenile animals are particularly promising in this context. Such an example is the development of a PBPK framework for studying oseltamivir's PK in healthy infants, neonates, and adult humans, through comparisons with simulations in adult and neonatal marmosets [7]. It is expected that PBPK models will also increasingly be used in (neonatal and juvenile) pigs, to improve the development of corresponding PBPK models in human populations. The pharmaceutical industry highly values the pig as a non-rodent model for use in toxicity studies due to the similarities to human physiology, anatomy, and biochemistry [6,8,9]. The Göttingen Minipig is the preferred pig strain in nonclinical drug development because its genetic consistency and well-documented characteristics, providing valuable historical control data for pharmaceutical companies in safety studies [1,10-14].

Physiologically based pharmacokinetic (PBPK) models, as illustrated by the I-PREDICT project [1], are built to anticipate drug exposure in neonates and to aid species selection for nonclinical safety studies [12]. However, the predictive performance of neonatal PBPK models at this stage is limited since high quality physiological and ADME data are largely lacking [12,15]. This chapter explores the available information to establish a database for the neonatal (juvenile) Göttingen Minipig model and highlights current knowledge gaps. Moreover, insights regarding the impact of TH versus control on PK (Chapter 4) to illustrate feasibility, together with literature findings, were used to develop a pilot neonatal Göttingen Minipig PBPK model.

2. Materials and methods

To provide a pilot of the applicability (and constraints) of neonatal Göttingen Minipig PBPK modeling, the materials and methods section was divided into two parts: (i) outlining the necessary data for PBPK model development, including an overview of the relevant literature, and (ii) detailing the actual model construction, verification, and refinement for two compounds (i.e., midazolam, MDZ; topiramate, TPM) under two conditions (i.e., normothermia and hypothermia), using PK-Sim® software (Open Systems Pharmacology Suite).

2.1. Required data for PBPK model construction

2.1.1. Physiology

Organ volume and blood flow

A prior study aimed to record body and organ weights, including brain, heart, gastrointestinal tract, kidneys, liver, lungs, and spleen, as well as measurements of the small and large intestines, and pH values of the gastrointestinal tract in Göttingen Minipigs, from the fetal stage to 5 months of age [16]. Data referring to postnatal day (PND) 1, <24 hours age, illustrated in Table 1, were implemented in our PBPK models.

Table 1. Organ volumes in neonatal Göttingen Minipigs, adapted from organ mass measurements in postnatal day 1 Göttingen Minipigs [16]. [1] Transformation to volume with density from Suenderhauf & Parrott [17].

Organ	Mass (g)	[1] Volume (mL)
Brain	20.4	20.82
Heart	4.08	3.89
Small intestine	19.6	18.15
Kidneys (2)	4.34	4.13
Liver	11.8	11.24
Lungs (deflated)	6.58	6.27
Spleen	0.72	0.69
Stomach	4.04	3.85

Next, a compilation of organ blood flow distributions, originating from 16 Göttingen Minipigs of 3 kg was available from Ellegaard Göttingen Minipigs A/S, Dalmose, Denmark (https://minipigs.dk/sites/default/files/2021-05/Hemodynamics.pdf [18]). These data, depicted in Table 2, were integrated in our MDZ and TPM normothermia PBPK models.

Table 2. Organ blood flow arithmetic means and standard deviations (±SD) originating from 16 Göttingen Minipigs of 3 kg available from Ellegaard Göttingen Minipigs A/S, (https://minipigs.dk/sites/default/files/2021-05/Hemodynamics.pdf [18]). * Gastrointestinal (GI).

| Organ	mL/min/100g organ (±SD)
Adrenals	82 (±62)
Brain	76 (±21)
Cecum	96 (±68)
Esophagus	16 (±11)
Fat tissues	11 (±6)
GI tract (total)	71 (±46)
Heart	118 (±45)
Small intestine	79 (±49)
Large intestine	43 (±30)
Kidneys	361 (±86)
Liver (total)	167 (±74)
Muscles	14 (±6)
Pancreas	147 (±166)
Skin	8 (±4)
Spleen	297 (±232)
Stomach	59 (±44)

In the context of hypothermia PBPK modelling, there is evidence that TH markedly reduces various physiological parameters [19]. In a juvenile conventional pig model (6 weeks old, 11.8±1.1 kg) under fentanyl anesthesia, hypothermia was associated with a significant % reduction in cardiac index (41±15%) and blood flows to various organs: kidney (38±32%), spleen (45±33%), stomach (53±31%), gut (49±26%), pancreas (49±46%). These blood flow changes were observed during different stages of the experiment, including the pre-hypothermic period (measuring point; MP1, MP2), after 6 hours of TH at 31.6±0.2 °C (MP3), after rewarming to normothermia at 37.7±0.3 °C (MP4), and at the end of the experiment, 6 hours after rewarming (MP5) [19]. These data, illustrated in Table 3 and Figure 1, were extracted from bar charts using WebPlotDigitizer (https://automeris.io/WebPlotDigitizer/) and were integrated in the MDZ and TPM hypothermia PBPK models.

Table 3. Blood flow arithmetic means and standard deviations (±SD) in a hypothermia juvenile conventional pig model undergoing fentanyl anesthesia. Table adapted from Fritz et al. [19]. * Baseline (MP1), control of baseline (MP2), after 6 hours of hypothermia at 32 °C (MP3), return of normothermia at 37.7±0.3 °C (MP4), end of the experiment (MP5); measuring point (MP).

Organ blood flow	Flow (mL/min/g) (±SD)	Organ blood flow	Flow (mL/min/g) (±SD)
Gut MP1	0.57(±0.25)	Pancreas MP1	0.88 (±0.36)
Gut MP2	0.57 (±0.21)	Pancreas MP2	0.82 (±0.32)
Gut MP3	0.31 (±0.14)	Pancreas MP3	0.43 (±0.29)
Gut MP4	0.68 (±0.31)	Pancreas MP4	0.45 (±0.4)
Gut MP5	0.51 (±0.16)	Pancreas MP5	0.53 (±0.16)
Hepatic artery MP1	0.22 (±0.09)	Spleen MP1	3.39 (±1.65)
Hepatic artery MP2	0.25 (±0.08)	Spleen MP2	2.78 (±1.2)

Hepatic artery MP3	0.26 (±0.05)	Spleen MP3	1.5 (±1.15)
Hepatic artery MP4	0.25 (±0.09)	Spleen MP4	3.07 (±2.14)
Hepatic artery MP5	0.28 (±0.1)	Spleen MP5	3.34 (±1.49)
Kidney MP1	2.5 (±0.4)	Stomach MP1	0.43 (±0.12)
Kidney MP2	2.19 (±0.49)	Stomach MP2	0.42 (±0.19)
Kidney MP3	1.57 (±0.5)	Stomach MP3	0.21 (±0.13)
Kidney MP4	2.17 (±0.6)	Stomach MP4	0.49 (±0.09)
Kidney MP5	2.17 (±0.37)	Stomach MP5	0.45 (±0.19)

Figure 1. Blood flows in a hypothermia juvenile conventional pig model undergoing fentanyl anesthesia. Line chart adapted from Fritz et al. [19]. * Baseline (MP1), control of baseline (MP2), after 6 hours of hypothermia at 32 °C (MP3), return of normothermia at 37.7±0.3 °C (MP4), end of the experiment (MP5); measuring point (MP).
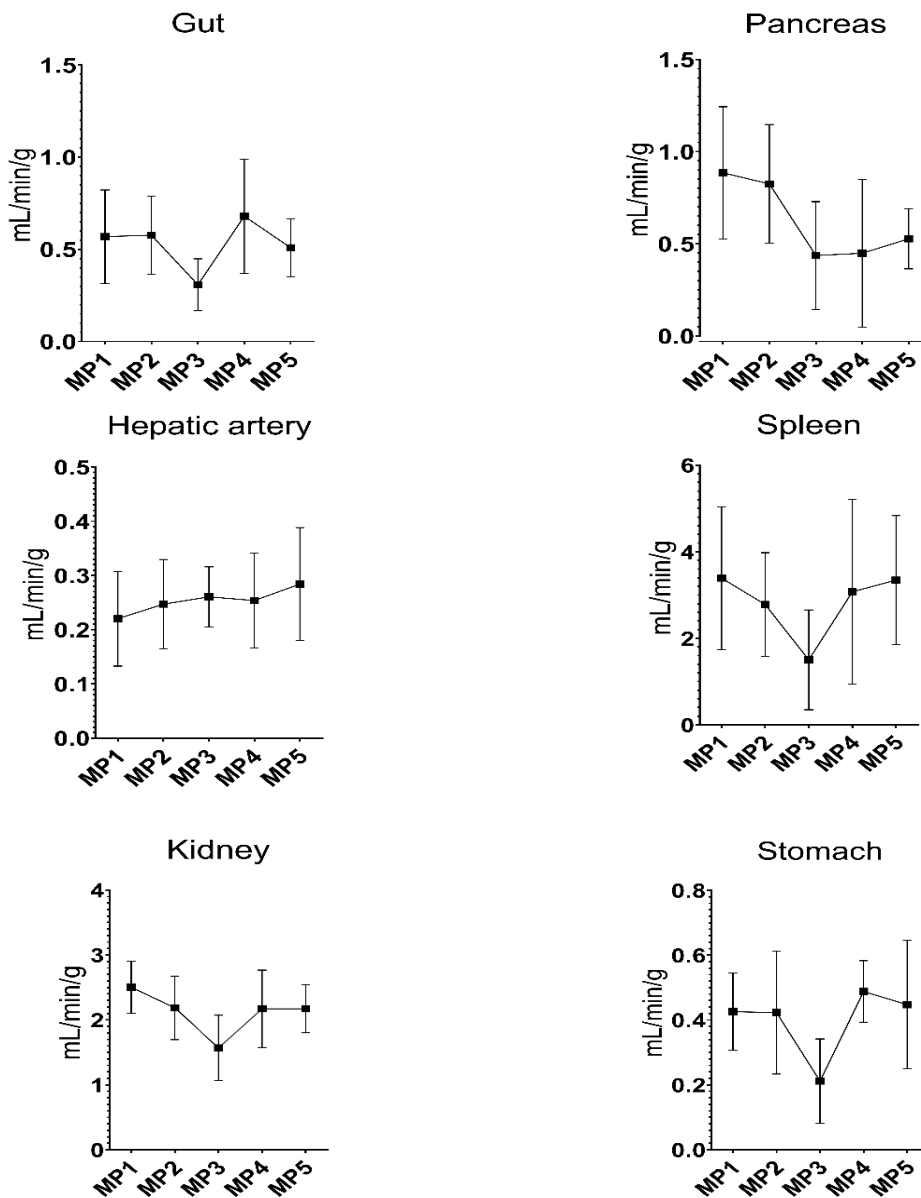
Estimated glomerular filtration rate

Kidneys are crucial organs influencing the PK and pharmacodynamics (PD) of several drugs. Glomerular filtration rate (GFR) is widely regarded as the most comprehensive indicator of glomerular function [20]. In practice, GFR is often estimated from the serum or plasma concentrations of endogenous creatinine [20,21]. In order to be able to compare individuals of different sizes, GFR is conventionally indexed to body surface area (BSA) [22]. However, this is controversial when calculating GFR in human infants [22], as well as for veterinary practice [20,23] (discussion section on Estimated glomerular filtration rate).

Creatinine levels in serum (and urine) were assessed using spectrophotometry on the Roche Cobas c702 machine at A.M.L. BV Lab. We estimated GFR based on BW, BSA, and kidney weight (KW, Supplementary Table 1). We incorporated GFR in relation to BW in the neonatal Göttingen Minipig PBPK model, drawing insights from prior studies conducted on developing conventional piglets [20]. From hypothermia PBPK modelling perspectives, our Göttingen Minipig data showed that urinary output is markedly reduced due to hypothermia (34.61%) respectively, hypothermia and hypoxia (39.10%) conditions (Table 4 and Figure 2). Therefore, the specific eGFR from the TH group was implemented in the hypothermia PBPK models.

Table 4. Urinary output in neonatal Göttingen Minipigs groups. The names of each group were abbreviated as the following - control (C), therapeutic hypothermia (TH), hypoxia (H), hypoxia and TH (H+TH). * body weight (BW).

Group	BW (kg)	Urine (mL) /24 hours	Urinary output mL/kg/24 hours	Urinary output mL/kg/h
C1	0.61	24	39.67	1.65
C2	0.55	23	38.01	1.58
C3	0.54	35	57.85	2.41
C4	0.47	19	31.40	1.31
C5	0.54	31	51.24	2.13
C6	0.63	24	39.67	1.65
H1	0.52	16	26.45	1.10
H2	0.50	15	24.79	1.03
H3	0.43	25	41.32	1.72
H4	0.53	23	38.02	1.58
H5	0.54	20	33.06	1.37
H6	0.59	23	38.02	1.58
TH1	0.66	27	44.63	1.86
TH2	0.56	31	51.24	2.13
TH3	0.44	4	6.61	0.27
TH4	0.62	6.5	10.74	0.45
TH5	0.51	8.5	14.05	0.58
TH6	0.60	25	41.32	1.72
H+TH1	0.53	25	41.32	1.72
H+TH2	0.61	21	34.71	1.44
[1] H+TH4	0.51	18	29.75	1.24

H+TH5	0.55	9	14.87	0.62
H+TH6	0.65	16	26.45	1.10
H+TH7	0.52	6	9.92	0.41

[1] For H+TH3 the systemic hypoxic insult and 24 hours experimental time was achieved. However, at the end of the experiment, misplacement of the epigastric catheter was noticed. Consequently, this subject was excluded from the pharmacokinetic analysis. Since this animal was excluded due to a technical and not a physiological issue, its blood gas analysis parameters were still considered for the assessment of the hypoxic insult (Chapter 3).

Figure 2. Urinary output in neonatal Göttingen Minipigs groups. The names of each group were abbreviated as the following - control (C), therapeutic hypothermia (TH), hypoxia (H), hypoxia and TH (H+TH).
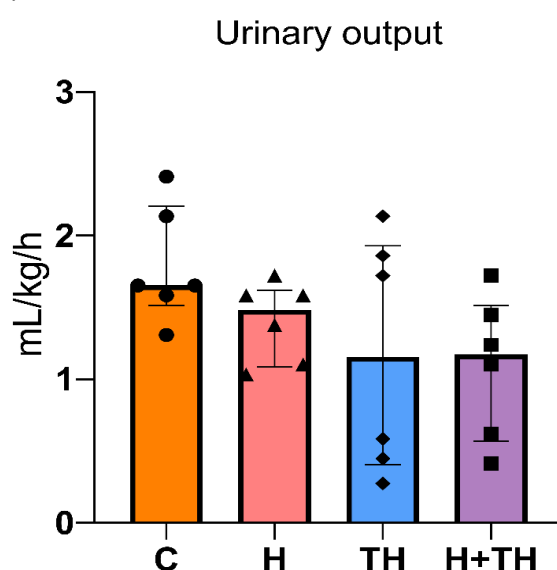
2.1.2. Drug metabolizing enzymes expression and activity

An automated workflow that generates whole-body gene expression databases for humans and other species relevant in drug development, animal health, nutritional sciences, and toxicology was previously developed [24]. Bulk ribonucleic acid (RNA)-seq data curated and provided by the Swiss Institute of Bioinformatics from healthy, normal, and untreated primary tissue samples were considered as an unbiased reference of normal gene expression [24]. Therefore, this minipig-specific database, operable in PK-Sim®, was used in constructing our PBPK models.

Regarding the in vitro drug metabolizing enzymes (DMEs) activity, large knowledge gaps still exist specially for developing (mini)pigs. Characterization of the DMEs systems in (mini)pigs were previously performed for various cytochrome P450 (CYP) enzymes [13,14,25,26] as well as for phase II metabolic pathways (i.e., uridine 5'-diphosphate glucuronosyltransferases [27]). However, these data relate to typical probe substrates (e.g., the ethoxyresorufin-O-deethylase (EROD) assay is one of the most commonly used fluorogenic tests to assess CYP1A activity; tolbutamide (CYP2C), dextromethorphan (CYP2D), and chlorzoxazone (CYP2E) [28]), while the data required for PBPK need to be related to the ADME of the drug in question (e.g., MDZ,

fentanyl, phenobarbital for the I-PREDICT project). Nevertheless, for the objective of our work, data on one of our model compounds (i.e., MDZ) could be found in the literature since it is also a substrate highly specific to both pig and human CYP3A and had been already used for various assays [14,28]. In a previous study, liver microsomes extracted from 16 conventional pigs (12 weeks of age, 8 females and 8 males) were incubated at 37 °C with MDZ. The final quantification was performed by liquid chromatography-tandem mass spectrometry (LC-MS/MS). The activity data were fitted against the standard Michaelis-Menten equation, and Michaelis-Menten constants (Km) and maximal reaction velocity (Vmax) were derived for each pig, in order to obtain the inter-individual variation. The resulting Michaelis-Menten parameters for MDZ activity, as implemented into the PBPK model, were the porcine Km (15.3 (±4.4) µM) and porcine Vmax (1848 (±637) pmol/min/mg protein) [28]. Based on these values, the turnover number (Kcat) was calculated for the whole organ by dividing the in vitro Vmax with the content of CYP protein in liver microsomes (i.e., porcine Kcat, 10.27 L/min). More specifically, assuming that k_{cat} is not influenced by in vivo factors, the equation employed for the calculation of this parameter was :

$$V_{max,organ} = k_{cat} * E_{0,organ}$$

where $V_{max,organ}$ is the tissue-specific maximum velocity, k_{cat} is the catalytic rate constant, 1/min and E_0 is the total enzyme concentration, µmol/L.

Regarding this last parameter, the content of CYP3A protein in liver microsomes was previously determined immunochemically in pigs and ranged between 0.14 and 0.18 nmol/mg protein [26].

2.2. Model construction, verification, and refinements

To preliminarily validate our neonatal Göttingen Minipig model, we simulated the plasma PK for two compounds: one predominantly cleared by the liver (MDZ), and one primarily cleared by the kidneys (TPM, with 80% excretion unchanged in urine). Table 5 summarizes the physicochemical parameters of the two compounds. The acidic function is only relevant at a pH greater than 9, which is not physiologically relevant. Additionally, the basic pKa of TPM is extremely low and thus irrelevant, making TPM a neutral compound. On the other hand, MDZ is positively charged only at acidic pH levels and is 10% charged at physiological pH (7.2-7.4). Therefore, it will be charged in acidic body compartments (e.g., stomach, lysosomes), and partially charged in the blood.

The simulations were conducted under two conditions, normothermia and hypothermia, resulting in 4 models: MDZ normothermia, MDZ hypothermia, TPM normothermia, and TPM hypothermia. The accuracy of these models was then assessed by comparing the simulated plasma concentrations with the observed data from the I-PREDICT project control group for normothermia PBPK respectively, the TH group for hypothermia PBPK models.

Table 5. Overview of midazolam and topiramate input physicochemical parameters. * Acid dissociation constant (pKa); octanol-water partition coefficient (LogP); molecular weight (MW).

Parameter	Midazolam			Topiramate		
	Data	Unit	Source	Data	Unit	Source
LogP	2.9	Log Units	PK-Sim®	1.26	Log Units	https://go.drugbank.com/salts/DBSALT002318
Binds to	Albumin	-		Unknown	-	Christensen et al. (2001) [29]
Fraction unbound	0.03	-		84	%	
Species	Minipig	-		Minipig	-	-
MW	325.78	g/mol		339.36	g/mol	https://pubchem.ncbi.nlm.nih.gov/compound/Topiramate
Halogens	1 Cl, 1 F	-		-	-	https://go.drugbank.com/salts/DBSALT002318
Effective MW	286.78	g/mol		339.36	g/mol	
pKa (Base)	6.2	-		-3.7	-	
pKa (Acid)	10.95	-		11.09	-	
Solubility	0.05	mg/mL		12.3	mg/mL	
Ref-pH	6.5	-		7	-	

2.2.1. PBPK model construction

In constructing an individual (i.e., a neonatal Göttingen Minipig), the weight of 0.49 kg (I-PREDICT) and the following steps were undertaken within PK-Sim®. Firstly, the default anatomical and physiological characteristics were incorporated, with specific customization for organ volumes [16], and blood flows [18] (Section 2.1., Required data for PBPK model construction). Secondly, for the hypothermia PBPK models, blood flows [19] and eGFR under hypothermic conditions were integrated accordingly. Lastly, regarding MDZ ADME data, CYP3A expression and activity [26,28] as explained previously, were implemented in both the normothermia and hypothermia PBPK models. Thirdly, PK-Sim® does not introduce any variability in the population results. Hence, populations for these PBPK models are not currently feasible to design, and variability in pathophysiology and possibly ADME cannot be explored in PK-Sim® software.

2.2.2. PBPK model verification

Plasma concentrations of MDZ and TPM over 24 hours were previously observed in 6 neonatal Göttingen Minipigs (Chapter 4). These individual and combined data (i.e., arithmetic mean ± standard deviation (SD) for each group and drug) coming from the I-PREDICT project were used for verification as observed data in the normothermic (i.e., control group) and hypothermic (i.e., TH group) PBPK models, with both drugs administered exclusively via intravenous (IV) routes. The MDZ drug administration protocol involved a loading dose of 0.3 mg/kg via IV bolus injection, followed by an IV continuous rate infusion (CRI) of 0.4 mg/kg/h at a constant rate of 2 mL/h until the end of the experiment. Topiramate was administered after 2.5 hours from the start of MDZ infusion and 12 hours later, at a dose of 20 mg/kg, via IV bolus injection. The administration protocols were the same for the normothermia and hypothermia PBPK models. Blood samples were collected at 0 (pre-dose) and 0.5, 2, 2.5, 3, 4,

4.5, 6, 8, 12, 24 hours post-drug administration. The MDZ and TPM plasma concentration profiles are depicted in Figure 3 and Figure 4, (A) control and (B) TH group. Figures were designed in GraphPad Prism version 8.0.2 (GraphPad Software, Inc. San Diego, California USA)).

Figure 3. Midazolam and 1-hydroxymidazolam plasma concentrations in 6 controls **(A)** and 6 hypothermic **(B)** neonatal Göttingen Minipigs. Blood samples were collected at 0 (pre-dose) and 0.5, 2, 2.5, 3, 4, 4.5, 6, 8, 12, 24 hours post-drug administration. * Control (C); hours (h); therapeutic hypothermia (TH).

(A) Midazolam control
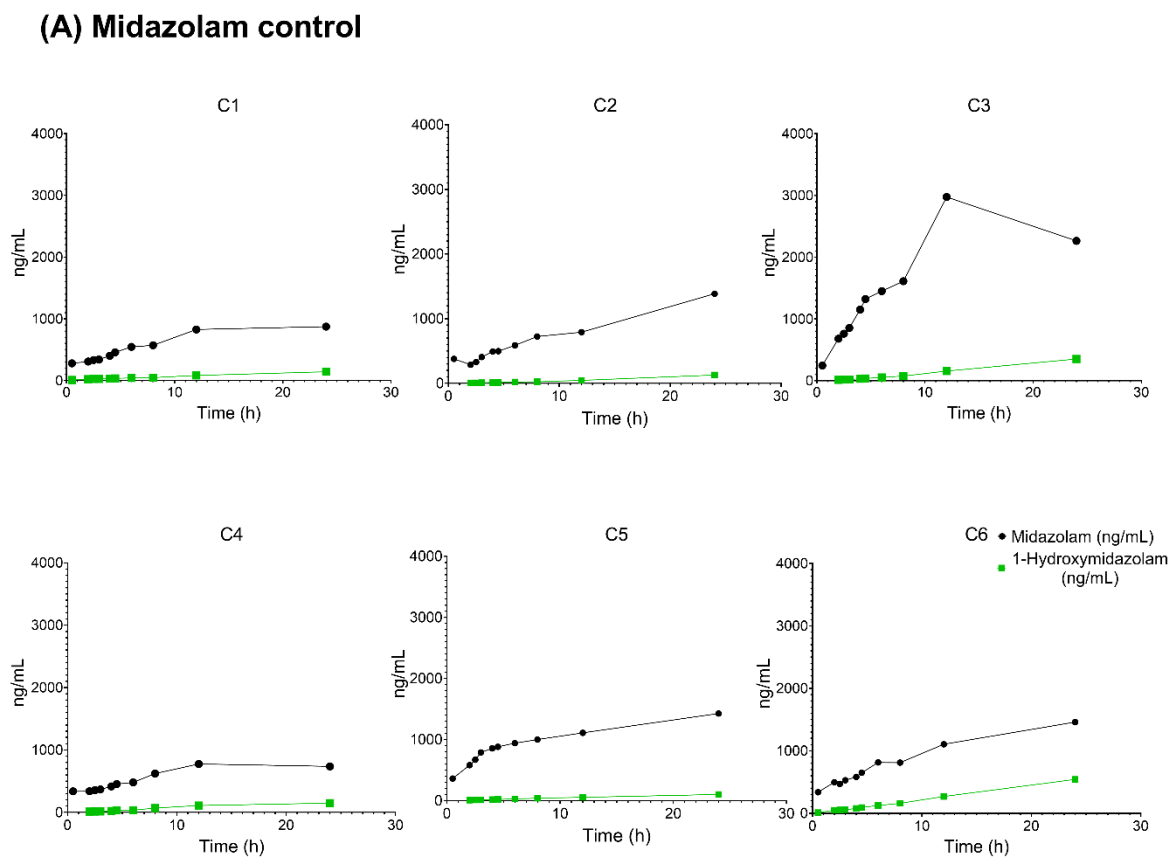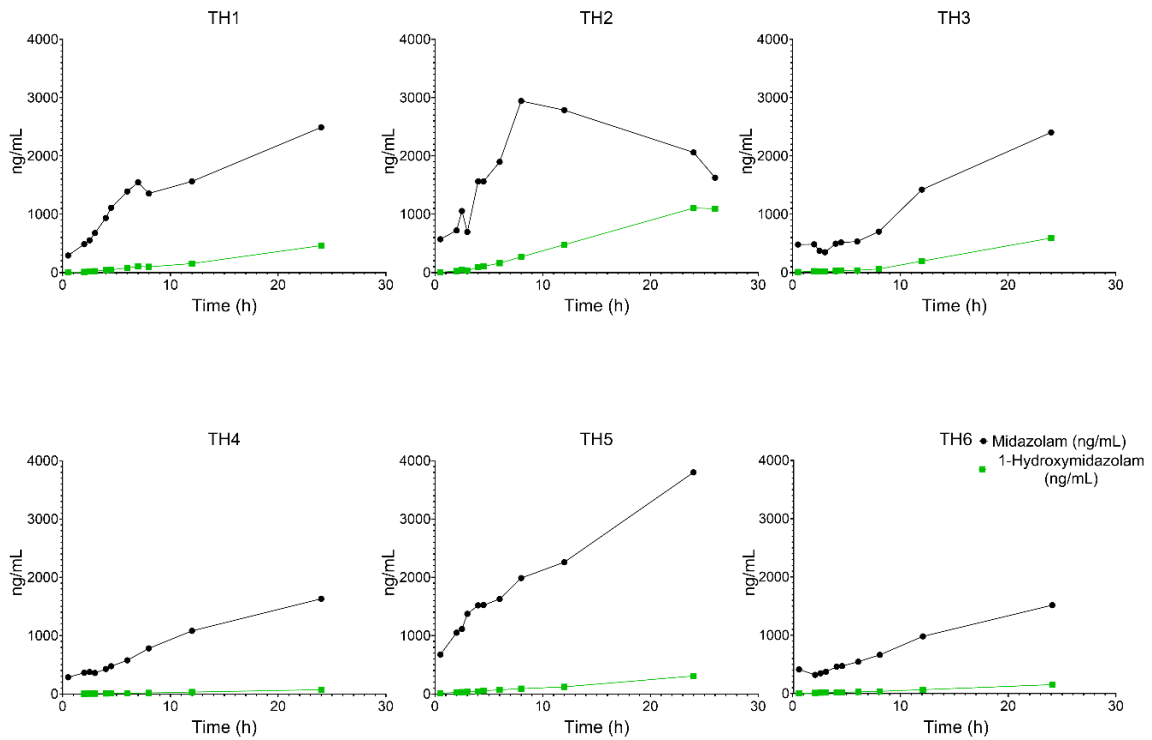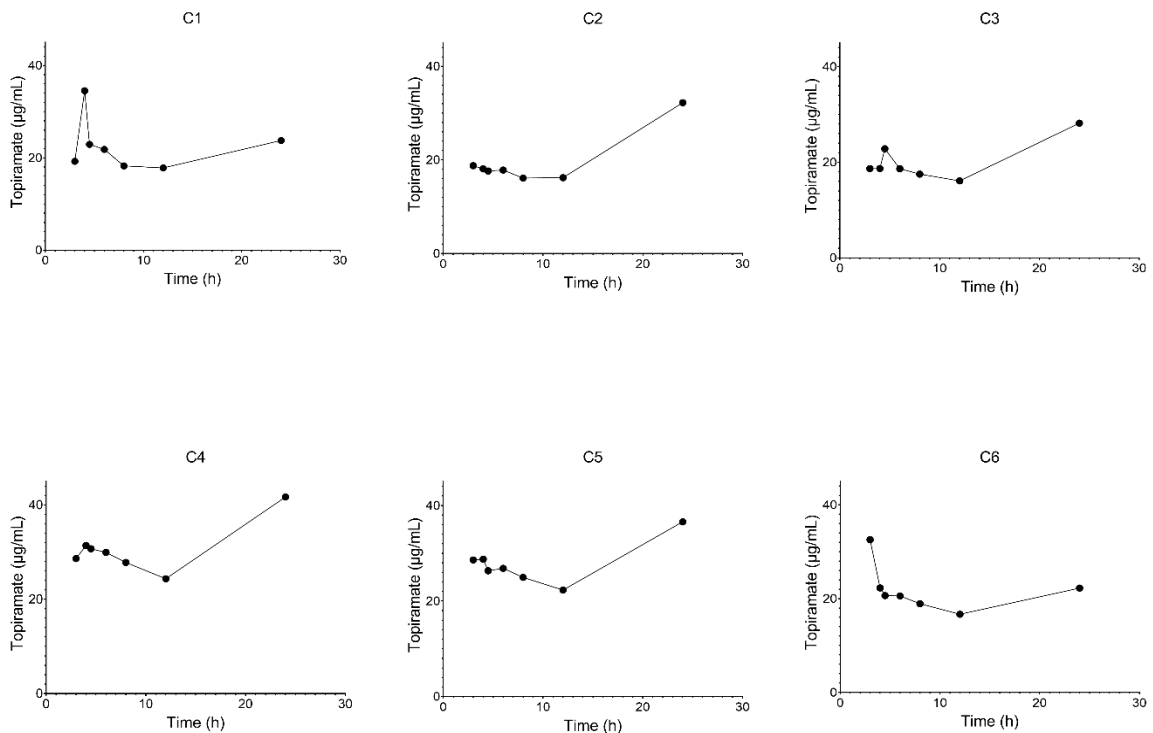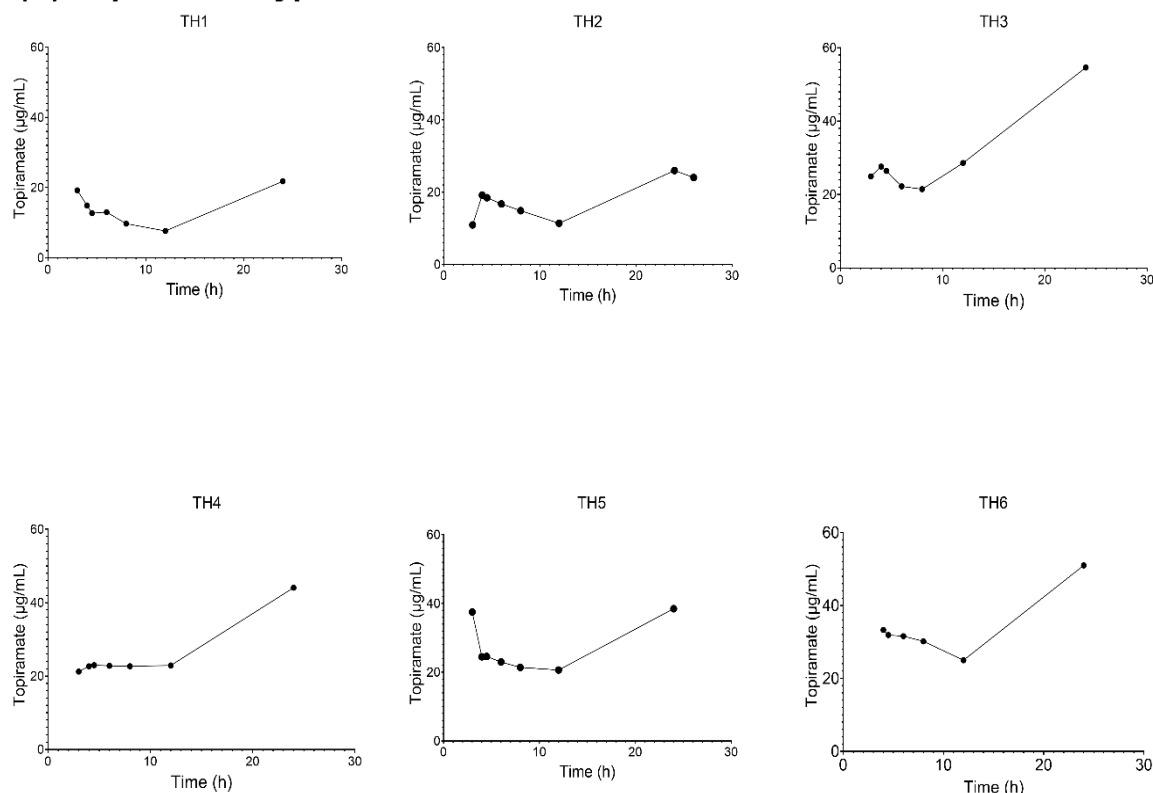
(B) Midazolam hypothermia

Figure 4. Topiramate plasma concentrations in 6 controls **(A)** and 6 hypothermic **(B)** neonatal Göttingen Minipigs. Blood samples were collected at 3, 4, 4.5, 6, 8, 12, 24 hours post-drug administration. * Control (C); hours (h); therapeutic hypothermia (TH).

(A) Topiramate control

(B) Topiramate hypothermia

2.2.3. PBPK model refinement

An important drug parameter in PBPK modeling is the tissue-to-plasma partition coefficient (K_p). There are five ways to calculate K_p in PK-Sim®: The PK-Sim® standard model and the approaches developed by Rodgers & Rowland, Schmitt, Poulin & Theil, and Berezhkovskiy. Cellular permeability, on the other hand, is calculated using three methods: PK-Sim® standard, charge dependent Schmitt, charge dependent Schmitt normalized to PK-Sim®. To enhance the alignment of predicted MDZ respectively, TPM concentration-time profiles with observed PK profiles, the distribution calculation in the PBPK model was optimized using the parameter identification module in PK-Sim®. This indicates that a middle-out approach was employed, meaning that these parameters were estimated by fitting to observed in vivo data. The assessment was based on visual inspection (Figure 5 and Figure 6) and numerically quantified by the total error, calculated as the sum of the squares of all residuals for each output:

$$Total\ error\ =\ \sum (residuals^2)$$

Firstly, regarding MDZ, the parameter identification module results showed overprediction by using the approaches proposed by Rodgers & Rowland (total error=1.78), Berezhkovskiy (total error=1.49) and Poulin & Theil (total error=0.71), while the PK-Sim® standard (total error=0.21) and Schmitt (total error=0.22) approaches were in good agreement with observed data (Figure

5). Secondly, regarding TPM, the parameter identification module results showed underprediction by using the approaches proposed by Schmitt (total error=1.12) and PK-Sim® standard (total error=1.16) and slight overprediction with Rodgers & Rowland (total error=0.16), while Berezhkovskiy (total error=0.15) and Poulin & Theil (total error=0.15) approaches were in good agreement with observed data (Figure 6). Therefore, the method selected for tissue distribution calculation was PK-Sim® standard method for MDZ respectively Poulin & Theil for TPM, while the PK-Sim® standard method was chosen for cellular permeability calculation for both compounds. Figures were designed in PK-Sim®.

Figure 5. Midazolam parameter identification module results showed overprediction by using the approaches proposed by Rodgers & Rowland (total error=1.78), Berezhkovskiy (total error=1.49) and Poulin & Theil (total error=0.71) while the PK-Sim® standard (total error=0.21) and Schmitt (total error=0.22) approaches were in good agreement with observed data. The distribution calculation was optimized using the parameter identification module in PK-Sim® on normothermia model (arithmetic mean ± standard deviation of the control neonatal Göttingen Minipigs).

Figure 6. Topiramate parameter identification module results showed underprediction by using the approaches proposed by Schmitt (total error=1.12) and PK-Sim® standard (total error=1.16) and slight overprediction with Rodgers & Rowland (total error=0.16), while Berezhkovskiy (total error=0.15) and Poulin & Theil (total error=0.15) approaches were in good agreement with observed data. The distribution calculation was optimized using the

parameter identification module in PK-Sim® on normothermia model (arithmetic mean ± standard deviation of the control neonatal Göttingen Minipigs).
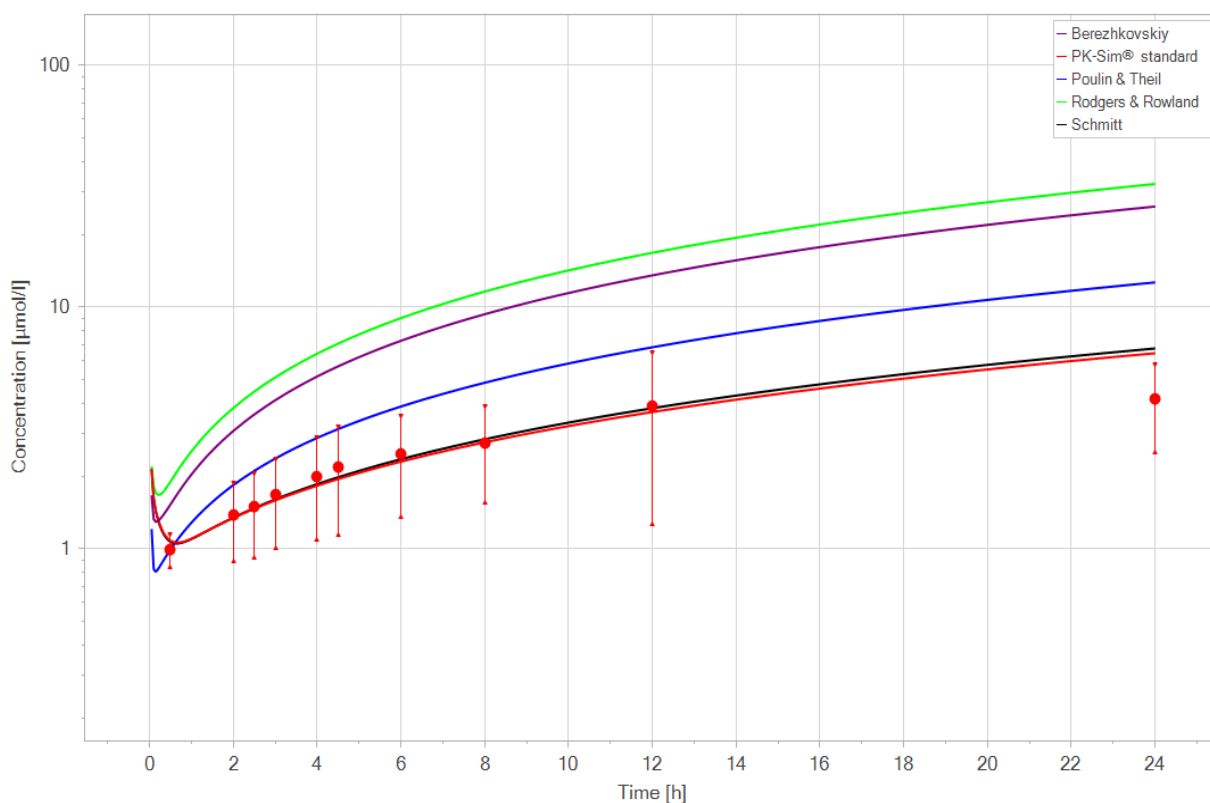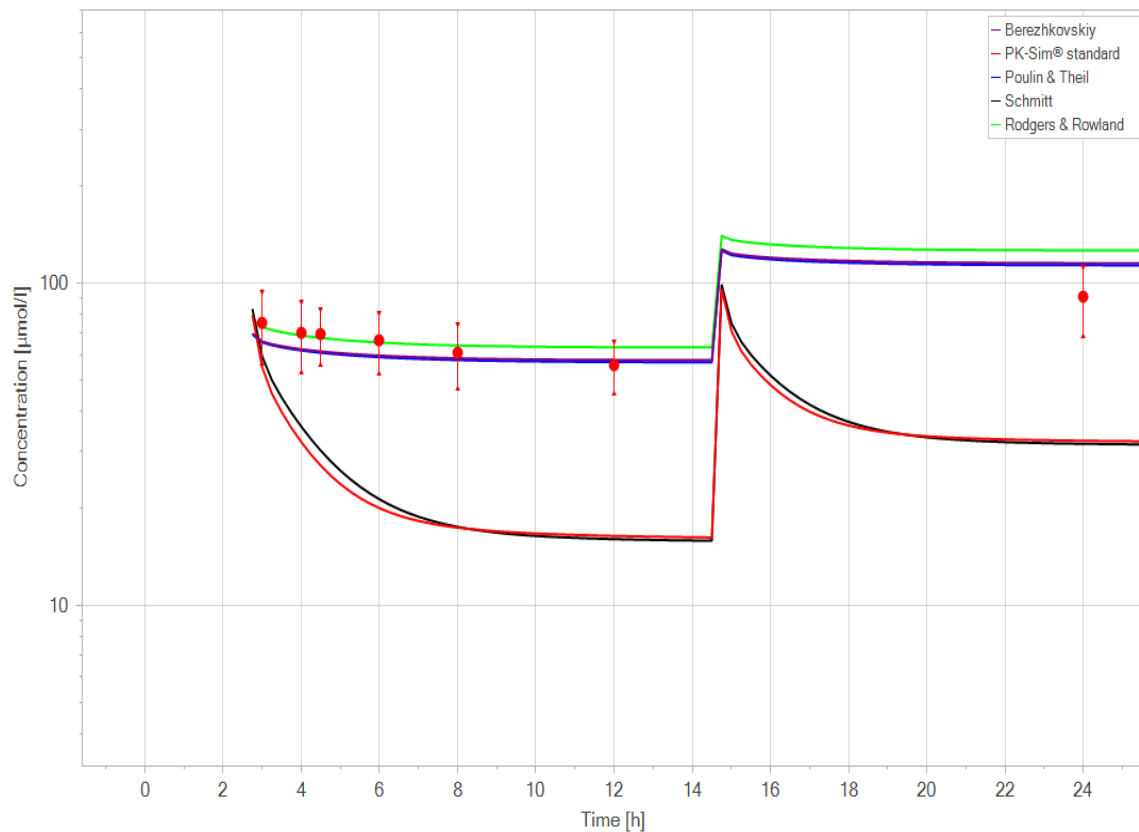

3. Results

The MDZ and TPM observed PK data for control, and TH groups respectively were used to validate the predictive performance of the PBPK models, by comparing the coincidence of predicted and observed PK profiles. Firstly, linear and logarithm representation of predicted and observed concentration profiles are provided in Figure 7 (i.e., MDZ) and Figure 8 (i.e., TPM).

Figure 7. Midazolam simulations on logarithmic **(A)** and linear **(B)** scales. The predicted concentrations are represented by the black line and the I-PREDICT observed concentrations (arithmetic mean ± standard deviations) are represented by the red (normothermia), respectively blue (hypothermia) dots. The midazolam drug administration protocol involved a loading dose of 0.3 mg/kg via IV bolus injection, followed by an IV continuous rate infusion (CRI) of 0.4 mg/kg/h at a constant rate of 2 mL/h until the end of the experiment. The administration protocol was the same for the normothermia and hypothermia PBPK models.

A. Logarithmic scale
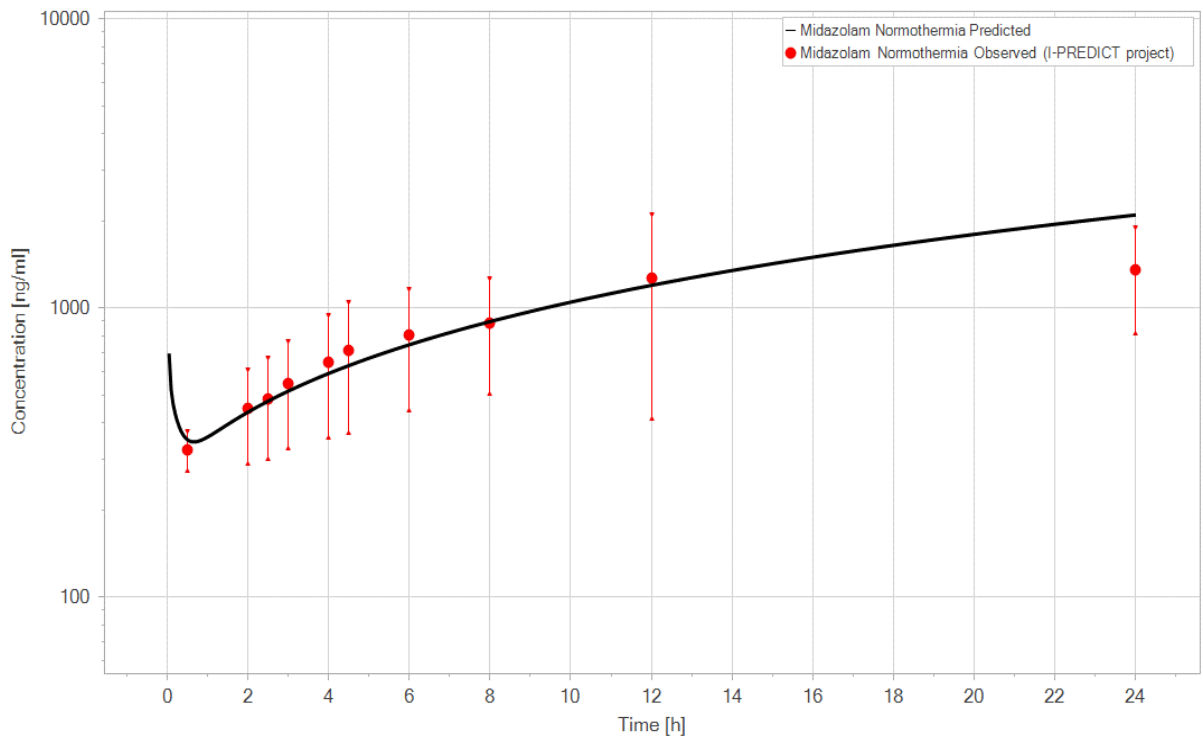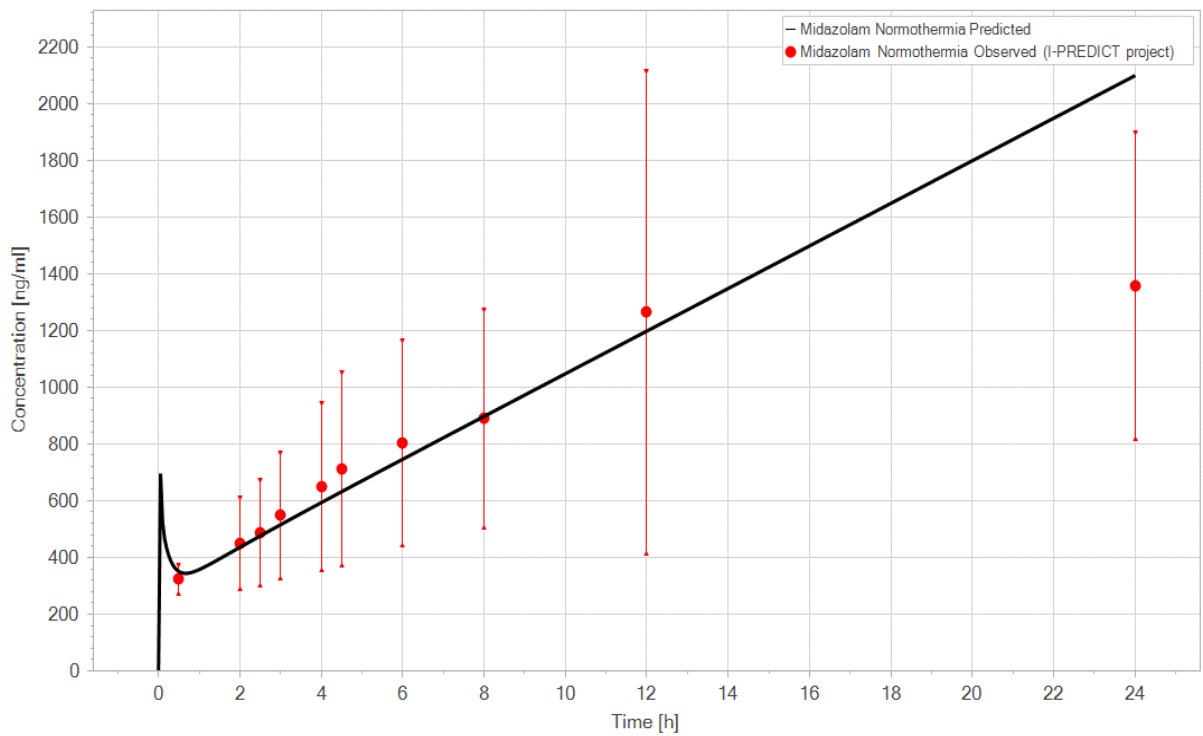
B. Linear scale

A. Logarithmic scale
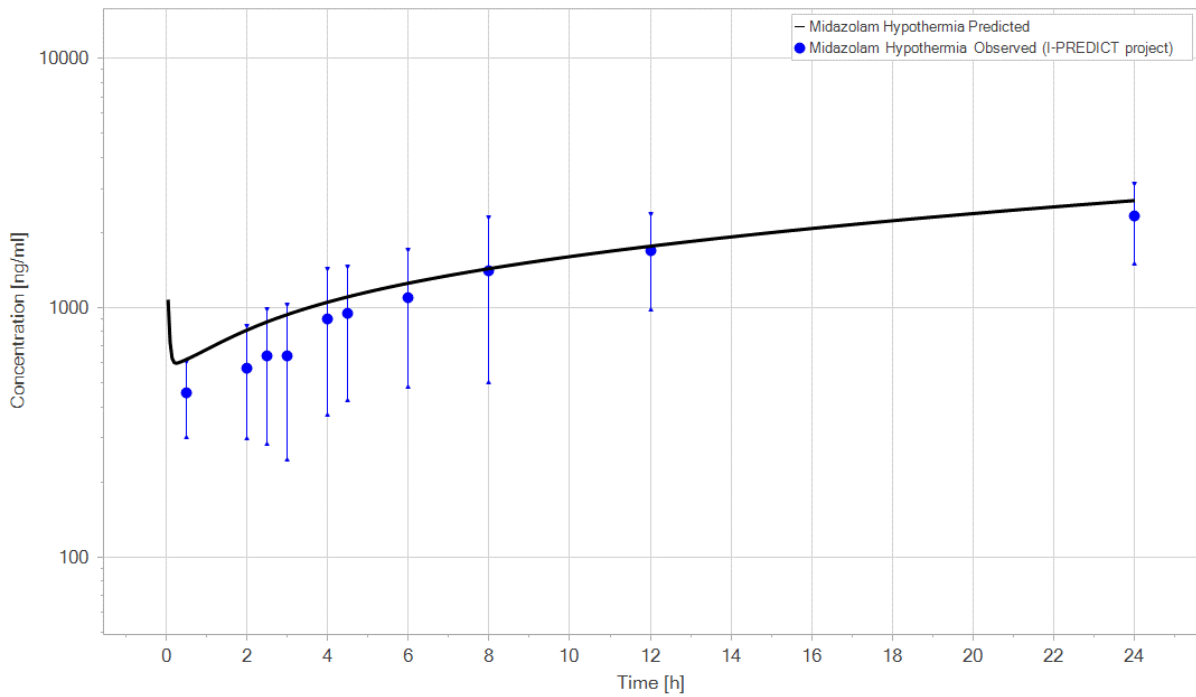
B. Linear scale
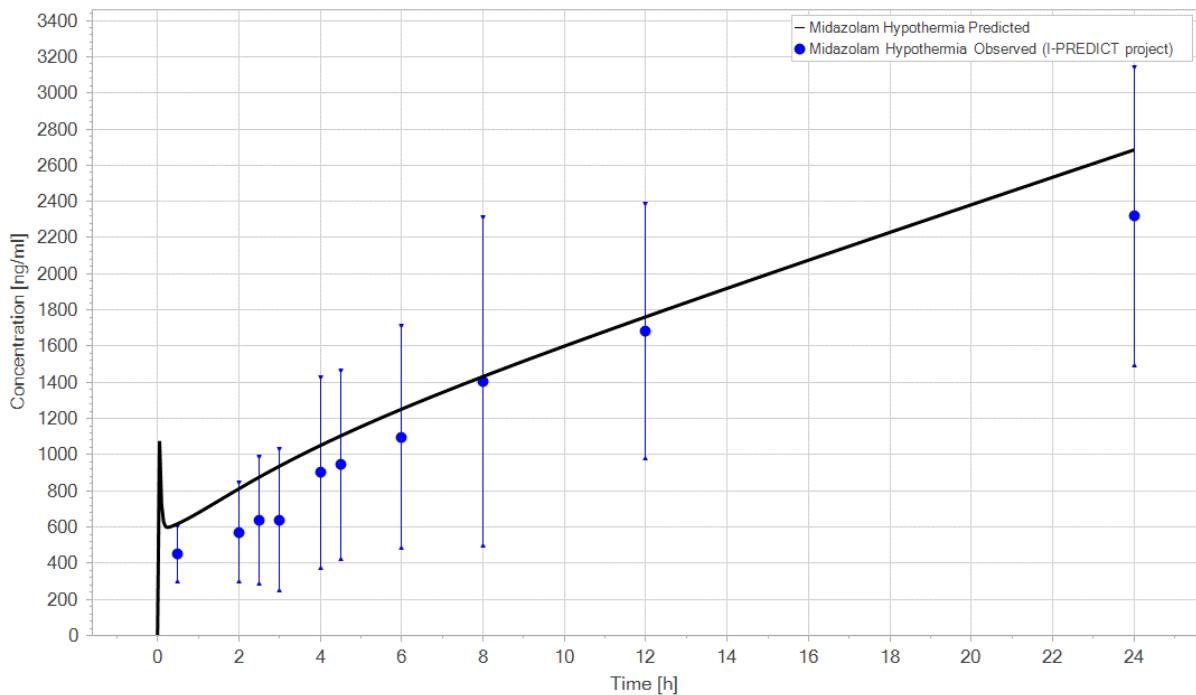
Figure 8. Topiramate simulations on logarithmic **(A)** and linear **(B)** scales. The predicted concentrations are represented by the black line and the I-PREDICT observed concentrations (arithmetic mean ± standard deviations) are represented by the red (normothermia), respectively blue (hypothermia) dots. The topiramate drug administration protocol was administered after 2.5 hours from the start of midazolam infusion and 12 hours later, at a

dose of 20 mg/kg, via IV bolus injection. The administration protocol was the same for the normothermia and hypothermia PBPK models.

A. Logarithmic scale
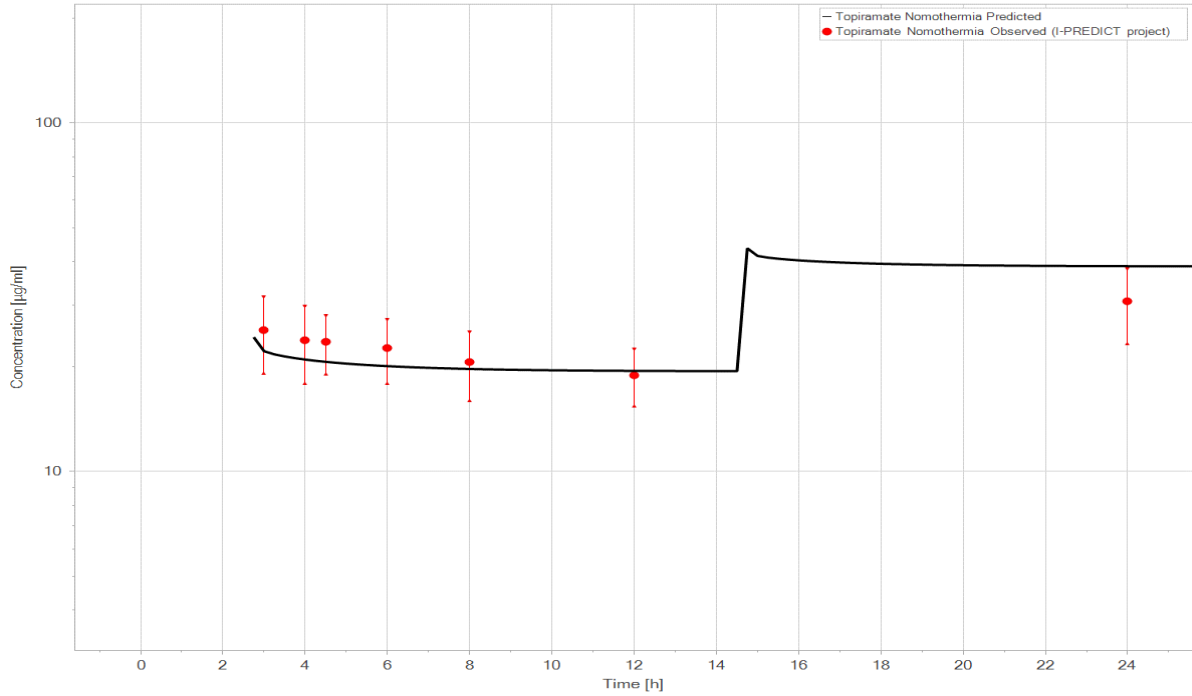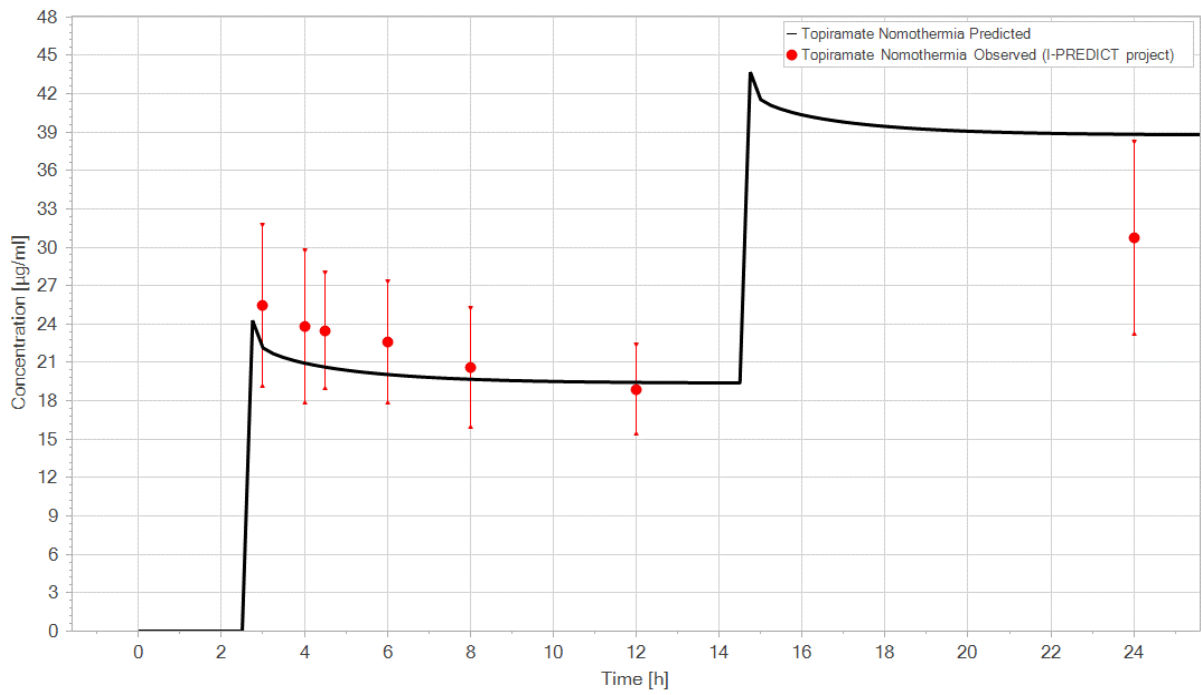
B. Linear scale

A. Logarithmic scale
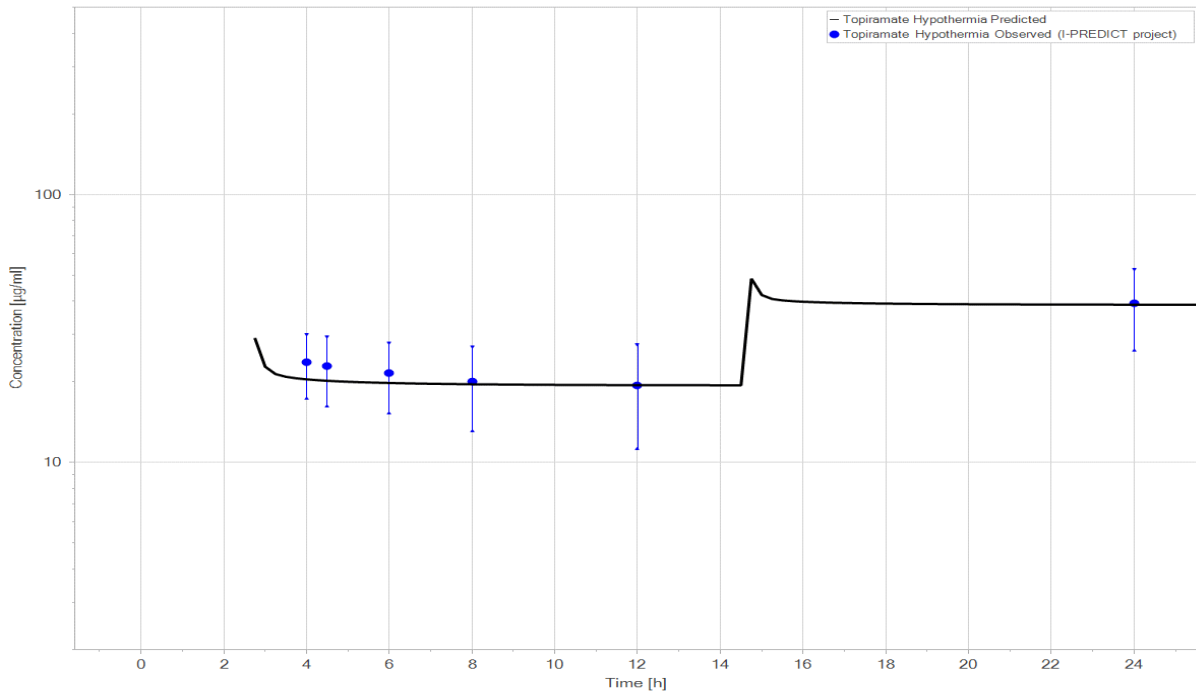
B. Linear scale
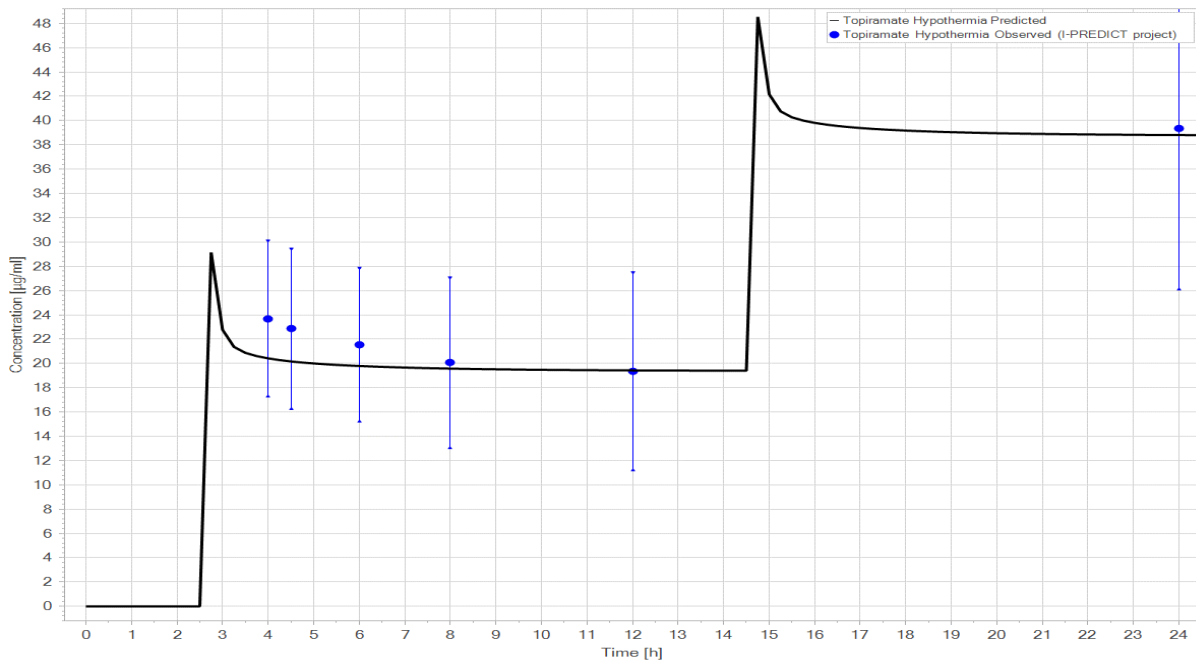
Next, the PK analysis provided the estimated PK parameters for the predicted and observed concentrations of both drugs, for normothermic and hypothermic conditions (Tables 6 and 7). Typically, acceptable criteria fall within the range of 0.5 to 2.0. This was assessed through two methods: (i) visually, by examining predicted and observed plots with 2-fold deviation lines shown in Figure 9, and (ii) by further verifying the model through a comparison of the predicted-to-observed ratio of the estimated PK parameters (fold error, FE), which should

ideally fall between 0.5 and 2.0 as presented in Tables 6 and 7. Generally, PBPK models are verified by comparing the predicted-to-observed ratio of the AUCs. For MDZ under normothermic conditions, the 12-hour plasma concentration predicted-to-observed ratio was 0.95, and the AUC predicted-to-observed ratio was 0.96 respectively, under hypothermic conditions, 1.04 and 1.12. For TPM under normothermic conditions, the AUC predicted-to-observed ratio was 0.93 respectively, under hypothermic conditions.

Table 6. Resulting midazolam (MDZ) estimated pharmacokinetic parameters comparatively presented for predicted and observed, under normothermic and hypothermic conditions. * Area under the curve (AUC), clearance (CL), half-life ($t_{1/2}$), elimination rate constant (k), ratio predicted versus observed concentrations (fold error, FE), volume of distribution (V_d).

Parameter	MDZ Normothermia Predicted	MDZ Normothermia Observed	FE	MDZ Hypothermia Predicted	MDZ Hypothermia Observed	FE
AUC_0.05_12 (h/nmol/mL)	27.48	28.53	0.96	44.82	40.02	1.12
AUC_0.05_12 (h/ng/mL)	8951.22	9293.69	0.96	14601.06	13038.98	1.12
12-hour plasma concentration (nmol/mL)	3.68	3.88	0.95	5.41	5.16	1.04
12-hour plasma concentration (ng/mL)	1197.88	1264.16	0.95	1762.44	1683.21	1.04
24-hour plasma concentration (nmol/mL)	6.44	4.17	1.54	8.24	7.11	1.19
24-hour plasma concentration (ng/mL)	2098.21	1358.06	1.54	2685.53	2318.26	1.19
V_d (L/kg)	2.41	1.97	1.22	1.12	1.67	0.67
CL (mL/min/kg)	3.62	5.11	0.71	3.37	2.86	1.19
k (1/h)	0.09	0.15	0.58	0.18	0.1	1.75
$t_{1/2}$ (h)	7.68	4.45	1.73	3.83	6.72	0.57

Table 7. Resulting topiramate (TPM) estimated pharmacokinetic parameters comparatively presented for predicted and observed, under normothermic and hypothermic conditions. *Area under the curve (AUC), clearance (CL), half-life ($t_{1/2}$), ratio predicted versus observed concentrations (fold error, FE), volume of distribution (V_d).

Parameter	TPM Normothermia Predicted	TPM Normothermia Observed	FE	TPM Hypothermia Predicted	TPM Hypothermia	FE
AUC_2.5_12 (h/nmol/mL)	564.96	607.6	0.93	556.03	598.12	0.93
AUC_2.5_12 (h/µg/mL)	191.73	206.2	0.93	188.7	202.98	0.93
24-hour plasma concentration (nmol/mL)	114.41	90.68	1.26	114.35	115.87	0.98
24-hour plasma concentration (µg/mL)	38.83	30.78	1.26	38.81	39.32	0.98
V_d (L/kg)	0.93	0.79	1.18	0.98	0.84	1.17
CL (mL/min/kg)	0.19	0.43	0.45	0.09	0.34	0.27
k (1/h)	0.01	0.03	0.38	0.006	0.02	0.23
$t_{½}$ (h)	56.17	21.53	2.61	120.86	27.99	4.32

Figure 9. Predicted and observed plots with 2-fold deviation lines for midazolam **(A)** and topiramate **(B)**, normothermia and hypothermia simulations.
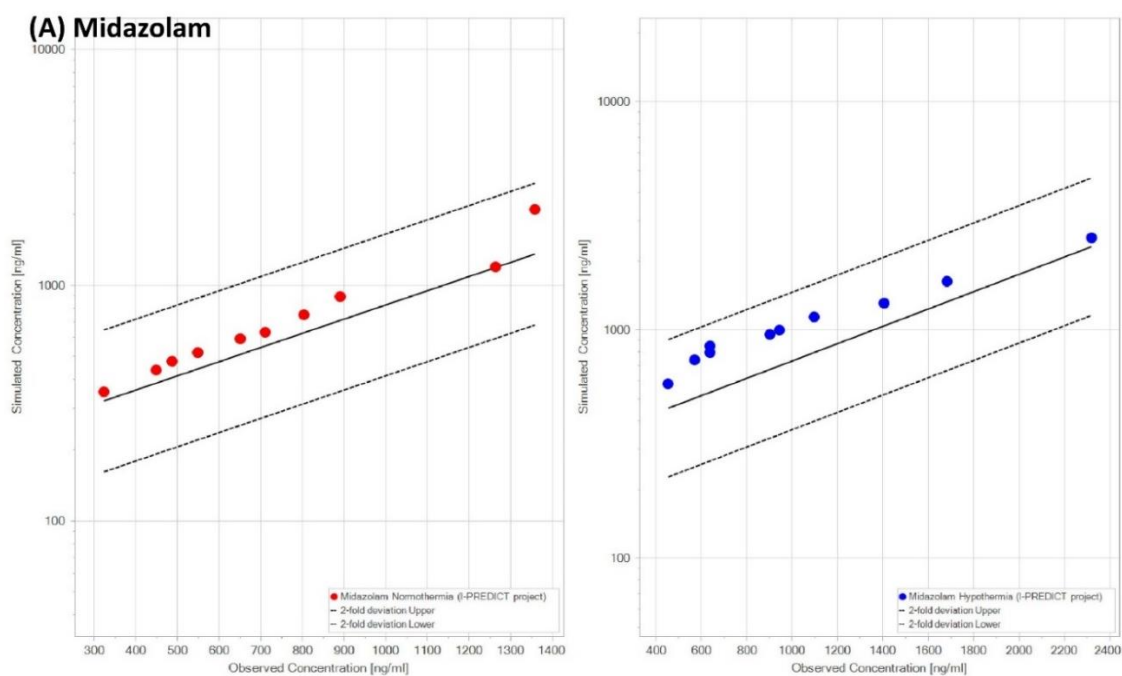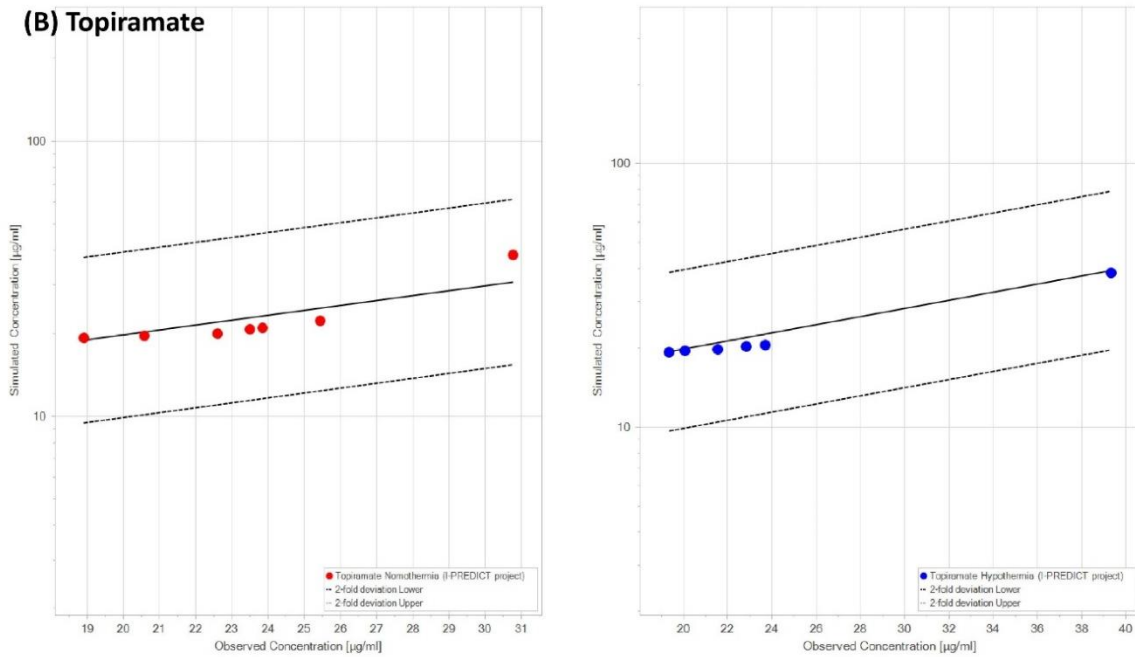
Lastly, a sensitivity analysis was conducted to identify the most sensitive parameters influencing AUC (Figure 10). In summary, this sensitivity analysis indicated that most modelling parameters had minimal impact on the AUC of MDZ and TPM, except for the lipophilicity of MDZ, which had a significantly influence. For AUC under normothermic conditions, the most sensitive parameter for MDZ was lipophilicity (-5.58), followed by dose (0.95), and for TPM, it was lipophilicity (-1.17) and dose (0.6).

Figure 10. Sensitivity analysis for midazolam **(A)** and topiramate **(B)** to identify the most sensitive parameters influencing area under the curve (AUC).

(A)
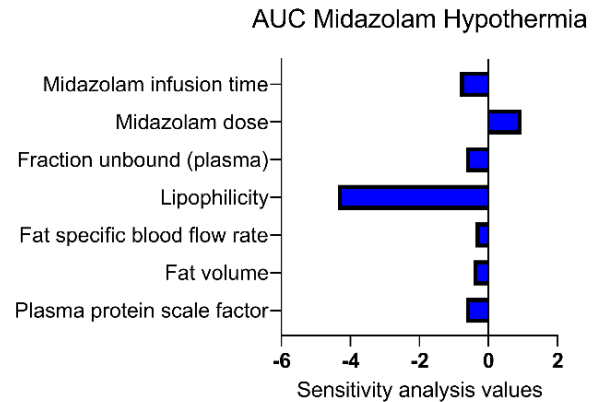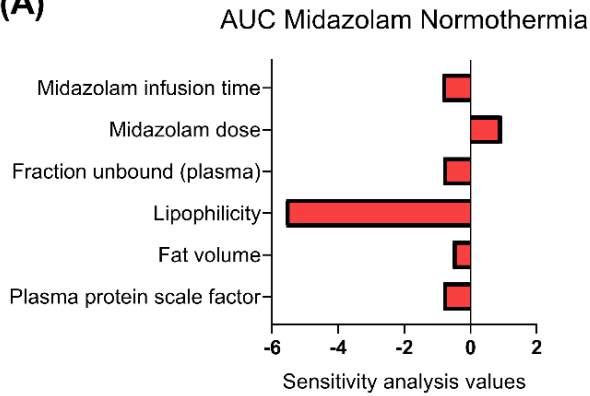
(B)
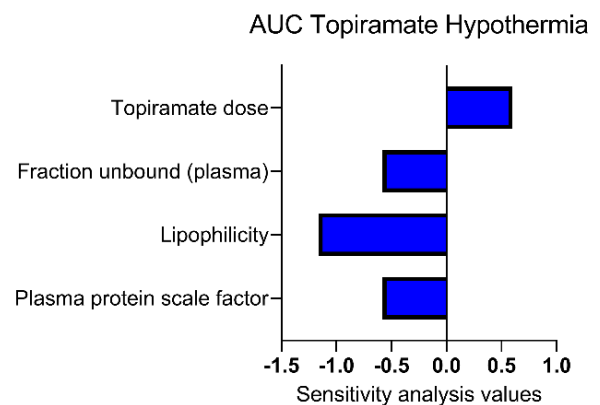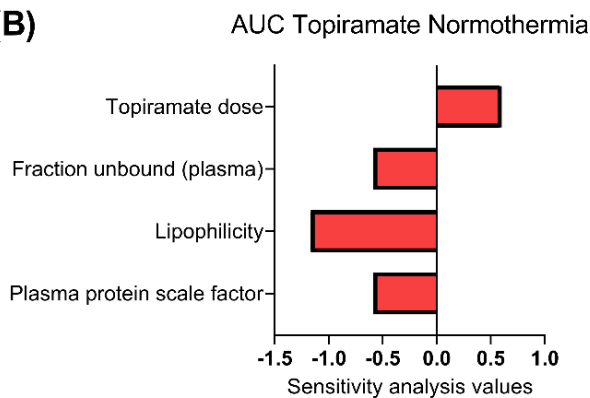
4. Discussion

To demonstrate the potential applicability of PBPK modeling using the neonatal Göttingen Minipig, we will discuss the necessary data for model construction and refinement, highlighting several gaps and challenges, and finalize by conclusions and outlook.

4.1. Organ volume and blood flow

In PBPK modelling, the body's tissues and organs are represented as interconnected compartments, each being characterized by specific volumes and K_p. Relevant volumes can be calculated from weight and density data [17]. Although specific organ densities for pigs have not been determined, it is reasonable to assume that these values do not vary significantly among mammals. As such, values of 0.98 kg/L for adipose and 1.05 kg/L for non-fat tissues have been adopted [17,30]. There is evidence that most of Göttingen Minipig organs are not following a linear growth curve during the first 5 months of life and the relative organ weights vary over time [16]. In general, the relative organ weights are the highest during the first week of life, while the major increases in absolute organ weights are observed during the first 3 to 4 months of life. Additionally, higher organ water content at the neonatal stage is observed. In contrast to the other organs, the spleen showed a low relative organ weight in neonates, which strongly increased during the first month of life [16]. Regarding conventional pigs, a previous study conducted to assess the natural longitudinal changes that organs undergo from birth through 150 kg body weight, showed that both absolute and relative measurements

(weight, volume, and length) of the organs were dependent on the body weight and age of the pig. More specifically, the relative weight of liver, kidney, heart, and lungs decreased after initially increasing within the first week of life (i.e., birth (pre-suckle), PND 1, 2, 3, 5, 7, 14, 21 (weaning), 22, 23, 24, 26, 28, 42, 49, and 63 of age), whereas the relative weight of all organs decreased as body weight increased (i.e., 30, 50, 75, 100, 125, and 150 kg) [31].

As part of the I-PREDICT project, we aimed to establish the neonatal Göttingen Minipig as a surgical model for investigating the impact of systemic hypoxia versus TH on drug disposition. This study demonstrated that various techniques previously considered challenging or even unfeasible in this new animal model, such as endotracheal intubation and catheterization of central (e.g., jugular, and umbilical veins) and peripheral (e.g., epigastric, and saphenous veins) vessels, are achievable when carried out by trained personnel (Chapter 3) [32]. However, obtaining organ blood flow in the neonatal Göttingen Minipigs at this stage was considered more challenging since this require extensive formal training for surgical sophisticated techniques. These advanced techniques refer to the catheterization of the abdominal aorta through the femoral artery, the left atrium via a left thoracotomy, as well as the pulmonary artery for blood sampling [19], and procedures like thoracotomy and laparotomy or flank incision with the isolation and catheterization of the superior mesenteric artery [33]. These procedures have been previously conducted in a juvenile conventional pig model of 6 weeks old, weighting 11.8±1.1 kg [19] and 1-3 days old, 1.5-2.5 kg [33] and potentially could contribute to the advancement of the neonatal Göttingen Minipig model for blood flow measurements in future research.

4.2. Estimated glomerular filtration rate

While performing neonatal Göttingen Minipig PBPK modelling, we acknowledged the significance of the eGFR parameter. Therefore, in obtaining an optimized neonatal Göttingen Minipig PBPK model we considered it important to implement renal parameters, such as eGFR specific to this age category. Next, it became widely accepted that, regardless of species, the metabolic rate is closely related to BSA [34]. As a result, it became common practice in humans to index physiological variables to BSA [22,34]. McIntosh et al. proposed indexing kidney function to BSA in one of the early papers describing the concept of renal CL. They proposed 1.73 m^2, since BSA correlates closely with kidney size of 25-year-old Americans of that time [35]. However, the appropriateness of normalizing to BSA is arguably in the pediatric population, as the formula to calculate the BSA tends to underestimate the true BSA and standardization to GFR/1.73 m^2 was 20% lower than GFR/12.9 L extracellular fluid volume (ECFV) [34]. This means that indexing GFR for BSA could have a clinically important overestimate or underestimate of true kidney function in an individual child [34]. Furthermore, GFR, ECFV, and BSA increase in a non-linear fashion as functions of age until about 13 years of age, corresponding to a BSA of about 1.35 m^2, which was taken as the cut-off point between children and adults [22]. As humans grow, their ratio of height to effective radius changes as a nonlinear function of surface area. Humans must therefore change shape as they grow. Moreover, the ECFV-to-weight ratio decreases as a function of body size, suggesting that humans also change body composition as they grow. Therefore, new equations give an iterative best fit to ECFV [22].

On the other hand, BW, which is widely used for indexing GFR in veterinary practice [20,23], is influenced by body fat content. Furthermore, plasma creatinine concentration is also affected by an animal's muscle mass which varies between individuals [23]. In a previous study

measuring eGFR in dogs, it was concluded that there is a strong reason why the GFR normalized with respect to ECFV may be a more suitable way of expressing GFR since it is the role of the kidney to filter the extracellular fluid and regulate its composition and volume [23]. Therefore, it was proposed the use of the GFR-to-ECFV ratio as a valid method for GFR normalization. This is particularly important in dogs because of the wide range of body sizes in different breeds [23]. In another study performed on developing conventional piglets, all GFR values were adjusted for BW, BSA or KW [20]. When indexed to BSA and KW, a statistically significant increase in GFR was observed. The increase in GFR indexed to BW was less pronounced than the GFR indexed to KW and BSA [20]. Therefore, based on these findings and the available data, we concluded that it is more appropriate to implement the GFR indexed to BW in our neonatal Göttingen Minipig PBPK models.

4.3. Metabolism

In the context of PBPK models, metabolic clearance is commonly extrapolated from in vitro data, such as drug kinetics measured in liver microsomes or hepatocytes [17]. Firstly, we used in vitro ADME data based on liver microsomes prepared from juvenile conventional pigs of both sexes to predict MDZ plasma concentrations in neonatal Göttingen Minipigs. Literature findings suggest that minipigs generally have CYP enzyme activities similar to those of conventional pigs [26]. Total CYP content in conventional pig microsomes aligns well with levels found in other pigs strains and humans [36]. Nevertheless, total CYP content in liver microsomes is slightly higher in minipigs compared to conventional pigs, and no sex difference was detected (Table 8) [26]. Therefore, in our MDZ PBPK model, we implemented the reported value for CYP3A enzyme content in pig liver microsomes (0.18 nmol/mg protein) [26]. Furthermore, as a possible future direction in order to make our pilot PBPK more bottom-up, given the available data on MDZ metabolism kinetics and CYP3A abundance in conventional pigs, one approach could be to indirectly derive the CYP activity ontogeny profiles in (mini)pigs and use this information for simulations.

Secondly, Michaelis-Menten parameters (i.e., porcine Km : 15.3 (±4.4) µM and porcine Vmax : 1848 (±637) pmol/min/mg protein [28]) were adopted from conventional pigs. In this regard, a previous study showed that mild hypothermia decreases fentanyl and MDZ clearance in a rat model of cardiac arrest, highlighting that metabolic capacity, rather than enzyme affinity, significantly influence the systemic clearance of these drugs [37]. This finding suggests a possible strategy to focus on evaluating temperature-dependent changes in Vmax (while keeping Km constant), when simulating MDZ levels. Therefore, the CYP3A enzyme content should be corrected for the ontogeny function as well as Vmax, that is age and strain dependent.

Table 8. Cytochrome P450 (CYP) concentration in liver microsomes from juvenile Göttingen Minipigs and conventional pigs [26]. * Bodyweight (BW).

Strain	Sex	Age (months)	BW (kg)	CYP (nmol/mg protein)
Göttingen Minipig	Female	4	12.7	1.03
			12.1	0.95

	Male		9.5	0.87
			9.9	0.95
Conventional Pig	Female	2	22	0.55
			31	0.45
			27	0.37
			25	0.35
	Male	5	85	0.38
			86	0.44
			79	0.39
			95	0.49

Another limitation in our model relates to the lack of ADME data regarding the impact of hypothermia on enzyme kinetics. Consequently, the same values for CYP3A protein content, Km, and Vmax were applied for both normothermia and hypothermia predictions, with hypothermia effects primarily considered based on physiological modifications (i.e., blood flow). Addressing this knowledge gap requires high-quality ADME data in Göttingen Minipigs and the quantification of Vmax, and CYP protein content in in vitro systems under hypothermia conditions. Based on in vitro short- and long-term hypothermia assessments, we can build hypotheses about the range of changes expected and assess the impact.

In the PBPK model construction, information on enzyme expression is crucial. Gene expression information can be used as surrogate for protein abundance and activity within PBPK models. It is important to acknowledge that the absolute and relative gene expression can differ between species and strains. This is affecting both, the PK and PD and is therefore posing a challenge for the extrapolation from preclinical findings to humans [24]. On the other hand, protein rather than mRNA quantification is considered superior, as transcription and translation are controlled separately and protein and mRNA levels do not necessarily correlate [17]. Currently, proteomics ontogeny data for Göttingen Minipigs at various developmental stages (i.e., gestational day (GD) 84–86, GD 108, PND 1, PND 3, PND 7, PND 28 and adult) are available [12], along with RT-qPCR and proteomics data under TH and hypoxia conditions, as part of the I-PREDICT project. Future steps will involve integrating these datasets into a workflow to generate comprehensive whole-body expression databases for developing Göttingen Minipig PBPK models.

4.4. Partition coefficients

Partition coefficients, and cellular permeabilities are crucial in predicting drug distribution in the body [38]. Partition coefficients are key parameters in PBPK models, yet the coefficients are impractical to measure in vivo [39]. Several mechanistic-based equations have been developed to predict K_p using tissue composition information and the compound's physicochemical properties, but it is not clear which, if any, of the methods is most appropriate under given circumstances [38]. In a previous study [38], five of the most widely used K_p methods were investigated: Poulin and Theil [40], Berezhkovskiy [41], Rodgers and Rowland [42], PK-Sim® standard [43] and Schmitt [44]. These methods were used to predict K_p for 11 drugs, classified as strong bases, weak bases, acids, neutrals, and zwitterions, among them MDZ as weak base.

Briefly, Poulin and Theil made the first attempt to develop and validate a mechanistic distribution model for predicting rat and human volume of distribution at steady state of 123 structurally unrelated compounds (acids, bases, and neutrals). The predicted data were compared with in vivo data. The approach proposed a K_p prediction method that accounts for dissolution into water and nonspecific binding to neutral lipids and phospholipids [40]. Berezhkovskiy modified the Poulin and Theil [40] method and assumed only drugs in the water fraction bind to tissues [41]. Rodgers and Rowland made improvements by proposing equations that incorporate expressions for dissolution in tissue water and partitioning into neutral lipids and neutral phospholipids, refinement that was not addressed in earlier equations [42]. On the other hand, the Schmitt approach offered a versatile method for estimating K_p values by considering tissue composition in terms of water, neutral lipids, neutral and acidic phospholipids, and proteins. It utilizes compound-specific parameters such as lipophilicity, binding to phospholipid membranes, acid dissociation constant (pKa), and unbound fraction in blood plasma. This method is universally applicable to various types of compounds, including neutral, acidic, basic, or multiply charged substances. A notable feature is its consideration for electrostatic interactions between positively charged molecules and acidic phospholipids, expanding its applicability compared to previous approaches [44]. Lastly, Willmann et al. introduced PK-Sim® standard method that considers partitioning into lipids, proteins, and water [43]. This approach incorporates membrane affinity as a measure of lipophilicity. To better mimic the partitioning into a biological membrane, it is assumed that the phospholipids in tissues have a lipophilicity similar to a mixture of 30% neutral lipids and 70% water. A tissue/plasma partition coefficient is then calculated using the volume fractions of the aqueous and the organic sub compartments of the respective organ and plasma [43]. Given that each of these methods relies on distinct assumptions and input information, they can yield different K_p predictions. No method is consistently more accurate than the others and in the context of PBPK modelling, it is then unclear which method should be used to predict plasma concentration profiles. The results from previous study investigating these five most commonly used methods, demonstrated that no method was consistently superior to the others, even within classes of drugs [38]. For strong bases, weak bases, acids, and neutrals, no single K_p method consistently produced PBPK model predictions that were more accurate than the other methods. Interestingly, the K_p for the adipose tissue was generally the most variable for every drug tested. Nevertheless, The PK-Sim® standard and Schmitt methods had the highest predictions for the adipose K_p for MDZ. This highlights the need to include the process of choosing the suitable method as part of the optimization process during PBPK model development [38]. This was also our approach in constructing the neonatal Göttingen Minipig PBPK models, this involving testing and comparing all five methods, ultimately selecting the one that provided the least misprediction. Using the implementation of the five most popular calculation methods as well as a standardized tissue composition data base would make the comparison, sensitivity, and optimization steps much more accessible and, thus, could eventually be part of the PBPK model-building routine [38]. To improve the alignment of predicted MDZ and TPM concentration-time profiles with observed PK profiles, the distribution calculation in the PBPK model was optimized using the parameter identification module in PK-Sim®. This optimization indicates the use of a middle-out approach, where predictions were partially estimated by fitting to observed data. It is important to clarify the extent to which the predictions were derived from a full bottom-up approach versus those that were adjusted by fitting to observed data.

Lastly, sensitivity analyses can help prioritize the collection of missing pathophysiological data for PA/TH. One consideration is to fit sensitive parameters using control data and then evaluate the impact on different populations (PA/TH). For example, Smits et al. [1] used MDZ as a model drug and conducted sensitivity analyses to assess the impact of TH on PK. They examined several parameters, including intrinsic hepatic clearance for 1-hydroxymidazolam, a 20% reduction in cardiac output, and changes in the blood/plasma ratio and unbound fraction in plasma (f_u_plasma). Changes in Km and Vmax for 1-hydroxymidazolam formation and f_u_plasma could significantly impact MDZ hepatic clearance, while a 20% reduction in cardiac output did not. Our pilot PBPK model's sensitivity analysis showed that most parameters minimally affected MDZ and TPM's AUC, except for MDZ's lipophilicity, which had a significant impact and warrants further analysis.

5. Conclusion

As no published neonatal Göttingen Minipig PBPK model exists, this work aimed to compile the necessary data to allow construction of such a model. While a considerable amount of data is available, important knowledge gaps still exist. Furthermore, the initial steps were taken to develop a pilot hypothermia PBPK model, incorporating TH as a non-maturational covariate. The preliminary simulated plasma concentrations were partially estimated by fitting to observed data, indicating the use of a middle-out approach. This method demonstrated good agreement with the observed data for the two different temperature groups and two compounds. The model remains adaptable and can be refined with new information, particularly on blood flow and metabolism in this specific age group, aiming for a more bottom-up approach. Future work should also focus on implementing population variability in physiological parameters. Currently, the variability in the population results makes it infeasible to design populations for these PBPK models, and variability in pathophysiology and possibly ADME cannot be explored in PK-Sim® software. Continuous adjustments based on in vivo data for reference compounds and different formulations are anticipated to enhance the model's predictive performance over time.

6. References

1.   Smits A, Annaert P, Van Cruchten S, et al. A Physiology-Based Pharmacokinetic Framework to Support Drug Development and Dose Precision During Therapeutic Hypothermia in Neonates. Front Pharmacol. 2020;11:587-587.
2.   Jacobs SE, Berg M, Hunt R, et al. Cooling for newborns with hypoxic ischaemic encephalopathy. Cochrane Database Syst Rev. 2013 Jan 31;2013(1):Cd003311.
3.   NICE. National Institute for Health and Care Excellence. Interventional procedures guidance [IPG347]. Therapeutic hypothermia with intracorporeal temperature monitoring for hypoxic perinatal brain injury. Published on 26 May 2010, accessed on 25 April 2023. 2010.
4.   Favié LMA, Groenendaal F, van den Broek MPH, et al. Phenobarbital, Midazolam Pharmacokinetics, Effectiveness, and Drug-Drug Interaction in Asphyxiated Neonates Undergoing Therapeutic Hypothermia. Neonatology. 2019;116(2):154-162.

5.   Michelet R, Bocxlaer JV, Vermeulen A. PBPK in Preterm and Term Neonates: A Review. Curr Pharm Des. 2017;23(38):5943-5954.

6.   Ayuso M, Buyssens L, Stroe M, et al. The Neonatal and Juvenile Pig in Pediatric Drug Discovery and Development. Pharmaceutics. 2021;13(1):44.

7.   Parrott N, Davies B, Hoffmann G, et al. Development of a Physiologically Based Model for Oseltamivir and Simulation of Pharmacokinetics in Neonates and Infants. Clinical Pharmacokinetics. 2011 2011/09/01;50(9):613-623.

8.   Helke KL, Swindle MM. Animal models of toxicology testing: the role of pigs. Expert Opin Drug Metab Toxicol. 2013 Feb;9(2):127-39.

9.   Singh VK, Thrall KD, Hauer-Jensen M. Minipigs as models in drug discovery. Expert Opin Drug Discov. 2016 Dec;11(12):1131-1134.

10.   Bode G, Clausing P, Gervais F, et al. The utility of the minipig as an animal model in regulatory toxicology. J Pharmacol Toxicol Methods. 2010 Nov-Dec;62(3):196-220.

11.   Valenzuela A, Tardiveau C, Ayuso M, et al. Safety Testing of an Antisense Oligonucleotide Intended for Pediatric Indications in the Juvenile Göttingen Minipig, including an Evaluation of the Ontogeny of Key Nucleases. Pharmaceutics. 2021;13(9):1442.

12.   Buyssens L, De Clerck L, Schelstraete W, et al. Hepatic Cytochrome P450 Abundance and Activity in the Developing and Adult Göttingen Minipig: Pivotal Data for PBPK Modeling. Front Pharmacol. 2021;12:665644.

13.   Van Peer E, De Bock L, Boussery K, et al. Age-related Differences in CYP3A Abundance and Activity in the Liver of the Göttingen Minipig. Basic Clin Pharmacol Toxicol. 2015 Nov;117(5):350-7.

14.   Van Peer E, Jacobs F, Snoeys J, et al. In vitro Phase I-and Phase II-drug metabolism in the liver of juvenile and adult Göttingen minipigs. Pharmaceutical research. 2017;34(4):750-764.

15.   Millecam J, De Clerck L, Govaert E, et al. The Ontogeny of Cytochrome P450 Enzyme Activity and Protein Abundance in Conventional Pigs in Support of Preclinical Pediatric Drug Research. Front Pharmacol. 2018;9:470.

16.   Van Peer E, Downes N, Casteleyn C, et al. Organ data from the developing Göttingen minipig: first steps towards a juvenile PBPK model. Journal of pharmacokinetics and pharmacodynamics. 2016;43:179-190.

17.   Suenderhauf C, Parrott N. A physiologically based pharmacokinetic model of the minipig: data compilation and model implementation. Pharmaceutical research. 2013;30(1):1-15.

18.   Beglinger R, Becker M. Herz und Kreislauf. Glodek P, Oldigs B Paul Parey, Berlin und Hamburg. 1981.

19.   Fritz HG, Holzmayr M, Walter B, et al. The effect of mild hypothermia on plasma fentanyl concentration and biotransformation in juvenile pigs. Anesth Analg. 2005 Apr;100(4):996-1002.

20.   Gasthuys E, Devreese M, Millecam J, et al. Postnatal Maturation of the Glomerular Filtration Rate in Conventional Growing Piglets As Potential Juvenile Animal Model for Preclinical Pharmaceutical Research [Original Research]. Front Pharmacol. 2017 2017-June-29;8.

21.   Dhondt L, Croubels S, De Paepe P, et al. Conventional Pig as Animal Model for Human Renal Drug Excretion Processes: Unravelling the Porcine Renal Function by Use of a

Cocktail of Exogenous Markers [Original Research]. Front Pharmacol. 2020 2020-June-12;11.

22. Bird NJ, Henderson BL, Lui D, et al. Indexing glomerular filtration rate to suit children. J Nucl Med. 2003 Jul;44(7):1037-43.

23. Gleadhill A, Peters AM, Michell AR. A simple method for measuring glomerular filtration rate in dogs. Research in Veterinary Science. 1995 1995/09/01/;59(2):118-123.

24. Cordes H, Rapp H. Gene expression databases for physiologically based pharmacokinetic modeling of humans and animal species. CPT Pharmacometrics Syst Pharmacol. 2023 Mar;12(3):311-319.

25. Skaanild MT, Friis C. Analyses of CYP2C in porcine microsomes. Basic Clin Pharmacol Toxicol. 2008 Nov;103(5):487-92.

26. Skaanild MT, Friis C. Characterization of the P450 system in Göttingen minipigs. Pharmacol Toxicol. 1997;80 Suppl 2:28-33.

27. Buyssens L, Valenzuela A, Prims S, et al. Ontogeny of CYP3A and UGT activity in preterm piglets: a translational model for drug metabolism in preterm newborns. Front Pharmacol. 2023;14:1177541.

28. Schelstraete W, Clerck LD, Govaert E, et al. Characterization of Porcine Hepatic and Intestinal Drug Metabolizing CYP450: Comparison with Human Orthologues from A Quantitative, Activity and Selectivity Perspective. Scientific Reports. 2019 2019/06/25;9(1):9233.

29. Christensen J, Højskov CS, Dam M, et al. Plasma concentration of topiramate correlates with cerebrospinal fluid concentration. Ther Drug Monit. 2001 Oct;23(5):529-35.

30. Price PS, Conolly RB, Chaisson CF, et al. Modeling interindividual variation in physiological factors used in PBPK models of humans. Crit Rev Toxicol. 2003;33(5):469-503.

31. Elefson SK, Lu N, Chevalier T, et al. Assessment of visceral organ growth in pigs from birth through 150 kg. Journal of Animal Science. 2021;99(9).

32. Stroe M-S, Van Bockstal L, Valenzuela AP, et al. Development of a neonatal Göttingen Minipig model for dose precision in perinatal asphyxia: technical opportunities, challenges, and potential further steps [Methods]. Front Pediatr. 2023;11:662.

33. Cheung P-Y, Gill RS, Bigam DL. A swine model of neonatal asphyxia. J Vis Exp. 2011 (56):3166.

34. Geddes CC, Woo YM, Brady S. Glomerular filtration rate—what is the rationale and justification of normalizing GFR for body surface area? Nephrology Dialysis Transplantation. 2007;23(1):4-6.

35. McIntosh JF, Möller E, Van Slyke DD. STUDIES OF UREA EXCRETION. III: The Influence of Body Size on Urea Output. J Clin Invest. 1928 Dec;6(3):467-83.

36. Skaanild MT. Porcine cytochrome P450 and metabolism. Curr Pharm Des. 2006;12(11):1421-7.

37. Empey PE, Miller TM, Philbrick AH, et al. Mild hypothermia decreases fentanyl and midazolam steady-state clearance in a rat model of cardiac arrest. Critical care medicine. 2012;40(4):1221.

38. Utsey K, Gastonguay MS, Russell S, et al. Quantification of the Impact of Partition Coefficient Prediction Methods on Physiologically Based Pharmacokinetic Model Output Using a Standardized Tissue Composition. Drug Metab Dispos. 2020 Oct;48(10):903-916.

39.   Jones H, Rowland-Yeo K. Basic concepts in physiologically based pharmacokinetic modeling in drug discovery and development. CPT: pharmacometrics & systems pharmacology. 2013;2(8):1-12.

40.   Poulin P, Theil FP. Prediction of pharmacokinetics prior to in vivo studies. 1. Mechanism-based prediction of volume of distribution. J Pharm Sci. 2002 Jan;91(1):129-56.

41.   Berezhkovskiy LM. Volume of distribution at steady state for a linear pharmacokinetic system with peripheral elimination. J Pharm Sci. 2004 Jun;93(6):1628-40.

42.   Rodgers T, Rowland M. Physiologically based pharmacokinetic modelling 2: predicting the tissue distribution of acids, very weak bases, neutrals and zwitterions. J Pharm Sci. 2006 Jun;95(6):1238-57.

43.   Willmann S, Lippert J, Schmitt W. From physicochemistry to absorption and distribution: predictive mechanistic modelling and computational tools. Expert Opin Drug Metab Toxicol. 2005 Jun;1(1):159-68.

44.   Schmitt W. General approach for the calculation of tissue to plasma partition coefficients. Toxicol In Vitro. 2008 Mar;22(2):457-67.

Supplementary Table 1.   Estimated Glomerular Filtration Rate (eGFR) normalized to bodyweight (BW), body surface (BSA) and kidney weight (KW) in in vivo Göttingen Minipigs. The names of each group were abbreviated as the following - control (C), therapeutic hypothermia (TH), hypoxia (H), hypoxia and TH (H+TH), PND1, untreated Göttingen Minipigs <24 hours age. * $Crea_{plasma}$, creatinine determined in plasma; $Crea_{urine}$, creatinine determined in urine, $eGFR_{BW}$, $eGFR_{KW}$, $eGFR_{BSA}$, eGFR calculated in function of BW, KW respectively, BSA.

Parameter	Formula	Reference
BSA (m²)	$BSA = (9 * BW\ (kg)^{(2/3)})/100$	Gathuys et al. 2017
eGFR (mL/min/kg)	$eGFR = (1.879*BW^{1.092})/ Crea_{plasma}^{0.601}$	
eGFR (mL/min/m²)	$eGFR = (1.879*BSA^{1.092})/ Crea_{plasma}^{0.601}$	
eGFR (mL/min/g)	$eGFR = (1.879*KW^{1.092})/ Crea_{plasma}^{0.601}$	

Group	BW (kg)	KW (g)	BSA (m²)	$Crea_{plasma}$ (mg/dL)	$eGFR_{BW}$ (mL/min/kg)	$eGFR_{KW}$ (mL/min/g)	$eGFR_{BSA}$ (mL/min/m²)	$Crea_{urine}$ (mg/dL)
C2	0.556	3.160	0.061	0.63	1.31	8.71	0.12	14
C3	0.544	2.800	0.06	0.51	1.45	8.67	0.13	14
C4	0.472	2.770	0.054	0.33	1.61	11.13	0.15	46
C5	0.542	2.950	0.06	0.38	1.72	10.95	0.15	15
C6	0.628	3.270	0.06	0.71	1.39	8.42	0.12	39
H1	0.521	2.810	0.058	0.75	1.09	6.90	0.1	45
H2	0.502	2.730	0.057	1.66	0.65	4.15	0.06	22
H3	0.430	2.260	0.051	0.51	1.12	6.86	0.11	19
H4	0.531	3.270	0.059	0.48	1.46	10.65	0.13	39
H5	0.547	3.310	0.06	0.72	1.18	8.46	0.11	59
H6	0.592	2.600	0.063	0.59	1.45	7.32	0.13	41
TH1	0.657	2.170	0.068	0.41	2.03	7.48	0.17	-
TH2	0.564	2.170	0.061	0.24	2.36	10.32	0.21	14
TH3	0.444	2.170	0.052	0.95	0.8	4.51	0.08	-
TH4	0.620	3.150	0.065	1.05	1.08	6.38	0.09	115
TH5	0.505	2.730	0.057	0.42	1.5	9.47	0.14	56
TH6	0.597	3.050	0.064	0.43	1.77	10.54	0.15	-
H+TH1	0.530	2.170	0.059	0.28	2.02	9.41	0.18	-
H+TH2	0.610	3.480	0.065	0.69	1.37	9.16	0.12	7
H+TH3	0.507	2.710	0.057	0.68	1.13	7.04	0.1	11
H+TH4	0.552	2.610	0.061	0.44	1.61	8.77	0.14	82
H+TH5	0.650	3.660	0.067	0.51	1.76	11.61	0.15	29
H+TH6	0.521	3.000	0.058	0.74	1.1	7.47	0.1	110
PND1 1	0.449	2.170	0.053	0.59	1.07	6.01	0.1	41
PND1 2	0.200	2.170	0.031	0.96	0.33	4.49	0.04	36
PND1 3	0.265	2.170	0.037	0.8	0.5	5.01	0.06	34
PND1 4	0.378	2.170	0.047	0.65	0.84	5.67	0.08	31
PND1 5	0.345	2.170	0.044	0.75	0.69	5.21	0.07	-

CHAPTER 7:
General Discussion

General Discussion

This study hypothesized that both systemic hypoxia and therapeutic hypothermia (TH) affect drug disposition. Given the effects of TH and perinatal asphyxia (PA) on physiology, our primary hypothesis was that TH significantly decreases metabolic clearance (CL) in asphyxiated neonates, necessitating adjustments in drug dosing. We also hypothesized that PA and TH influence enzyme functionality, including gene and protein expression and enzymatic activities. To investigate these effects, a neonatal Göttingen Minipig model was developed. Supporting drug development for this population involves integrating clinical observations (pharmacokinetic (PK) data and real-world physiological data), preclinical data (in vitro and in vivo animal models), and molecular and cellular biology insights into a physiologically-based pharmacokinetic (PBPK) model. Therefore, an optimized PBPK model, the ultimate goal of this study, is expected to be a reliable tool for accurately predicting drug exposure in asphyxiated neonates undergoing TH.

Chapter 7 offers the general discussion of this PhD thesis, containing three key aspects: (1) a comparative analysis of conventional pigs versus the neonatal Göttingen Minipig model developed for PA, (2) an examination of various pharmacological strategies applicable to asphyxiated neonates undergoing TH and (3) future prospects on (neonatal) Göttingen Minipig PBPK modelling. To understand the differences between the two PA models, the conventional pig and the Göttingen Minipig, **Section 1** explores the methodological considerations in establishing in vivo asphyxia models. **Section 2** provides a summary of human neonatal PK as supportive pharmacotherapy to improve neurodevelopmental outcomes (adapted from "Pharmacokinetics during therapeutic hypothermia in neonates: from pathophysiology to translational knowledge and physiologically-based pharmacokinetic (PBPK) modelling"), along with an evaluation of the effects of PA/TH on the disposition of our study drugs in human and animal studies. **Section 3** resumes the strategy for PBPK model evaluation together with future prospects on developing PBPK models, using the neonatal Göttingen Minipig. Lastly, **Section 4** offers the general conclusion of this PhD thesis.

1. Pig asphyxia models

1.1. Methodological considerations

Amongst the PA animal models, the conventional piglet is a well-established and relevant model to study cerebral blood flow and cerebral metabolism [1]. The developmental similarities with the (near)term human neonates represents an advantage over other species, such as rodents and even dogs and non-human primates (NHPs), since this larger pig's body size at birth allows for sampling at early stages without hampering the physiology and also facilitates the adaptation of neonatal intensive care unit (NICU) equipment for its use in pigs [2]. Furthermore, the confounding variables of hypoxia and hemodynamic derangements can be controlled [2]. Before setting up our protocol, we analyzed some hypoxia pig models for a comparative methodology and knowledge of limitations, that will be further presented.

Fetal and early postnatal (<24 hours after birth) procedures to induce PA in piglets were previously published [3]. Fetal procedures offer the advantage that the piglets have not been

exposed yet to the external environment and as such may better mimic PA. However, the induced asphyxia by umbilical cord clamping appears to be not as severe as expected in human neonates as well as the final outcome is also very variable in the animal model [3]. Therefore, early postnatal procedures (<24 hours after birth) are more commonly used and several protocols are reported. Cheung et al. [4] described an experimental protocol of severe hypoxemia induced via normocapnic alveolar hypoxia. The neonatal piglets are surgically instrumented in a non-survival experiment, which allows the establishment of mechanical ventilation, arterial and central venous access and the placement of catheters and flow probes for the continuous monitoring of intra-vascular pressure and blood flow, across different arteries. In this protocol, the severe hypoxemia is achieved by decreasing the inspired oxygen concentration (FiO_2) to 10-15% and by increasing the concentration of inhaled nitrogen gas, for two hours, aiming for arterial oxygen saturations of 30-40%. This degree of hypoxemia produces clinical asphyxia, with severe metabolic acidosis, systemic hypotension, and cardiogenic shock with hypoperfusion to vital organs [4]. A similar piglet model for PA has been described by O'Brien et al. [5] via whole-body hypoxia-asphyxia. This was induced by decreasing the inhaled oxygen to 10%, for 45 minutes in combination with the occlusion of the endotracheal tube, for 7 minutes [5]. Global hypoxia-ischemia was established by Kyng et al. [6], combining ischemia through hypotension, with low FiO_2 via nitrogen gas, for a flat trace amplitude integrated electroencephalogram (aEEG), indicative of cerebral hypoxia. Survival was improved by adjusting oxygenation according to the aEEG response and arterial blood pressure. A different approach for inducing transient hypoxia-ischemia was presented by Ezzati et al. [7], by remote occlusion of both common carotid arteries, using inflatable vascular occluders, at the level of the fourth cervical vertebra, with low FiO_2 of 0.09. Regarding our Göttingen Minipig study [8], the monitoring of the laboratory clues for acidosis, via blood gas analysis, and the perfusion and cardiac function, via ECG, allowed for adjustments according to each piglet´s tolerance to hypoxia, thus ensuring a high survival rate.

Whether dealing with conventional piglets or minipigs, the development of a neonatal pig asphyxia model requires careful consideration and monitoring of factors such as the selection of medication, the approach to controlling insult duration and severity, post-insult resuscitation and care, and the evaluation of the outcomes [6]. In expected clinical asphyxia, severe metabolic acidosis, systemic hypotension, and cardiogenic shock with hypoperfusion of vital organs may occur. In case of hypotension, dobutamine, norepinephrine and crystalloids can be used to maintain the mean arterial blood pressure above 45 mmHg, which is the lower limit of autoregulation in neonatal swine [5]. Bolus infusions of 0.9% saline, at 10 mL/kg, dopamine and dobutamine (5-20 µg/kg/min), adrenaline (0.1-1.5 µg/kg/min) and noradrenaline (0.02-1 µg/kg/min) could sustain the mean arterial blood pressure above 40 mmHg [7]. Neuromuscular blocking agents (NMBAs), such as vecuronium (0.2 mg/kg/h), are often used to prevent shivering and to provide consistent anesthesia [5]. Sodium bicarbonate and calcium chloride can be administered to correct metabolic acidosis and hypocalcemia if necessary [5,7,9].

Nevertheless, there are also some limitations of the swine model for PA. The side effects, related to anesthesia and surgical trauma stress, limit this model in terms of survival length and number of invasive procedures performed. The survival length may be increased with an adequate stabilizing period, appropriate use of anesthetic medications and refined surgical techniques [4]. Regarding the latter, skilled personnel that has experience in surgery and anesthesia of neonatal piglets is the key for these types of experiments. Other limitations

include the logistical aspects of getting neonatal piglets in the research facility when no (pregnant) sows are housed on-site. As transportation of neonatal piglets is prohibited, transportation of pregnant sows to the facility will be needed and this results in a high number of piglets that need to be instrumented in a short time frame (< 24 hours) when she delivers. Using older piglets (two or more days of age) risks weakening the clinical relevance of the piglet model, as the model should mimic human PA [10].

1.2. Comparative evaluation of the Gottingen Minipig and the conventional piglet as distinctive models for perinatal asphyxia

As noted, the conventional piglet serves as a well-established model for PA. However, the neonatal Göttingen Minipig stands out as the most frequently employed pig strain in nonclinical drug development [11]. Considering the specific objectives of our study, which involve enhancing dose precision under PA/TH conditions, the neonatal Göttingen Minipig model was considered more suitable than the conventional pig model. However, both strains have translational value and present strengths and limitations. Some technical, logistical as well as metabolic and biochemical aspects are resumed in Table 1 and will be further discussed.

At birth, pigs are smaller than humans, with a weight of approximately 0.5 kg for a Göttingen Minipig and 1.5 kg for a conventional pig. However, they undergo rapid growth, with Göttingen Minipigs exhibiting linear growth up to around 18 months, in contrast with the conventional pigs, that follow more of an exponential growth curve until the age of 4 months [2]. In particular, this larger birth size of conventional piglets presents an advantage over the Göttingen Minipigs, a strength that will be further highlighted from various perspectives. Firstly, in Brodbelt's study on perioperative mortality, various factors were identified as significant contributors to mortality [12]. Notably, extremes of weight were found to be associated with an increased likelihood of anesthetic-related deaths. For instance, in the 0-2 kg weight range, the odds ratio was 15.7 compared to the 2-6 kg range, where the odds ratio was 1 (study performed on small animals) [12]. Secondly, since the piglet asphyxia model is well-characterized, this opens opportunities for new pharmacological interventions (e.g., melatonin and/or erythropoietin [13], xenon [14]) and technologies applied in the clinical setting, (e.g., aEEG [6], magnetic resonance spectroscopy (MRS) [15], cerebral magnetic resonance or neurological hypoxic-ischemic encephalopathy (HIE) biomarkers [16]). Interestingly, in a study conducted by Iwata et al. [17] was shown that body weight critically modulates regional cerebral hypothermic temperatures. This study explored the body weight dependency of regional cerebral temperature in 14 neonatal conventional piglets subjected to normothermia (38.5 °C), whole-body cooling (36.5 °C, 34.5 °C, 32.5 °C, and 30.5 °C), or systemic hypothermic circulatory arrest (20 °C, 15 °C, and 10 °C). The findings demonstrated that the superficial brain is cooler in smaller piglets and the efficiency of brain cooling increased with lower body weight, attributed to the greater head surface area-to-volume ratios [17]. Given the implications that body weight has on regional cerebral hypothermic temperatures, wherein smaller piglets exhibit cooler superficial brains and enhanced brain cooling efficiency due to their greater head surface area-to-volume ratios, the conventional piglet model may be deemed more advantageous over Göttingen Minipigs for this purpose, as it closely resembles the size of human neonates at birth, thereby providing a closer physiological resemblance to humans. In the context of the CoolCap Trial (controlled trial of

selective head cooling with systemic hypothermia (rectal temperature, 34 °C to 35 °C for 72 hours [18]), it is noted that low body weight human neonates may have experienced excessive cooling. To achieve consistent regional temperatures and optimize neuroprotection, adjustments based on body weight may be necessary for both whole-body cooling and systemic hypothermic circulatory arrest [17].

In view of animal experimentation, the larger size of conventional piglets enables for larger sample amounts, such as increased blood volumes in view of PK studies, or the conduct of more extensive or prolonged experiments with frequent sampling time points [8]. Furthermore, this size of conventional piglets aligns well with NICU equipment and medical devices, better resembling the size of (near)term neonates. One example is the percutaneous external jugular vein catheterization, using the triangulation technique [19], that was feasible in the conventional piglet model but not in the Göttingen Minipig. This guide-wire-assisted percutaneous technique have become standard practice in both human and veterinary medicine due to the minimization of the soft tissue and vessel damage, facilitating rapid and easy central venous access by using palpable anatomical landmarks and triangulation [19]. Due to the larger size of the conventional piglet model, the anatomical landmarks were easier identified, and the catheter easier manipulated in the vessel. Nevertheless, despite the inherent challenges, the successful instrumentation and stabilization of our Göttingen Minipigs throughout the 24-hour experiment demonstrated the feasibility of using this model as well. Through ongoing refinement of techniques and specialized training, there is potential to extend the experimental duration in future studies.

While there are numerous pig breeds, only few have been thoroughly characterized in terms of both DMEs and background pathology findings. Helke et al. conducted a review with focus on the Göttingen Minipig, emphasizing background pathology changes and, specifically, exploring breed differences [20]. The estimation of total cytochrome P450 (CYP) content in liver microsomes was previously conducted for both conventional pigs and Göttingen Minipigs [21]. The Göttingen Minipigs have higher CYP concentration overall relative to three conventional pig breeds and two human races [21-23] (i.e., minipigs exhibited 0.81 nmol/mg protein, while various strains of conventional pigs showed concentrations of 0.57 nmol/mg, 0.22 nmol/mg, and 0.46 nmol/mg). This comparison highlights that conventional pigs CYP concentrations are comparable to the total human CYP of 0.43 nmol/mg protein and 0.26 nmol/mg protein in Caucasian and Japanese individuals, respectively [21,24].

Beside the total CYP content in liver microsomes, specific CYP isoforms were examined in the context of breed differences [20]. For example, CYP1A activity exhibits sex-related differences in both minipigs and humans, although the patterns differ [20]. In minipigs, females demonstrate 2 to 4 times higher activity than males, while in humans, Caucasian males have 2 to 4 times higher activity than females [22,24]. In another study, focusing on wild pigs, revealed lower levels of CYP1A in dams compared to piglets, suggesting a decline in CYP1A with age in pigs [25]. Notable species and sex differences exist in CYP2A activity [20]. Porcine CYP2A19 exhibits a 99% homology between Göttingen and conventional breed pigs. However, female Göttingen Minipigs display a 70-fold higher activity than males (0.35 nmol/mg protein versus 0.005 nmol/mg protein), and when males are castrated, the CYP2A activity increases by 10-fold [21]. Yucatan miniature pigs also show sex differences, with females having a 5-fold higher activity than males [26]. While sex differences in CYP activity have not been reported in humans, variations in protein levels have been noted in both pigs and humans [22], and distinctions among human races are also apparent [20]. Transcriptional regulation of CYP3A

differs between humans and pigs, with similar tissue expression patterns but detected interindividual variances [27]. Notably, Yucatan miniature pigs exhibit higher CYP3A activity compared to Göttingen and conventional pigs [22,23,26]. Additionally, tissue expression patterns of CYP3A undergo changes with age [28-30] (discussed in Chapter 5 of this thesis). There are significant discrepancies in interpretation of CYP levels and substrate specificities. Both inducibility and the magnitude of induction differ across tissues and cell types even when exposed to the same inducer [20,31]. Porcine CYP2C enzymes show cross-reactivity towards many human test substrates, but not those specific for human CYP2C, making extrapolation between pigs and humans for CYP2C difficult [31]. For example, the CYP2C substrate, tolbutamide, which is fairly specific for human CYP2C9, has been tested in pigs. The tolbutamide hydroxylation was measured in both conventional pigs and minipigs, showing that the minipigs had lower activity compared to human activity [32]. CYP2D in pigs has not undergone comprehensive examination, and several substrates specific to human CYP2D are metabolized by porcine CYP2B [21]. A study investigating drug CL in pigs found that CYP2D6 substrate metabolism was faster in pigs compared to other species [33].

As discussed, various pig breeds exhibit distinct amounts of CYP and varying levels of CYP activity [20,34]. The CYP mRNA levels may change with age and differ between sexes [22,23,35]. The CYP diversity is influenced by additional factors such as epigenetics and diet, with dietary fat known to modulate CYP in pigs through transcriptional and posttranscriptional mechanisms [36]. Conventional pigs typically have ad libitum feeding until reaching maturity, at which point restricted feeding is implemented to prevent obesity and related health issues affecting skeletal and cardiovascular functions [37]. In contrast, Göttingen Minipigs are bred under controlled conditions, ensuring genetic coherence, specific pathogen-free status, and non-pigmented skin [38]. They are provided with a specialized diet designed for minipigs, preventing obesity in females or fat atrophy in males while ensuring adequate nutrient intake [39]. This controlled breeding and feeding regimen offers advantages from a research perspective, reducing variability and contributing to refinement practices that enhance animal welfare [37].

Lastly, the knowledge gained from our study, will be applied to inform, and construct a physiologically-based pharmacokinetic (PBPK) model (Chapter 6). This aligns with the overarching objective of the I-PREDICT project, which is useful for drug exposure prediction in human neonates. It is crucial to underscore that the PBPK platform relies on a minipig database, as this species is extensively characterized and commonly employed in nonclinical drug development [40]. Using data from other pig strains may compromise the predictive accuracy of this in silico technique.

Table 1. Strengths and limitations of Göttingen Minipigs and the conventional pig, as distinctive models for perinatal asphyxia (PA) /hypoxic-ischemic encephalopathy (HIE). * Cytochrome P450 (CYP); Intrauterine growth restriction (IUGR); pharmacokinetics (PK); therapeutic hypothermia (TH).

Animal model for PA/HIE	Strengths	Limitations

Conventional Pig	- well-established model for PA/HIE, this opens opportunities for new pharmacological interventions (e.g., melatonin and/or erythropoietin [13], xenon [14]), technologies (e.g., neurological investigations [6,15] [16]), and procedures applied in a clinical setting (e.g., TH [15] [16] [17]). - body systems and size at birth (1.5-2 kg) comparable with (near)term human neonate [2]. - larger body size at birth facilitates the sampling (i.e., increased blood volumes for PK studies, or the conduct of more extensive or prolonged experiments) and the adaptation of NICU equipment. - spontaneously occurring IUGR and preterm pigs are commonly observed in pig production, providing valuable opportunities for translational research [41,42]. - CYP concentrations are comparable to the total human CYP [21,24].	- since there are different strains, the amount of historical control data is limited [11]. - not bread under controlled conditions (e.g., diet can modulate CYPs in pigs [36], therefore can increase variability). - not used by pharmaceutical companies for drug discovery or development [11]. - PBPK platform relies on a minipig database [40]; therefore, using data from other pig strains may compromise the predictive accuracy.
Göttingen Minipig	- commonly used pig strain by the pharmaceutical industry, as they are genetically coherent and well-characterized, and by using the same strain, pharmaceutical companies can rely on historical control data when interpreting findings in drug safety studies [11]. - animal models for several clinical applications such as cardiovascular [43], dental conditions [44], diabetes [45], heart disease [46], skin conditions [47,48], and acute and chronic intestinal inflammation [49,50]. - Growing evidence on the developmental characteristics of Göttingen Minipigs reveals a significant resemblance to human neonates [28,29,51-53].	- the total CYP activity in minipigs is approximately 2-3 times higher than human [21]. - smaller size 0.45 (0.3-0.55) kg [37] making more challenging the instrumentation and stabilization through surgery and anesthesia [8]. - increased likelihood of anesthetic-related deaths [12]. - limitation in amount of fluid sampling (e.g., blood volumes for PK studies, or the conduct of more extensive or prolonged experiments with frequent sampling time points) [8].

2. Pharmacological strategies for asphyxiated neonates undergoing therapeutic hypothermia

Despite the positive effect of TH, PA still accounts for a relevant portion of neonatal mortality and morbidity in (near)term neonates. Therefore, interventions to further improve outcomes are urgently needed. From a drug development aspect, PA qualifies as an orphan disease. The Committee for Orphan Medicinal Products estimates that about 15 000 neonates (0.3/10 000 EU inhabitants) are affected annually. The modulation of the pathophysiology by TH in asphyxiated neonates is relevant for dosing of the commonly used drugs (antibiotics, analgosedatives, anti-epileptics, inotropes). For example, Lutz et al. analyzed 36 studies using 15 compounds. The impact of PA/TH on drug CL was dependent on the route of elimination and was most pronounced for renal elimination during TH (i.e., no difference for PHB, -25% for 1-hydroxymidazolam, -24% for lidocaine; -21% to -47% for morphine) [54]. Mannitol and amikacin CL (-40% to -60%) were estimated in the first 24-48 hours of life [55,56]. Based on gentamicin disposition in PA/TH cases, CL was initially decreased (25-35%), with a subsequent increase observed after normothermia (96-120 hours) [57]. Consequently, prolonging the dosing interval resulted in better target attainment for amikacin and gentamicin, characterized by renal elimination [56,58]. Population PK model-based dosing for neonates with PA receiving TH has been published for some commonly used drugs, like amikacin [56]. Nevertheless, therapeutic drug monitoring of compounds with a small therapeutic window (e.g., aminoglycosides) is still recommended in these critically ill neonates to obtain safe and effective therapy.

For drugs undergoing metabolic elimination, the decreased CL may reflect overall lower enzymatic activity with decreasing temperature or reduced hepatic blood flow. However, the underlying pathophysiological mechanisms still need further exploration and research [59]. Besides opioids, alpha-2-adrenergic receptor agonists like dexmedetomidine are increasingly used for sedation and their opioid-sparing effect in neonates. The drug undergoes hydroxylation (mainly by CYP2A6) and direct N-glucuronidation in adults [60]. The efficacy and short-term safety of dexmedetomidine were described in 19 neonates receiving TH [61]. Despite an association with lower heart rate, Elliott et al. concluded that the compound can be used successfully in neonates with HIE receiving TH [62]. In 2020, a phase 1 study was published in 7 neonates with PA/TH receiving dexmedetomidine [63]. Clearance was comparable to slightly lower, and the volume of distribution was larger compared to a non-HIE, non-hypothermia neonatal cohort but not statistically significant [63]. Compared to FNT, dexmedetomidine appears to provide comparable control of agitation, reducing the need for additional sedatives, shorter time to extubation, and discontinuation of sedatives [64]. Although the compounds seem promising, further research on optimal analgosedative pharmacotherapy in the setting of TH is requested and ongoing [65,66]. In addition to clinical studies, preclinical research plays a crucial role in acquiring insights in this field. In this respect, we will next discuss our main study findings and examine how they align with other preclinical and human clinical data.

Our findings revealed a notable impact on FNT metabolism, characterized by a significant decrease in CL by 66%, resulting in an approximately threefold increase in half-live ($t_{1/2}$) in the TH group compared to controls. This could be attributed to the reduced CYP3A activity, but also due to the diminished liver blood flow [67,68]. Notably, the reduced liver blood flow is particular important for the metabolic capacity of drugs with a high extraction ratio (ER; e.g.,

FNT), these being more affected by TH compared to intermediate- (e.g., MDZ) and low- ER drugs (e.g., PHB) [69,70]. This illustrates that both decreased intrinsic CL and reduced liver blood flow have to be considered during TH. For instance, in a juvenile porcine model undergoing TH and FNT anesthesia [71], FNT plasma concentrations increased by 25±11% during hypothermia and remained elevated after rewarming (i.e., the plasma FNT concentration increased significantly to 7.0±0.6 ng/mL; therefore, after rewarming and 6 hours at normothermia, decreased significantly to 6.3±0.6 ng/mL). These changes were associated with a significant reduction in cardiac index (41±15%) and blood flows of various organs: kidney (38±32%), spleen (45±33%), stomach (53±31%), gut (49±26%), pancreas (49±46%) [71]. Similarly, in a rat model of asphyxia cardiac arrest, mild hypothermia was found to decrease the FNT systemic CL from 61.5±11.5 to 48.9±8.95 mL/kg/min [72]. These findings underscore the significant impact of hypothermia on the PK of high ER drugs like FNT, which consequently affects pharmacodynamic (PD) responses such as cardiac index, highlighting the importance of considering both aspects in nonclinical studies.

Our Göttingen Minipig data indicate that TH does not significantly affect the CL of PHB and MDZ. A similar conclusion was reached in a study on neonates with HIE, which included 113 neonates treated with PHB, 118 with MDZ, and 68 with both drugs [73]. Although not statistically significant, trends towards lower CL and longer $t_{\frac{1}{2}}$ were observed in the TH and H+TH groups for MDZ and PHB. Similar trends were observed by Pokorná et al. for PHB during TH, although not statistically significant [74]. Another example is a neonatal rhesus monkey study designed to explore whether mild hypothermia (i.e., 35 °C-36.5 °C) can prevent neurotoxicity due to the combined treatment of PHB and MDZ, with plasma concentrations and duration that are clinically relevant for the management of HIE in human neonates [75]. Plasma concentrations of PHB on day 1 were 28.00±9.58 µg/mL, 36.93±6.25 µg/mL on day 2 in the normothermia group and 34.20±10.62 µg/mL at 4 hours and 40.52±7.60 µg/mL at 24 hours in the hypothermia group [75]. Was concluded that PHB plasma concentrations between the normothermic and hypothermic groups at the 4- or the 24-hour time points in the neonatal rhesus monkeys were also non statistically significant [75]. However, these findings contradict those from an asphyxia cardiac arrest rat model where mild hypothermia (33 °C) increased MDZ plasma concentrations and resulted in a significant decrease in the MDZ CL (17.5% decrease) after cardiac arrest [72]. Contrary to MDZ in humans and pigs, MDZ has a high extraction in rats with ratios of hepatic CL to blood flow of 0.86 [72,76]. The variations in physiological characteristics between our model and the cardiac arrest rat model could be the reason for the differing conclusions. Midazolam CL may therefore be more dependent on hepatic blood flow rather than significantly affected by changes in hepatic metabolic capacity in rats [72]. Based on these interspecies differences, (mini)pigs may offer a more representative model for human MDZ metabolism and should be favored over the rodent model in nonclinical studies due to their closer resemblance to human PK and PD responses.

Topiramate was included in our study to evaluate the impact on renal CL. In one PK study with neonatal conventional pigs following IV TPM administration, a proportional increase in drug exposure was found when the dose increased from 5 to 40 mg/kg, suggesting linearity over this dose range [77]. Furthermore, a dose of 5 mg/kg appeared to be sufficient to maintain plasma drug concentrations >10 µM, a concentration associated with neuroprotection in primary neuronal (astroglial) cultures [78]. In another study, involving 5 dogs with naturally occurring epilepsy treated with TPM IV formulation, at a low dose (10 mg/kg) and a high dose (20 mg/kg), demonstrated that IV TPM shows a relatively rapid onset of action and these doses appear to be safe [79]. The CL, volume of distribution (V_d), and $t_{\frac{1}{2}}$ were similar for both studied

dose groups. However, when PHB was co-administered, a higher dose of TPM was needed to achieve the desired concentrations. This was due to a significant increase in CL by approximately 5.6-fold and a reduction in $t_{1/2}$ by about 4-fold. In dogs receiving PHB, the CL ranged from 8.33 to 11.66 mL/kg/min, while the $t_{1/2}$ was between 0.5 and 1 hour, compared to dogs that were not receiving PHB, where the CL was 1.66 mL/kg/min and the $t_{1/2}$ ranged from 3.7 to 5 hours. Therefore, this suggests that PHB induces hepatic enzymes, impacting TPM elimination [79]. Regardless of whether PHB was co-administered or not, the CL in naturally occurring epileptic dogs was higher and the $t_{1/2}$ was notably shorter compared to the human adult situation (i.e., $t_{1/2}$ of 16-32 hours [80]) and our model (i.e., $t_{1/2}$ of 24.28±10.99 hours in controls) showing that the pig might be a better model than the dog for TPM PK studies.

3. Reflections on Göttingen Minipig PBPK models

The European Medicines Agency strongly encourage the use of modelling and simulation (M&S) approaches during drug development. These methods aim to integrate data from different domains and as such help decision making during early drug development, improve study design, reduce costs and the use of laboratory animals, save time, and finally enhance success rates [81]. According to the European Medicines Agency Guideline (EMA/CHMP/458101/2016, 13 December 2018), PBPK efforts supporting regulatory submissions require: (i) a platform (e.g., commercially available or in-house built platforms) that needs to be qualified for the intended use with well characterized in vivo data, and (ii) the demonstration of predictive performance of PBPK models [81]. Furthermore, it is emphasized that simulations should encompass a large number of subjects to better predict population variability of the outcomes. These recommendations are equally pertinent in the development of a PBPK platform for predicting drug exposure in human neonates undergoing TH. Notably, this guideline underscores that PBPK models tailored for pediatric dosing are deemed high-impact applications, particularly in regulatory contexts [11].

Commercially available PBPK platforms such as Simcyp®, PK-Sim®, and Gastroplus® currently include animal models (e.g., mouse, rat, dog, NHPs, minipigs) to aid in selecting the most suitable species for nonclinical studies. A particular challenge associated with this is the much more limited physiological database for animal models compared to humans [82]. Furthermore, although neonatal and juvenile (mini)pigs are gaining interest in pediatric programs due to their similarities to humans [28,83], they are not yet included in these platforms due to a lack of historical data.

When performing the pilot (neonatal/juvenile) Göttingen Minipig PBPK modelling (Chapter 6), using the PK-Sim® software, we uncovered various gaps and potential challenges. Firstly, the current PK-Sim® software only represents a 40-kg minipig and applies linear scaling for organ volume. This approach may not accurately reflect neonatal organ maturation and development, whereas allometric scaling would be more appropriate. Secondly, a critical gap lies in the available data on DMEs, including ADME and gene expression databases, particularly regarding ontogeny- and covariate- related differences. Further characterization of ADME properties is necessary to provide sufficient input data for developing Göttingen Minipig PBPK models for adults, juveniles, and neonates. As a possible future direction in order to make our pilot PBPK more bottom-up, given the available data on MDZ metabolism kinetics and CYP3A abundance in conventional pigs, one approach could be to indirectly derive the CYP activity ontogeny profiles in (mini)pigs and use this information for simulations. On the

other hand, a previous study showed that mild hypothermia decreases FNT and MDZ CL in a rat model of cardiac arrest, highlighting that metabolic capacity, rather than enzyme affinity, significantly influence the systemic CL of these drugs [72]. This finding suggests a possible strategy to focus on evaluating temperature-dependent changes in Vmax (while keeping Km constant) when simulating MDZ levels. Regarding proteomics ontogeny data for Göttingen Minipigs, data at various developmental stages (i.e., gestational day (GD) 84–86, GD 108, PND 1, PND 3, PND 7, PND 28 and adult) [53], along with gene and protein expression data under TH and hypoxia conditions, as part of the I-PREDICT project, are currently available. Future steps will involve integrating these datasets into a workflow to generate comprehensive whole-body expression databases for developing Göttingen Minipig PBPK models.

Parameters such as flow rates, glomerular filtration rate (GFR), and organ composition can be considered for modification when building a PBPK model for the neonatal PA/TH population. For instance, acquiring organ blood flow data in neonatal Göttingen Minipigs at this juncture was deemed more complex, as it necessitates extensive formal training for surgical techniques, which have already been demonstrated in the conventional piglet model [4,71]. Nonetheless, this presents an opportunity for future investigations.

As already mentioned, the European Medicines Agency guideline also provides a framework for evaluation of the predictive performance of the drug-specific PBPK models [81]. This entails evaluating the model's performance across various scenarios: different populations, single versus multiple dosing, dose-dependency, various dosage forms and routes of administration, and supportive evidence from corresponding nonclinical PBPK models. Notably, for pediatric applications an overview of available PK information in other age groups, such as older children and adults, should be presented. Additionally, it is essential to examine the impact of ontogeny, including potential quantitative shifts in the contributions of various elimination pathways across pediatric age subgroups [81]. This form of extrapolation from adult to pediatric PBPK models has been demonstrated previously for FNT and lorazepam [84,85]. Although, preliminary adult Göttingen Minipig PBPK models had already been made and data on physiology regarding organ volumes and/or blood flow, as well as cardiac output (CO) are available for this population [86,87], limited and fragmented data on observed plasma concentrations from adult Göttingen Minipigs of our study drugs are currently available in the public domain. Consequently, the development of MDZ or TPM neonatal Göttingen Minipig PBPK models starting from adult Göttingen Minipig PBPK models remains challenging due to limited PK data in order to verify the predictions made.

Finally, developed PBPK models should undergo sensitivity analyses to understand the impact of imprecise input variables on predicted drug exposure. Sensitivity analyses may inform prioritization for collecting pathophysiological data currently lacking for PA/TH [82]. An illustrative case is the example using MDZ as model drug provided in the review paper by Smits et al. [11], where several sensitivity analyses were conducted to evaluate the possible impact of TH on the PK. Anticipated temperature-induced alterations were examined for several parameters: (i) intrinsic hepatic CL for 1-hydroxymidazolam (CYP3A4); (ii) a 20% reduction in CO; and (iii) changes in the blood/plasma ratio and/or the unbound fraction in plasma (f_u_plasma). Changes in the Michaelis-Menten constant (Km) and/or maximal velocity of the reaction (Vmax) for 1-hydroxymidazolam formation, as well as in f_u_plasma (rather than the B/P ratio), could have a potentially clinically significant impact on the MDZ in vivo hepatic CL. Conversely, a 20% reduction in CO did not substantially impact the predicted CL. We also conducted a sensitivity analysis in our pilot PBPK model, which revealed that most modeling

parameters had minimal impact on the AUC of MDZ and TPM. However, the lipophilicity of MDZ significantly influenced AUC, indicating that this parameter warrants further analysis. While additional in vitro ADME data and in vivo (patho)physiological data (including the effects of TH/PA) are needed, this pilot neonatal (juvenile) Göttingen Minipig PBPK model demonstrates the usefulness of PBPK modelling for this population. The predictive performance of such models will depend significantly on the scope and quality of the input data. Nevertheless, PBPK M&S can bridge the gap between in vitro observations to real in vivo impact, aiding in decision-making regarding drug dose selection for specific patient populations. The strategy for developing and evaluating a neonatal hypothermia PBPK model, outlined in this thesis, can be applied to personalized drug therapy and drug development.

4. General conclusion

A neonatal Göttingen Minipig model was used to assess the impact of systemic hypoxia and TH separately on drug disposition, which provided insights that are difficult to obtain in a clinical setting. The following results were obtained:

(i) Demonstrated the feasibility of challenging in vivo procedures (i.e., endotracheal intubation, vascular access, anesthesia, and mechanical ventilation), important in nonclinical animal experimentation.

(ii) Established a novel pig asphyxia model using the neonatal Göttingen Minipig.

(iii) Unveiled insights into the effects of systemic hypoxia and TH on drug disposition, notably alterations in PK parameters like plasma levels and $t_{1/2}$ across various drugs:

    a. Notably, a statistically significant decrease in FNT CL by 66% with an approximately 3-fold increase in $t_{1/2}$ was observed in the TH group. The H+TH group exhibited a 17% decrease in FNT CL compared to the controls, however not statistically significant.

    b. Trends toward reduced CL and prolonged $t_{1/2}$ were noticed due to TH for MDZ and PHB, though not statistically significant.

    c. TPM showcased a 28% reduction in CL in the H group compared to controls.

(iv) Revealed the significant impact of systemic hypoxia and TH on PD, particularly the influence of TH on heart rate in neonatal Göttingen Minipigs, aligning with its documented effect in human neonates, notably affecting high ER drugs, like FNT.

(v) Provided insights into the influence of age, TH, systemic hypoxia, and medical interventions on CYP enzymes in Göttingen Minipigs:

    a. In vitro investigations highlighted differences in CYP gene expression and activity between neonatal and adult Göttingen Minipigs, emphasizing the role of maturation in drug metabolism.

    b. CYP activity in adult liver microsomes decreased by 36% following exposure to in vitro hypothermia. While no differences were observed in gene expression in response to in vivo TH, alterations in the expression of CYP3A29, CYP2C33, and CYP2C42 genes occurred due to hypoxia in neonatal Göttingen Minipigs.

    c. Medical treatments and interventions over 24 hours, alongside the covariates (systemic hypoxia/TH), influenced the protein abundance of CYP51A1, CYP2B22, CYP2C34, CYP2C42, CYP2D6, and CYP2E1.

While laying the foundation for a neonatal Göttingen Minipig PBPK model, this PhD thesis also highlights existing knowledge gaps. Continuous efforts to refine and update the model with new data, particularly regarding neonatal metabolism, are imperative for enhancing predictive accuracy and clinical relevance over time. Our study underscores the potential of neonatal Göttingen Minipigs as a promising translational model for evaluating therapy safety for pediatric conditions, marking a significant step toward developing a neonatal Göttingen Minipig PBPK model.

5. References

1. Mallard C, Vexler ZS. Modeling Ischemia in the Immature Brain. Stroke. 2015;46(10):3006-3011.
2. Ayuso M, Buyssens L, Stroe M, et al. The Neonatal and Juvenile Pig in Pediatric Drug Discovery and Development. Pharmaceutics. 2021;13(1):44.
3. van Dijk AJ, van Loon JPAM, Taverne MAM, et al. Umbilical cord clamping in term piglets: A useful model to study perinatal asphyxia? Theriogenology. 2008 2008/09/01/;70(4):662-674.
4. Cheung P-Y, Gill RS, Bigam DL. A swine model of neonatal asphyxia. J Vis Exp. 2011 (56):3166.
5. O'Brien CE, Santos PT, Kulikowicz E, et al. Hypoxia-ischemia and hypothermia independently and interactively affect neuronal pathology in neonatal piglets with short-term recovery. Developmental neuroscience. 2019;41(1-2):17-33.
6. Kyng KJ, Skajaa T, Kerrn-Jespersen S, et al. A Piglet Model of Neonatal Hypoxic-Ischemic Encephalopathy. J Vis Exp. 2015 (99):e52454-e52454.
7. Ezzati M, Broad K, Kawano G, et al. Pharmacokinetics of dexmedetomidine combined with therapeutic hypothermia in a piglet asphyxia model. Acta Anaesthesiol Scand. 2014 Jul;58(6):733-42.
8. Stroe M-S, Van Bockstal L, Valenzuela AP, et al. Development of a neonatal Göttingen Minipig model for dose precision in perinatal asphyxia: technical opportunities, challenges, and potential further steps [Methods]. Front Pediatr. 2023;11:662.
9. Wang B, Armstrong JS, Lee J-H, et al. Rewarming from therapeutic hypothermia induces cortical neuron apoptosis in a swine model of neonatal hypoxic-ischemic encephalopathy. Journal of cerebral blood flow and metabolism : official journal of the International Society of Cerebral Blood Flow and Metabolism. 2015;35(5):781-793.
10. Whitaker EE, Zheng CZ, Bissonnette B, et al. Use of a Piglet Model for the Study of Anesthetic-induced Developmental Neurotoxicity (AIDN): A Translational Neuroscience Approach. J Vis Exp. 2017 Jun 11(124).
11. Smits A, Annaert P, Van Cruchten S, et al. A Physiology-Based Pharmacokinetic Framework to Support Drug Development and Dose Precision During Therapeutic Hypothermia in Neonates. Front Pharmacol. 2020;11:587-587.
12. Brodbelt D. Perioperative mortality in small animal anaesthesia. The Veterinary Journal. 2009;182(2):152-161.
13. Pang R, Avdic-Belltheus A, Meehan C, et al. Melatonin and/or erythropoietin combined with hypothermia in a piglet model of perinatal asphyxia. Brain Commun. 2021;3(1):fcaa211.

14. Faulkner S, Bainbridge A, Kato T, et al. Xenon augmented hypothermia reduces early lactate/N-acetylaspartate and cell death in perinatal asphyxia. Ann Neurol. 2011 Jul;70(1):133-50.

15. Martinello KA, Meehan C, Avdic-Belltheus A, et al. Hypothermia is not therapeutic in a neonatal piglet model of inflammation-sensitized hypoxia–ischemia. Pediatric Research. 2022 2022/05/01;91(6):1416-1427.

16. Thayyil S, Chandrasekaran M, Taylor A, et al. Cerebral magnetic resonance biomarkers in neonatal encephalopathy: a meta-analysis. Pediatrics. 2010 Feb;125(2):e382-95.

17. Iwata S, Iwata O, Thornton JS, et al. Superficial brain is cooler in small piglets: neonatal hypothermia implications. Ann Neurol. 2006 Nov;60(5):578-585.

18. Gluckman PD, Wyatt JS, Azzopardi D, et al. Selective head cooling with mild systemic hypothermia after neonatal encephalopathy: multicentre randomised trial. Lancet. 2005 Feb 19-25;365(9460):663-70.

19. Flournoy WS, Mani S. Percutaneous external jugular vein catheterization in piglets using a triangulation technique. Lab Anim. 2009 Oct;43(4):344-9.

20. Helke KL, Nelson KN, Sargeant AM, et al. Pigs in Toxicology: Breed Differences in Metabolism and Background Findings. Toxicol Pathol. 2016 Jun;44(4):575-90.

21. Skaanild MT. Porcine cytochrome P450 and metabolism. Curr Pharm Des. 2006;12(11):1421-7.

22. Skaanild MT, Friis C. Cytochrome P450 sex differences in minipigs and conventional pigs. Pharmacol Toxicol. 1999 Oct;85(4):174-80.

23. Skaanild MT, Friis C. Characterization of the P450 system in Göttingen minipigs. Pharmacol Toxicol. 1997;80 Suppl 2:28-33.

24. Shimada T, Yamazaki H, Mimura M, et al. Interindividual variations in human liver cytochrome P-450 enzymes involved in the oxidation of drugs, carcinogens and toxic chemicals: studies with liver microsomes of 30 Japanese and 30 Caucasians. J Pharmacol Exp Ther. 1994 Jul;270(1):414-23.

25. Mizukawa H, Nomiyama K, Kunisue T, et al. Organohalogens and their hydroxylated metabolites in the blood of pigs from an open waste dumping site in south India: association with hepatic cytochrome P450. Environ Res. 2015 Apr;138:255-63.

26. Bogaards JJ, Bertrand M, Jackson P, et al. Determining the best animal model for human cytochrome P450 activities: a comparison of mouse, rat, rabbit, dog, micropig, monkey and man. Xenobiotica. 2000 Dec;30(12):1131-52.

27. Shang H, Yang J, Liu Y, et al. Tissue distribution of CYP3A29 mRNA expression in Bama miniature pig by quantitative reverse transcriptase-polymerase chain reaction (RT-PCR). Xenobiotica. 2009 Jun;39(6):423-9.

28. Van Peer E, De Bock L, Boussery K, et al. Age-related Differences in CYP3A Abundance and Activity in the Liver of the Göttingen Minipig. Basic Clin Pharmacol Toxicol. 2015 Nov;117(5):350-7.

29. Van Peer E, Jacobs F, Snoeys J, et al. In vitro Phase I-and Phase II-drug metabolism in the liver of juvenile and adult Göttingen minipigs. Pharmaceutical research. 2017;34(4):750-764.

30. Van Peer E, Verbueken E, Saad M, et al. Ontogeny of CYP3A and P-glycoprotein in the liver and the small intestine of the Göttingen minipig: an immunohistochemical evaluation. Basic Clin Pharmacol Toxicol. 2014 May;114(5):387-94.

31. Skaanild MT, Friis C. Analyses of CYP2C in porcine microsomes. Basic Clin Pharmacol Toxicol. 2008 Nov;103(5):487-92.

32. Anzenbacher P, Soucek P, Anzenbacherová E, et al. Presence and activity of cytochrome P450 isoforms in minipig liver microsomes. Comparison with human liver samples. Drug Metab Dispos. 1998 Jan;26(1):56-9.

33. Mogi M, Toda A, Iwasaki K, et al. Simultaneous pharmacokinetics assessment of caffeine, warfarin, omeprazole, metoprolol, and midazolam intravenously or orally administered to Microminipigs. J Toxicol Sci. 2012;37(6):1157-64.

34. Helke KL, Swindle MM. Animal models of toxicology testing: the role of pigs. Expert Opin Drug Metab Toxicol. 2013 Feb;9(2):127-39.

35. Sakuma T, Shimojima T, Miwa K, et al. CLONING CYP2D21 AND CYP3A22 CDNAS FROM LIVER OF MINIATURE PIGS. Drug Metabolism and Disposition. 2004;32(4):376.

36. Puccinelli E, Gervasi PG, Pelosi G, et al. Modulation of cytochrome P450 enzymes in response to continuous or intermittent high-fat diet in pigs. Xenobiotica. 2013 Aug;43(8):686-98.

37. Ellegaard L, Cunningham A, Edwards S, et al. Welfare of the minipig with special reference to use in regulatory toxicology studies. Journal of Pharmacological and Toxicological Methods. 2010 2010/11/01/;62(3):167-183.

38. Swindle MM, Makin A, Herron AJ, et al. Swine as models in biomedical research and toxicology testing. Vet Pathol. 2012 Mar;49(2):344-56.

39. Bollen P, Skydsgaard M. Restricted feeding may induce serous fat atrophy in male Göttingen minipigs. Exp Toxicol Pathol. 2006 Jul;57(5-6):347-9.

40. Cordes H, Rapp H. Gene expression databases for physiologically based pharmacokinetic modeling of humans and animal species. CPT Pharmacometrics Syst Pharmacol. 2023 Mar;12(3):311-319.

41. Van Ginneken C, Ayuso M, Van Bockstal L, et al. Preweaning performance in intrauterine growth-restricted piglets: Characteristics and interventions. Mol Reprod Dev. 2023 Jul;90(7):697-707.

42. Vanden Hole C, Ayuso M, Aerts P, et al. Preterm Birth Affects Early Motor Development in Pigs. Front Pediatr. 2021;9:731877.

43. Pearson N, Boiczyk GM, Kote VB, et al. A Strain Rate-Dependent Constitutive Model for Göttingen Minipig Cerebral Arteries. J Biomech Eng. 2022 Aug 1;144(8).

44. Musskopf ML, Finger Stadler A, Wikesjö UME, et al. The minipig intraoral dental implant model: A systematic review and meta-analysis. PLOS ONE. 2022;17(2):e0264475.

45. Larsen MO, Rolin B. Use of the Göttingen minipig as a model of diabetes, with special focus on type 1 diabetes research. Ilar j. 2004;45(3):303-13.

46. Roh J, Hill JA, Singh A, et al. Heart Failure With Preserved Ejection Fraction: Heterogeneous Syndrome, Diverse Preclinical Models. Circulation Research. 2022;130(12):1906-1925.

47. Eirefelt S, Stahlhut M, Svitacheva N, et al. Characterization of a novel non-steroidal glucocorticoid receptor agonist optimized for topical treatment. Scientific Reports. 2022 2022/01/27;12(1):1501.

48. Eisler W, Baur J-O, Held M, et al. Assessment of Two Commonly used Dermal Regeneration Templates in a Swine Model without Skin Grafting. Applied Sciences. 2022;12(6):3205.

49. Singh VK, Thrall KD, Hauer-Jensen M. Minipigs as models in drug discovery. Expert Opinion on Drug Discovery. 2016 2016/12/01;11(12):1131-1134.

50. Stricker-Krongrad A, Shoemake CR, Pereira ME, et al. Miniature Swine Breeds in Toxicology and Drug Safety Assessments: What to Expect during Clinical and Pathology Evaluations. Toxicologic Pathology. 2015 2016/04/01;44(3):421-427.

51. Bode G, Clausing P, Gervais F, et al. The utility of the minipig as an animal model in regulatory toxicology. J Pharmacol Toxicol Methods. 2010 Nov-Dec;62(3):196-220.

52. Valenzuela A, Tardiveau C, Ayuso M, et al. Safety Testing of an Antisense Oligonucleotide Intended for Pediatric Indications in the Juvenile Göttingen Minipig, including an Evaluation of the Ontogeny of Key Nucleases. Pharmaceutics. 2021;13(9):1442.

53. Buyssens L, De Clerck L, Schelstraete W, et al. Hepatic Cytochrome P450 Abundance and Activity in the Developing and Adult Göttingen Minipig: Pivotal Data for PBPK Modeling. Front Pharmacol. 2021;12:665644.

54. Lutz IC, Allegaert K, de Hoon JN, et al. Pharmacokinetics during therapeutic hypothermia for neonatal hypoxic ischaemic encephalopathy: a literature review. BMJ Paediatr Open. 2020;4(1):e000685.

55. Deferm N, Annink KV, Faelens R, et al. Glomerular Filtration Rate in Asphyxiated Neonates Under Therapeutic Whole-Body Hypothermia, Quantified by Mannitol Clearance. Clin Pharmacokinet. 2021 Jul;60(7):897-906.

56. Cristea S, Smits A, Kulo A, et al. Amikacin Pharmacokinetics To Optimize Dosing in Neonates with Perinatal Asphyxia Treated with Hypothermia. Antimicrob Agents Chemother. 2017 Dec;61(12).

57. Bijleveld YA, de Haan TR, van der Lee HJ, et al. Altered gentamicin pharmacokinetics in term neonates undergoing controlled hypothermia. Br J Clin Pharmacol. 2016 Jun;81(6):1067-77.

58. Frymoyer A, Lee S, Bonifacio SL, et al. Every 36-h gentamicin dosing in neonates with hypoxic-ischemic encephalopathy receiving hypothermia. J Perinatol. 2013 Oct;33(10):778-82.

59. **Smits A, Annaert P, Van Cruchten S, et al. A Physiology-Based Pharmacokinetic Framework to Support Drug Development and Dose Precision During Therapeutic Hypothermia in Neonates [Review]. Front Pharmacol. 2020 2020-May-13;11.

60. Weerink MAS, Struys M, Hannivoort LN, et al. Clinical Pharmacokinetics and Pharmacodynamics of Dexmedetomidine. Clin Pharmacokinet. 2017 Aug;56(8):893-913.

61. O'Mara K, Weiss MD. Dexmedetomidine for Sedation of Neonates with HIE Undergoing Therapeutic Hypothermia: A Single-Center Experience. AJP Rep. 2018 Jul;8(3):e168-e173.

62. Elliott M, Burnsed J, Heinan K, et al. Effect of dexmedetomidine on heart rate in neonates with hypoxic ischemic encephalopathy undergoing therapeutic hypothermia. J Neonatal Perinatal Med. 2022;15(1):47-54.

63. McAdams RM, Pak D, Lalovic B, et al. Dexmedetomidine pharmacokinetics in neonates with hypoxic-ischemic encephalopathy receiving hypothermia. Anesthesiology Research and Practice. 2020;2020.

64. Naveed M, Bondi DS, Shah PA. Dexmedetomidine Versus Fentanyl for Neonates With Hypoxic Ischemic Encephalopathy Undergoing Therapeutic Hypothermia. J Pediatr Pharmacol Ther. 2022;27(4):352-357.

65. Bäcke P, Bruschettini M, Sibrecht G, et al. Pharmacological interventions for pain and sedation management in newborn infants undergoing therapeutic hypothermia. Cochrane Database Syst Rev. 2022 Nov 10;11(11):Cd015023.

66. Baserga M, DuPont TL, Ostrander B, et al. Dexmedetomidine Use in Infants Undergoing Cooling Due to Neonatal Encephalopathy (DICE Trial): A Randomized Controlled Trial: Background, Aims and Study Protocol. Front Pain Res (Lausanne). 2021;2:770511.

67. Hines RN. Ontogeny of human hepatic cytochromes P450. J Biochem Mol Toxicol. 2007;21(4):169-75.

68. Gow PJ, Ghabrial H, Smallwood RA, et al. Neonatal hepatic drug elimination. Pharmacol Toxicol. 2001 Jan;88(1):3-15.

69. Koren G, Barker C, Goresky G, et al. The influence of hypothermia on the disposition of fentanyl--human and animal studies. Eur J Clin Pharmacol. 1987;32(4):373-6.

70. van den Broek MP, Groenendaal F, Egberts AC, et al. Effects of hypothermia on pharmacokinetics and pharmacodynamics: a systematic review of preclinical and clinical studies. Clin Pharmacokinet. 2010 May;49(5):277-94.

71. Fritz HG, Holzmayr M, Walter B, et al. The effect of mild hypothermia on plasma fentanyl concentration and biotransformation in juvenile pigs. Anesth Analg. 2005 Apr;100(4):996-1002.

72. Empey PE, Miller TM, Philbrick AH, et al. Mild hypothermia decreases fentanyl and midazolam steady-state clearance in a rat model of cardiac arrest. Critical care medicine. 2012;40(4):1221.

73. Favié LMA, Groenendaal F, van den Broek MPH, et al. Phenobarbital, Midazolam Pharmacokinetics, Effectiveness, and Drug-Drug Interaction in Asphyxiated Neonates Undergoing Therapeutic Hypothermia. Neonatology. 2019;116(2):154-162.

74. Pokorná P, Posch L, Šíma M, et al. Severity of asphyxia is a covariate of phenobarbital clearance in newborns undergoing hypothermia. The Journal of Maternal-Fetal & Neonatal Medicine. 2019 2019/07/18;32(14):2302-2309.

75. Ikonomidou C, Wang SH, Fuhler NA, et al. Mild hypothermia fails to protect infant macaques from brain injury caused by prolonged exposure to Antiseizure drugs. Neurobiol Dis. 2022 Sep;171:105814.

76. Björkman S, Redke F. Clearance of fentanyl, alfentanil, methohexitone, thiopentone and ketamine in relation to estimated hepatic blood flow in several animal species: application to prediction of clearance in man. Journal of pharmacy and pharmacology. 2000;52(9):1065-1074.

77. Galinkin JL, Kurth CD, Shi H, et al. The plasma pharmacokinetics and cerebral spinal fluid penetration of intravenous topiramate in newborn pigs. Biopharmaceutics & drug disposition. 2004;25(6):265-271.

78. Angehagen M, Ben-Menachem E, Rönnbäck L, et al. Topiramate protects against glutamate- and kainate-induced neurotoxicity in primary neuronal-astroglial cultures. Epilepsy Res. 2003 Apr;54(1):63-71.

79. Vuu I, Coles LD, Maglalang P, et al. Intravenous Topiramate: Pharmacokinetics in Dogs with Naturally Occurring Epilepsy [Original Research]. Frontiers in Veterinary Science. 2016 2016-December-05;3(107).

80. Glauser TA, Miles MV, Tang P, et al. Topiramate Pharmacokinetics in Infants. Epilepsia. 1999;40(6):788-791.

81. Agency EM. Guideline on the reporting of physiologically based pharmacokinetic (PBPK) modelling and simulation. 2018.

82. [#a]Leys K, and[#b]Stroe M-S, Annaert P, et al. Pharmacokinetics during therapeutic hypothermia in neonates: from pathophysiology to translational knowledge and physiologically-based pharmacokinetic (PBPK) modeling. Expert Opinion on Drug Metabolism & Toxicology. 2023:1-17.

83. Van Peer E, Downes N, Casteleyn C, et al. Organ data from the developing Göttingen minipig: first steps towards a juvenile PBPK model. Journal of pharmacokinetics and pharmacodynamics. 2016;43:179-190.

84. Kovar L, Weber A, Zemlin M, et al. Physiologically-Based Pharmacokinetic (PBPK) Modeling Providing Insights into Fentanyl Pharmacokinetics in Adults and Pediatric Patients. Pharmaceutics. 2020 Sep 23;12(10).

85. Maharaj AR, Barrett JS, Edginton AN. A Workflow Example of PBPK Modeling to Support Pediatric Research and Development: Case Study with Lorazepam. The AAPS Journal. 2013 2013/04/01;15(2):455-464.

86. Suenderhauf C, Parrott N. A physiologically based pharmacokinetic model of the minipig: data compilation and model implementation. Pharmaceutical research. 2013;30(1):1-15.

87. Suenderhauf C, Tuffin G, Lorentsen H, et al. Pharmacokinetics of paracetamol in Göttingen minipigs: in vivo studies and modeling to elucidate physiological determinants of absorption. Pharmaceutical research. 2014;31:2696-2707.

CHAPTER 8:
Challenges, limitations, and future perspectives

Challenges, limitations, and future perspectives

The final chapter of this thesis revisits the challenges and limitations encountered during our study while offering insights into future perspectives. The content of **Section 1** was modified from the methods article "Development of a neonatal Göttingen Minipig asphyxia model for dose precision in perinatal asphyxia: technical opportunities, challenges, and potential further steps" to provide a more comprehensive understanding within the framework of this thesis. Additionally, this chapter integrates the content from a report detailing the outcomes of a Short-Term Scientific Mission (STSM) titled "An Interdisciplinary Approach to Electroencephalography in Perinatal Asphyxia: Capacity Building for Future Human-Piglet Translational Work" (**Section 2**). The STSM was conducted from July 16, 2023, to July 28, 2023, at the University College London, UK, as part of the European Cooperation in Science & Technology (COST) action "Maximizing Impact of Multidisciplinary Research in Early Diagnosis of Neonatal Brain Injury (AI-4-NICU)" (action number CA20124). Stroe M-S contributed to funding acquisition and the development of the work during this period.

1. Challenges, limitations, and future perspectives

The aim of this experimental study was to develop a neonatal in vivo model to assess the impact of systemic hypoxia and therapeutic hypothermia (TH) on drug disposition, to support improved drug dosing and drug development in asphyxiated neonates. As the potential role of hypoxia and TH cannot be explored separately in the clinical situation, this model is of utmost importance since it allows this distinction. The I-PREDICT project mainly focuses on drug metabolism and elimination, targeting the liver and the kidneys. However, regarding investigations, the limitation referring to the examination of other organs (i.e., brain) and systems that were not performed in this study needs to be emphasized. We developed a novel animal model for drug disposition and not an animal model for hypoxic-ischemic encephalopathy (HIE), and thus not to assess brain damage. The construct validity of this model was based on blood lactate and pH, biomarkers in the determination of systemic hypoxia and not necessary on neuropathological assessment, since HIE was out of our scope. Therefore, when considering our model for HIE research, additional diagnostic tools are needed to assess its validity. Some of them are discussed below.

1.1. Additional diagnostic modalities for perinatal asphyxia and hypoxic-ischemic encephalopathy

In the neonatal intensive care unit (NICU), the diagnosis of perinatal asphyxia (PA) is based on clinical endpoints (e.g., Apgar score ≤5 at 10 minutes after birth [1,2]), failure to initiate or sustain spontaneous breathing at birth [3] leading to impaired gas exchange [4], clinical chemistry results, such as metabolic acidosis identified via the blood sampling obtained within the first hour after birth [5]. For diagnosing HIE, clinical scoring or more sophisticated tools

like electroencephalography (EEG) are used. In addition, neuroimaging is used to evaluate the impact of asphyxia on brain structures [3,6]. Also, the pathological diagnosis of PA is important, which is based on histological markers of tissue hypoxia, with a relevant role in vascular changes [7]. All these diagnostic parameters could prove useful as well when performing a research study. These will provide important evidence for better understanding the mechanisms of PA and confirming the degree of hypoxia. However, the selection of the parameters and the interpretation of the results should be carefully carried out. Therefore, when designing a PA/HIE animal study several considerations need to be taken into account: species-tailored clinical diagnostic, the maturational stage of the brain at the time of injury which differs from species to species [8], the use of anesthesia (which may alter the neurological examination [3]), but also the neuroprotection protocols (TH, medication), the special training for more sophisticated techniques, the presence of a multi-disciplinary team to perform full monitoring and critical care, and the costs and logistics for making all these techniques available in the research setup. These diagnostic modalities have already been used in PA/HIE translational research, using the conventional pig model [9-11]. While it should be technically feasible to extrapolate these modalities to the minipig, this necessitates further studies.

1.2. Neurological assessment

Amplitude-integrated electroencephalography (aEEG) is a technique for simplified EEG, which is applied in the NICU. Its main value lies in allowing to monitor baseline brain activity, and real-time detection of electrographic seizures, providing the opportunity for treatment at the time they occur, without requiring extensive formal training for their interpretation [12]. To avoid artefacts misdiagnosed as seizures, the aEEG trace preferably must be reviewed by conventional, full, EEG. However, the interpretation of conventional EEG requires more specific expertise [12]. Overall, neurological assessment (clinical as well as by EEG) to diagnose HIE, is ideally performed before the administration of sedatives that may alter the neurological examination. The final (a)EEG pattern is indeed a combined reflection of the disease state, medication administered and the impact of TH (potential accumulation of sedatives, affecting the (a)EEG [13]). Previous preclinical studies with the pig model have shown that a more consistent brain injury can be achieved, with an enhanced survival rate, by individualizing the hypoxic insult according to each subject's cerebral response evaluated by aEEG. Models of global hypoxia-ischemia titrated by aEEG suppression (aEEG flat trace, upper margin <7 µV), have demonstrated encephalopathy that is clinically, and neuropathologically comparable to the condition found in asphyxiated term human neonates [9,11].

Doppler sonography and cranial ultrasound proved useful adjuncts in early diagnostic imaging. Magnetic Resonance Imaging (MRI) has been demonstrated to have good diagnostic ability to detect brain injury in cases with HIE, when performed at the end of the first post-natal week of life, and it can support prognosis [3]. Magnetic Resonance Imaging has also shown value in the animal setting, e.g. due to the correlation of MRI findings with the degree of brain injury in a PA piglet model [10]; MRI at 72 hours also revealed lesions corresponding to diffuse ischemic infarction in another global hypoxia-ischemia pig model [9].

1.3. Histopathological examination

In human neonates, PA can cause pathological changes in multiple organs, with HIE representing one of the most severe consequences, and occasionally leading to a multi-organ dysfunction syndrome. The pathological diagnosis of PA is complex, histological markers of tissue hypoxia often overlap with pathological changes due to other causes. The endothelial lesions, represented by swelling, apoptosis, detachment, and loss of the endothelial barrier, are the most relevant pathological changes induced by hypoxia in all organs [7]. In the pig model, brain injury after PA is hypoxic-ischemic in nature, and the injury pattern includes selective neuronal ischemic necrosis [9,14]. Additionally, the lungs are commonly affected by PA. Pulmonary hypertension, hemorrhage, and significant coagulopathy are frequent complications [15]. The finding of increased hepatic hematopoiesis represents one of the most important markers of chronic tissue hypoxia. Neonates with PA are known to have an increased risk of ischemic heart injury due to decreased cardiac output and decreased coronary perfusion [16]. The cardiac injury diagnostic is determined by the presence of high levels of cardiac enzymes; however, the immediate and long-term structural consequences are not well known, since reported histological findings are minimal [17,18]. Therefore, for future PA animal model development, we recommend the analysis of the brain through electrophysiology and neuroimaging, together with the histopathological examination of the brain and other organs such as lungs, heart, liver, and kidneys. With the current survival rate (i.e., 24 hours), the sampling time, or strategies to improve postnatal survival should be further considered.

2. Maximizing the impact of multidisciplinary research in early diagnosis of neonatal brain injury (AI-4-NICU)

Electroencephalography, a technology applied in the NICU, allows continuous monitoring of the brain activity and real-time detection of seizures, providing the opportunity to treat seizures at the time they occur [12]. Electroencephalography is useful in the understanding of PA, as well as the impact of treatment modalities such as TH [19] and add-on medication on (neuro)physiology. In view of translational research, EEG has also been used in the PA piglet model [9-11], which is a relevant model to study cerebral blood flow and cerebral metabolism [8,20]. The aim of this STSM consisted of studying EEG data collected from neonates in the NICU, as part of a collaboration between Dr Kimberley Whitehead - with expertise in clinical neurophysiology [21-23] and Stroe M-S. This collaboration offered the opportunity to combine the academic strengths and allowed Stroe M-S to improve as a scientist, for potentially advancing the translatability of this technology into animal model-based research. This potentially could pave the way to develop future human-piglet translational work by bringing together two research groups, Dr Whitehead's Lab, at the University College London, UK, and Comparative Perinatal Development, at the University of Antwerp, Belgium.

In this mission, Stroe M-S spent two weeks at Dr. Whitehead's Lab, to conduct a pilot quantitative analysis on neonatal EEG data. The data had already been collected by Dr. Whitehead in a NICU in London, comprising a cohort of 37 neonates, 8 controls, 14 with mild HIE (non-TH), and 15 with moderate HIE, undergoing TH (Table 1). For these patients, EEG, electrocardiogram (ECG), and a respiratory movement trace, annotated with individual drug exposure and whether they were receiving TH, as well as outcome data, were available.

Table 1. Demographic data collected in NICU, University College Hospital, London for a cohort of 37 neonates in view of a pilot quantitative analysis of neonatal EEG data.
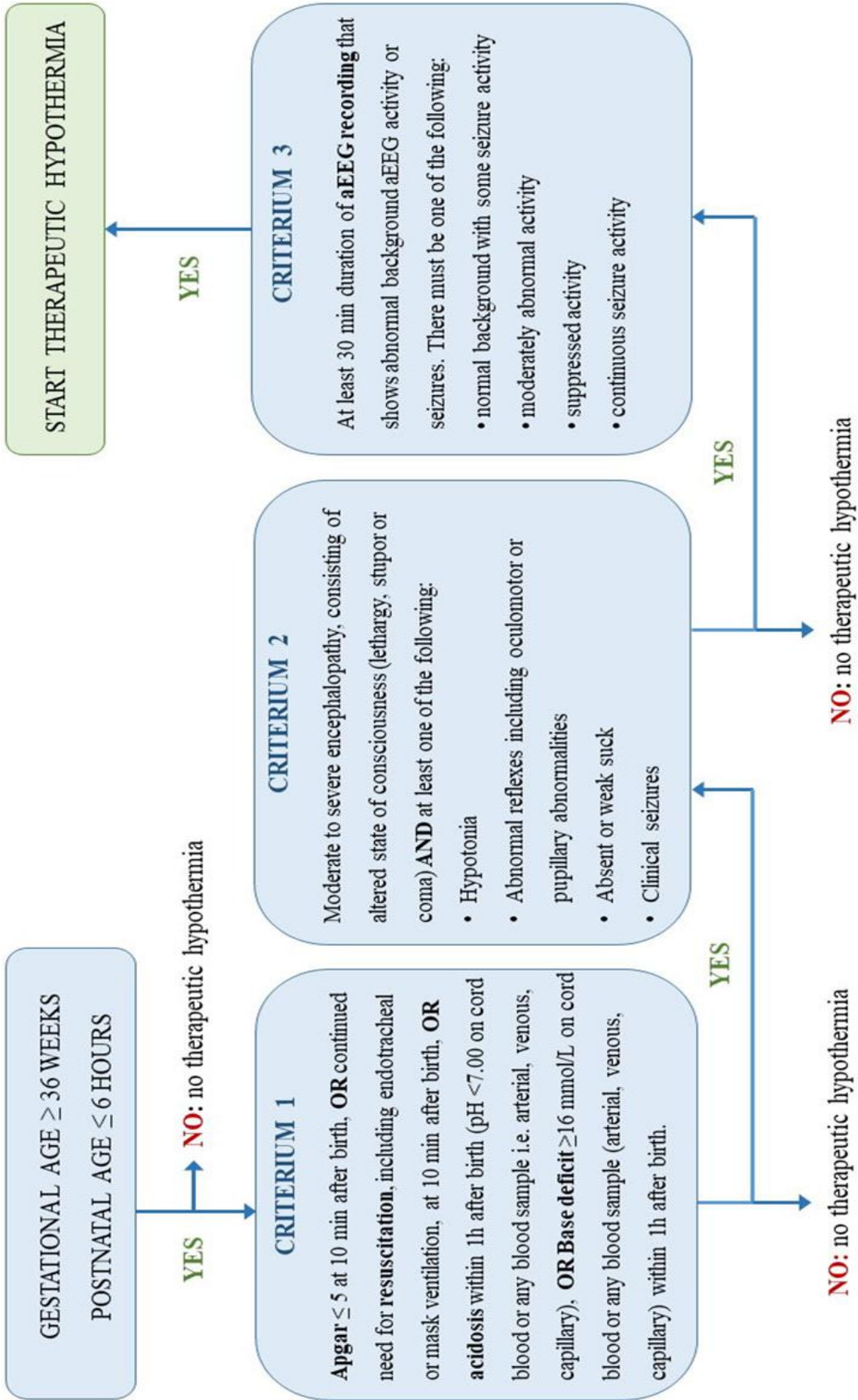
Parameter / Group		Control	Mild HIE	HIE
Number of neonates		8	14	15
Number of females (%)		0	8 (57.14%)	8 (53.33%)
GA at birth (weeks)		39.91 (±1.3)	39.14 (±2.04)	39.49 (±1.79)
Birth weight (g)		3462.12 (±471.25)	2983.5 (±579.13)	3276.2 (±750.97)
Apgar 1 minute		7.62 (±2.19)	3.28 (±2.05)	2.46 (±2.26)
Apgar 5 minutes		9.25 (±1.16)	5.57 (±1.78)	4.86 (±2.41)
First pH		7.28 (±0.1)	6.93 (±0.13)	6.91 (±0.11)
First BE		-5.4 (±4.70)	-15.53 (±5.23)	-18.54 (±3.91)
First Lactate		5.1 (±3.11)	10.86 (±3.57)	14.17 (±2.24)
Hours old EEG start		19.87 (±14.16)	4.89 (±4.39)	7.67 (±3.59)
Cooling / Rewarming	Passively cooling	0	5 (35.71%)	0
	Actively cooling		3 (20%)	15 (100%)
	No cooling	8	6 (42.85%)	0

The objective was to assess how cortical activity is acutely affected by the hypoxic insult and whether a severity-dependent pattern could be observed in the two hypoxic groups (i.e., comparison between mild HIE, non-TH (A) and moderate (B) to severe HIE (C), subjected to TH treatment). For a better understanding, the most important criteria for defining mild, moderate, and severe HIE are presented in Table 2 [24,25]. Moreover, as the distinction between mild (A), moderate (B), and severe (C) HIE is pertinent to the application of TH, assessing the criteria for initiating TH in neonates becomes crucial. These criteria may vary between studies. Figure 1 visually outlines the criteria used in the TOBY trial [1,2].

Table 2. Criteria for defining mild **(A)**, moderate **(B)** and severe **(C)** encephalopathy. Adapted from Shankaran et al. [24] and Sarnat, H. B., & Sarnat, M. S. [25].

	Mild HIE **(A)**	Moderate HIE **(B)**	Severe HIE **(C)**
Level of consciousness	Hyperalert	Lethargic	Stuporous/Coma
Neuromuscular control			
Muscle tone	Normal	Mild hypotonia	Flaccid
Posture	Mild distal flexion	Strong distal flexion	Intermittent decerebration
Complex reflexes			
Suck	Normal/Weak	Weak/Absent	Absent
Moro	Strong	Weak	Absent
Oculovestibular	Normal	Overactive	Weak/Absent
Tonic neck	Slight	Strong	Absent
Autonomic function			
Autonomic function	Generalized sympathetic	Generalized parasympathetic	Both systems depressed
Pupils	Mydriasis	Miosis	Variable; often unequal; poor light reflex
Heart rate	Tachycardia	Bradycardia	Variable
Seizures	Absent	Common	Frequent/ Difficult to control
Treatment	non-TH	TH	

Figure 1. A graphical representation illustrating the step-by-step assessment of the criteria employed in the TOBY trial to decide whether therapeutic hypothermia should be initiated in neonates [1]. Reproduced from Smits et al. [2].

START THERAPEUTIC HYPOTHERMIA

GESTATIONAL AGE ≥ 36 WEEKS

POSTNATAL AGE ≤ 6 HOURS

YES → **NO:** no therapeutic hypothermia

YES

CRITERIUM 1

Apgar ≤ 5 at 10 min after birth, **OR** continued need for **resuscitation**, including endotracheal or mask ventilation, at 10 min after birth, **OR** **acidosis** within 1h after birth (pH <7.00 on cord blood or any blood sample i.e. arterial, venous, capillary), **OR Base deficit** ≥16 mmol/L on cord blood or any blood sample (arterial, venous, capillary) within 1h after birth.

YES

NO: no therapeutic hypothermia

CRITERIUM 2

Moderate to severe encephalopathy, consisting of altered state of consciousness (lethargy, stupor or coma) **AND** at least one of the following:

- Hypotonia
- Abnormal reflexes including oculomotor or pupillary abnormalities
- Absent or weak suck
- Clinical seizures

YES

NO: no therapeutic hypothermia

CRITERIUM 3

At least 30 min duration of **aEEG recording** that shows abnormal background aEEG activity or seizures. There must be one of the following:

- normal background with some seizure activity
- moderately abnormal activity
- suppressed activity
- continuous seizure activity

YES

2.1. Materials and methods

Electroencephalography data was recorded via 9 scalp electrodes (two visual (O1, O2); 2 auditory (T3, T4); 2 for association (F3, F4) and 3 somatosensory (C3, Cz, C4)), and other relevant patient information (ECG, and respiratory movement trace, sex, gestational age, birthweight, first blood gas analysis values, drug exposure and active/passive cooling, outcome data) were available. The first 11 minutes of artefact-free EEG during the 14 hours post birth, excluding segments within 6 hours after anti-epileptic drug administration or during seizures, were compared with the control group matched by age, intensive care nursing, and recording system. Data was manually de-noised for muscle, heart, movement, or equipment artifacts; artefactual independent components were selected manually. Data was not filtered or down-sampled and was analyzed in the frequency domain. Analyzing these preprocessed and denoised data, Stroe M-S conducted a study in EEGLAB, involving the precomputation and plotting of channel measures. 2 analysis techniques, topography (Figure 2), and single channel (Figure 3) were employed on manually de-noised data. Statistical analyses, including One-Way Analysis of variance (ANOVA) with a post hoc Tukey's-Kramer honestly significant difference (HSD), and linear mixed modelling, to detect potential interactions, were conducted to evaluate differences between groups. The assumptions linearity and homoscedasticity testing ensured data met the parametric testing requirements, with a logarithm transformation applied if these assumptions were violated. If data was not normally distributed even after transformation, the Wilcoxon test with Dunn method for Joint Ranking was employed. Raw data was computed in MATLAB (2023a, MathWorks, Inc.) and EEGLAB (version 5.2); graphs were made in GraphPad Prism version 8.0.2 and EEGLAB, statistical analysis in JMP® Pro 16.

2.2. Results

In this pilot analysis were found significant differences in cortical activity between moderate HIE and control, as well as between moderate HIE and mild HIE. Firstly, topography analyses (Figure 2) indicated higher standard deviation and higher coefficient of variation across scalp in the moderate HIE group (mean 5.88%) compared to control (mean 3.98%) and mild HIE (mean 3.87%). Statistical analysis together with the graphical presentation of the topography per group performed in EEGLAB (parametric test, $P < 0.05$), at 2 different frequencies (0.2-2 Hz and 2-8 Hz), revealed statistical significance for all scalp electrodes between groups with a gradual decrease in activity from control to mild HIE to moderate HIE.

Figure 2. The topography plots were derived for each individual, including 8 controls (**A**), 13 mild HIE cases (**B**, non-TH), and 15 moderate HIE cases (**C**, undergoing TH). The amplitude for each scalp electrode (μV^2) was extracted, and the standard deviation across the scalp for each participant was calculated and graphically presented. Statistical analysis, along with graphical representation of the topography for each group, was conducted in EEGLAB, considering two different frequency ranges (0.2-2 Hz and 2-8 Hz), as illustrated in the bottom box.
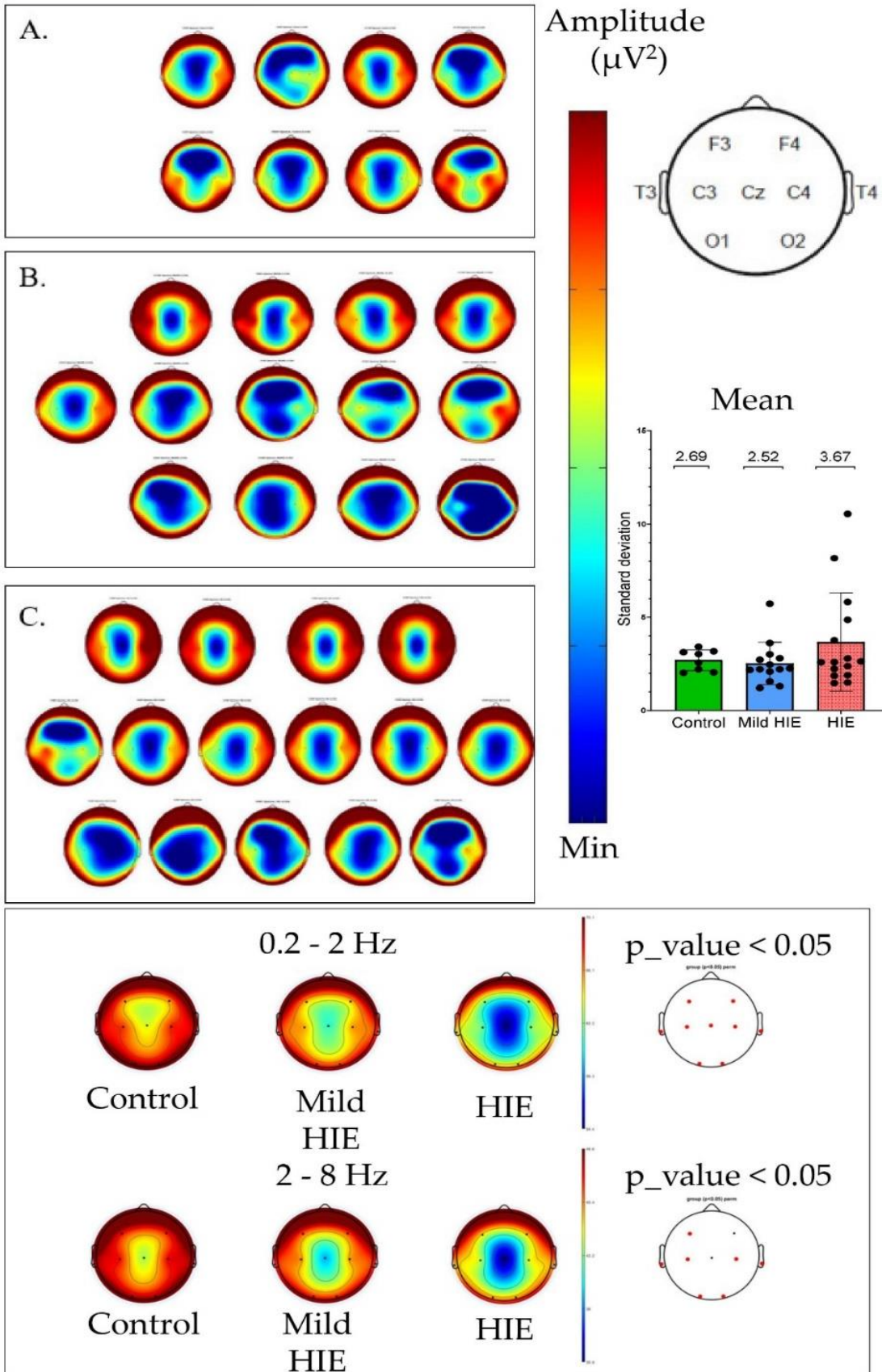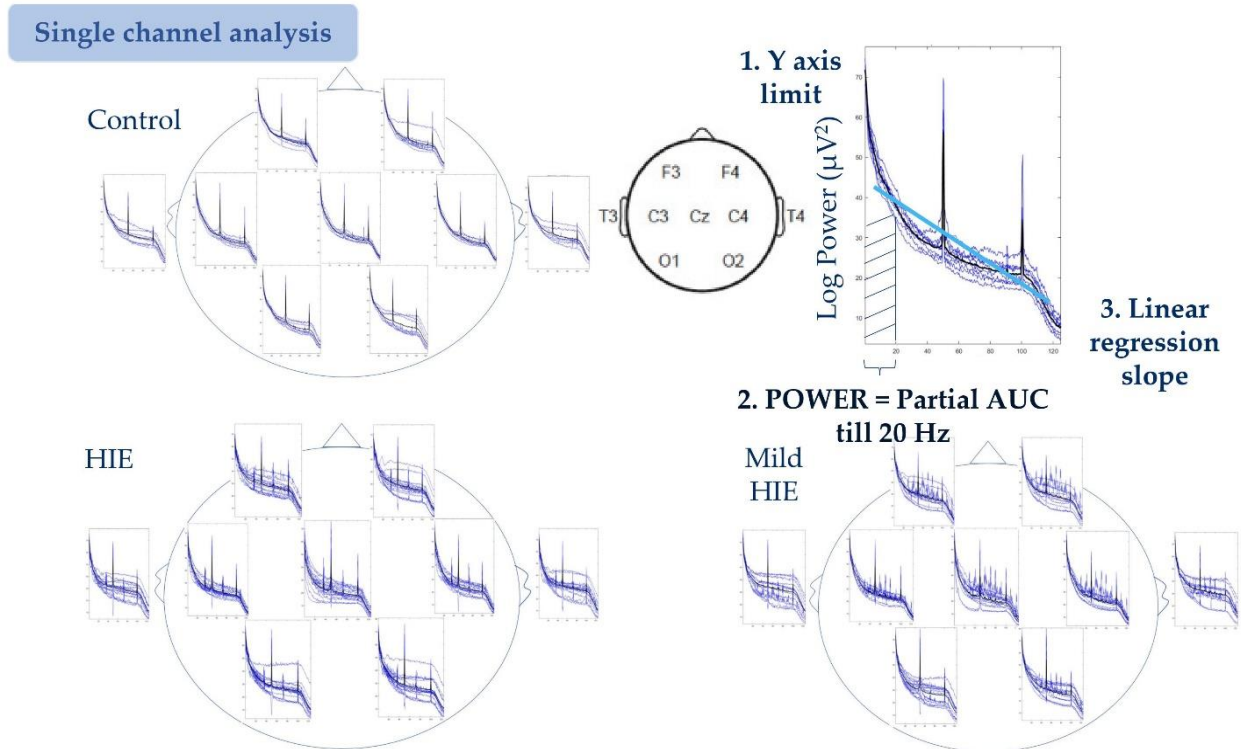
Topography

Figure 3. The single channel analysis was derived for each individual, including 8 controls, 13 mild HIE cases (non-TH), and 15 moderate HIE cases (undergoing TH). This descriptively demonstrated more variability in the mild and moderate HIE compared to controls.


Secondly, single channel analyses (Figure 3) revealed more variability in cortical activity for both hypoxic groups compared to controls. Further, to statistically investigate the cortical activity differences between the groups, Y limit (Figure 4 (A), the maximal amplitude, log power (μV^2)) and the power till 20 Hz (Figure 4 (B), area under the curve) for the O1, C3, F3, Cz, and T3 scalp electrodes were investigated. Statistically significant differences were found between HIE and Control group, as well as between HIE and mild HIE. However, no significant differences were observed between the Control and mild HIE groups.

Figure 4. The statistical analysis was performed on the Y limit (**(A)**, representing the maximal amplitude, log power (μV^2)) and the power till 20 Hz (**(B)**, area under the curve) for the O1, C3, F3, Cz, and T3 scalp electrodes. Significant differences were identified between the HIE and control groups, as well as between the HIE and mild HIE groups. However, no statistically significant differences were observed between the control and mild HIE groups in the measured outcomes. p-value: *, $P<0.05$; **, $P<0.005$; ***, $P<0.0005$; ****, $P<0.0001$.

(A)
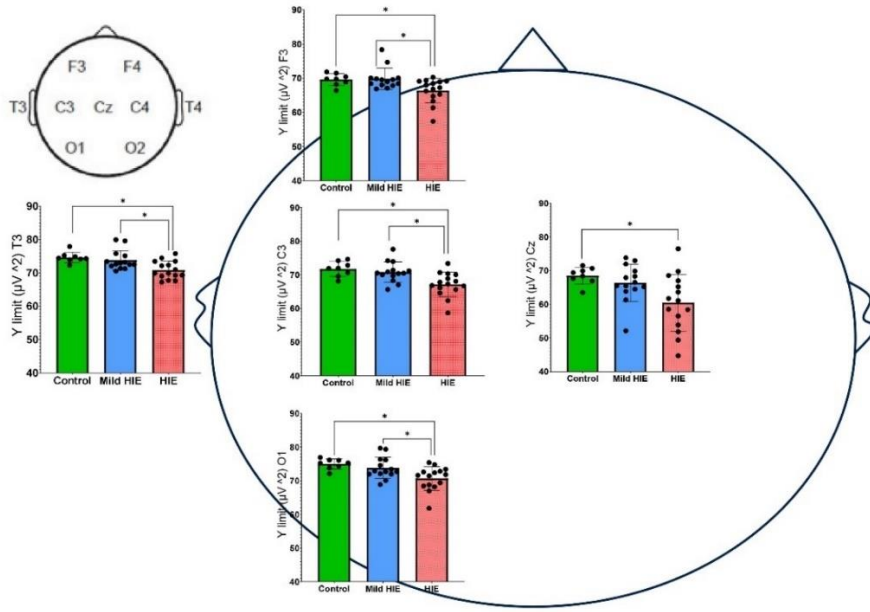
(B)
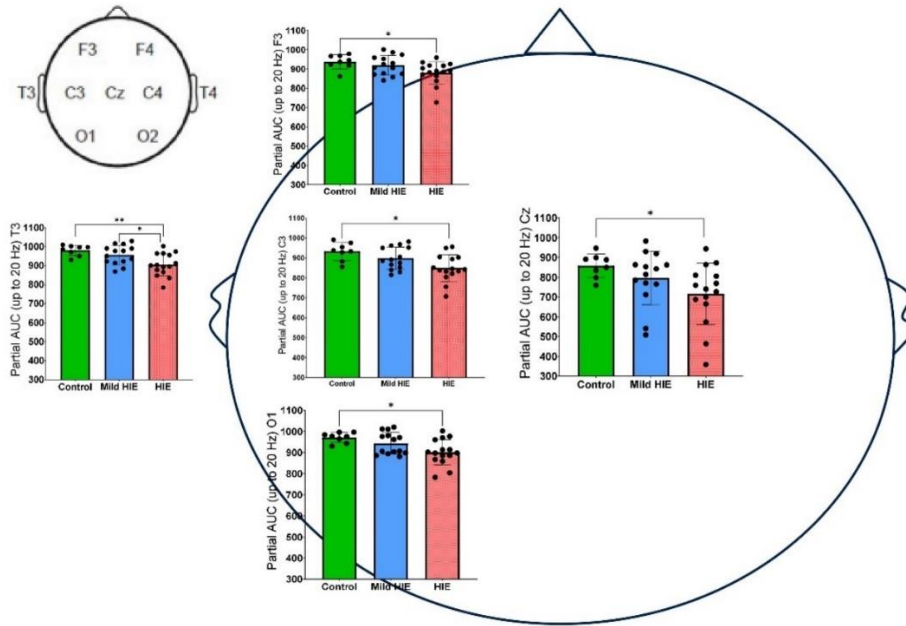
Thirdly, differences between groups on blood gas analysis parameters and Apgar score were also investigated, by plotting the pH, base excess (BE), lactate, Apgar_1 (first Apgar score after birth) and Apgar_5 (Apgar score in 5 minutes after birth) of each individual in function of group (Figure 5).

Figure 5. Blood gas analysis parameters (i.e., pH, base excess (BE), lactate) and Apgar score for each individual, including 8 controls (A), 13 mild HIE cases (B, non-TH), and 15 moderate HIE cases (C, undergoing TH). p-value: *, $P<0.05$; **, $P<0.005$; ***, $P<0.0005$; ****, $P<0.0001$.
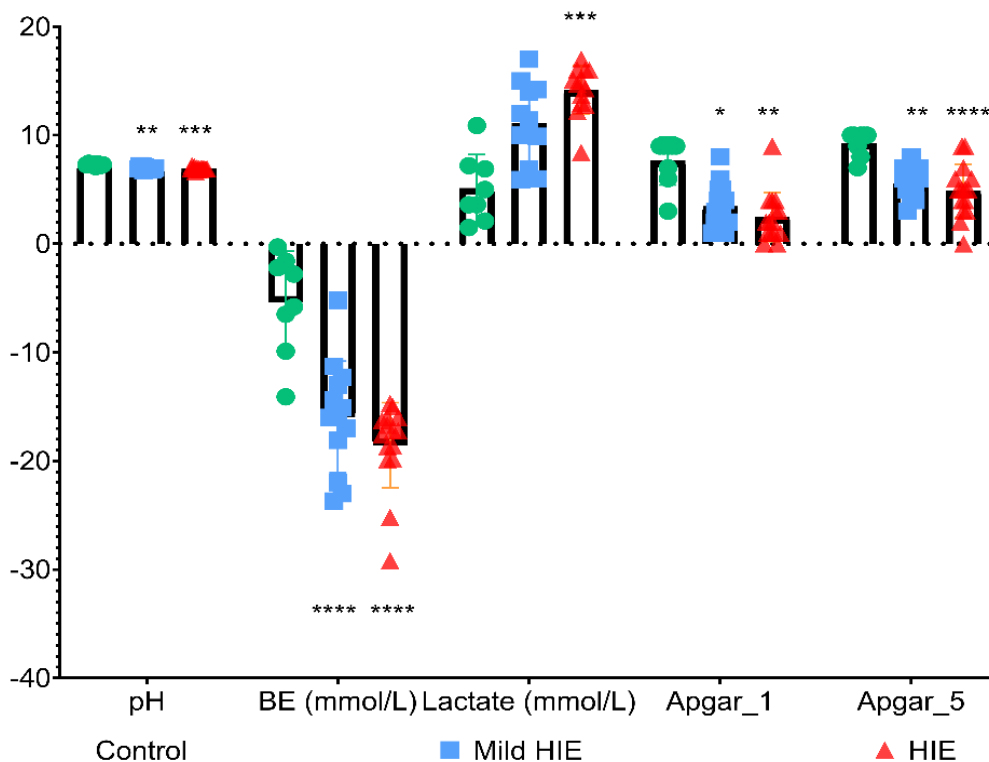

One step further in the data analysis was represented by the investigation of the EEG data in function of the biochemical biomarkers (i.e., pH, BE, lactate; Figure 6 (A)) and Apgar score (Figure 6 (B)). The maximal amplitude (i.e., Y limit) was selected as the most reliable parameter extracted from the EEG. There was a trend driven by the moderate HIE group in having especially a lower pH and a lower lactate in association with lower cortical activity (Figure 6 (A)). This association was less remarkable for the BE and not present when plotting Y limits in function of the Apgar score (Apgar_1 and Apgar_5, Figure 6 (B)). Furthermore, the trend was reproduceable for all the scalp electrodes investigated here, with more variability for the Cz (possible since this is a scalp electrode positioned next to the anterior fontanelle, soft spot of the scalp in neonates, frequently targeted for brain ultrasound in hypoxia cases, this increasing the risks for more artefacts due to movements as well not reliable adherence between the electrode and the scalp since it is soft).

Figure 6. Electroencephalogram (EEG) data plots in function of the biochemical biomarkers (i.e., pH, base excess (BE), lactate; **(A)**) and Apgar score **(B).** The maximal amplitude (i.e., Y

limit) was selected as the most reliable parameter extracted from the EEG. There was a trend lead by the moderate HIE group in having especially a lower pH and a lower lactate in association with lower cortical activity.

(A) BGA vs EEG
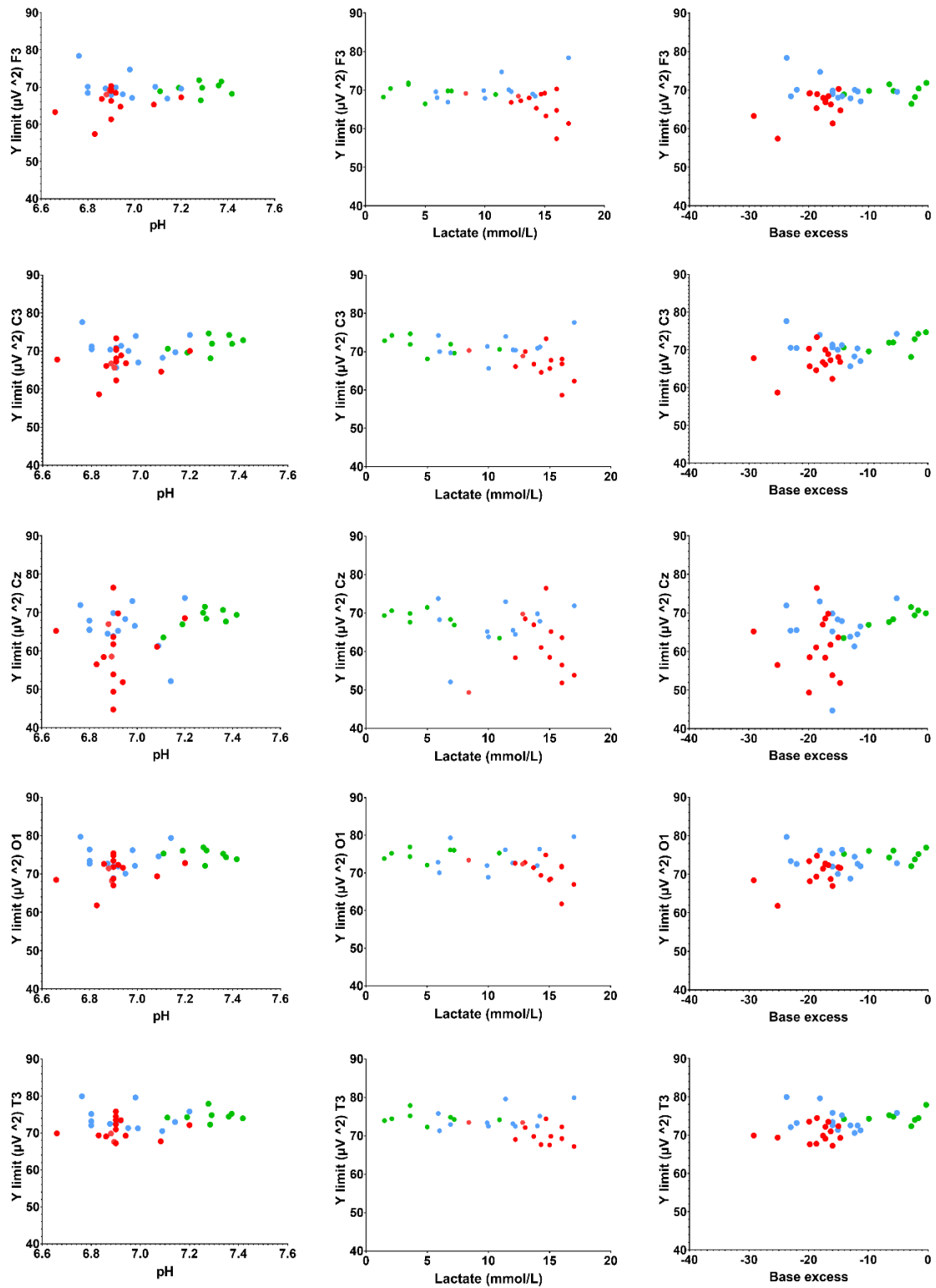
(B) Apgar vs EEG
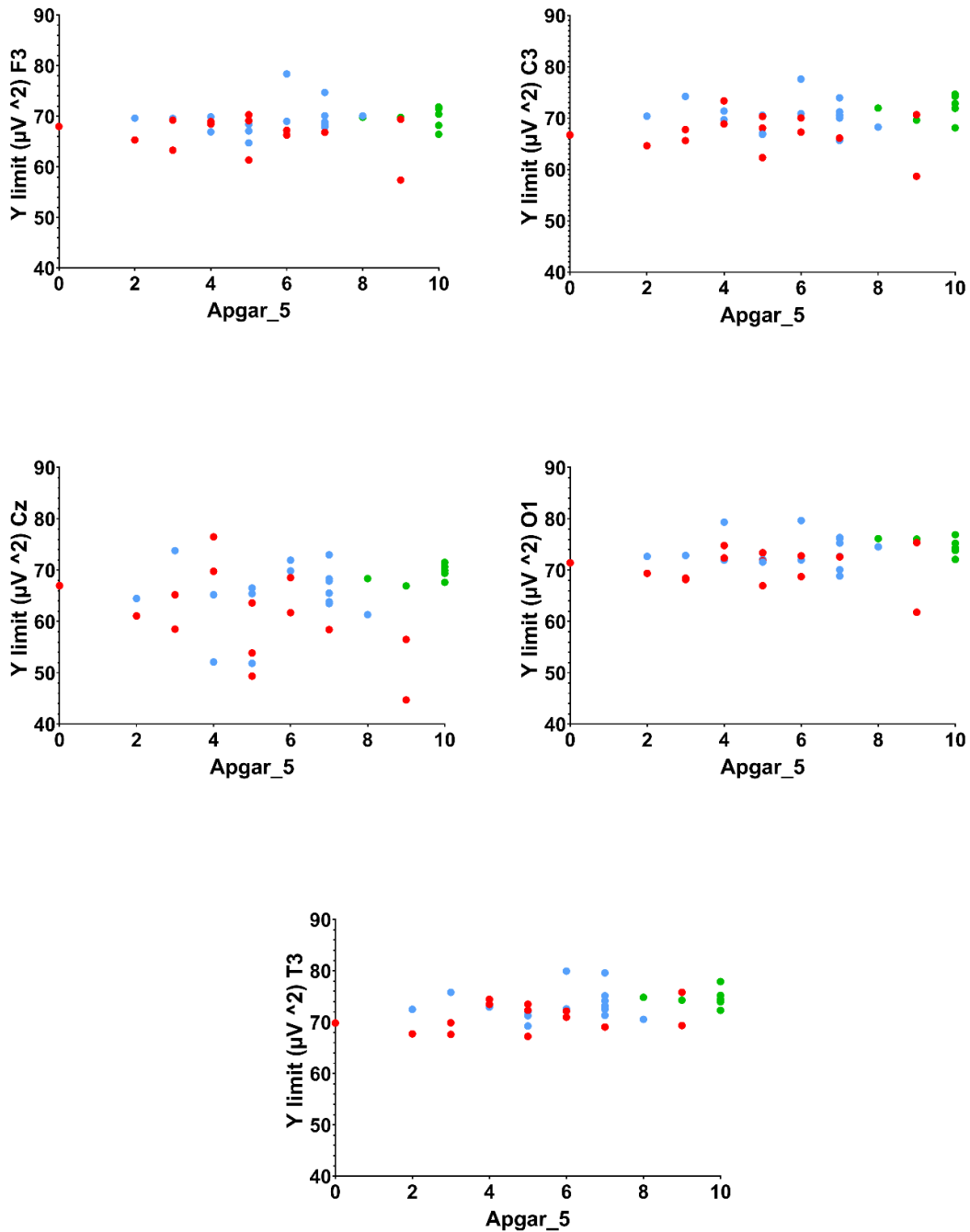
Lastly, the linear mixed modelling approach was used to detect the driving factor responsible for the significant effect on the cortical activity in these human neonates, and the possible interactions between the factors investigated here. The fixed factors were for model 1, the group and for model 2 the group, Apgar_5 and lactate together with their interaction. The starting model was gradually simplified using stepwise backward modelling, where the non-significant effects were removed step by step. The assumptions linearity and homoscedasticity were tested on the residuals. Statistical significance was set at $P<0.05$. After analyzing model 1 (i.e., the simple mixed model including as factor the group), it was detected that the activity with all scalp electrodes is significantly affected (C3: $P=0.002$; O1:

P=0.004; F3: *P*=0.0091; Cz: *P*=0.0153; T3: *P*=0.0018). For the second model, the group factor showed significantly differences for T3 (*P*=0.0018) and O1 (*P*=0.0040) scalp electrodes, while the interaction between group*lactate was significant for F3 (*P*=0.0267) and C3 (*P*=0.0384) (Figure 7). In the regard of Cz, the linear model could not be fitted since the data was not normally distributed and failed to fulfil the assumption by several transformations.

Figure 7. The linear mixed modelling approach was used to detect the driving factor responsible for the significant effect on the cortical activity in these human neonates, and the possible interactions between the factors investigated here. The group factor showed significantly differences for T3 (*P*=0.0018) and O1 (*P*=0.0040) scalp electrodes, while the interaction between group*lactate was significant for F3 (*P*=0.0267) and C3 (*P*=0.0384).
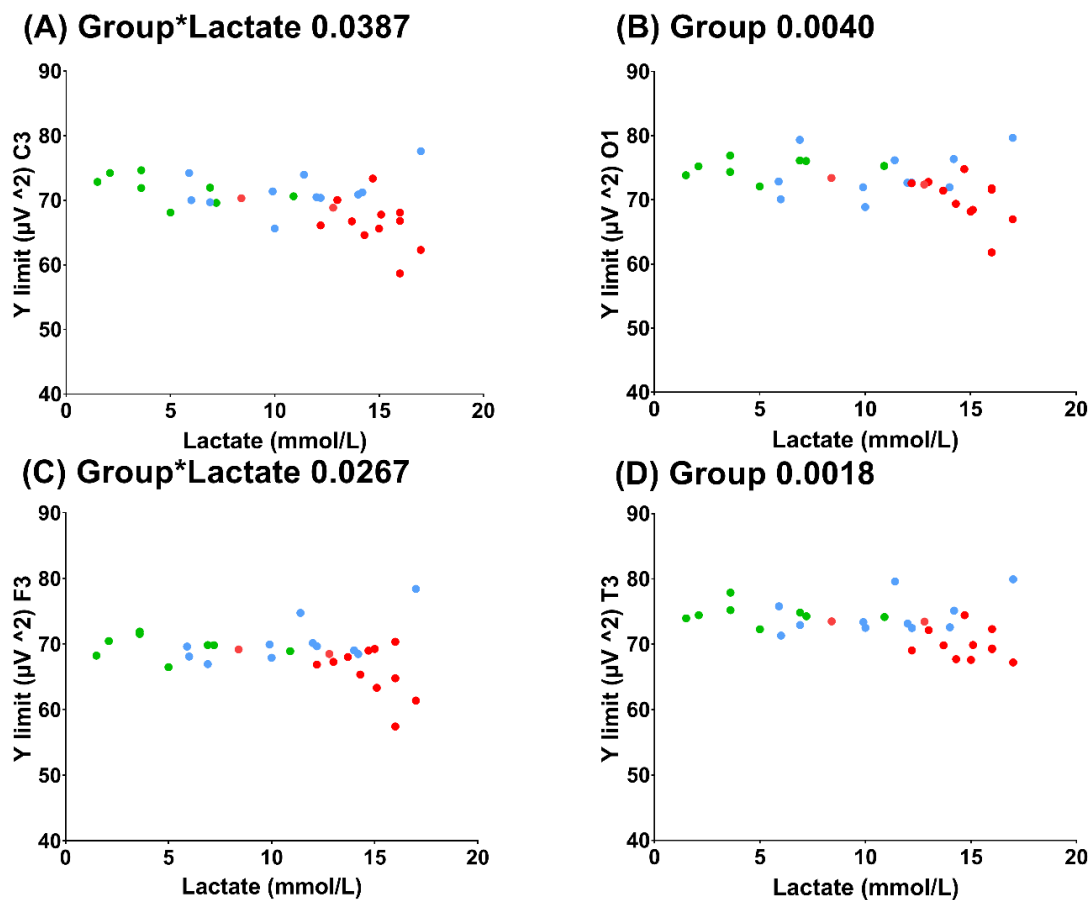
2.3. Description of the STSM main achievements, limitations, and conclusion

This study findings suggest that HIE leads to acute cortical activity depression in a severity-dependent manner, with more pronounced effects observed in the moderate HIE group. This suggests that the severity of the hypoxic-ischemic insult plays a crucial role in determining the extent of cortical activity disruption. In the context of AI-4-NICU, the initial data indicated a correlation between cortical activity and lactate levels. This correlation could provide a promising avenue for further exploration, potentially leading to the development of a machine learning algorithm capable of predicting outcomes based on lactate values. By using artificial intelligence techniques and machine learning algorithms to predict outcomes based on lactate

levels, we can potentially improve the care and treatment of neonates affected by PA/HIE, ultimately leading to better neurological outcomes for these vulnerable infants.

Furthermore, the study revealed substantial interindividual variability in responses to HIE, meaning that different individuals might exhibit diverse cortical activity patterns in response to the same hypoxic-ischemic insult. This variability highlights the complexity and heterogeneity of the brain's response to HIE, and it might be influenced by various factors, including individual differences in physiological, genetic, and environmental factors. In addition to the variability seen in the HIE group, there was also observed variability within the mild HIE group. This suggests that even within the milder cases of hypoxic-ischemic insult, there can be different degrees of cortical activity depression among individuals. This could be influenced by factors such as pre-existing health conditions, age, sex, and the presence of other potential confounding variables (e.g., hypothermia, sepsis) that might impact the response to mild HIE.

The study faced limitations due to the small sample size, imbalanced group sizes, and absence of females in the control group. Other covariates, such as hypothermia and sepsis, were not fully accounted in the mild HIE group, which could impact the interpretation of results. Although, this study is highly clinically relevant since it reflects the real-world data and analyze real HIE cases. These results have important clinical implications, as they underline the individual differences and the severity of the insult in understanding the neurological consequences of hypoxic-ischemic events. However, the study's limitations should be considered when interpreting the results, and future research with larger and more balanced sample sizes is essential to validate and expand upon these findings.

3. References

1.   Azzopardi D, Brocklehurst P, Edwards D, et al. The TOBY Study. Whole body hypothermia for the treatment of perinatal asphyxial encephalopathy: A randomised controlled trial. BMC Pediatrics. 2008 2008/04/30;8(1):17.

2.   Smits A, Annaert P, Van Cruchten S, et al. A Physiology-Based Pharmacokinetic Framework to Support Drug Development and Dose Precision During Therapeutic Hypothermia in Neonates. Front Pharmacol. 2020;11:587-587.

3.   O'Dea M, Sweetman D, Bonifacio SL, et al. Management of multi organ dysfunction in neonatal encephalopathy. Front Pediatr. 2020;8:239.

4.   Moshiro R, Mdoe P, Perlman JM. A global view of neonatal asphyxia and resuscitation. Front Pediatr. 2019;7:489.

5.   Gomella TL, Cunningham MD, Eyal FG, et al. Perinatal Asphyxia. Neonatology: Management, Procedures, On-Call Problems, Diseases, and Drugs, 7e. New York, NY: McGraw-Hill Education; 2013.

6.   Hines RN. The ontogeny of drug metabolism enzymes and implications for adverse drug events. Pharmacol Ther. 2008 May;118(2):250-67.

7.   Gerosa C, Fanni D, Puddu M, et al. Histological markers of neonatal asphyxia: the relevant role of vascular changes. Journal of Pediatric and Neonatal Individualized Medicine (JPNIM). 2014 10/21;3(2):e030275.

8.   Mallard C, Vexler ZS. Modeling Ischemia in the Immature Brain. Stroke. 2015;46(10):3006-3011.

9. Kyng KJ, Skajaa T, Kerrn-Jespersen S, et al. A Piglet Model of Neonatal Hypoxic-Ischemic Encephalopathy. J Vis Exp. 2015 (99):e52454-e52454.

10. Robertson NJ, Thayyil S, B. Cady E, et al. Magnetic Resonance Spectroscopy Biomarkers in Term Perinatal Asphyxial Encephalopathy: From Neuropathological Correlates to Future Clinical Applications. Current Pediatric Reviews. 2014;10(1):37-47.

11. Liu X, Tooley J, Løberg EM, et al. Immediate Hypothermia Reduces Cardiac Troponin I After Hypoxic-Ischemic Encephalopathy in Newborn Pigs. Pediatric Research. 2011 2011/10/01;70(4):352-356.

12. Gacio S. Amplitude-integrated electroencephalography for neonatal seizure detection. An electrophysiological point of view. Arq Neuropsiquiatr. 2019 Feb;77(2):122-130.

13. Shankaran S, Pappas A, McDonald SA, et al. Predictive value of an early amplitude integrated electroencephalogram and neurologic examination. Pediatrics. 2011 Jul;128(1):e112-20.

14. O'Brien CE, Santos PT, Kulikowicz E, et al. Hypoxia-ischemia and hypothermia independently and interactively affect neuronal pathology in neonatal piglets with short-term recovery. Developmental neuroscience. 2019;41(1-2):17-33.

15. Forman KR, Diab Y, Wong EC, et al. Coagulopathy in newborns with hypoxic ischemic encephalopathy (HIE) treated with therapeutic hypothermia: a retrospective case-control study. BMC Pediatr. 2014 Nov 3;14:277.

16. Sehgal A, Wong F, Mehta S. Reduced cardiac output and its correlation with coronary blood flow and troponin in asphyxiated infants treated with therapeutic hypothermia. Eur J Pediatr. 2012 Oct;171(10):1511-7.

17. Mota-Rojas D, Villanueva-García D, Solimano A, et al. Pathophysiology of Perinatal Asphyxia in Humans and Animal Models. Biomedicines. 2022 Feb 1;10(2).

18. LaRosa DA, Ellery SJ, Walker DW, et al. Understanding the Full Spectrum of Organ Injury Following Intrapartum Asphyxia. Front Pediatr. 2017;5:16.

19. NICE. National Institute for Health and Care Excellence. Interventional procedures guidance [IPG347]. Therapeutic hypothermia with intracorporeal temperature monitoring for hypoxic perinatal brain injury. Published on 26 May 2010, accessed on 25 April 2023. 2010.

20. Ayuso M, Buyssens L, Stroe M, et al. The Neonatal and Juvenile Pig in Pediatric Drug Discovery and Development. Pharmaceutics. 2021;13(1):44.

21. Koskela T, Kendall GS, Memon S, et al. Prognostic value of neonatal EEG following therapeutic hypothermia in survivors of hypoxic-ischemic encephalopathy. Clin Neurophysiol. 2021 Sep;132(9):2091-2100.

22. Georgoulas A, Jones L, Laudiano-Dray MP, et al. Sleep-wake regulation in preterm and term infants. Sleep. 2021 Jan 21;44(1).

23. Whitehead K, Pressler R, Fabrizi L. Characteristics and clinical significance of delta brushes in the EEG of premature infants. Clin Neurophysiol Pract. 2017;2:12-18.

24. Shankaran S, Laptook AR, Ehrenkranz RA, et al. Whole-body hypothermia for neonates with hypoxic-ischemic encephalopathy. N Engl J Med. 2005 Oct 13;353(15):1574-84.

25. Sarnat HB, Sarnat MS. Neonatal encephalopathy following fetal distress. A clinical and electroencephalographic study. Arch Neurol. 1976 Oct;33(10):696-705.

Summary

Pediatric drug therapy, presents significant challenges due to the pronounced growth and development during early life stages, affecting drug response. Perinatal asphyxia (PA) is a critical condition in neonates often requiring therapeutic hypothermia (TH) and intensive care to reduce morbidity and mortality. Animal models, such as the neonatal Göttingen Minipig, are valuable for understanding the mechanisms of conditions and therapies in pediatric populations. This study hypothesized that systemic hypoxia, as well as TH, affect drug disposition, including enzyme functionality. Given the effects of TH and PA on physiology, the primary hypothesis was that TH significantly decreases metabolic clearance (CL) in asphyxiated neonates, necessitating drug dosing adjustments. To address this, in vitro and in vivo data from neonatal Göttingen Minipigs will be used to develop a physiology-based pharmacokinetic (PBPK) model to ensure accurate drug dosing for asphyxiated neonates. An experimental study was carried out to examine the pharmacokinetics of midazolam, fentanyl, phenobarbital, and topiramate under 4 conditions: therapeutic hypothermia (group TH), hypoxia (group H), hypoxia and therapeutic hypothermia (group H+TH), and controls (group C). 6 healthy male Göttingen Minipigs, within 24 hours of birth per condition, were anesthetized for drug administration and blood sampling. Whole-body hypothermia was induced by lowering the Göttingen Minipigs' body temperature to 33.5°C, while systemic hypoxia was induced using a low-oxygen gas mixture. The gene and protein expression, as well as the activity of specific cytochrome P450 (CYP) enzymes were evaluated using in vitro methods. Hepatic CYP expression levels and activity were assessed in both adult and neonatal Göttingen Minipigs, in addition to the 24 experimental Göttingen Minipigs.

The study confirmed the feasibility of conducting complex in vivo procedures in neonatal Göttingen Minipigs, including endotracheal intubation, vascular access, anesthesia, and mechanical ventilation, which are critical for nonclinical animal experimentation. Furthermore, a novel pig model of asphyxia was successfully established, providing valuable insights into PA and related therapies. The drug disposition investigation conducted for 24 hours highlighted several alterations. Fentanyl was mostly affected since TH led to a 66% decrease in CL and approximately a 3-fold increase in the half-life ($t_{\frac{1}{2}}$). The study also explored the pharmacodynamic effects of TH, revealing notable impacts on heart rate in neonatal Göttingen Minipigs, consistent with documented effects in human neonates. These effects are particularly important for high extraction ratio drugs like fentanyl, due to their dependence on liver blood flow for their subsequent metabolism. Additionally, the research provided insights into the influence of age, hypothermia, and hypoxia on CYP enzymes. The vitro studies revealed differences in CYP expression and activity between neonatal and adult Göttingen Minipigs, underscoring the role of maturation in drug metabolism. Additionally, adult liver microsomes exhibited a 36% reduction in CYP activity following in vitro hypothermia exposure. In vivo hypothermia did not significantly alter CYP gene expression. However, alterations in the expression of CYP3A29 and CYP2E1 occurred due to hypoxia in neonatal Göttingen Minipigs. Lastly, this PhD thesis underscores the importance of refining and updating the PBPK model to improve its predictive accuracy and clinical relevance, marking a significant advancement in using neonatal Göttingen Minipigs for evaluating pediatric drug therapies.

Samenvatting

De pediatrische geneesmiddelentherapie, staat voor grote uitdagingen vanwege de snelle groei en ontwikkeling tijdens de vroege levensfasen, wat de reactie op geneesmiddelen beïnvloedt. Perinatale asfyxie (PA) is een kritieke toestand bij pasgeborenen die vaak therapeutische hypothermie (TH) en intensieve zorg vereist om de morbiditeit en mortaliteit te verminderen. Diermodellen, zoals de neonatale Göttingen Minipig, zijn waardevol voor het begrijpen van de mechanismen van aandoeningen en therapieën in pediatrische populaties. In deze studie werd onderzocht hoe systemische hypoxie en TH de geneesmiddelendispositie beïnvloeden, met behulp van een neonataal Göttingen Minivarkenmodel. Gezien de effecten van TH en PA op de fysiologie was de primaire hypothese dat TH de metabole klaring bij verstikte pasgeborenen aanzienlijk vermindert, waardoor de dosering van geneesmiddelen moet worden aangepast. Daarom voerden we een experimentele studie uit waarin in vitro en in vivo gegevens van neonatale Göttingen Minipigs werden gecombineerd om een fysiologisch gebaseerd farmacokinetisch (PBPK) kader te ontwikkelen met als doel dosisprecisie te bereiken bij verstikte pasgeborenen. De farmacokinetiek van midazolam, fentanyl, fenobarbital, en topiramaat werd onderzocht onder verschillende omstandigheden, zoals hypoxie, TH, of een combinatie van beide, evenals bij controleomstandigheden. Het onderzoek omvatte ook de evaluatie van gen- en eiwitexpressie en activiteit van hepatische cytochroom P450-enzymen. Het ontwikkelde fysiologie-gebaseerde farmacokinetische raamwerk had als doel dosisnauwkeurigheid te bereiken bij asfyctische pasgeborenen. De studie benadrukte de waarde van diermodellen zoals het Göttingen Minivarken voor het begrijpen van pediatrische farmacokinetiek en de impact van therapeutische interventies. De samenvatting van dit onderzoek biedt inzicht in de complexe interacties tussen ziekte, therapie en geneesmiddelenreacties bij neonatale patiënten, met het oog op verbeterde klinische behandelingen en zorg.

De studie bevestigde de haalbaarheid van het uitvoeren van complexe in vivo-procedures bij neonatale Göttingen Minipigs, waaronder endotracheale intubatie, vasculaire toegang, anesthesie en mechanische ventilatie, die cruciaal zijn voor niet-klinische dierexperimenten. Verder werd een nieuw varkensmodel van asfyxie succesvol ontwikkeld, wat waardevolle inzichten biedt in PA en gerelateerde therapieën. Het onderzoek naar de medicijnafgifte onthulde verschillende veranderingen. Voor fentanyl leidde TH tot een afname van 66% in de klaring en een ongeveer 3-voudige verhoging van de halfwaardetijdDe studie onderzocht ook de farmacodynamische effecten van TH, waarbij aanzienlijke effecten op de hartslag bij neonatale Göttingen Minipigs werden onthuld, in overeenstemming met gedocumenteerde effecten bij menselijke neonaten. Deze effecten zijn bijzonder belangrijk voor geneesmiddelen met een hoge extractieratio zoals fentanyl, die voor hun klaring en metabolisme hoofdzakelijk afhankelijk zijn van de leverdoorbloeding. Bovendien verschaft het onderzoek inzichten in de invloed van leeftijd, TH, systemische hypoxie en medische interventies op CYP-enzymen. In vitro studies onthulden verschillen in CYP-genexpressie en -activiteit tussen neonatale en volwassen Göttingen Minipigs, wat de rol van rijping in medicijnmetabolisme onderstreept. Bovendien vertoonden volwassen levermicrosomen een afname van 36% in CYP-activiteit na blootstelling aan in vitro hypothermie. In vivo veranderde therapeutische hypothermie de CYP-genexpressie niet significant, maar er traden veranderingen op in de expressie van CYP3A29 en CYP2E1 door hypoxie bij neonatale Göttingen Minipigs. Deze PhD-thesis legt een

basis voor een PBPK-model van neonatale Göttingen Minipigs. Het onderstreept het belang van het verfijnen en bijwerken van het model met nieuwe gegevens om de voorspellende nauwkeurigheid en klinische relevantie te verbeteren, en markeert een significante vooruitgang in het gebruik van neonatale Göttingen Minipigs voor de evaluatie van pediatrische geneesmiddeltherapieën.

Acknowledgements

This thesis is a tribute to all the people who made my academic journey worthwhile.

I would like to extend my heartfelt thanks to my promoter, Steven Van Cruchten, for trusting me and selecting me for this project. His immense availability, countless meetings spent answering my questions, and unwavering support during all the key moments have been invaluable. I am deeply grateful to my co-promoters: Karel Allegaert, who was always prompt in addressing my questions; Anne Smits, for her positive energy and dedication to the group; and Pieter Annaert, for his guidance in analyzing samples and data and his patience in answering my queries. Their unwavering support has been instrumental in the completion of this thesis and the publication of several articles.

I owe a great debt of gratitude to my colleagues. Karen, who shared this journey with me, working on the same project simultaneously, has been a constant source of support. I am also thankful to Lieselotte, Allan, and Miriam, who accompanied me to Denmark, participated in the in vivo experiments, and spent countless hours with me and the minipigs, making significant efforts for the animal experiments. Special acknowledgments go to the laboratory technicians, Katty Huybrechts and Gunther Vrolix, for their administrative and technical support, ordering numerous new supplies, and assisting with my in vitro work and in vivo experiments, including visits to the farm. I am also grateful to Prof. Chris Van Ginneken for her guidance in animal experimentation and the publication of several articles, as well as to my colleagues Sara, Marlotte, Laura, Jente, Kris, Steve, Kevin, Chloe, and Elias.

The completion of this thesis is the culmination of efforts from various individuals to whom I would like to express my sincere appreciation. I thank the team from Ellegaard Göttingen Minipigs A/S, Dalmose, Denmark for enabling the experiments on site, Adrian Zeltner for his involvement and expertise, and Jens Ellegaard for housing us and welcoming us warmly.

I would like to express my gratitude to the internal committee members, Prof. Dr. Peter Bols and Prof. Dr. Antonius Mulder, and external committee members, Prof. Dr. Thomas Thymann and Dr. Tim Bosmans, whose meticulous proofreading greatly improved my thesis.

Special thanks go to my family, whose constant encouragement fueled my perseverance during the completion of this dissertation. Firstly, to Martin, who believed in me and encouraged me at every step of my PhD journey and beyond, sharing not only the everyday challenges but also great moments. Now, we embark on a new adventure as parents to our little Marius. I am immensely thankful to my family and my in-laws for their presence, encouragement, and attention throughout this journey.

To those I have not mentioned specifically but who have become part of my life, both academically and personally, I extend my deepest gratitude.

Marina Stroe, DVM, PhD

Bruxelles | +32 470 277 148 | marina_stroe2000@yahoo.com

Professional summary :

With a background in laboratory animal sciences, anesthesiology, pharmacokinetics, and molecular biology, I am a veterinarian driven by the passion for uncovering new research questions. My PhD research focused on innovative drug development, specifically studying the effects of hypoxia and hypothermia on pharmacokinetics in neonates using the minipig model. This research not only improved my scientific skills but also deepened my enthusiasm for translational science. As an experienced small animal anesthesiologist, I have developed a strong interest in surgery and clinical pathology. Committed to education, I believe in collaborating with other researchers to create a collaborative and enriching learning environment.

Education & Experience :

UNIVERSITY OF ANTWERP,
FACULTY OF PHARMACEUTICAL, BIOMEDICAL AND VETERINARY SCIENCES
01.10.2020 - **22.11.2024 Public Defense PhD** - I-PREDICT: Innovative physiology-based pharmacokinetic (PBPK) model to predict drug exposure in neonates undergoing cooling therapy | Promoter: Prof. Steven Van Cruchten (UA) | Co-promoters: Prof. Allegaert Karel, Prof. Annaert Pieter, Prof. Smits Anne (KU Leuven)

UNIVERSITY OF GHENT
FACULTY OF VETERINARY MEDICINE, SMALL ANIMAL DIVISION
06.2019 - 09.2020 | Anesthesia Clinician

UNIVERSITY OF LIÈGE
FACULTY OF VETERINARY MEDICINE, SMALL ANIMAL DIVISION
01.2018 - 01.2019 | Anesthesia & Reanimation

UNIVERSITY OF AGRONOMIC SCIENCES AND VETERINARY MEDICINE OF BUCHAREST, FACULTY OF VETERINARY MEDICINE
10.2011 - 07.2017
Master's degree in **Veterinary Medicine**

DI-VET MEDICAL VETERINARY EMERGENCY CLINIC (Bucharest, Romania)
11.2015 - 12.2017 and 01.2019 - 04.2019

Scientific publications :

Stroe M-S, Van Bockstal L, et al. Development of a neonatal Göttingen Minipig model for dose precision in perinatal asphyxia: technical opportunities, challenges, and potential further steps. Front. Pediatr. Sec. Children and Health. 2023 (11), doi: 10.3389/fped.2023.1163100

Stroe M-S, Huang M-C, et al. Drug disposition in neonatal Göttingen Minipigs: Exploring Effects of Perinatal Asphyxia and Therapeutic Hypothermia. Drug Metab Dispos (2024), doi: 10.1124/dmd.124.001677

Stroe M-S, De Clerck L, et al. In vitro assessment of the effects of hypothermia and hypoxia on cytochrome P450-mediated drug metabolism in neonatal Göttingen Minipigs, Basic Clinical Pharmacology & Toxicology, (2024) doi: 10.1111/bcpt.14081

Leys K[a#] & **Stroe M-S**[b#], et al. Pharmacokinetics during therapeutic hypothermia in neonates: from pathophysiology to translational knowledge and physiologically-based pharmacokinetic (PBPK) modeling. Expert opinion on drug metabolism & toxicology, (2023) 19(7), 461–477. https://doi.org/10.1080/17425255.2023.2237412

Ayuso M, Buyssens L, **Stroe M-S**, et al. The Neonatal and Juvenile Pig in Pediatric Drug Discovery and Development. Pharmaceutics. 2020;13(1):44. Published 2020 Dec 30. doi:10.3390/pharmaceutics13010044

Tubeeckx M, Laga S, Jacobs C, **Stroe M-S**, Van Cruchten S, Goovaerts B, Van Fraeyenhove J, Miljoen H, De Meyer G, De Keulenaer G, Heidbuchel H, Segers V. Sterile Pericarditis in Aachener Minipigs As a Model for Atrial Myopathy and Atrial Fibrillation. J. Vis. Exp (175), e63094, doi:10.3791/63094 (2021)

Science Communication :

Stroe M-S, Van Bockstal L, Van Cruchten S. Developing a perinatal asphyxia model with newborn Göttingen Minipigs at the Ellegaard Göttingen Minipigs A/S research facility, Göttingen Minipigs Magazine, #64, Winter 2023, https://minipigs.dk/about-us/gottingen-minipigs-magazine

Stroe M-S, Van Bockstal L, et al. The Neonatal Göttingen Minipig as Translational Model for Perinatal Asphyxia and Therapeutic Hypothermia, Poster presentation, Beltox Annual Meeting 2022, 7 December 2022, Antwerp, Belgium, https://beltox.be/wp-content/uploads/2022/12/Abstract-book-AM22.pdf

Stroe M-S, The neonatal Göttingen Minipig model for dose precision in perinatal asphyxia, Oral presentation, 11th Juvenile Toxicity Symposium 20-21 April 2023, Janssen R&D, Belgium

Stroe M-S, Ayuso M, et al. The Neonatal Göttingen Minipig Model for Dose Precision in Perinatal Asphyxia and Therapeutic Hypothermia, Poster presentation, 15th Minipig Research Forum, 10-12 May 2023, Amsterdam, the Netherlands, Poster https://www.uantwerpen.be/en/research-groups/coped/projects-and-publications/publications/poster-presentations/

Stroe M-S, Effects of Perinatal Asphyxia and Therapeutic Hypothermia on Drug Disposition in Neonates using a Translational Approach, Oral presentation, 51st European Teratology Society Conference, September 17-20, 2023, Madrid, Spain

Skills :

- **Catheterization, surgery & anesthesia, necropsy in small and laboratory animals**
- **Molecular biology:** mRNA extraction & purification, DNA and tissues manipulation, quantitative PCR; cell isolation & culture (hepatocytes); proteomics; fluorometry; microsomal preparation
- **Pharmacokinetics**, drug dosing & sampling, in silico PBPK modeling
- Multitasking, project management, communication, presentation
- **English (B2), French (B2), Dutch (A1), Romanian (native speaker)**

Short-Term Scientific Mission Grant :

16.07.2023 - 28.07.2023
COST | European Cooperation in Science and Technology
CA20124 Maximising impact of multidisciplinary research in early diagnosis of neonatal brain injury (AI-4-NICU) | Supervisor: Dr. Kimberley Whitehead, EGA Institute for Women's Health, University College London, UK

Awards :

- Elsevier Young Scientist Award for Best Poster, 50th European Teratology Society Conference, September 25-28, 2022, Antwerp, Belgium
-
- Elsevier Young Scientist Award for Best Presentation, 51st European Teratology Society Conference, September 17-20, 2023, Madrid, Spain

Training :

- **FELASA B & C** (2020)
- Radboud Summer School: PK/PD (2021)
- Statistics: Antwerp Doctoral School, Flames, Statua courses

Teaching :

- Laboratory Animal Science Course
- Hands-on anesthesia training for final-year veterinary students